CHARLES UNIVERSITY IN PRAGUE

FACULTY OF SCIENCE

Ph.D. study program: Developmental and Cell Biology

Sweetu Susan Sunny, MS.c

The role of transcription factors in mouse eye development

Úloha transkripčních faktorů při vývoji oka myši

Ph.D. Thesis

Supervisor : RNDr. Zbynek Kozmik, CSc.

Prague 2023

STATEMENT

The work presented in this dissertation has been carried out by me under the supervision of Dr. Zbynek Kozmik.

This work has not been submitted in part or in full for a degree, a diploma or a fellowship to any other university or institution. Whenever contributions of others are involved, every effort is made to indicate this clearly, with due acknowledgement of collaborative research and discussions. This thesis is a bonafide record of original work done by me and all sources listed within have been detailed in the bibliography

Dated: Sweetu Susan Sunny, MS.c

ACKNOWLEDGEMENT

I would like to take this opportunity to express my sincere gratitude to my supervisor Dr. Zbynek Kozmik for his guidance, encouragement and funding throughout my PhD studies. His teaching, enthusiasm and dedication to work have motivated me to pursue research.

I am deeply indebted to Jitka Lachova who introduced me to mouse work and to the lab members namely, Dr. Naoko Dupacova, and Dr. Jana Smolikova, for their support and helpful discussions. Their contributions have greatly enriched my research experience. I am grateful to Veronika Noskova and Anna Zitova for their technical support.

To my friends, Reshma R, Swathi Jayaram, Parvathy *Surendranadh and Nikol Dikus,* I extend my heartfelt gratitude for their love and motivation. I feel fortunate to have had their unwavering support throughout my stay in Prague.

Finally, I would like to express my deepest gratitude to my family for their unconditional love, encouragement and support.

This work was supported by the Grant Agency of the Czech Republic (21-27364S, 18-20759S), the Ministry of Education, Youth and Sports of the Czech Republic (RVO68378050-KAV-NPUI and LQ1604) and partial mouse costs are covered by Czech Center for Phenogenomics (LM2018126, OP VaVpI CZ.1.05/2.1.00/19.0395, and CZ.1.05/1.1.00 /02.0109.)

ABSTRACT

Vision is a complex process that begins with the transmission and refraction of light through a highly specialised transparent tissue called the cornea. The cornea acts as a protective barrier and contributes to the focusing power of the eye. The development of mammalian cornea is a multiphase process involving the formation of the corneal epithelium (CE), stroma and endothelium (CEn) during embryogenesis, followed by the postnatal stratification of epithelium and constant renewal of desquamated outermost cells.

Paired box protein (Pax) 6 is an evolutionarily conserved transcription factor important for the proper development of the eye. To provide further insights into the role of Pax6 in corneal development, we took the advantage of Cre-*loxP* system for selectively inactivating Pax6 in two ocular domains, specifically, the postnatal CE and the ocular surface epithelium (OSE) (cornea, limbus, and conjunctiva). We generated a novel postnatal CE-specific Cre-expressing transgenic mouse line, *Aldh3-Cre*. Inactivation of Pax6 in the postnatal CE using *Aldh3-Cre* resulted in the abnormal thin cornea with defective cell-cell adhesion, thus providing direct evidence for the function of Pax6 in postnatal corneal development. Subsequently, the OSE-specific depletion of Pax6 using *K14-Cre*, resulted in the conjunctivalisation of the CE and limbal epithelium, suggesting the importance of limbal Pax6 in preventing the conjunctival outgrowth into the cornea.

The genetic causation of posterior polymorphous corneal dystrophy (PPCD) 1 is the mutations in the highly conserved promoter region of the Ovo-like zinc finger 2 (OVOL2) gene causing ectopic OVOL2 expression in CEn. In this part of the study, we generated and characterised seven Ovol2 promoter mutations in mice, including human PPCD1 pathogenic variant c.-307T>C using CRISPR- Cas9 approach. Despite of high degree of sequence conservation, only two mutations lead to phenotypic effects. Mice harbouring c.-307T>C or c.-307_-320del showed significant upregulation of Ovol2 mRNA but did not demonstrate the hallmarks of corneal endothelial dystrophy, suggesting species-specific variation in the CEn development. Interestingly some mutants showed ocular phenotypes such as iridocorneal adhesion, persistent hyperplastic primary vitreous, and dysplastic retina implying the role of Ovol2 in early eye development.

Altogether, the main part of this thesis provides insights into the role of transcription factor Pax6 in corneal development and the effects of *Ovol2* promoter mutations on the pathogenicity of PPCD1 in mouse models.

In addition, this thesis also presents the role of the chromatin remodeling factor sucrose non-fermenting 2-homolog (Snf2h) during retinal development. Snf2h is expressed in retinal progenitors and post-mitotic retinal cells. Our studies show that conditional depletion of Snf2h in retinal progenitor cells resulted in a thin retina with the absence of the photoreceptor layer. Immunofluorescence studies revealed that all other retinal cell types are specified in Snf2h depleted retina, suggesting that Snf2h is not required for the generation and maintenance of other retinal cell types. On the contrary, it is important for the proliferation of retinal progenitor cells. The loss of Snf2h in retinal progenitor cells led to cell cycle abnormalities and an increase in apoptosis, which ultimately culminated in the destruction of photoreceptors and the lamination of the retina. Together, our data suggest that Snf2h is important for retinal cell proliferation and maintenance of photoreceptors.

ABSTRAKT

Vidění /zrak je složitý proces, který začíná přenosem a lomem světla přes vysoce specializovanou průhlednou tkáň nazývanou rohovka. Rohovka slouží jako ochranná bariéra a přispívá k zaostřovací schopnosti oka. Vývoj savčí rohovky sestává z několika fází, zahrnující tvorbu rohovkového epitelu (CE), rohovkového stromatu a endotelu (CEn) během embryogeneze, následované postnatální stratifikací epitelu a pravidelnou obnovou odlupovaných povrchových buněk epitelu.

Transkripční faktor Paired box protein (Pax)6 je evolučně konzervovaný transkripční factor, důležitý pro správný vývoj oka. Pro další porozumění úloze Pax6 při vývoji rohovky jsme využili systém Cre-*loxP* k selektivní inaktivaci Pax6 ve dvou tkáních oka, konkrétně postnatálním CE a tkání "epitelu očního povrchu*"* (OSE) (rohovka, limbus a spojivka). Vytvořili jsme novou transgenní myší linii s postnatálně specifickou expresí Cre-rekombinázy v CE, *Aldh3-Cre*. Inaktivace Pax6 v postnatálním CE pomocí *Aldh3-Cre* vedla k abnormálně tenké rohovce s defekty v buněčné adhezi. Tím jsme přímo prokázali, že Pax6 hraje klíčovou roli v postnatálním vývoji rohovky. Poté jsme selektivně inaktivovali Pax6 v OSE pomocí další specifické myší linie *K14-Cre*. U těchto myší docházelo ke "konjunktivalizaci" CE a epitelu limbu (přeměně tkáně CE a limbu v tkáň morfologicky podobnou spojivce). Což ukazuje, že Pax6 je nepostradatelný při vývoji limbu a celkově je jeho exprese nezbytná pro správnou morfologii a funkci tkání OSE (rohovky,limbu a spojivky).

Genetickou příčinou zadní polymorfní dystrofie rohovky (PPCD) 1 jsou mutace vysoce konzervované oblasti promotoru genu *OVOL2 (*ovo-like zinc finger 2), které způsobují ektopickou expresi OVOL2 v CEn. V této části studie jsme pomocí metody CRISPR-Cas9 vytvořili a charakterizovali sedm transgenních kmenů myší nesoucích mutace promotoru *Ovol2*, včetně lidské PPCD1 patogenní varianty, c.-307T>C. Přestože je sekvence promotoru vysoce konzervovaná, pouze dvě mutace měly fenotypické účinky. Myši s mutacemi c.-307T>C nebo c.-307_-320del vykazovaly významné zvýšení hladiny *Ovol2* mRNA, ale nevykazovaly charakteristické znaky dystrofie rohovkového endotelu, což naznačuje druhově specifickou variaci ve vývoji CEn. U některých myších mutantů jsme popsali oční fenotypy, jako je adheze duhovky a rohovky, abnormality v primárním sklivci a dysplastické sítnice, což naznačuje možnou roli Ovol2 při raném vývoji oka.

Tato práce poskytuje především nové poznatky o úloze transkripčního faktoru Pax6 při vývoji rohovky; dále popisuje fenotyp nových myších kmenů nesoucích mutace v promotoru *Ovol2* a tímto hledá souvislost s lidskou rohovkovou distrofií PPCD1.

Kromě toho tato práce představuje úlohu faktoru chromatinového remodelingu Snf2h (sucrose nonfermenting 2-homolog) během vývoje sítnice. Snf2h je exprimován v progenitorech sítnice a postmitotických buněčných typech v sítnici. Naše studie ukazují, že podmíněná deplece Snf2h v progenitorech sítnice vede k ztenčení sítnice kvůli absenci vrstvy fotoreceptorů. Imunofluorescenční studie odhalily, že všechny ostatní typy buněk sítnice jsou ve Snf2h-depletované sítnici specifikovány, což naznačuje, že Snf2h není potřeba pro vznik a udržování ostatních buněčných typů sítnice. Naopak je důležitý pro proliferaci progenitorových buněk sítnice. Ztráta Snf2h u progenitorových buněk sítnice vedla k abnormalitám v buněčném cyklu a zvýšení apoptózy, což nakonec vedlo ke změnáve vrstvení sítnice a k zániku fotoreceptorů. Naše data naznačují, že Snf2h je důležitý pro proliferaci buněk sítnice a udržování/viabilitu fotoreceptorů

CONTENTS

1. PREFACE

Human survival skills depend heavily on the ability of our senses to gather information and respond to our surroundings. Of the five senses, vision is considered to be of high importance, since it is a vital tool for social interaction, proper functioning of daily activities, perceiving beauty and achieving personal fulfilment. Eye morphogenesis is a highly complex process which starts very early during embryonic development and any abnormalities in this normal programme of development will result in serious ocular disorders, for instance, aniridia, anophthalmia, corneal dystrophies, Axenfeld- Reiger syndrome, coloboma. These are mainly caused by the mutations in genes which are important during eye development. Studies in animal models have greatly improved our understanding of the roles of each of these genes, in the cause and progression of these disorders.

This Ph.D. thesis is mainly focused on the role of transcription factor Pax6 during corneal development and the effect of *Ovol2* promoter mutations in developing posterior polymorphous corneal dystrophy using the mouse as a model organism. It also briefly touches on the function of the chromatin remodeling protein Snf2h in the development of the mouse retina.

This thesis consists of four publications as follows:

1. **Generation and characterization of *Aldh3-Cre* transgenic mice as a tool for conditional gene deletion in postnatal cornea.**
   Sunny.SS, Lachova J, Dupacova N, Zitova A, Kozmik Z
   Sci Rep. 2020 Jun 3:10 (1):9083, doi: 10.1038/s41598-020-65878-1, PMID: 32493941
2. **Multiple roles of Pax6 in postnatal cornea development.**
   Sunny.SS, Lachova J, Dupacova N, Kozmik Z
   Dev Biol. 2022 Nov; 491:1-12. doi: 10.1016/j.ydbio.2022.08.006, PMID: 36049534
3. **Investigating the effect of the *Ovol2* promoter mutations and their possible association with Posterior polymorphous corneal dystrophy (PPCD) 1 in the mouse model.**
   Sunny SS, Lachova J, Kaspaerek P, Prochazka J, Sedlacek R, Liskova P, Kozmik Z.
   Prepared for submission
4. **Chromatin remodeling enzyme Snf2h is essential for retinal cell proliferation and photoreceptor maintenance**
   Kuzelova A, Dupacova N, Antosova B, Sunny SS, Kozmik Z, Paces J, Skoultchi AI, Stopka T, Kozmik Z
   Cells. 2023 Mar 28; 12 (7):1035. doi: 10.3390/cells12071035. PMID: 37048108

2. LIST OF ABBREVIATIONS

aa	Aminoacid
ALDH	Aldehyde dehydrogenase
Ap-2	Adapter-related protein complex 2
CE	Corneal epithelium
CEn	Corneal endothelium
cKO	Conditional knockout
Dkk	Dickkopf-2
DNA	Deoxyribonucleic acid
DVL	Disheveled
E	Embryonic day
EBS	Epidermolysis bullosa simplex
EFTF	Eye field transcription factor
EMT	Epithelial to mesenchymal transition
GRHL2	Grainy head-like transcription factor 2
HD	Homeodomain
IF	Intermediate filament
KLF	Kruppel-like transcription factor
Krt	Cytokeratin
LP	Lens Placode
LV	Lens Vesicle
LSC	Limbal stem cell
LSCD	Limbal stem cell deficiency
MET	Mesenchymal to epithelial transition
miR	MicroRNA
mRNA	Messenger ribonucleic acid
NR	Neural Retina
OC	Optic cup
OSE	Ocular surface ectoderm
OV	Optic Vesicle
OVOL2	Ovo-like zinc finger 2
Pax6	Paired box 6
PD	Paired Domain
PHPV	Persistent hyperplastic primary vitreous
PPCD	Posterior polymorphous corneal dystrophy
PN	Postnatal day
PST	Proline- Serine-Threonine
RPC	Retinal progenitor cells
RPE	Retinal pigment epithelium
SE	Surface ectoderm
SD-OCT	Spectral domain optical coherence tomography
Snf2h	Sucrose non-fermenting 2 homolog
Snf2l	Sucrose non-fermenting 2-like protein
TAC	Transient amplifying cell
Tkt	Transketolase
ZEB1	Zinc finger E-box binding homeobox 1
Zo	Zona occludens

3. LITERATURE OVERVIEW

3.1 Overview of mammalian eye development

Eye development in mammals involves a series of coordinated inductive events between the anterior surface ectoderm, neuroectoderm and surrounding extraocular mesenchyme, derived from mesoderm and neural crest (Graw, 2010).

The developing eye is organized as a single eye field in the anterior neural plate during late gastrulation. This single eye field then separates and evaginates laterally towards non-neural surface ectoderm (SE) to form optic vesicles (OVs) at embryonic day (E) 9.5 in the mouse (Figure 1A). Interactions between OV and SE induce a thickening in the latter called lens placode (LP) (Figure 1B). Subsequently, the LP coordinately invaginate with the OV forming the lens pit and a double-layered optic cup (OC), respectively (at E10.0 in mouse) (Figure 1C). The outer layer of the optic cup will differentiate to form retinal pigment epithelium (RPE), and the inner layer will form the neural retina (NR). Laterally, the lens pit invaginate until it detaches from the SE to form a lens vesicle (LV) (E11.0) (Figure 1D) and LV differentiates to form the mature lens (Graw, 2010).

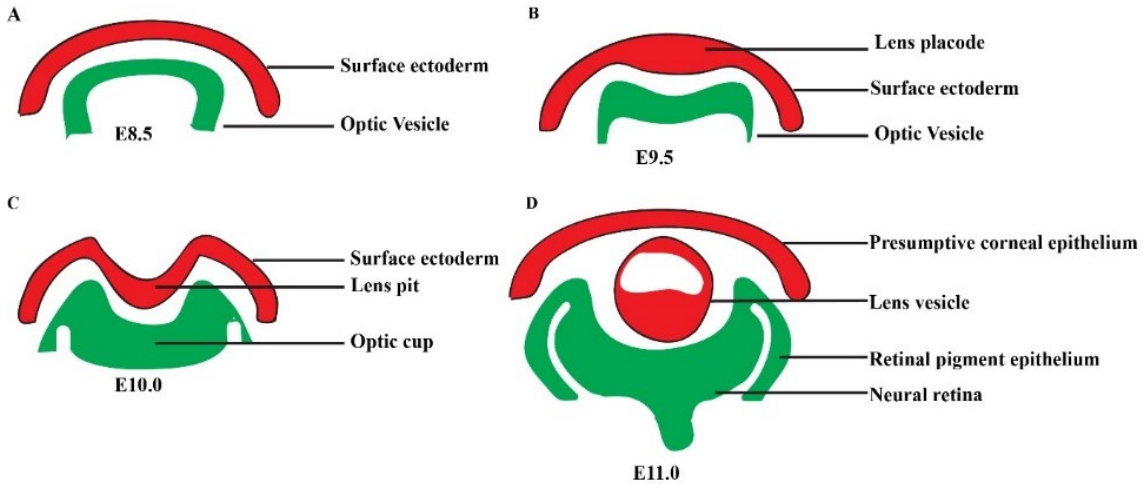

Figure 1: Overview of mammalian eye development (**A**) Evagination of diencephalon forms optic vesicle (**B**) Optic vesicle induces the overlying surface ectoderm to form lens placode. (**C, D**) Co- ordinated invagination of lens placode and optic cup forms lens vesicle and double -layered optic cup respectively. Laterally, the outer layer of the optic cup gives rise to retinal pigment epithelium and the inner layer forms the neural retina. Lens vesicle detaches from the surface ectoderm and the surface ectoderm reassembles to form presumptive corneal epithelium. The colour indicates the tissue of origin, Red: the surface ectoderm, Green: the neuroectoderm.

3.1.1 Corneal development

Shortly after LV formation, SE reassembles to form corneal epithelium (CE), which remains 1-2 layered until birth. Around E12.5-E13.5, mesenchymal cells of neural crest origin migrate to the space between CE and LV (Figure 2A) and condense to form 4-6 flat layers that are separated from each other by a loose extracellular matrix (Figure 2B). During E14.5 -15.5, the posterior-most mesenchymal cells get flatten and make intercellular contacts with adjacent cells to form monolayered corneal endothelium (CEn) (Figure 2C)

(Cvekl and Tamm, 2004; Dublin, 1970; Flugel-Koch et al., 2002; Kidson et al., 1999; Pei and Rhodin, 1970; Reneker et al., 2000). Mesenchymal cell layers between CE and CEn differentiate to form corneal stromal keratocytes, which later secretes a highly specialised extracellular matrix of the corneal stroma (Pei and Rhodin, 1970; Swamynathan, 2013). The CE continues to develop postnatally, coincident with eye-opening (postnatal day (PN) 14), it starts dividing rapidly and differentiates to form 6-8 layered stratified epithelium by PN28 (Figure 2D-E) (Hay, 1980; Zieske, 2004).

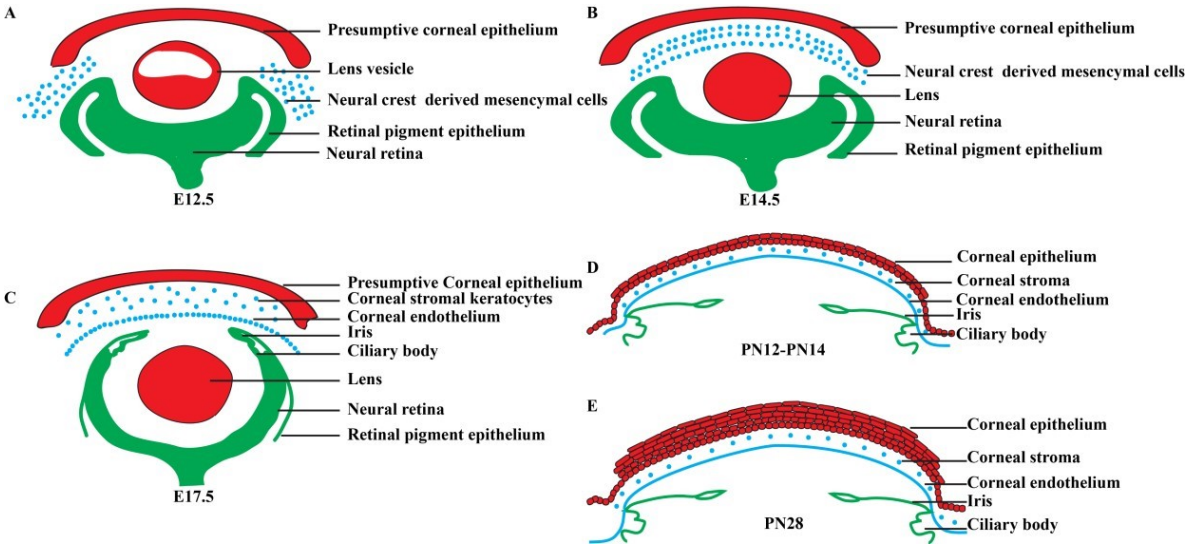

Figure 2: Overview of embryonic and postnatal corneal development (A) Neural crest-derived mesenchymal cells migrates to the space between the lens and corneal epithelium**. (B)**These cells condense to form 3-4 layers. **(C)** Posterior most mesenchymal cells flatten and make contact with the adjacent cells to form monolayered corneal endothelium and others differentiate to form stromal keratocytes. **(D)** Corneal epithelium remains 2-3 layered until eye-opening (around PN12-PN14). **(E)** Upon eye-opening, corneal epithelium starts dividing rapidly and stratifies to form 6-8 layers by PN28. The colour indicates the tissue of origin, Red: surface ectoderm, Green: the neuroectoderm, Blue: the neural crest.

3.1.2 Retina, iris and ciliary development

When the lens and cornea are formed, OC differentiates to form neuronal and non-neuronal tissue types. This process begins at around E12.5 and the resulting tissues include the NR, the RPE, the iris and the ciliary body. The neural retina is composed of retinal progenitor cells (RPC), which undergo proliferation and expansion to form three distinct cell layers. These layers include the outer nuclear layer, which contains cone and rod photoreceptors, and the inner nuclear layer, which is populated by horizontal, bipolar, amacrine and Muller glial cells and ganglion cell layer. Retina reaches full development a few days after birth in mice (Figure 3) (Graw, 2010).

In mice, development of the iris and the ciliary body begins at around E15.5, when the marginal cells of the optic cup are well distinguished with the absence of neuronal markers. By E17.5, these progenitor cells differentiate to form the iris epithelium. Cells located at the root of the iris continue to differentiate and form a ciliary body (Figure 2C-E).

Mesenchymal cells migrating along the iris and ciliary body epithelium differentiate to form stroma. (Cvekl and Tamm, 2004; Davis-Silberman and Ashery-Padan, 2008).

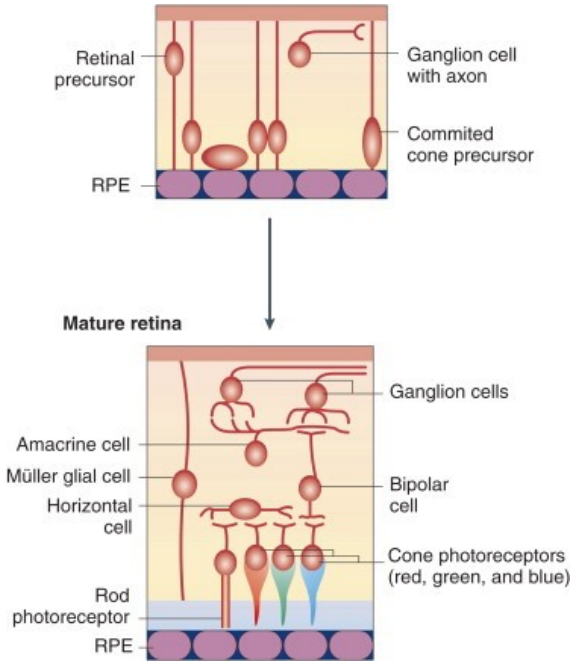

Figure 3: Development of retina. The outer layer of the optic cup differentiates to form retinal pigment epithelium and the inner layer contributes to the neural retina. The retinal precursor cells further differentiate to form three distinct layers with seven cell types. Cone and rod photoreceptors form the outer nuclear layer, and horizontal, bipolar, Muller glial and amacrine cells populate the inner nuclear layer, whereas ganglion cells reside in the innermost layer, ganglion cell layer. Adapted from (Graw, 2010).

3.2 Structure and the function of adult mouse cornea

The optimal phototransduction process of the retina is highly dependent on specialized structures present in the front of the eye. The cornea is a highly specialized, avascular, transparent tissue that forms the anterior-most part of the eye. It contributes to 60-70% of the total refractive power of the eye and acts as a protective barrier as well as provides mechanical stability for the eye (DelMonte and Kim, 2011). The cornea consists of mainly five layers; CE, Bowman's layer, stroma, Descemet's membrane and CEn, each with a specific structure and function (Figure 4).

Stratified non-keratinized squamous epithelium forms the outermost layer of the cornea. The CE is in direct contact with the mucin layer of the tear film, which is produced by the conjunctival globet cells. The close interaction of the mucin layer with CE allows the hydrophilic spreading of the tear, as each time eye blinks (Sridhar, 2018). The primary function of CE is to provide a barrier against pathogens and maintain a clear and smooth transmission of light. An adult mouse eye has 6-8 layered CE, and it is continuously renewed by a population of stem cells located at the juncture between the cornea and conjunctiva called the limbus. Limbal stem cells (LSC) divide asymmetrically and give rise to a stem-like daughter cell that remains in the limbus and a transient amplifying cell (TAC) that migrates centripetally through the basal epithelium. TACs undergo multiple rounds of

replication and gradually lose their stemness as they migrate anteriorly, transforming into post-mitotic suprabasal wing cells and ultimately to terminally differentiated superficial cells. These superficial cells are constantly shed from the surface through natural exfoliation. The entire mouse CE is renewed every 7-8 weeks (Collinson et al., 2002; Cotsarelis et al., 1989; Lavker et al., 1991; Nagasaki and Zhao, 2003; Thoft and Friend, 1983; Yoon et al., 2014)

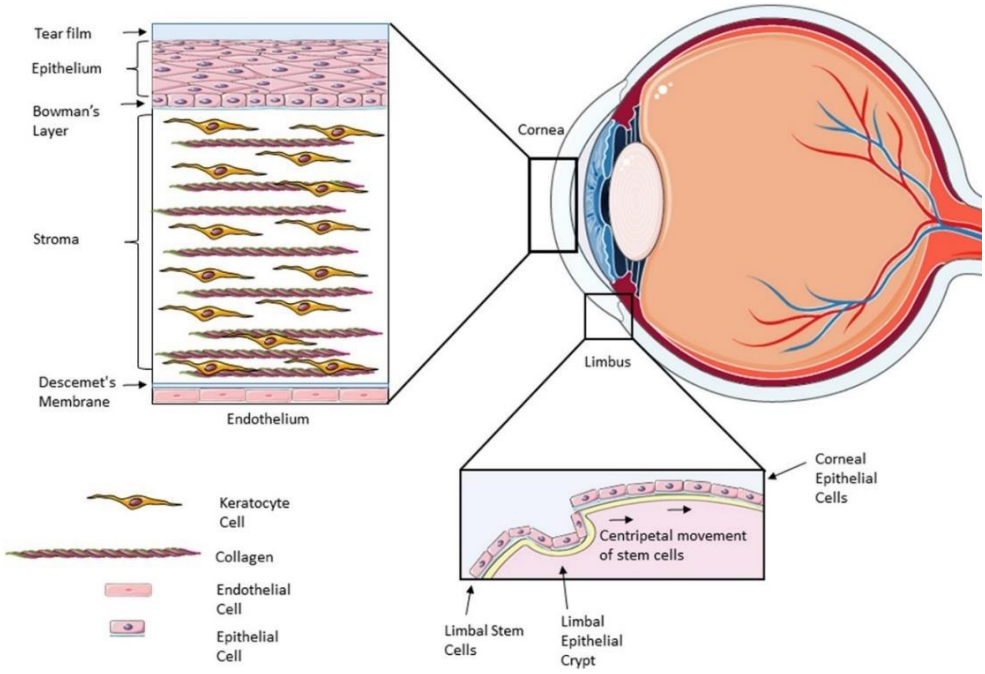

Figure 4: Schematic representation of the structure of the cornea. The cornea forms the outermost layer of the eye which provides protection and the first refractive surface for the transmission of light. The cornea mainly consists of five layers, the corneal epithelium, Bowman's layer, stroma, Descemet's layer and corneal endothelium. Corneal epithelial homeostasis is maintained by stem cells located at the junction between the cornea and conjunctiva, called limbus (Masterton and Ahearne, 2018).

Dysfunction or loss of LSCs by genetic conditions, thermal or chemical burn, or autoimmune disorders, will result in a condition called limbal stem cell deficiency (LSCD) where corneal epithelial renewal function and barrier role is compromised (Chen and Tseng, 1990; Tseng, 1989). Symptoms of LSCD include conjunctivalisation, vascularisation of the cornea, pain, oedema, redness, tear, and ultimately blindness (Dua et al., 2000; Menzel-Severing, 2011). In these cases, limbal stem cell transplantation or limbal-derived cell grafts may be necessary to restore the function of the CE and improve vision (Bonnet et al., 2021; Kenyon and Tseng, 1989; Le et al., 2020; Pellegrini et al., 1997).

The CE lies on a fibrous meshwork called Bowman's layer. It consists of collagen fibers and proteoglycans which provide structural support for the cornea. Corneal stroma forms the central and thickest layer of the cornea. More than 97% of stroma consists of collagen fibers and extracellular matrix proteins secreted by the sparsely dispersed keratocytes. Stroma reduces light scattering by precise patterning of collagen fibers (Price et al., 2021).

Descemet's membrane is a thin, acellular layer located between the stroma and CEn. It provides structural support and aids in the diffusion of nutrients and waste products (Sridhar, 2018).

The CEn is a single layer of hexagonal-shaped cells located at the innermost surface of the cornea. The CEn must perform two functions to maintain nourishment and transparency of the cornea: it should allow the passive transport of nutrients and other molecules from the aqueous humour and must regulate stromal hydration to a level that minimum amount of light scatters. This problem is solved by the pump-leaky mechanism in the endothelium. Endothelial cells have incomplete tight junctions between the adjacent cells. This leaky barrier together with imbibition pressure caused by highly charged stromal proteoglycans, allows the diffusion of nutrients and extracellular fluid into the stroma. At the same time, endothelium maintains stromal hydration by the active pumps that move stromal ions and water osmotically to the aqueous humour and thus prevents inhomogeneities in collagen pattern and light scattering (Bonanno, 2012; Klyce, 2020; Maurice, 1962). The CEn cells have limited regenerative capability since they are arrested at the G1 phase of the cell cycle (Senoo and Joyce, 2000). As a result, loss of endothelial cells due to toxic insult, injury or diseases can cause irreversible endothelial dysfunction which leads to corneal edema, and thus loss of visual acuity (Koizumi et al., 2012; Park et al., 2021; Tuft and Coster, 1990). Together, these layers contribute to the unique structure and function of the mouse cornea.

3.3 Transcription factors regulating corneal epithelial development, maturation and maintenance

Studies utilizing the advantages of transgenic and knockout models have uncovered the role of various transcription factors in the development, maturation and maintenance of cornea. A concise overview of how these transcription factors contribute to corneal development and homeostasis is discussed below.

3.3.1 Transcription factor Pax6 and its role in corneal development

3.3.1.1 Transcription factor Pax6

Paired box genes encode for a family of transcription factors which are crucial for various aspects of early development. Paired box (Pax) 6 is a highly conserved member of the Pax gene family which first gained attention due to its role in eye development (Chi and Epstein, 2002; Kozmik, 2005; Pichaud and Desplan, 2002). In addition to its role in eye morphogenesis, Pax6 is also important for the development of the central nervous system, olfactory system and pancreas (Hanson and Van Heyningen, 1995; Shaham et al., 2012; Simpson and Price, 2002).

The mammalian Pax6 gene consists of 16 exons spanning around 28 kb of genomic DNA (Glaser et al., 1992; Kammandel et al., 1999; Kim and Lauderdale, 2006). Transcription of Pax6 can start from three promoters, P0, P1 and internal promoter Pα (Plaza et al., 1995b; Walther and Gruss, 1991; Xu and Saunders, 1997) (Figure 5A). Primary transcripts from P0 and P1 encodes Pax6 (46 kDa) and its alternatively spliced isoform Pax6 5a (48 kDa), whereas from Pα encodes a truncated Pax6 (33kDa) (Carriere et al., 1993; Xu et al., 1999b). Even though different transcripts are generated as a result of alternate splicing and differential

selection of promoters as described above, the most abundant and widely studied is the canonical Pax6 (46kDa) (Czerny et al., 1999; Quiring et al., 1994).

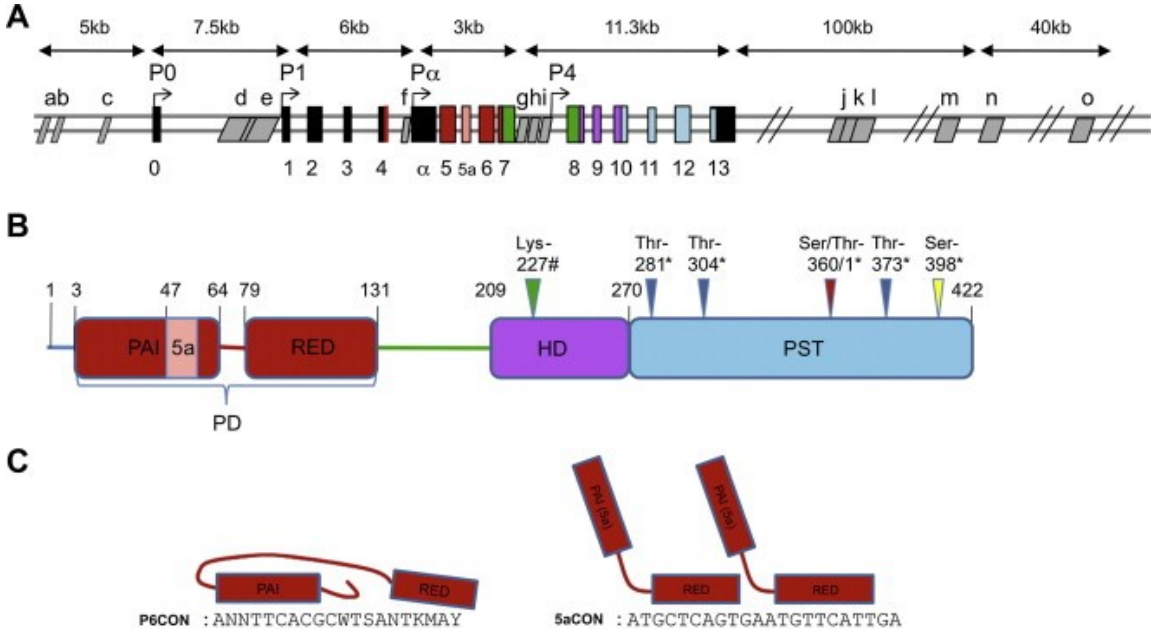

Figure 5: Schematic representation of locus of Pax6 gene, protein domains and the DNA binding motifs. **(A)** Genomic organization of mouse Pax6 gene. Colored boxes with numbers represent coding exons, their colour represents the locus of respective protein domains and black boxes indicate non-coding exons. Promoters are represented as P0, P1 and Pα and arrows denote the transcription start site. Grey rhomboids labelled with lowercase alphabets represent the cis-regulatory elements. **(B)** Schematic representation of two main Pax6 isoforms, Pax6 and Pax6 (5a) with their functional domains. PD: Paired domain, PAI; N-terminal domain of PD, RED: C-terminal domain of PD, HD: homeodomain, PST: Proline-Serine-Threonine domain. Asterisk (*) and hash (#) represent the phosphorylation and sumoylation sites respectively. **(C)** Optimal SELEX-driven binding sites for functional domains of Pax6 (P6CON) and Pax6 (5a) (5aCON). Adapted from **(Shaham et al., 2012).**

Canonical Pax6 has two Deoxyribonucleic acid (DNA) binding domains, a 128 amino acid (aa) bipartite paired domain (PD) and 61 aa paired homeodomain (HD) (Walther and Gruss, 1991; Wilson et al., 1993). These two DNA binding domains are separated by a glycine-rich 78 aa linker (Figure 5B). The mammalian paired domain which is encoded by 4-7 exons has two independent subdomains, termed PAI (N-terminal) and RED (C-terminal) (Epstein et al., 1994b; Jun and Desplan, 1996; Xu et al., 1999a). Previously the optimal binding site of Pax6 PD has been derived using SELEX (systematic evolution of ligands by exponential enrichment), known as P6CON ((Figure 5C). This 20 base pair (bp) long consensus sequence is a bipartite region, in which 5' half is recognized by the PAI subdomain and 3' half is recognized by the RED subdomain (Czerny et al., 1993; Epstein et al., 1994a). Lately, the sequences identified by unbiased genome-wide Pax6 ChIP-seq studies in the lens and forebrain showed consensus sequences comparable to P6CON (Sun et al., 2015). The specificity of PD depends mainly on three aa, asparagine 64, glutamine 61, and isoleucine 59, which are located within the PAI subdomain (Czerny and Busslinger, 1995).

Remarkably the DNA binding site of Pax6 5a (called 5aCON) is different from the canonical Pax6, as 42bp insertion within the PAI domain disrupts the DNA binding capacity

of the same and leaving RED and HD for recognition (Epstein et al., 1994b; Xie and Cvekl, 2011) (Figure 5C).

The mammalian paired type homeodomain is encoded by exons 8-10 (Wilson et al., 1993). Paired type homeodomains bind co-operatively as hetero or homo dimers to palindromic sequence with two inverted ATTA separated by 2 or 3 bp (Czerny and Busslinger, 1995; Shaham et al., 2012; Wilson et al., 1993; Wilson et al., 1995).

The C-terminal part of the Pax6 protein is rich in proline, serine and threonine (PST) residues and important for transactivation (Czerny and Busslinger, 1995; Duncan et al.,2000; Mikkola et al., 1999; Singh et al., 1998; Tang et al., 1998). These residues are prone to phosphorylation by ERK and p38 kinases (Mikkola et al., 1999). Paired and homeodomain have also been shown to participate in protein-protein interactions apart from the PST domain (Cvekl et al., 1999; Mikkola et al., 2001).

Studies investigating the effects of somatic mutations or conditionally deleted alleles on Pax6 have revealed its functions as a transcriptional repressor in addition to its well-known role as a transcriptional activator, (Huang et al., 2011; Numayama-Tsuruta et al.,2010; Sansom et al., 2009; Shaham et al., 2013; Walcher et al., 2013; Wolf et al., 2013; Wolf et al., 2009). The mechanisms by which Pax6 represses transcription are varied and may involve the recruitment of co-repressors, competition for promoter occupancy, and regulation of negative regulators of gene expression or sequence-specific repression (Cvekl and Callaerts, 2017; Duncan et al., 1998). Additionally, Pax6 also regulate microRNAs (miR), including miR-204, miR-135b, and miR-124 (Bhinge et al., 2014; Fang et al., 2014; Shaham et al., 2013).

The highly complex and dynamic spatiotemporal expression pattern of Pax6 is controlled by the coordinated and redundant action of cis-regulatory elements (Antosova et al., 2016). These cis-elements are located upstream, downstream and within introns of the Pax6 gene. Some of these regulatory elements are active in the eye (Figure 5A, c, e, f, g, j, k, l, m, n), pancreas (Figure 5A, a, c), brain (Figure 5Ad, h, I, m, n, o) or in the olfactory region (Figure 5Aj, k, l) (Kammandel et al., 1999; Kleinjan et al., 2004; Kleinjan et al., 2001; Plaza et al., 1995a; Schweitzer, 1981; Williams et al., 1998; Xu et al., 1999b). Identifying Pax6 regulatory modules has the additional advantage of facilitating the generation of tissue-specific Cre lines. For example, the *Le-Cre* transgenic line (including regions a, b, and c of Figure 5A) (Ashery-Padan et al., 2000) and *α-Cre* line (including regions f in Figure 5A) (Marquardt et al., 2001) were developed and are commonly used in the study of gene function in the lens and retina, respectively, using Cre-*loxP* technology (Shaham et al., 2012).

3.3.1.2. Pax6 in corneal development

Pax6 is a gene of great significance, as it is highly conserved and plays a critical role in the development of eyes in both invertebrates and vertebrates. The discovery of spontaneously occurring loss of function mutations in Pax6 in two model organisms, *Drosophila* and mice, has provided valuable insights into the role of this gene in eye development. In *Drosophila,* the mutation resulted in a complete absence of eyes, known as the eyeless phenotype (Sturtevant, 1951), while in mice, it led to the 'Small Eye' phenotype, (Roberts 1967), which is characterized by a failure of lens development and stunted eye growth. In humans, over the last few decades, there have been numerous reports of Pax6

mutations, which result in a semi-dominant condition termed aniridia (Cadenas, 1955). This condition is characterised by several ocular abnormalities including hypoplasia of the iris and ciliary body, dislocation of the lens, cataracts, corneal opacity, foveal dysplasia, and glaucoma (Brown et al., 1998; Kokotas and Petersen, 2010; Lee et al., 2008; Lima Cunha et al., 2019).

The ectopic expression of human Pax6 in non-mammalian models such as *Drosophila* and *Xenopus* results in the formation of ectopic eye structures, indicating that Pax6 is a key regulator of a highly conserved genetic pathway that initiates eye development (Chow et al., 1999; Halder et al., 1995). This remarkable ability of Pax6 to induce ectopic eye formation has led to its classification as a "master control gene" of eye development, positioned at the top of a gene cascade that triggers eye formation (Gehring and Ikeo, 1999). However, in mammals, the process of eye formation is more complex, requiring the interaction of several transcription factors and reciprocal interactions among multiple tissues.

Pax6 is among the earliest expressed eye field transcription factor (ETTF) in the eye field of mice, with expression occurring in both the SE and OV. Later in development, Pax6 is expressed in developing NR, RPE and all SE-derived parts lens, CE, limbus and conjunctiva.

As the retina differentiates, Pax6 expression becomes limited to specific cells, such as retinal ganglion cells, amacrine cells, horizontal cells, and Müller glial cells. Whereas Pax6 expression remained strong in adult CE, limbus and conjunctival epithelium (Koroma et al., 1997; Walther and Gruss, 1991). Heterozygosity in Pax6 mutations results in various congenital eye abnormalities including aniridia, Peter's anomaly in humans and *Small eye* (*Sey*) in mice and rats (Glaser et al., 1992; Hanson et al., 1993; Hill et al., 1991; Jordan et al., 1992; Matsuo et al., 1993). Homozygous *Sey* mutant lacks eyes and nasal cavity and dies at birth (Hogan et al., 1986). Heterozygous *Sey* mutant ($Pax6^{+/-}$) exhibits abnormalities in the retina, lens, iris, ciliary body and cornea (Collinson et al., 2001; Davis et al., 2003; Hill et al., 1991; Ramaesh et al., 2003; Ramaesh et al., 2005; van Raamsdonk and Tilghman, 2000). Prenatally, corneas of $Pax6^{+/-}$ exhibit thin epithelium and thickened hypocellular stroma. Postnatally, the cornea collapses further with inflammatory cell infiltration, neovascularisation, erosions, and globet cells accumulation in the epithelium reducing wound healing capability, and leading to corneal opacity (Davis et al., 2003; Kucerova et al., 2006; Ramaesh et al., 2003; Ramaesh et al., 2005). Further studies on factors contributing to cornea's pathogenesis in $Pax6^{+/-}$ mutants revealed enhanced cell turnover, decreased levels of β-catenin, γ-catenin, and desmoglein, delayed expression of cytokeratin (Krt)12, abnormal migration of neural crest cells and defective centripetal migration of LSCs (Davis et al., 2003; Douvaras et al., 2013; Kanakubo et al., 2006; Ramaesh et al., 2003; Ramaesh et al., 2005).

Pax6 activity in the cornea is dosage dependent, as evidenced by the impaired morphogenesis observed in response to its either over or under-expression. Overexpression of Pax6 in mice resulted in disturbed epithelial proliferation and homeostasis, which further leads to inflammation and neovascularisation (Davis and Piatigorsky, 2011; Ouyang et al., 2006). On the other hand, an interaction between normal pax6 dosage and hedgehog

signalling is important for the modulation of cell proliferation and migration in CE cells (Kucerova et al., 2012). Furthermore, normal Pax6 dosage is not only important for CE but also for corneal stroma and CEn, underscoring the significance of appropriate Pax6 levels in the development of all layers of mouse cornea (Mort et al., 2011).

Pax6 regulates ocular surface development directly as well as indirectly through the control of other transcription factors including c-Maf, MafA/L-Maf, Sox2, Prox1, Foxe3 and Six3 (Cvekl and Tamm, 2004; Swamynathan, 2013).In addition to its role in development, Pax6 plays a critical role in adult CE wound healing, as evidenced by its interaction with the hedgehog and gelatinase B (Mmp-9). Pax6 controls gel B promoter activity by directly interacting with one of the two binding sites and indirectly interacting with the other through cooperative interactions with Ap2-α (Sivak et al., 2004). These findings highlight the significant role of Pax6 in various stages of corneal development and maintenance.

3.3.2 Wnt/β-catenin signalling in corneal development

The Wnt signalling pathway plays a crucial role in controlling various cellular processes such as cell fate, proliferation, apoptosis and differentiation during development, maintenance of stem cells and tissue homeostasis in adults (Logan and Nusse, 2004; Nusslein-Volhard and Wieschaus, 1980; Zhang et al., 2010). These proteins are highly conserved among various species, including humans and *Drosophila*. Wnt proteins are secreted glycoproteins with a cleavable N-terminal signal peptide that directs secretion. Wnt proteins activate intracellular signalling pathways by binding to a dual receptor complex consisting of Frizzled and either LRP6 or LRP5. This leads to the stabilisation and nuclear translocation of β-catenin, which subsequently interacts with TCF/LEF to regulate the transcription of downstream target genes (Figure 6) (Wang et al., 2019). During eye development, multiple components of the Wnt / β-catenin pathway are expressed in various ocular tissue, and studies on conditional knockout models (cKO) revealed its importance in regulating the correct patterning of ocular tissue (Reviewed in (Fujimura, 2016). However, here I will be discussing the role of Wnt/β-catenin signalling in corneal development.

The strict regulation of Wnt/β-catenin signalling in terms of its spatiotemporal control is crucial for determining the cell fate and differentiation of progenitor cells into non-keratinized stratified CE cells. Studies have demonstrated that persistent expression of β-catenin in differentiated CE cells can lead to ocular neoplasia and neovascularization. In such cases, an increase in the expression of proliferative markers such as Pcna and p63 was observed, while the expression of Pax6 and Krt12 decreased. Moreover, epithelial E-cadherin and laminins were also decreased, while Mmp-7 levels were elevated. There was also an ectopic extension of limbal-type K15 to CE. Nuclear translocation of β-catenin leads to the up/downregulation of genes, which disrupts the differentiation of CE cells, increases proliferation, and elevates proangiogenic factors, eventually leading to corneal neoplasia (Walker et al., 2020; Zhang et al., 2010).

Dickkopf-2 (Dkk2) is an antagonist of Wnt-β-catenin signalling. Its expression is initially limited to the stromal mesenchyme at E11.5, but by E14.5, it expands to both epithelium and mesenchyme and continues to be expressed in postnatal tissues (Mukhopadhyay et al., 2006). When Dkk2 or its upstream transcription factor Pitx2 is ablated, aberrant Wnt/β-catenin signalling commences in CE, which suppresses Pax6 and causes ectopic expression of a conjunctival phenotype in CE cells. These findings suggest

that the abnormal expression of Wnt/β-catenin signalling could result in the conjunctivalisation of CE cells (Gage et al., 2014; Gage et al., 2008; Walker et al., 2020).

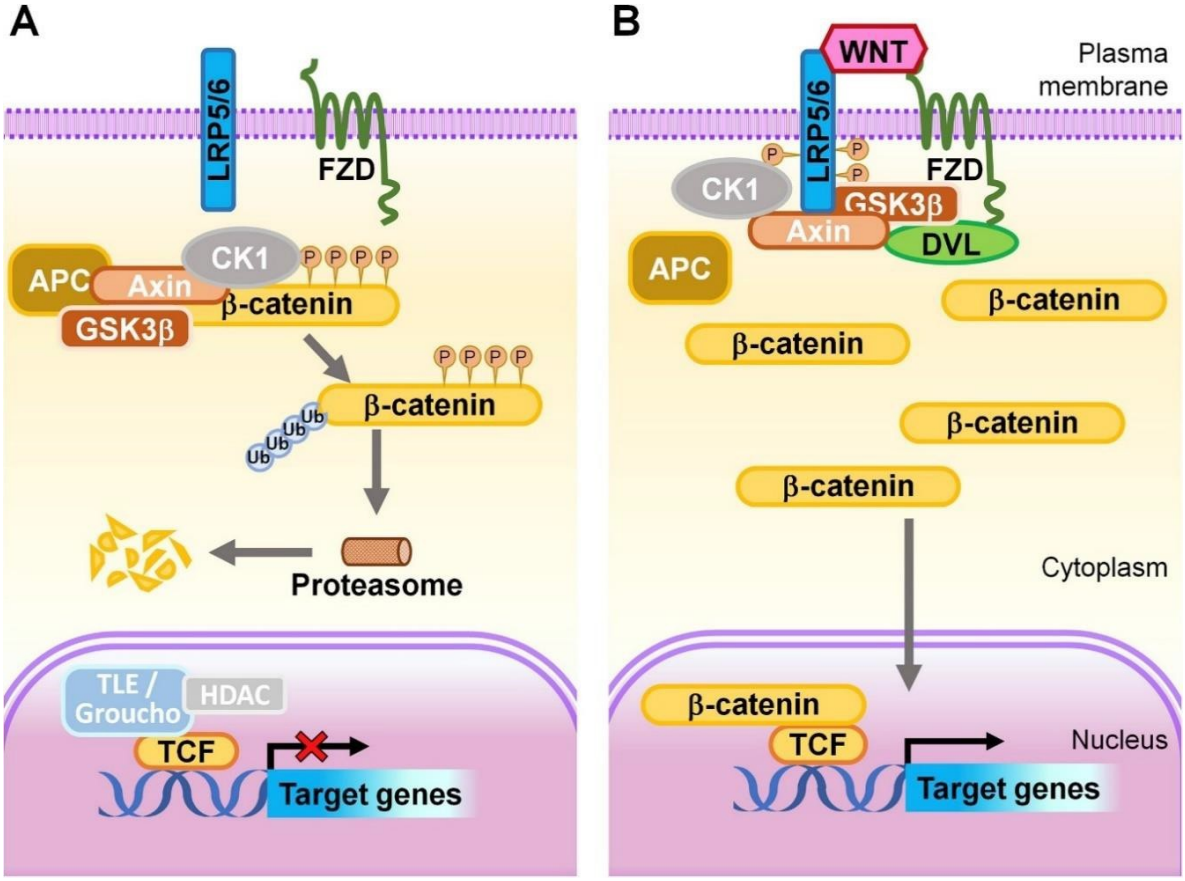

Figure 6: Overview of Wnt/ β-catenin signalling mechanism. (A) In the absence of Wnt ligand, β-catenin forms a degradation complex with Axin, APC, CK1, and GSK3β. Within the degradation complex, GSK3β and CK1α mediate the phosphorylation of β-catenin, which leads to its ubiquitination and subsequent proteasomal –mediated degradation. **(B)** In the presence of Wnt ligands, Wnt glycoproteins bind with Frizzled receptors and LRP5/6 co-receptors, recruiting cytoplasmic Disheveled (DVL). The co-receptor LRP5/6 is then sequentially phosphorylates by GSK3β and CK1 α and Axin is recruited to the plasma membrane. As a result, β-catenin is no longer phosphorylated or ubiquitinated due to the disassembly of the degradation complex. Stabilized β-catenin then translocates to the nucleus, where it displaces the co-repressor Groucho and interacts TCF/LEF transcription factors to regulate target gene transcription. Adapted from (Wang et al., 2019).

In mice, stratification of CE cells is a postnatal event and (Zhang et al., 2015) have shown that coordinated epithelial-mesenchymal communication by cross-talk between Bmp4 and Wnt/ β-catenin signalling is important for the stratification and differentiation of CE cells. Aberrant expression of β-catenin in stromal keratocytes results in reduced stratification of CE cells, whereas its ablation results in precocious stratification. Further analysis on these gain or loss of function mutants showed that active Wnt/β-catenin signalling in stroma is necessary to prevent Bmp4-mediated precocious CE stratification, before eyelid opening. Although, expression of nuclear β-catenin in corneal stroma is gradually declined from PN7-PN21 so that paracrine factor Bmp4 will be upregulated, which further triggers epithelial stratification via Smad1/5 and Mapk3/1 phosphorylation (Walker et al., 2020; Zhang et al., 2019; Zhang et al., 2015).

Taken together, abnormal Wnt signalling in the cornea can result in different effects depending on the stage and region of activation. CE cells may undergo dedifferentiation to a more progenitor-like state or change fate to become conjunctival cells or undergo impaired stratification.

3.3.3 Other transcription factors regulating corneal epithelial development

3.3.3.1 Kruppel-like transcription factors

The Kruppel-like transcription factor 4 (Klf4) is one of the highly expressed transcription factors in mouse cornea (Norman et al., 2004). Klf4 is expressed in the ocular surface from E10 and its expression is maintained in the adult cornea. Conditional depletion of Klf4 in ocular surface ectoderm (OSE) (cornea-limbus-conjunctiva) from E10 resulted in multiple ocular defects including thinner CE, vacuolated, swollen basal epithelial and endothelial cells, edematous stroma and lack of conjunctival globet cells (Swamynathan et al., 2007). Microarray analysis on these Klf4 cKO mutants showed that Klf4 maintains corneal epithelial homeostasis by regulating a subset of genes with specific functions in the progression of the cell cycle, maintenance of corneal hydration, cell-cell adhesion, crystallins, and epithelial barrier function. Of these genes, it has been discovered that Klf4 directly regulates the expression of intermediate filament: Krt12, aquaporins: Aqp3, Aqp5, and corneal crystallins: Aldh3a1 and Tkt (Swamynathan et al., 2008). Moreover, it has been shown that Klf4 promotes epithelial barrier function through the regulation of various desmosomal components such as desmoplakin, desmoglein and basement membrane components such as laminin-α3, laminin-β3, and laminin-β1–1(Swamynathan et al., 2011).

More restricted spatiotemporal ablation of Klf4 in adult CE, resulted in increased expression of mesenchymal markers (vimentin, cyclin D1, survivin, and β-catenin), increased EMT transcription factors (Zeb1, Zeb2, Twist1, Twist2, Slug, Snail) downregulation of epithelial markers (claudins, E-cadherin, and Krt12) and faster wound healing in a manner suggestive of epithelial to mesenchymal transition (EMT) (Delp et al.,2015). Additionally, Klf4 suppresses EMT and promotes CE differentiation by the inhibition of Smad2/3 mediated TGF-β signalling and directly upregulating cyclin- dependent kinase inhibitors p27 and p16 (Tiwari et al., 2019). Together, Klf4 is essential for corneal maturation as well as for the maintenance of adult CE cell identity and homeostasis.

Another KLF family member which is highly abundant in the cornea is Kruppel-like factor 5 (Klf5) (Norman et al., 2004). Even though, Klf5 is structurally related to Klf4; they play a nonredundant function in the anterior eye development. Conditional depletion of Klf5 as early as E12 resulted in multiple ocular defects such as abnormal eyelids, malformed Meibomian glands, and lack of conjunctival globet cells (Kenchegowda et al., 2011). More restricted depletion of Klf5 in adult CE resulted in decreased expression of desmosomal (Dsg1) and tight junction components (Tjp1, Gkn1) contributing to the loss of barrier function; decreased cyclin D1 and upregulated levels of p27 contributing to reduced proliferation; and absence of significant change in the expression of CE markers such as Krt12, E-cadherin and β-catenin. Altogether, this suggests that Klf5 is important for CE cell proliferation and barrier function (Loughner et al., 2017).

3.3.3.2 Adapter-related protein complex 2 (Ap-2)

The Ap-2 family of transcription factors are retinoic acid-responsive genes, which are

important for epithelial differentiation (Swamynathan et al, 2013). To date, five homologous members are known as Ap2-α, Ap2-β, Ap2γ, Ap2-δ and Ap2-ε. Ap2-α commences its expression from the OC stage in presumptive CE whereas, in the adult cornea, its expression is restricted to the basal epithelium (West-Mays et al., 2003). Ap2-α null embryos exhibited a range of ocular phenotypes from a complete lack of eyes to persistent attachment of lens stalk to the cornea (West-Mays et al., 1999). Targeted depletion of Ap2- α in SE derivatives, including CE, resulted in thinner CE despite of no change in proliferation or apoptosis, suppressed expression of cell-cell adhesion molecule E-cadherin, altered expression of basement membrane proteins like laminin, entactin and type IV collagen, indicating that Ap2-α is important for proper corneal morphogenesis (Dwivedi et al., 2005).

3.4 Other genes with important functions in the cornea

3.4.1 Corneal crystallins

Corneas abundantly accumulate a few water-soluble proteins/enzymes called corneal crystallins in a taxon-specific manner. They function as metabolic enzymes or chaperons that protect the cells from UV light-induced damage. In addition to this, it has been proposed that they also contribute to structural function by providing a short-range order within the cytoplasm of corneal keratocytes and thus directly reducing light scattering (reviewed in Jester et al, 2008)

Aldh3a1 (Aldehyde dehydrogenase 3 a1), contributes to 50% of the water-soluble protein present in the mammalian cornea (Abedinia et al., 1990). Aldh3a1 is known to protect against oxidative damage through multiple mechanisms (Estey et al., 2007). Like other members of the ALDH family, ALDH3A1 aids in the elimination of toxic aldehydes that arise due to lipid peroxidation and generates the antioxidant co-factor NADPH. Additionally, ALDH3A1 has also been found to directly absorb UV light, act as a chaperone, and scavenge reactive oxygen species (reviewed in (Estey et al., 2007). In mice, endogenous expression of Aldh3 begins from PN9 and increases by approximately 100-fold between birth and 6 weeks of age. A 4.4 kb promoter fragment from the mouse *Aldh3a1* gene regulates its expression in the CE cells and its promoter activity is co-operatively regulated by Pax6, p300 and Oct1 (Davis et al., 2008; Kays and Piatigorsky, 1997). While the absence of Aldh3a1 does not affect corneal transparency in mice, it does make their eyes more vulnerable to UV-induced cataracts and corneal opacities compared to age-matched controls (Lassen et al., 2007). Aldh1a1 is another corneal crystallin which is present in very low levels in the cornea and lens. *Aldh1a1/ Aldh3a1* double knockout mice showed increased proliferation in CE cells although no change in single knockout mice, which suggest the possibility that both Aldh's compensate for each other in the cornea (Koppaka et al., 2016).

Transketolase (Tkt) is the second significant crystallin in mouse cornea, with mRNA levels increasing by six-fold coincident with eye-opening. This increase is attributed to oxidative stress and exposure to light (Sax et al., 2000). Currently, there is limited information on the transcription factors responsible for regulating *Tkt* promoter, apart from Klf4 (Swamynathan et al., 2008).

3.4.2 Cytokeratin

Cytokeratin are the building blocks of intermediate filaments (IF) which play, a crucial

role in providing mechanical strength and establishing desmosomes between cells, as well as hemi desmosomes with basement membrane to maintain the structural integrity of epithelial tissues. One of the distinctive characteristics of keratin IF is the pairing of type I and type II keratins to form heterodimers during normal assembly. For instance, Krt5 (type I)/ Krt12 (type II) are paired and expressed by differentiated CE cells. It is worth noting that unpaired keratins are quickly degraded within the cells (Moll et al., 2008). As a result, missense mutations in keratin can lead to detrimental pathological effects in the stratified epithelial tissues (Chamcheu et al., 2011; Hassan et al., 2013).

During mouse embryonic development, the single layer of SE begins the expression of Krt8/Krt18 at E8.5. Around E13.5, the SE (presumptive CE) stratifies and forms a non-keratinized, two-cell layered epithelium, where suprabasal cells continue to express Krt8/Krt18 and basal cells commence Krt5/Krt14 expression. From E15.5, suprabasal cells express Krt12 and maintain this expression until birth. At birth, there is a dynamic change in Krt12 expression and it is re-expressed from PN4, when CE starts stratification again. Krt5 /K14 expression persists in the basal layer of CE, which slowly differentiates and co- express Krt5/Krt14, and Krt5/Krt12. The mouse limbus consists of 2-3 stratified layers with Krt5/Krt14 expressing basal stem cells and Krt5/Krt12 suprabasal/ superficial cells (Figure 7) (reviewed in (Kao, 2020).

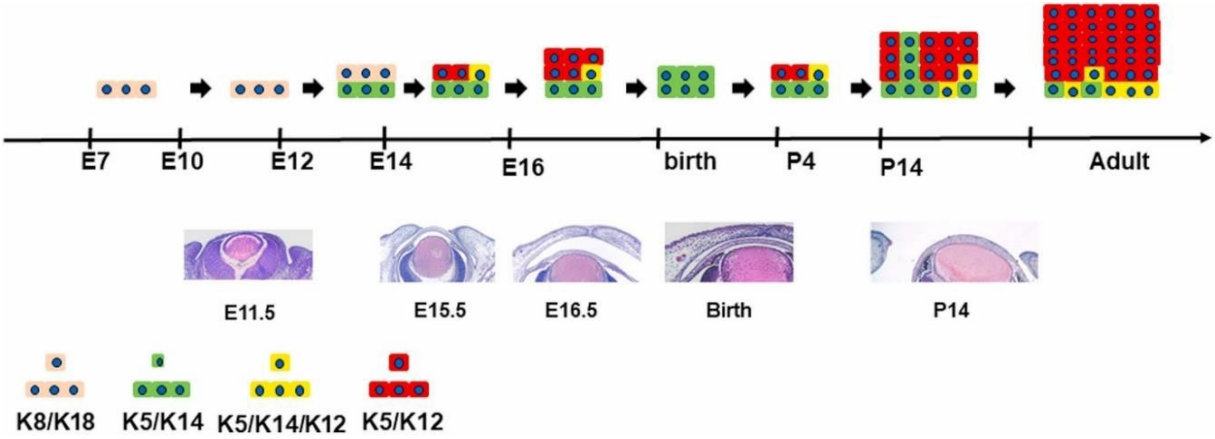

Figure 7: Cytokeratin expression pattern during corneal development. During the early stages of mouse corneal development, progenitors derived from the SE express Krt8/Krt18 IF, which is a marker for non-keratinised simple epithelium. By 13.5, these cells begin to stratify and form two-layered epithelium, where the basal layer commences the expression of Krt5/Krt14 IF. From E15, Krt5/Krt12 expression starts sporadically in the suprabasal cells, while basal cells continue to express Krt5/Krt14 IF. At the time of birth, CE is negative for Krt12 and is regained by PN4. From PN4, CE begins to stratify and re-expresses Krt12, when eyes open at PN14. In young adults, Krt5/Krt14 cells persist at the basal layer, slowly committing to differentiation and co-expressing Krt5/Krt14 and Krt5/Krt12. P4 =PN4, and K=Krt. Adapted from (Kao, 2020)

As discussed above, CE expresses various type I keratins such as Krt12, Krt14, Krt15, Krt18, and Krt19 and type II keratins such as Krt3, Krt5 and Krt8. Of these only Krt3/Krt12 and Krt5/Krt12 IF expression is specifically for CE differentiation. As a result, mutations in Krt3/ Krt12 specifically result in Meesmann's corneal dystrophy, while a mutation in other keratins like Krt14, Krt18 and Krt5 causes pathogenesis in multiple organs derived from SE.

Krt5/ Krt14 IF is expressed in all stratified epithelium including keratinised and non-keratinised tissues. Thus, the dominant negative mutation in Krt14 or Krt5 leads to epidermolysis bullous simplex (EBS), which is characterised by the blistering of the skin (Peters et al., 2001). In the case of the knockout model for Krt14 and Krt5 (Lloyd et al.,1995; Lu et al., 2006), most of the newborn pups die shortly after birth. In Krt14 $^{-/-}$ mice, some pups survive with severe EBS symptoms and the CE of these mice has fewer cell layers with basal layer cytolysis (Lloyd et al., 1995). Whereas no pathological changes were observed on Krt5$^{-/-}$ CE due to the ectopic expression of Krt4 which heterodimerize with Krt12 in the absence of Krt5 (Lu et al., 2006). Unlike other keratin knockout mice, Krt12$^{-/-}$ is viable and fertile and their CE is fragile with intracellular cysts of keratin aggregates (reviewed in (Kao, 2020)).

Particle-mediated gene transfer was utilised to identify CE-specific regulatory elements within a 2.5kb *Krt12* promoter region (Shiraishi et al., 1998). It was discovered that Krt12 promoter activity is regulated by Pax6, Klf4 and Klf6 (Chiambaretta et al., 2002; Liu et al., 1999; Swamynathan et al., 2008; Swamynathan et al., 2007). This was further supported by the downregulation and delayed expression of Krt12 in *Pax6*$^{-/-}$ mutants (Ramaesh et al., 2005). Intriguingly, Pax6 overexpression also affected the expression of Krt12, which indicates the importance of Pax6 dosage in *Krt12* promoter activity (Davis and Piatigorsky, 2011).

3.4.3 Adhesion-related genes

Corneal epithelium provides the first line of barrier against pathogens, dirt and foreign particles. These barrier functions are performed by four types of cell-cell junctions present in the CE; gap junctions, tight junctions, desmosomes, and adherens junctions (Figure 8).

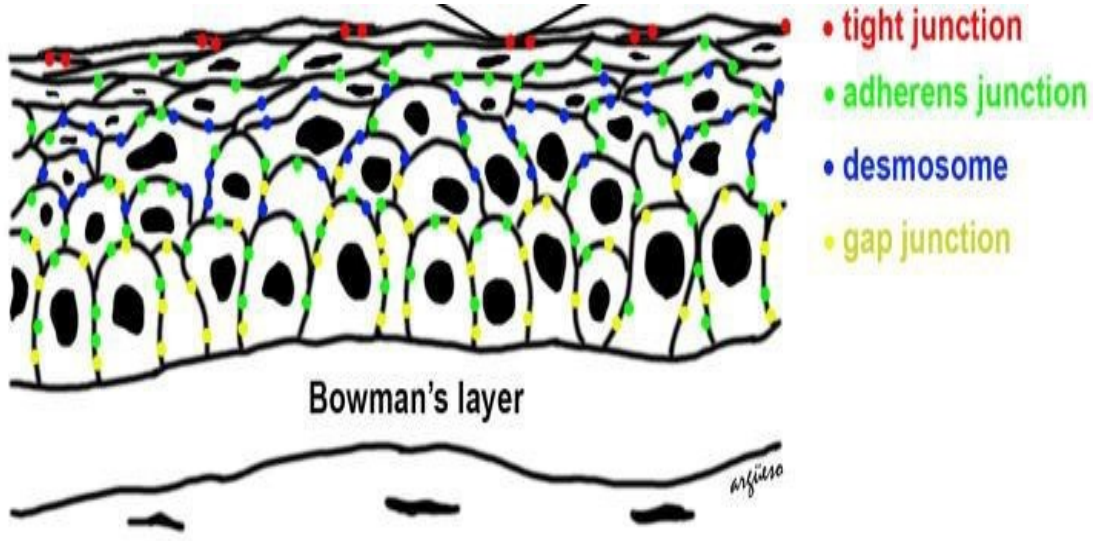

Figure 8: Spatial distribution of cell–cell junctions in corneal epithelial cells. Gap junctions are distributed in all basal cell layers of corneal epithelium. Desmosomes are abundantly present in wing cells and tight junctions are found highly in superficial cells. Adherens junctions are distributed in all stratified layers of corneal epithelium. Adapted from (Mantelli et al., 2013).

Gap junctions are present in all basal layers of CE (Mantelli et al., 2013), which is important for intercellular communication. Gap junctions are formed by transmembrane proteins called connexins in vertebrates (Nielsen et al., 2012). Connexin 43 is a major gap junction protein which contributes to corneal epithelial integrity in the mouse.

Downregulation of connexin 43 is found in pathology associated with keratoconus, whereas it is not clear whether alteration in connexin 43 levels is directly associated with pathogenesis (Gatzioufas et al., 2008).

Desmosomes are abundant in wing cells of CE (Mantelli et al., 2013) and mediate adjacent cell-cell adhesion by the interaction of desmosomal proteins to the IF cytoskeleton. Desmosomes are formed by transmembrane glycoproteins of the desmosomal cadherins family (desmogleins and desmocollins), which recruit plakoglobins, plakophilins, and desmoplakin, which in turn couples with IF cytoskeleton (Kowalczyk and Green, 2013; Mantelli et al., 2013). Adherens junctions are present in all stratified layers of CE (Mantelli et al., 2013). Adherens junctions are formed by transmembrane cadherins such as E- cadherin, which binds to δ-catenin (p120), near the plasma membrane, which in turn recruits β-catenin and α catenin. The β-catenin binds directly to the C-terminal tail of E-cadherin, which in turn binds to α-catenin which attaches to actin cytoskeleton (Hartsock and Nelson, 2008). As discussed in section 3.3, null mutation of various transcription factors like Pax6 (Davis et al., 2003), Klf4 (Tiwari et al., 2017), and Ap2-α (Dwivedi et al., 2005) resulted in fragile thinner CE, which attributes to reduced expression of components of adherens junction or desmosomes and thus suggesting the importance of these cell-cell junctions in maintain epithelial integrity and barrier function.

The tight junctions form a continuous intercellular barrier between the superficial CE cells, which prevents the passive diffusion of molecules through the paracellular pathway. The major components of the tight junction complex include integral transmembrane proteins (Occludins, Claudins, and Junctional adhesion molecule-A), which interact with actin filaments through adapter proteins such as Zona occludens (Zo) (Mantelli et al., 2013; Sugrue and Zieske, 1997). It has been shown that altering the levels of Zo-1 and Zo-2 or changes in its distribution in CE cells results in disruption of CE barrier function, which makes it more prone to infections and irritations (Chen et al., 2012; Xiang et al., 2018; Yi et al., 2000).

3.5 Posterior Polymorphous corneal dystrophy

Corneal dystrophies are a group of rare genetic diseases that are associated with single or more layers of the cornea (Lin et al., 2016). Posterior polymorphous corneal dystrophy (PPCD) is a rare autosomal dominant disorder predominantly affecting CEn, which is first described by Koeppe in 1916. Symptoms of PPCD are highly variable from vesicular, band-like or diffused lesions in the CEn to corneal edema, which necessitates corneal transplantation. In PPCD, CEn cells differentiate aberrantly and these cells express several epithelial-like characteristics such as keratin, desmosomes and numerous microvilli. These abnormal cells are not only restricted to the CEn but in many cases, they migrate to the iridocorneal angle and peripheral iris surface, which results in anterior synechia (Iris adhesion to the cornea), resulting in angle closure and subsequently to secondary glaucoma (Bourgeois et al., 1984) (Grayson, 1974).

The genetic cause of PPCD is heterogeneous, so far mutations in 4 different genes are described in its genesis, designated as PPCD1 to PPCD4. PPCD1 is caused by the heterozygous mutation in the promoter region of the Ovo-like zinc finger 2 *(OVOL2)* gene (Davidson et al., 2016). PPCD2 is due to the non –synonymous mutation in the *COL8A2* gene. PPCD3 is associated with Zinc finger E-box binding homeobox 1 (*ZEB1*) truncating deletions leading to ZEB1 haploinsufficiency (Aldave et al., 2007; Krafchak et al., 2005). PPCD4 is associated with

promoter mutations in the Grainy head-like transcription factor 2 (*GRHL2*) gene (Liskova et al., 2018).

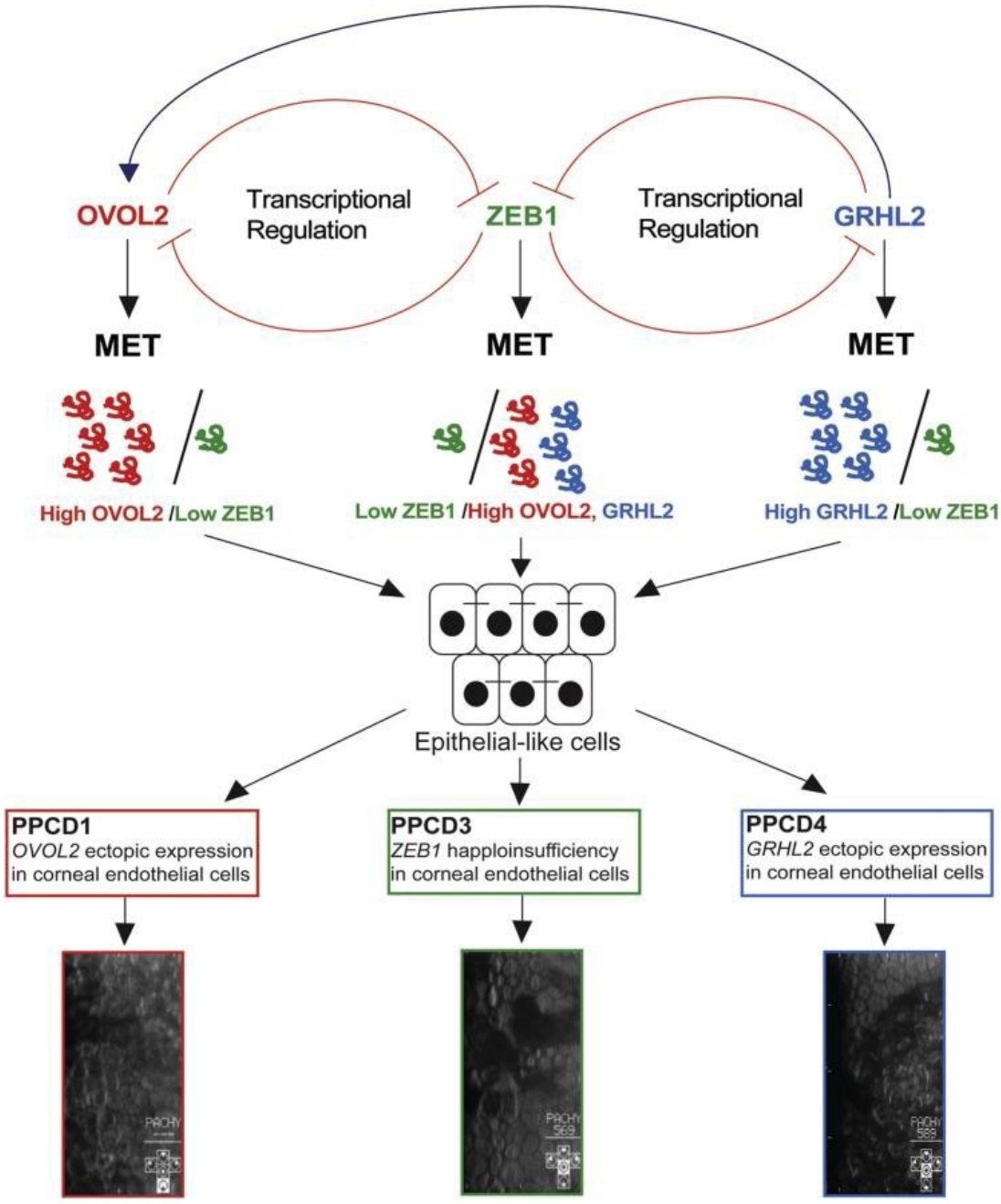

Figure 9: The pathogenic mechanism in PPCD. ZEB1 induces EMT and maintains the homeostasis of corneal endothelial cells. OVOL2 and GRHL2 promote MET by directly repressing ZEB1. ZEB1 also can repress the expression of both OVOL2 and GRHL2. In PPCD3, mutations affecting the *ZEB1* gene results in ZEB1 haploinsufficiency and thus a reduced expression of ZEB1 leading to stratified, epithelial-like corneal endothelial cells. In PPCD1 and PPCD4, mutations result in the ectopic expression of OVOL2 and GRHL2 respectively and thus to pathogenicity. Adapted from (Liskova et al., 2018).

Three of the genes linked with PPCD together control cell fate transitions like epithelial to mesenchymal transition (EMT) and its reverse process mesenchymal to epithelial transition (MET) (Chung et al., 2019; Liskova et al., 2018). For example, ZEB1 regulates EMT. EMT is a process in which polarised epithelial cells are transformed into extracellular matrix-secreting mesenchymal cells. ZEB1 induces EMT by repressing epithelial genes such as CDH1,

OVOL2 and GRHL2 (Cieply et al., 2013; Hong et al., 2015;Vandewalle et al., 2009; Werner et al., 2013). Three of the genes linked with PPCD together control cell fate transitions like

epithelial to mesenchymal transition (EMT) and its reverse process mesenchymal to epithelial transition (MET) (Chung et al., 2019; Liskova et al., 2018). For example, ZEB1 regulates EMT. EMT is a process in which polarised epithelial cells are transformed into extracellular matrix-secreting mesenchymal cells. ZEB1 induces EMT by repressing epithelial genes such as CDH1, OVOL2 and GRHL2 (Cieply et al., 2013; Hong et al., 2015;Vandewalle et al., 2009; Werner et al., 2013). EMT is critical for the delamination of neural crest cells from the dorsal neural tube (Nieto, 2001) and ZEB1 seems to have a role in neural crest cell migration and thus for the development of neural crest-derived CEn (Darling et al.,2003; Liu et al., 2008). PPCD3-associated *ZEB1* mutations result in ZEB1 haploinsufficiency and thus an altered endothelial expression of genes regulated by ZEB1, resulting in abnormal endothelial proliferation, corneal thickening and iridocorneal adhesions (Chung et al., 2017; Liskova et al., 2016).

In contrast to ZEB1, GRHL2 and OVOL2 encode transcription factors that promote MET, by directly repressing ZEB1 (Cieply et al., 2013; Hong et al., 2015; Mooney et al.,2017; Roca et al., 2013; Werner et al., 2013). OVOL2 and GRHL2 are expressed in the CE but are not present in the CEn (Davidson et al., 2016; Liskova et al., 2018). Thus the pathogenic consequences linked to PPCD1 and PPCD4 are due to the ectopic expression of OVOL2 and GRHL2 respectively, which subsequently represses the expression of ZEB1 (Chung et al., 2019). So the pathogenic mechanisms associated with PPCD are due to the deregulation of the OVOL2-ZEB1-GRHL2 axis (Figure 9)

4. AIMS OF THE STUDY

Vision is a complex process, which starts with the transmission and refraction of light through a specialised transparent tissue called cornea. The proper development, maintenance and homeostasis of the cornea are quite important for normal socio-economic human life since any abnormalities in these processes will lead to corneal blindness, which is the fourth leading cause of blindness. This thesis mainly focuses on the role of certain transcription factors in corneal development and its homeostasis. Specific aims are as follows:

1. Unlike other ocular tissues, the cornea continues to develop postnatally and its function is also dependent on its postnatal development and homeostasis. Conventional gene knockout mouse models are valuable sources for deciphering gene function in vivo, however, they present challenges when it comes to studying gene functions beyond embryonic stages due to prenatal fatality or developmental arrests. Generation of cKO models using the Cre-*loxP* system allow us to overcome these challenges. Several Cre drivers are available for the inactivation of the gene of interest in the ocular surface, nevertheless, they start their activity during embryonic stages, which prevents the understanding of the role of the gene of interest during postnatal corneal development and maturation. So we aimed at generating and characterizing a Cre recombinase expressing transgenic mouse line for inactivation of the gene of interest during postnatal corneal development.
2. During the last decades, a lot has been revealed about the function of transcription factor Pax6 in various ocular tissues using cKO models, whereas its spatiotemporal function during embryonic or postnatal corneal development is not well understood. Therefore we investigated the role of Pax6 in CE by taking advantage of Cre drivers specific for postnatal CE or OSE.
3. PPCD1 is caused by mutations in the evolutionarily conserved promoter region of the *OVOL2* gene, resulting in its upregulation in the CEn. However, the disease mechanism leading to PPCD1 phenotypes is not well understood. Hence, we intended for generating and characterising the allelic series of *Ovol2* promoter mutations in mice including human disease-associated variant c. -307T>C using CRISPR-Cas9 gene editing.
4. Chromatin remodeling complexes are important for the regulation of gene expression, DNA replication, and DNA repair. However, its function in the mammalian retina is not well studied. Thence, we focussed on understanding the role of chromatin remodeler Snf2h in retinal development by taking advantage of Cre –*loxP* technology.

5. LIST OF METHODS

Nucleic acid manipulation

RNA isolation

Polymerase chain reaction, Quantitative PCR (qRT-PCR)

PCR- based mouse genotyping

Tissue collection

Dissection and collection of embryonic and postnatal mouse tissues

Histology

Immunohistochemistry

β- galactosidase assay

Hematoxylin and Eosin staining

Alcian blue staining

Fluorescence confocal microscopy

BrdU incorporation assay

6. RESULTS AND DISCUSSIONS

6.1 Generation and characterization of *Aldh3-Cre* transgenic mice as a tool for conditional gene deletion in postnatal cornea.

Eye morphogenesis in mammals is a complex process which involves cascades of sequential and reciprocal inductive events (Cvekl and Piatigorsky, 1996). Classical gene knockout mouse models have been widely used for in vivo studies of gene function. However, the analysis of gene function during postnatal stages can be complicated by issues such as embryonic lethality or developmental arrest (Hill et al., 1991; Hogan et al., 1986). In contrast, the development of conditional knockout mice using the Cre-*loxP* system has addressed these challenges. With conditional gene knockout models, the expression of the gene of interest can be specifically deactivated by controlling the spatiotemporal expression of the Cre driver, offering greater precision and flexibility in studying gene function (Gu et al., 1994; Gu et al., 1993).

Several Cre driver lines are accessible for conditional gene deletion in the OSE. However, these driver lines begin the process of Cre -mediated recombination during embryonic development (Joo et al., 2010; Swamynathan et al., 2007). This poses a challenge for determining whether the defects in the maturation and self-renewal of the cornea are caused by abnormal development or gene function during postnatal stages, especially for genes that are vital for embryonic and postnatal corneal development like Pax6.

In this study, we used regulatory sequences of the mouse *Aldh3a1* gene to generate *Aldh3-Cre* transgenic line to direct the Cre expression in the postnatal cornea. Using a set of floxed alleles, we characterised the Cre expression pattern and the efficiency of Cre- mediated recombination. Our data suggest that *Aldh3-Cre* is a very useful tool for the functional analysis of genes which is crucial for the postnatal development of cornea and conjunctiva.

My contribution to this work: I generated the majority of the experimental data and wrote the manuscript of the published paper *Sunny SS et al, 2020* (presented on pages 29-38 of this thesis).

SCIENTIFIC REPORTS
nature research

OPEN

Generation and characterization of *Aldh3-Cre* transgenic mice as a tool for conditional gene deletion in postnatal cornea

Sweetu Susan Sunny[1], Jitka Lachova[1], Naoko Dupacova[1], Anna Zitova[1,2] & Zbynek Kozmik[1,2]✉

Conditional gene targeting in mice by means of Cre-loxP strategy represents a powerful approach to study mammalian gene function. This approach is however dependent on the availability of suitable strains of mice with a tissue or time restricted activity of the Cre recombinase. Here we describe *Aldh3-Cre* transgenic mice as a useful tool to conditionally delete genes in cornea, a specialized transparent tissue found on the anterior-most part of the eye, which acts as a protective barrier and contributes to the refractive power. Using a set of floxed alleles we demonstrate high Aldh3-Cre activity in corneal epithelial cells, corneal stroma and conjunctival epithelial cells at postnatal stages. Aldh3-Cre will thus be particularly beneficial for functional analysis of genes which are vital for postnatal development of cornea and conjunctiva.

Vision is a complex process which begins with the refraction of light through the cornea, a highly specialised tissue with unprecedented transparency, refractive and protective properties. In mouse, the adult cornea comprises of mainly three layers, anterior non-keratinised stratified squamous epithelium which is 6–8 cell layers thick, collagenous stroma with sparsely dispersed keratocytes, and posterior monolayered endothelium[1,2]. Corneal morphogenesis involves differentiation of surface ectoderm to two-layer thick corneal epithelium and migration of neural crest-derived mesenchymal cells to space between the lens and corneal epithelium, which forms stromal keratocytes and endothelium[3,4]. Corneal epithelium continues to develop after birth; coincident with eye-opening corneal epithelium cells proliferate and differentiate to form 4–5 layered epithelium by postnatal day (PN)21 and form matured 6–8 layered tissue by eight weeks after birth. In the mature cornea, superficial cells of corneal epithelium are regularly sloughed off and constantly replaced by apically moving differentiated basal cells, which in turn are maintained by limbal epithelial stem cells present in limbus which forms a transition between cornea and conjunctiva[5–7]. Any abnormalities in the development and maintenance of cornea result in loss of corneal transparency and thus reduced visual acuity[8].

Classical gene knockout mouse models are excellent tools for studying gene function *in vivo*, but embryonic lethality or developmental arrest complicates the dissection of gene function during postnatal stages[9,10]. In contrast, the generation of conditional gene knockout mice using the Cre-*loxP* system resolved these difficulties. In conditional gene knockout models, spatiotemporal expression of Cre driver controls Cre mediated inactivation of the gene of interest[11,12].

Various Cre driver lines are available for conditional gene deletion in the ocular surface. However, these driver lines start Cre-mediated recombination during embryonic development[13–18]. In the case of genes which are essential for embryonic and postnatal corneal development, it makes it difficult to determine whether the defects in maturation and self-renewal of the cornea is due to abnormal development or gene function at the postnatal stages. Hence the generation of Cre driver line, which is restricted to postnatal corneal development would permit a more precise understanding of gene function.

[1]Laboratory of Eye Biology, Institute of Molecular Genetics of the Czech Academy of Sciences, Division BIOCEV, Prumyslova 595, 252 50, Vestec, Czech Republic. [2]Laboratory of Transcriptional Regulation, Institute of Molecular Genetics of the Czech Academy of Sciences, Videnska 1083, Praha 4, 142 20, Czech Republic. ✉e-mail: kozmik@img.cas.cz

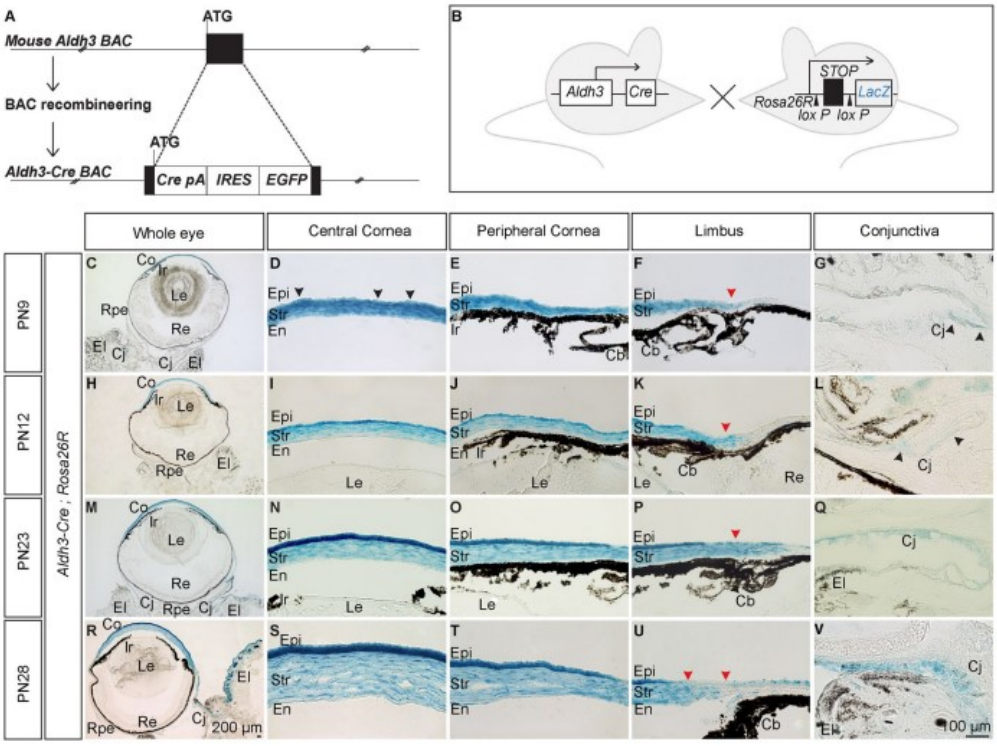

Figure 1. Generation of *Aldh3-Cre* BAC transgenic mice and characterisation of Cre expression pattern. (**A**) Schematic representation of the modification of a BAC clone containing *Aldh3* gene by BAC recombineering. A cassette containing the coding sequence of *Cre* recombinase (Cre-pA) and the coding sequence of *EGFP* linked by *IRES* sequence was inserted into the first translational start site (ATG) of *Aldh3* gene. Black box indicates exons. (**B**) Schematic of mouse lines used to characterise Cre expression pattern. *Aldh3-Cre* driver line was crossed with *Rosa26* reporter strain. This reporter strain has stop cassette flanked by *loxP* sites precedent to *LacZ* gene. In the presence of Cre recombinase, the *LacZ* gene will be expressed upon deletion of *loxP* flanked stop cassette. (**C–V**) Coronal section of the eye at indicated stages was stained with X-gal to show Cre activity in the ocular surface. (**F,K,P,U**) Red arrowheads indicate regions without Cre activity in the limbus region. (**D,G,L**) Black arrowheads indicate few lacZ^{+} ve cells in corneal epithelial cells and conjunctival epithelial cells. Scale bar −100 µm except for (**C,H,M,R**) −200 µm. Abbreviations used in this figure and consecutive images: Co, Cornea; Le, Lens; Re, Retina; Rpe, Retinal pigment epithelium; El, Eyelid; Epi, Corneal epithelium; Str, Corneal stroma; En, Corneal endothelium; Cb, ciliary body; Ir, Iris; Cj, Conjunctival epithelium.

Aldehyde dehydrogenase III (Aldh3), encoded by *Aldh3A1* gene, constitutes nearly one half of total water-soluble protein fraction in the mammalian adult cornea[19]. Aldh3 plays a vital role in protecting the eye from ultraviolet radiation as well in maintaining corneal transparency[20,21]. Endogenous expression of Aldh3 starts at PN9 in very low levels and increases robustly by PN13 in corneal epithelial cells of mouse cornea, coincident with eye-opening[22]. This expression pattern suggests Aldh3 as a promising candidate for driving the Cre expression to cornea specifically at postnatal stages. In the present study we generated BAC transgenic mice expressing Cre recombinase under cis-regulatory control of *Aldh3* gene. We characterised the Cre expression pattern as well as the efficiency of Cre-mediated recombination. Our data suggest that Aldh3-Cre is a very useful tool for postnatal deletion in case of genes which specifically expressed only in the corneal epithelial cells.

Results

Generation of *Aldh3 -Cre* transgenic mice and characterisation of Cre activity using *Rosa26R* reporter strain. To generate *Aldh3-Cre* transgenic mice, we used a large BAC-based construct harbouring regulatory sequences of *Aldh3A1* gene. A cassette carrying Cre recombinase and EGFP coupled via internal ribosomal entry site (IRES) was introduced into the translation start site of the *Aldh3A1* by BAC recombineering, and the modified BAC clone was then used for pronuclear injections (Fig. 1A). Founders were screened for the presence of the BAC and a single transgenic line was established by breeding to *C57Bl/6*. To visualise the Cre recombinase activity, we mated *Aldh3-Cre* transgenic mice with *Rosa26R* reporter strain. In *Aldh3-Cre; Rosa26R*

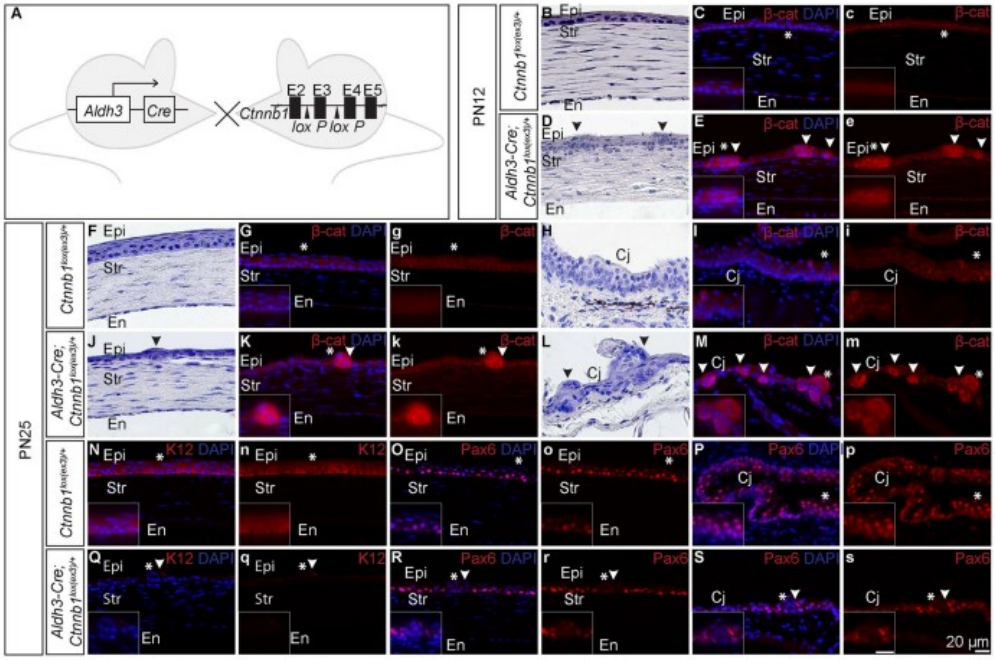

Figure 2. Ectopic expression of β-catenin using Aldh3-Cre results in epithelial hyperplasia. (**A**) Schematic of mouse lines used for ectopic expression of *Ctnnb1* gene. Generation of *Aldh3-Cre; Ctnnb1*$^{lox(ex3)/+}$ double transgenic mice, by crossing *Aldh3-Cre* driver line with *Ctnnb1*$^{lox(ex3)/+}$ transgenic mice, which harbours *loxP* sites flanking exon3 of *Ctnnb1* gene. Cre mediated deletion results in the accumulation of a stabilised Ctnnb1 protein in the cells. (**B–S**) Corneal sections from PN12 and PN25 of wild type and gain of function mutant were subjected to H & E staining and antibodies indicated. Epithelial protrusions (arrowheads) were found on (**B–K**) corneal and (**L,M**) conjunctival epithelial cells of gain of function mutant. (**N,Q**) Loss of K12 expression in the entire corneal epithelium of gain of function mutant. Diminished Pax6 expression in epithelial protrusions found on (**O,R**) corneal and (**P,S**) conjunctival epithelium. Inserts are the higher magnification of corresponding panels and asterisks (*) indicates its position. Scale Bar- 20 µm.

double transgenic mice, Cre induced recombination activated the expression of *LacZ* under *Rosa26* promoter by excision of *loxP*-flanked stop cassette. (Fig. 1B)[23]. As a result, X-gal staining in *Aldh3-Cre; Rosa26R* mice reveals the spatio-temporal activity of Cre *in vivo*.

Beginning by embryonic day (E)15.5, weak X-gal staining was found in few cells in the presumptive corneal stroma (Supplementary Fig. S1). By PN6 X-gal staining spreads over the anterior corneal stroma (Supplementary Fig. S1). Later on, by PN9 the Cre activity starts in few corneal epithelial cells, in addition to intense X-gal staining throughout the corneal stroma (Fig. 1C–F). A more conspicuous X-gal staining becomes apparent in corneal epithelial cells by PN12 (Fig. 1H–J) with a further sharp increase from PN12 to PN28 (Compare Fig. 1H–J with M-O, R-T). Besides this, we observed mosaic X-gal staining in conjunctival epithelial cells in PN9 and PN12 (Fig. 1G,L) and considerably stronger expression in later postnatal stages (Fig. 1Q,V). In accordance with the previous report[24], we found weak or no X-gal staining in limbal epithelial cells in all indicated stages (Fig. 1F,K,P,U). We found no X-gal staining on age-matched *Rosa26R* mice, used as negative controls, upon parallel incubations (Supplementary Fig. S1).

Our experiments demonstrated the spatio-temporal expression pattern of Aldh3-Cre, in which highly mosaic Cre activity was found at embryonic stages, whereas a strong rate of recombination was detected at postnatal stages in the cornea, concurrent with eye-opening.

Ectopic expression of β-catenin using Aldh3-Cre results in the formation of corneal epithelial nodules. In order to evaluate the utility of Aldh3-Cre in conditional gene modification, we crossed *Aldh3-Cre* transgenic mice with a mouse strain that harbours a conditional allele of *β-catenin*, *Ctnnb1*$^{lox(ex3)/+}$ (Fig. 2A). Upon Cre-mediated recombination *loxP* sites flanking exon3 of *Ctnnb1* gene will be excised which results in mutant β-catenin protein resistant to phosphorylation and proteasome-mediated degradation. This stabilised mutant β-catenin protein accumulates in the cell and mimics activation of canonical Wnt signaling (β-catenin gain-of-function situation)[25]. For the sake of simplicity, now onwards we refer *Ctnnb1*$^{lox(ex3)/+}$ as wildtype and *Aldh3-Cre; Ctnnb1*$^{lox(ex3)/+}$ as a gain-of-function mutant in the subsequent text. To investigate the effect of ectopic

β-*catenin* expression in the ocular surface of the gain-of-function mutant we performed morphological analysis of different developmental stages from PN6 to PN25. We observed no conspicuous changes in the ocular surface until PN9 (Supplementary Fig. S2). However, epithelial protrusions began to appear in the corneal epithelium of gain of function mutant from PN12 (Fig. 2D,J) and conjunctival epithelium by PN25 (Fig. 2L), whereas age-matched wildtype exhibited normal corneal (Fig. 2B,F) and conjunctival epithelium (Fig. 1H). This observation is consistent with a previous study showing that the gain-of-function of β-catenin induces hyperplastic transformation in corneal epithelial cells[26].

In addition to the phenotype described above, H & E staining also revealed that unlike wildtype, which possessed 5–6 layers at PN25 (Fig. 2F), the gain-of-function mutant exhibited thinner epithelium with only 2–3 layers (Fig. 2J). This phenotype corroborates previous study showing that the aberrant β-catenin expression in stromal keratocytes prevents corneal stratification[27].

To confirm that phenotypic consequences in the cornea of β-catenin gain-of-function mutant are due to the increased level of β-catenin we performed immunohistochemistry staining using an antibody that recognises C-terminus of the protein. Indeed, we confirmed that compared to wildtype, there was a significant increase of β-catenin staining in corneal epithelial cells and stroma from PN12 (Fig. 2C,E,G,K) and conjunctival epithelial cells by PN25 (Fig. 2I,M).

Next we investigated whether corneal epithelial differentiation is affected upon β-catenin overexpression. Immunohistochemistry staining showed diminished expression of Pax6 in the epithelial nodules formed in the corneal (Fig. 2O,R) and conjunctival epithelium (Fig. 2P,S) of the gain-of-function mutant. Furthermore, in contrast to wildtype corneal epithelium which exhibited a typical keratin 12 (K12) expression (Fig. 2N), the gain-of-function mutant completely lost K12 expression in the entire corneal epithelium (Fig. 2Q). This data indicates that corneal character is lost upon β-catenin activation, as reported previously[26].

Combined, our data suggest that Aldh3-Cre mediated recombination is high in the corneal stroma, corneal epithelial cells and conjunctival epithelial cells postnatally. Furthermore, Aldh3-Cre is capable of efficiently generating stabilised β-catenin protein upon breeding to *Ctnnb1*$^{lox(ex3)}$ to replicate previously described phenotypes.

Postnatal inactivation of β-catenin in cornea using Aldh3-Cre. To further assess the efficacy of Aldh3-Cre in conditional gene deletion, we generated *Aldh3-Cre; Ctnnb1*$^{lox(ex2-6)/lox(ex2-6)}$ mice, in which *loxP* sites flank exons 2–6 of the *β-catenin* gene (Fig. 3A)[28]. Cre mediated deletion removes exons 2–6 of the floxed allele and results in depletion of β-catenin in the cells. For the sake of simplicity, from now onwards we refer to *Aldh3-Cre; Ctnnb1*$^{lox(ex2-6)/lox(ex2-6)}$ as a loss-of-function mutant and *Ctnnb1*$^{lox(ex2-6)/lox(ex2-6)}$ as a wildtype. Immunohistochemistry staining showed depletion of β-catenin in corneal epithelial cells of loss-of-function mutant compared to wildtype by PN14, whereas we found no significant decrease in β-catenin staining in limbal epithelial cells and conjunctival cells at this stage (Fig. 3F–K). However, we observed a notable depletion of β-catenin protein in corneal and conjunctival epithelial cells by PN23 (Fig. 3L–Q). As expected, even at PN23 we found no evidence of β-catenin gene deletion in limbal epithelial cells (Fig. 3M,P). Next we determined the phenotypic consequence of β-catenin gene deletion in *Aldh3-Cre; Ctnnb1*$^{lox(ex2-6)/lox(ex2-6)}$ mice. Histological analysis of postnatal corneas at PN14 and PN23 showed that unlike control littermates the loss-of-function mutants have thicker epithelium (Fig. 3B–E). This result is in agreement with the previous findings that the loss of β-catenin in stromal keratocytes results in precocious stratification[29]. Taken together, these experiments demonstrated that Aldh3-Cre-mediated excision of β-catenin floxed allele resulted in the depletion of β-catenin protein from postnatal corneal and conjunctival epithelial cells. Combined, our data suggest that Aldh3-Cre is a useful tool for gene modification for elucidating biological functions of any gene of interest during postnatal corneal (or conjunctival) development.

Discussion

Based on serial analysis of gene expression data (SAGE) demonstrating that *Aldh3* is one of the most abundant genes in the postnatal cornea[30], we generated an *Aldh3-Cre* transgenic driver mouse line for conditional gene modification in the postnatal cornea. We characterised the expression pattern of Cre recombinase by X-gal staining after breeding *Cre* driver line with *Rosa26R* reporter mice. Endogenous expression of Aldh3 protein starts at PN9[22] and is restricted to corneal epithelial cells of the mouse cornea[24]. In contrast, we observed mosaic Cre activity in the corneal stroma by E15.5 (Supplementary Fig. S1) and strong Cre activity throughout the corneal stroma by PN9 (Fig. 1C–V). We also noted that X-gal staining starts in few corneal epithelial cells at PN9, and becomes stronger coincidentally with eye-opening, as described previously[22]. BAC transgenes carry extensive cis-regulatory sequences of the corresponding gene, and thus usually Cre recombinase activity recapitulates endogenous gene expression. One possible explanation for the difference that we noted between the endogenous Aldh3 expression and Cre activity is that the BAC clone used by us does not possess all of the regulatory information of the *Aldh3A1* gene.

We further assessed the functionality of Aldh3-Cre by generating mouse strains *Aldh3-Cre; Ctnnb1*$^{lox(ex3)/+}$ and *Aldh3-Cre; Ctnnb1*$^{lox(ex2-6)/lox(ex2-6)}$. In both cases, we found that Aldh3-Cre-mediated recombination resulted in excision of the floxed genomic region, and generated a gain- and loss-of-function mutant for β-catenin, respectively, that recapitulated previously described phenotypes (Figs. 2 and 3). A recent study showed a constitutive expression of active β-catenin in postnatal corneal epithelial cells and dynamic expression in the corneal stroma during PN1 to PN21[29]. This expression pattern will make it difficult to determine whether the phenotypic consequences on corneal epithelial cells are precisely due to loss/gain of β-catenin in corneal epithelial cells or due to its loss/gain in the corneal stroma. Despite this limitation, *Aldh3-Cre* strain described here is a highly efficient driver line for postnatal gene ablation in case of genes which are specifically expressed in corneal epithelial cells. Furthermore, Aldh3-Cre is a useful tool for deletion of genes that cause developmental arrest during embryonic development, allowing to determine their function in the postnatal stages. Finally, we propose that the late onset

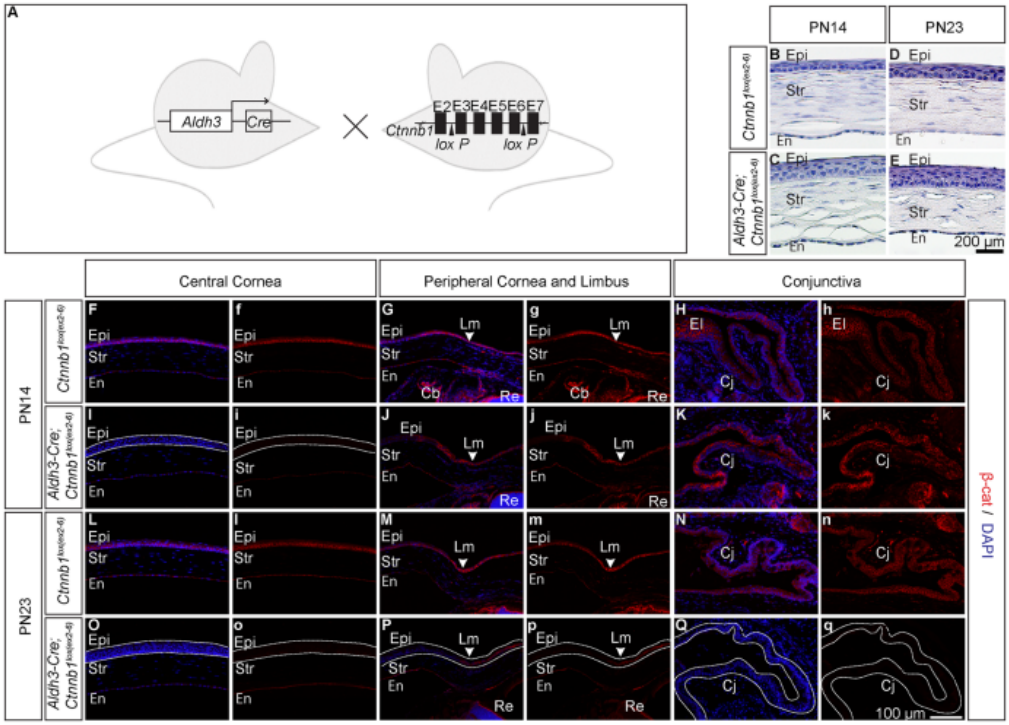

Figure 3. Postnatal deletion of β-catenin using Aldh3-Cre. (**A**) Schematic of mouse lines used for conditional inactivation of β-catenin. (**B–E**) H & E staining on corneal sections of wildtype and loss of function mutant from PN14 and PN23 old mice. Corneal epithelium of loss of function mutant had more layers at PN14 and PN23 in comparison to age-matched control epithelium. (**F–Q**) β-catenin staining on corneal and conjunctival sections from PN14 and PN23 old mice of wild type and loss of function mutant. (**F,I,L,O**) Loss of β-catenin in corneal epithelial cells from PN14 and (**H,K,N,Q**) conjunctival epithelial cells by PN23.(**G,J,M,P**) Depletion of β-catenin in the peripheral cornea at indicated stages, but note that staining retained in limbal epithelial cells. The dashed line indicates a region with β-catenin deletion. White arrowheads indicate the position of the limbus. Abbreviations: Lm, Limbus. Scale bar (**B–E**) −200 µm (**F–Q**) −100 µm.

of Cre expression in conjunctival epithelial cells will be beneficial for the functional analysis of genes which are vital for its postnatal development.

Methods

Ethics statement. Experimental mice were housed and *in vivo* experiments were executed in compliance with the European Communities Council Directive of 24 November 1986 (86/609/EEC) and national and institutional guidelines. Experimental procedures for handling the mice were approved by the Animal Care Committee of the Institute of Molecular Genetics (no. 71/2014). This work did not include human subjects.

Mouse strains. A 164 kb bacterial Artificial Chromosome (BAC) (RP24–338F21) harboring the mouse *Aldh3A1* gene was purchased from Children's Hospital Oakland Research Institute. To generate *Aldh3-Cre* BAC, the open reading frame of Cre recombinase fused to EGFP via IRES was inserted into the exon 1 containing the translation initiation codon of *Aldh3A1* using a method of BAC recombineering[31]; http://web.ncifcrf.gov/research/brb/protocol.aspx). The CreIRESEGFP-FRT-neo-FRT targeting cassette was PCR-amplified from pCS- CreIRESEGFP-FRT-neo-FRT using *Aldh3* forward and reverse targeting primers: 5′-gccatcctccttcctctgatgcaaagtgttctctatccccagttaccatgtccaatttactgaccgtaca-3′; 5′-gcgctgcaacgcctccagctgctcaacccggaactgcagcggtcgagtctgctattccagaagtagtgag-3′. The PCR product was purified using QIAEX Gel extraction Kit (Qiagen) and treated with DpnI to destroy the template plasmid. The PCR product was electroporated into bacterial strain EL250 carrying RP24–338F21 BAC, and colonies were tested for homologous recombination by PCR. The kanamycin resistance cassette was next removed by induction of flipase activity in EL250 cells. Modified *Aldh3-Cre* BAC DNA was isolated and used for pronuclear injection. Mice were genotyped using primers that recognize the recombination junction, with forward primer located upstream of the Aldh3 translation start site (5′-aattagcatagtggtggagtca-3′) and reverse primer located in Cre recombinase coding region (5′-cgttgcatcgaccggtaatgca-3′). For analysis of Cre activity, the animals of the tenth and later generations

from the original founder were used for genetic crossing. Samples exhibited reproducible Cre-mediated recombination regardless of the breeding generation.

Following are the other genetically modified mouse strains used for this study; *Rosa26R*[23] (Jackson Laboratory, stock no. 003309), *Ctnnb*$^{lox(ex3)}$[25], and *Ctnnb*$^{lox(ex2-6)}$[28]. The genotype of each mouse was identified by PCR analysis of tail DNA.

X-gal staining for LacZ activity. We harvested mouse eyes at different developmental stages from PN9. Enucleated eyes were fixed in 0.2% formaldehyde in 1x PBS for 15 min at room temperature on ice, washed 2 × 5 minutes with the rinse buffer (0.1 M phosphate buffer pH 7.3, 2 mM $MgCl_2$, 0.01% sodium deoxycholate and 0.02% Nonidet P-40), followed by incubation in X-gal staining solution (rinse buffer,5 mM potassium ferrocyanide, 5 mM potassium ferricyanide, 20 mM Tris pH 7.3, 1 mg/ml X-gal) for 1 hour at 37 °C and overnight at room temperature. Eyes were postfixed in 4% formaldehyde in 1x PBS overnight at 4 °C, cryoprotected in 30% sucrose and frozen in OCT (Tissue Tek, Sakura). Frozen tissues were sectioned at 18 µm thickness.

Histology and Immunohistochemistry for corneal characterisation. Enucleated eyes were fixed in 4% formaldehyde in 1x PBS for overnight at 4 °C, washed 3 × 10 minutes in 1x PBS and followed by paraffin embedding. For histology analysis, paraffin sections (6 µm) were deparaffinised, rehydrated with ethanol series and stained with Hematoxylin and Eosin (H & E). For immunofluorescence, paraffin sections (6 µm) were deparaffinised, rehydrated with ethanol series, followed by antigen retrieval in sodium citrate buffer (10 mM sodium citrate buffer, 0.05% Tween 20, pH-6.0). The sections were blocked in 10% BSA/0.1% PBT for 30 minutes and incubated with primary antibodies in 1% BSA/0.1% PBT for overnight. On the following day, samples were washed in 1x PBS for 3 × 10 minutes, incubated with secondary antibodies in 1% BSA/0.1% PBT for 1 hour, washed in 1x PBS, counterstained with DAPI (1 µg/ml) and mounted in Mowiol (Sigma). Following are the antibodies used for this study: rabbit anti-β-catenin (1:1000, Sigma, C2206), rabbit anti- Pax6 (1:1000, Covance, PRP-278P), goat anti-K12 (1: 300, Santa Cruz Biotec Inc, Sc-17101), anti-rabbit Alexa 594, and anti-goat Alexa 594 (all 1:500, Molecular Probes). Stained sections were analysed with Zeis Imager Z2 (Zeis, Germany).

Data availability

All the data generated and analysed in our study are included in this article.

Received: 13 March 2020; Accepted: 12 May 2020;
Published online: 03 June 2020

References

1. Zieske, J. D. Corneal development associated with eyelid opening. *Int. J. Dev. Biol.* **48**, 903–911, https://doi.org/10.1387/ijdb.041860jz (2004).
2. Hay, E. D. Development of the vertebrate cornea. *Int. Rev. Cytol.* **63**, 263–322, https://doi.org/10.1016/s0074-7696(08)61760-x (1980).
3. Pei, Y. F. & Rhodin, J. A. Electron microscopic study of the development of the mouse corneal epithelium. *Invest. Ophthalmol.* **10**, 811–825 (1971).
4. Haustein, J. On the ultrastructure of the developing and adult mouse corneal stroma. *Anat. Embryol.* **168**, 291–305, https://doi.org/10.1007/bf00315823 (1983).
5. Collinson, J. M. *et al.* Clonal analysis of patterns of growth, stem cell activity, and cell movement during the development and maintenance of the murine corneal epithelium. *Dev. Dyn.* **224**, 432–440, https://doi.org/10.1002/dvdy.10124 (2002).
6. Nagasaki, T. & Zhao, J. Centripetal movement of corneal epithelial cells in the normal adult mouse. *Invest. Ophthalmol. Vis. Sci.* **44**, 558–566, https://doi.org/10.1167/iovs.02-0705 (2003).
7. Cotsarelis, G., Cheng, S. Z., Dong, G., Sun, T. T. & Lavker, R. M. Existence of slow-cycling limbal epithelial basal cells that can be preferentially stimulated to proliferate: implications on epithelial stem cells. *Cell* **57**, 201–209, https://doi.org/10.1016/0092-8674(89)90958-6 (1989).
8. Klintworth, G. K. The molecular genetics of the corneal dystrophies–current status. *Front. Biosci.* **8**, d687–713, https://doi.org/10.2741/1018 (2003).
9. Hogan, B. L. *et al.* Small eyes (Sey): a homozygous lethal mutation on chromosome 2 which affects the differentiation of both lens and nasal placodes in the mouse. *J. Embryol. Exp. Morphol.* **97**, 95–110 (1986).
10. Hill, R. E. *et al.* Mouse small eye results from mutations in a paired-like homeobox-containing gene. *Nature* **354**, 522–525, https://doi.org/10.1038/354522a0 (1991).
11. Gu, H., Marth, J. D., Orban, P. C., Mossmann, H. & Rajewsky, K. Deletion of a DNA polymerase beta gene segment in T cells using cell type-specific gene targeting. *Science* **265**, 103–106, https://doi.org/10.1126/science.8016642 (1994).
12. Gu, H., Zou, Y. R. & Rajewsky, K. Independent control of immunoglobulin switch recombination at individual switch regions evidenced through Cre-loxP-mediated gene targeting. *Cell* **73**, 1155–1164, https://doi.org/10.1016/0092-8674(93)90644-6 (1993).
13. Swamynathan, S. K. *et al.* Conditional deletion of the mouse Klf4 gene results in corneal epithelial fragility, stromal edema, and loss of conjunctival goblet cells. *Mol. Cell Biol.* **27**, 182–194, https://doi.org/10.1128/MCB.00846-06 (2007).
14. Lu, H., Lu, Q., Zheng, Y. & Li, Q. Notch signaling promotes the corneal epithelium wound healing. *Mol. Vis.* **18**, 403–411 (2012).
15. Kokado, M. *et al.* Lack of plakoglobin impairs integrity and wound healing in corneal epithelium in mice. *Lab. Invest.* **98**, 1375–1383, https://doi.org/10.1038/s41374-018-0082-z (2018).
16. Tanifuji-Terai, N., Terai, K., Hayashi, Y., Chikama, T. & Kao, W. W. Expression of keratin 12 and maturation of corneal epithelium during development and postnatal growth. *Invest. Ophthalmol. Vis. Sci.* **47**, 545–551, https://doi.org/10.1167/iovs.05-1182 (2006).
17. Weng, D. Y. *et al.* Promiscuous recombination of LoxP alleles during gametogenesis in cornea Cre driver mice. *Mol. Vis.* **14**, 562–571 (2008).
18. Joo, J. H., Kim, Y. H., Dunn, N. W. & Sugrue, S. P. Disruption of mouse corneal epithelial differentiation by conditional inactivation of pnn. *Invest. Ophthalmol. Vis. Sci.* **51**, 1927–1934, https://doi.org/10.1167/iovs.09-4591 (2010).
19. Abedinia, M., Pain, T., Algar, E. M. & Holmes, R. S. Bovine corneal aldehyde dehydrogenase: the major soluble corneal protein with a possible dual protective role for the eye. *Exp. Eye Res.* **51**, 419–426, https://doi.org/10.1016/0014-4835(90)90154-m (1990).
20. Pappa, A., Sophos, N. A. & Vasiliou, V. Corneal and stomach expression of aldehyde dehydrogenases: from fish to mammals. *Chem. Biol. Interact.* **130-132**, 181–191, https://doi.org/10.1016/s0009-2797(00)00233-7 (2001).

21. Chen, Y., Thompson, D. C., Koppaka, V., Jester, J. V. & Vasiliou, V. Ocular aldehyde dehydrogenases: protection against ultraviolet damage and maintenance of transparency for vision. *Prog. Retin. Eye Res.* **33**, 28–39, https://doi.org/10.1016/j.preteyeres.2012.10.001 (2013).
22. Davis, J., Davis, D., Norman, B. & Piatigorsky, J. Gene expression of the mouse corneal crystallin Aldh3a1: activation by Pax6, Oct1, and p300. *Invest. Ophthalmol. Vis. Sci.* **49**, 1814–1826, https://doi.org/10.1167/iovs.07-1057 (2008).
23. Soriano, P. Generalized lacZ expression with the ROSA26 Cre reporter strain. *Nat. Genet.* **21**, 70–71, https://doi.org/10.1038/5007 (1999).
24. Kays, W. T. & Piatigorsky, J. Aldehyde dehydrogenase class 3 expression: identification of a cornea-preferred gene promoter in transgenic mice. *Proc. Natl Acad. Sci. USA* **94**, 13594–13599, https://doi.org/10.1073/pnas.94.25.13594 (1997).
25. Harada, N. *et al.* Intestinal polyposis in mice with a dominant stable mutation of the beta-catenin gene. *EMBO J.* **18**, 5931–5942, https://doi.org/10.1093/emboj/18.21.5931 (1999).
26. Zhang, Y. *et al.* Aberrant expression of a beta-catenin gain-of-function mutant induces hyperplastic transformation in the mouse cornea. *J. Cell Sci.* **123**, 1285–1294, https://doi.org/10.1242/jcs.063321 (2010).
27. Zhang, L. *et al.* Aberrant expression of a stabilized beta-catenin mutant in keratocytes inhibits mouse corneal epithelial stratification. *Sci. Rep.* **9**, 1919, https://doi.org/10.1038/s41598-018-36392-2 (2019).
28. Brault, V. *et al.* Inactivation of the beta-catenin gene by Wnt1-Cre-mediated deletion results in dramatic brain malformation and failure of craniofacial development. *Development* **128**, 1253–1264 (2001).
29. Zhang, Y. *et al.* Wnt/beta-catenin signaling modulates corneal epithelium stratification via inhibition of Bmp4 during mouse development. *Development* **142**, 3383–3393, https://doi.org/10.1242/dev.125393 (2015).
30. Norman, B., Davis, J. & Piatigorsky, J. Postnatal gene expression in the normal mouse cornea by SAGE. *Invest. Ophthalmol. Vis. Sci.* **45**, 429–440, https://doi.org/10.1167/iovs.03-0449 (2004).
31. Lee, E. C. *et al.* A highly efficient Escherichia coli-based chromosome engineering system adapted for recombinogenic targeting and subcloning of BAC DNA. *Genomics* **73**, 56–65, https://doi.org/10.1006/geno.2000.6451 (2001).

Acknowledgements

This work was supported by GACR 18-20759S (awarded to ZK). Research on animal models in ZK laboratory is supported by RVO68378050-KAV-NPUI and LQ1604 (MEYS). Mouse costs were partially covered by the CCP infrastructure supported by LM2018126, OP VaVpI CZ.1.05/2.1.00/19.0395, CZ.1.05/1.1.00/02.0109 (MEYS). We wish to thank Dr. R. Kemler and M. Taketo for providing mice.

Author contributions

Designed experiments: S.S.S. and Z.K. Performed experiments: S.S.S., J.L., A.Z., Z.K. Data analysis and interpretation: S.S.S., J.L., N.D., Z.K. Wrote the manuscript: S.S.S. and Z.K. Revising the manuscript's content and approving the final version of the manuscript: all authors.

Competing interests

The authors declare no competing interests.

Additional information

Supplementary information is available for this paper at https://doi.org/10.1038/s41598-020-65878-1.

Correspondence and requests for materials should be addressed to Z.K.

Reprints and permissions information is available at www.nature.com/reprints.

Publisher's note Springer Nature remains neutral with regard to jurisdictional claims in published maps and institutional affiliations.

Supplementary Information

Generation and characterization of *Aldh3-Cre* transgenic mice as a tool for conditional gene deletion in postnatal cornea.

Sweetu Susan Sunny[1], Jitka Lachova[1], Naoko Dupacova[1], Anna Zitova[1,2] and Zbynek Kozmik[1,2*]

[1] Laboratory of Eye Biology, Institute of Molecular Genetics of the Czech Academy of Sciences, Division BIOCEV, Prumyslova 595, 252 50 Vestec, Czech Republic

[2] Laboratory of Transcriptional Regulation, Institute of Molecular Genetics of the Czech Academy of Sciences, Videnska 1083, Praha 4, 142 20, Czech Republic

[*] Corresponding author: Institute of Molecular Genetics of the Czech Academy of Sciences, Videnska 1083, Praha 4, 142 20, Czech Republic

E-mail: kozmik@img.cas.cz

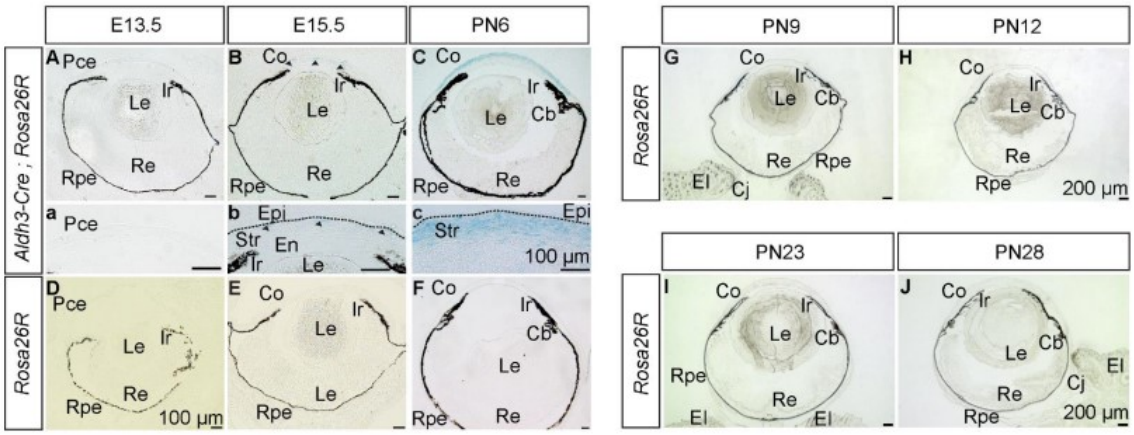

Supplementary Figure S1. Mosaic Cre activity starts at E15.5 and no endogenous lacZ expression upon X-gal incubation. (A-C) X-gal staining on frontal sections from indicated stages revealed (B, b) mosaic Cre activity on corneal stroma (black arrowheads) at E15.5 and (C, c) more spreaded activity by PN6 (D-J) No Cre activity in age-matched *Rosa26R* sections and (A,a) sections from E13.5. Abbreviations: Pce, Presumptive corneal epithelium. Scale bar: (A-F) - 100 µm, (G-J) - 200 µm

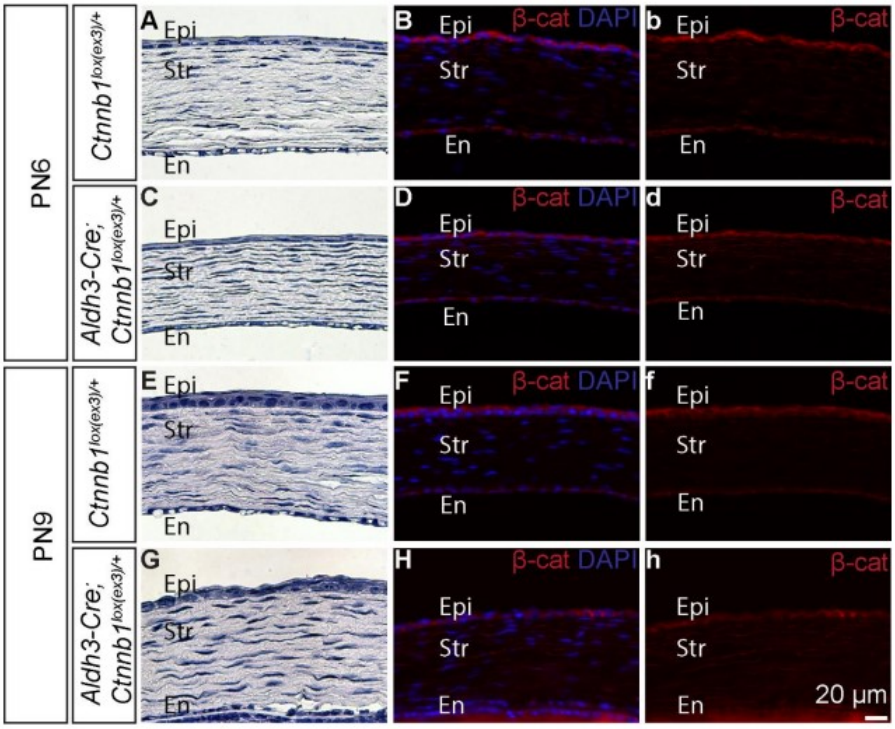

Supplementary Figure S2. **No epithelial protrusions until PN9 upon ectopic β-catenin activation**. (A-H) H & E staining and immunostaining with β-catenin on corneal sections from PN6 and PN9. (A, C, E, G) No significant morphological changes till PN9. (B, D, F, H) No significant increase in β-catenin levels in corneal epithelial cells, but there is an increase in the corneal stroma at PN9. Scale bar- 20μm

6.2 Multiple roles of Pax6 in postnatal cornea development.

It has been reported that Pax6 plays an important role in corneal morphogenesis (Davis et al., 2003; Douvaras et al., 2013; Ramaesh et al., 2003; Ramaesh et al., 2005). However, the consecutive induction of lens and cornea from SE, the impact of the lens in the morphogenesis of the anterior segment (Collinson et al., 2001; Genis-Galvez, 1966; Genis-Galvez et al., 1967; van Raamsdonk and Tilghman, 2000) and continued expression of Pax6 in the adult lens and cornea (Koroma et al., 1997), makes it challenging to discriminate spatial and temporal function of Pax6 in CE using *Pax6*$^{+/-}$ mutants. Here we took advantage of the Cre-*loxP* system for selectively inactivating Pax6 either in the CE or OSE.

In this study, we used two independent Cre recombinase systems with different spatiotemporal Cre activity, first *Aldh3-Cre* where Cre activity is controlled by promoter-specific for postnatal CE and second, *K14-Cre* where Cre activity is controlled by promoter-specific for basal keratinocyte, which is expressed in OSE. We show that specific depletion of Pax6 from CEs upon eye opening leads to an abnormal cornea with reduced thickness, in spite of increased proliferation. Immunostaining studies revealed the loss of CE-specific intermediate filament Krt12, the diffused expression pattern of adherens junction components, E-cadherin and β-catenin and decreased expression of tight junction protein, Zo-1 suggesting defective cell-cell adhesion. Besides that, the expansion of Krt14, a basal cell marker in apical layers, indicates impaired differentiation. Taken together, this provides direct evidence for the role of Pax6 in maintaining proper cell-cell adhesion and differentiation in postnatal CE. While Pax6 ablation using *K14-Cre* from OSE at early postnatal stages (PN1-PN9) resulted in conjunctivalisation of the CEs, suggesting the importance of limbal Pax6 in maintaining the corneal-conjunctival barrier.

My contribution to this work: I generated the majority of the experimental data and wrote the manuscript of the published paper *Sunny SS et al, 2022* (presented on pages 40-60 of this thesis).

Developmental Biology 491 (2022) 1–12

Contents lists available at ScienceDirect

Developmental Biology

journal homepage: www.elsevier.com/locate/developmentalbiology

Multiple roles of Pax6 in postnatal cornea development

Sweetu Susan Sunny, Jitka Lachova, Naoko Dupacova, Zbynek Kozmik *

Laboratory of Transcriptional Regulation, Institute of Molecular Genetics of the Czech Academy of Sciences, Videnska 1083, Praha 4, 142 20, Czech Republic

ARTICLE INFO

Keywords:
Eye
Development
Cornea
Pax6
Conditional knockout
E-cadherin
Keratins

ABSTRACT

Mammalian corneal development is a multistep process, including formation of the corneal epithelium (CE), endothelium and stroma during embryogenesis, followed by postnatal stratification of the epithelial layers and continuous renewal of the epithelium to replace the outermost corneal cells. Here, we employed the Cre-*loxP* system to conditionally deplete Pax6 proteins in two domains of ocular cells, i.e., the ocular surface epithelium (cornea, limbus and conjunctiva) (OSE) or postnatal CE via *K14-cre* or *Aldh3-cre*, respectively. Earlier and broader inactivation of Pax6 in the OSE resulted in thickened OSE with CE and limbal cells adopting the conjunctival keratin expression pattern. More restricted depletion of Pax6 in postnatal CE resulted in an abnormal cornea marked by reduced epithelial thickness despite increased epithelial cell proliferation. Immunofluorescence studies revealed loss of intermediate filament Cytokeratin 12 and diffused expression of adherens junction components, together with reduced tight junction protein, Zonula occludens-1. Furthermore, the expression of Cytokeratin 14, a basal cell marker in apical layers, indicates impaired differentiation of CE cells. Collectively, our data demonstrate that Pax6 is essential for maintaining proper differentiation and strong intercellular adhesion in postnatal CE cells, whereas limbal Pax6 is required to prevent the outgrowth of conjunctival cells to the cornea.

1. Introduction

The complex process of vision starts with the light transmission and refraction through the multilayered cornea, a transparent avascular tissue, which contributes to 60–70% of the eye's total refractive power and functions as a protective barrier (Sridhar, 2018). The cornea is composed of three main compartments; outermost non-keratinized stratified squamous epithelium, central collagenous stroma with sparsely dispersed keratocytes and innermost monolayered endothelium (Hay, 1980; Zieske, 2004). Any defects in corneal development or maintenance of its homeostasis result in loss of vision (Vincent et al., 2005; Klintworth, 2003).

Mammalian corneal development is a multistep process originating at the early optic cup stage with formation of the presumptive corneal epithelium from the surface ectoderm, followed by formation of the corneal endothelium and keratocytes during two migratory waves of the neural crest-derived periocular mesenchyme. Postnatal stratification of the epithelial layers and continuous epithelial renewal are central processes of adult corneal cell biology (Cvekl and Tamm, 2004; Dhouailly et al., 2014; Lwigale, 2015; Lavker et al., 2020; Walker et al., 2020). Mouse corneal development is a leading mammalian model for understanding cellular, molecular and genetic mechanisms underlying corneal development and homeostasis. Coincident with eyelid opening around postnatal day14 (PN14), 1–2 layered corneal epithelium (CE) divides and differentiates into 4–6 layers by PN21 and forms mature 6–8 layered tissue by 8–10 weeks after birth (Hay, 1980; Zieske, 2004; Collinson et al., 2002). In the mature cornea, most superficial cells are shed off and replaced regularly by differentiated cells that move apically from the underlying layers, which are replenished by centripetal migration of stem cells from the limbus located at the juncture between the cornea and the conjunctiva (Collinson et al., 2002; Cotsarelis et al., 1989; Nagasaki and Zhao, 2003; Lavker et al., 1991; Thoft and Friend, 1983).

Paired domain and homeodomain-containing transcription factor Pax6 is an evolutionarily conserved regulator of eye development in vertebrates and invertebrates (Cvekl and Callaerts, 2017; Kozmik, 2008).

In the mouse, Pax6 is expressed in the surface ectoderm, giving rise first to the prospective lens ectoderm and then to CE (Walther and Gruss, 1991). Pax6 is also expressed in the corneal limbus, where stem cells reside, and in the conjunctiva (Li et al., 2007; Secker and Daniels, 2008).

Several mutated *Pax6* alleles have been used to dissect both cell type- and stage-specific roles of this transcription factor in mouse eye development, including the cornea (Hill et al., 1991; van Raamsdonk and Tilghman, 2000; Collinson et al., 2001; Davis et al., 2003; Ramaesh et al., 2003, 2005; Ambati et al., 2006; Masse et al., 2007; Ashery-Padan et al.,

* Corresponding author. Institute of Molecular Genetics of the Czech Academy of Sciences, Videnska 1083, Praha 4, 142 20, Czech Republic.
E-mail address: kozmik@img.cas.cz (Z. Kozmik).

https://doi.org/10.1016/j.ydbio.2022.08.006
Received 1 May 2022; Received in revised form 20 August 2022; Accepted 23 August 2022
Available online 29 August 2022

2000; Marquardt et al., 2001; Raviv et al., 2014; Klimova and Kozmik, 2014; Antosova et al., 2016).

Heterozygous mutations in both human *PAX6* and mouse *Pax6* genes cause a range of ocular and postnatal developmental abnormalities (i.e., human aniridia and Peters' anomaly) that affect all ocular tissues at variable degrees depending on the type and location of each mutation (Hingorani et al., 2012; Lima Cunha et al., 2019). In the cornea, the prevailing PAX6-associated defects are aniridia-associated keratopathy (Ihnatko et al., 2016; Latta et al., 2021) and limbal stem cell deficiency (Tseng et al., 2020). In contrast, *Pax6* homozygous mutants such as *Sey/Sey* lack the eyes, exhibit brain, olfactory placode and pancreas abnormalities and die at birth (Hogan et al., 1986).

Prenatally, $Pax6^{+/-}$ corneas exhibit thin epithelium and thickened hypocellular stroma. Postnatally, the cornea collapses further with inflammatory cell infiltration, neovascularisation, erosions, and goblet cell accumulation in the epithelium, leading to corneal opacity (Davis et al., 2003; Ramaesh et al., 2003, 2005; Ambati et al., 2006; Leiper et al., 2009). Further studies on factors contributing to corneal pathogenesis in $Pax6^{+/-}$ mutants revealed enhanced cell turnover, delayed expression of Cytokeratin 12 (Krt12) and defective centripetal migration of limbal stem cells (LSC) (Davis et al., 2003; Ramaesh et al., 2003, 2005; Douvaras et al., 2013). However, the lethality of homozygous Sey mutants, consecutive induction of the lens and cornea from SE, the impact of the lens in morphogenesis of the anterior segment (van Raamsdonk and Tilghman, 2000; Collinson et al., 2001; Genis-Galvez et al., 1967; Genis-Galvez, 1966) and continued expression of Pax6 in the adult lens and cornea (Koroma et al., 1997) make it challenging to dissect both spatial and temporal functions of Pax6 in CE using classical knockout models.

Analysis of mouse Pax6 heterozygous mutations offers some insight into its corneal function; however, loss-of-function studies resulting in complete depletion of the Pax6 protein provide key mechanistic insights into how this transcription factor functions in different corneal cellular compartments. Here, we thus took advantage of the Cre-*loxP* system for selectively inactivating Pax6 either in the ocular surface epithelium (OSE) (cornea, limbus, and conjunctiva) or CE. We used two Cre drivers: *K14-Cre,* where cre activity is controlled by Keratin 14 promoter, specific for basal keratinocytes in OSE (Andl et al., 2004), and *Aldh3-Cre,* where cre activity is controlled by the Aldh3/Aldh1a3 promoter specific for postnatal CE (Sunny et al., 2020). Pax6 ablation using *K14-Cre* from OSE at early postnatal stages (PN1-PN9) resulted in conjunctivalisation of the CE and limbal epithelium, suggesting the importance of limbal Pax6 in preventing the overgrowth of conjunctival epithelia to the cornea. In contrast, specific deletion of Pax6 from CE upon eyelid opening leads to an abnormal thin cornea with defective cell-cell adhesion, thus providing direct evidence for the function of Pax6 in postnatal corneal development.

2. Methods

2.1. Ethics statement

The housing of mice and in vivo experiments were done in concurrence with the European Communities Council Directive 86/609/EEC of November 24, 1986 and institutional and national guidelines. All experimental methods and animal care were approved by the Animal Care Committee of the Institute of Molecular Genetics (no. 71/2014). This work did not include human subjects.

2.2. Mouse strains

The following genetically modified mouse strains were used for this study: *Aldh3-Cre* (Sunny et al., 2020), *K14- Cre* (Andl et al., 2004) and $Pax6^{fl/fl}$ (Klimova and Kozmik, 2014).

2.3. Histology and immunofluorescence

Eyeballs from pups of desired age were enucleated, fixed in 4% formaldehyde in 1x PBS (Phosphate-Buffered Saline) overnight at 4 °C, then washed 3 × 10 min in 1x PBS, dehydrated in ethanol series, cleared in xylene, and then processed to paraffin wax.

For histological analysis, sections (6 μm) were deparaffinized, rehydrated with ethanol series, stained with Hematoxylin and Eosin (H & E), and mounted in glycerol. For immunofluorescence, deparaffinized sections were heat-treated with sodium citrate buffer (10 mM sodium citrate buffer, 0.05% Tween 20, pH-6.0) for antigen retrieval. Non-specific binding was blocked by incubation in 10% BSA (Bovine Serum Albumin)/0.1% PBT (PBS with 0.1% Tween-20) for 30 min and then incubated with primary antibodies in 1% BSA/0.1% PBT overnight. Subsequently, samples were washed in 1x PBS for 3 × 10 min, followed by incubation for 1 h in secondary antibodies in 1% BSA/0.1% PBT, washed in 1x PBS, 2 × 10 min, counterstained with DAPI (1 μg/ml) and mounted using Mowiol (Sigma).

For staining with antibodies related to adhesion, eyeballs collected were fixed for 1 h in 4% formaldehyde/1x PBS, washed in 1x PBS for 2 × 5 min, cryopreserved in 30% sucrose/PBS and later frozen in OCT. Cryosections (6μm) were permeabilized by incubation with 0.1% PBT for 15 min, followed by a heat-induced antigen retrieval step using sodium citrate buffer. Successive steps were the same as for paraffin sections (as described above).

Whole-mount staining of the cornea was performed to analyze tight junction marker ZO-1. Enucleated eyes were fixed for 1 h in 4% PFA in 1x PBS. Corneal buttons were dissected from the remaining parts of the eye and washed for 3 × 5 min in 1x PBS, then permeabilized with 0.3%PBT (PBS with 0.3% Triton x-100) for 1 h, blocked with 10% BSA/0.1% PBT for 1 h, and further antibody incubation steps were the same as for corneal sections. Then, corneal buttons were radially cut to flatten and mounted. The primary antibodies used in this study are listed in Table S1 and secondary antibodies were fused to Alexa fluorophore (Molecular Probes, 1:500). All stained sections were analyzed with Zeis Imager Z2 (Zeis, Germany).

2.4. Phalloidin staining

Fresh frozen samples were cut at 6μm thickness, air-dried for 30 min, fixed for 8 min at 4°C, washed in 1x PBS for 2 × 5 min, permeabilized with 0.5% PBT for 15 min, blocked with 10% BSA/0.1% PBT for 30 min, followed by overnight incubation with Pax6 primary antibody in 1% BSA/0.1% PBT. Sections were washed with 0.1% PBT for 3 × 10 min, incubated with a solution containing secondary antibody (Anti-rabbit Alexa fluor 488) and Alexa fluor 594 Phalloidin (Invitrogen, A12381) in 1% BSA/0.1% PBT for 1 h and washed with 0.1% PBT, 2 × 10 min, counterstained with DAPI, washed with 1x PBS for 2 × 5 min, and mounted in Mowiol.

2.5. BrdU labeling

To determine proliferation in wild-type and mutant mice, animals of desired age were injected intraperitoneally with BrdU (Sigma B9285, 0.1 mg/g body weight) and sacrificed by cervical dislocation after 2 h. Enucleated eyes were fixed in 4% formaldehyde and processed to embed in paraffin wax. Paraffin sections were cut at 6μm thickness, dewaxed and hydrated with ethanol series. The antigen retrieval step was done by heating in sodium citrate buffer (10 mM sodium citrate buffer, 0.05% Tween 20, pH-6.0), followed by incubation in 2N HCl for 30 min and 20 min neutralization using 0.1M borate buffer (pH 8.3). Subsequently, they were washed with PBT for 10 min, blocked with 10% BSA for 1 h and incubated at 4 °C overnight with rat anti-BrdU antibody (1:500, Abcam, ab6326) and rabbit anti-Pax6 in 1% BSA in PBT. Follow-up steps were the same as described above for paraffin sections.

The ratio of proliferating cells and the number of $DAPI^+$ cells for each genotype were always calculated by counting 5–6 central sections from at least three different samples. The statistical significance was determined by Student's t-test.

3. Results

3.1. Pax6 depletion in postnatal corneal epithelium results in an abnormal cornea with reduced thickness

For conditional inactivation of Pax6 during postnatal development of CE, we used *Aldh3-Cre* transgenic mice (Sunny et al., 2020) in which Cre recombinase expression is controlled by the cis-regulatory regions of the mouse Aldh3 gene within a large BAC clone (Fig. S1). To visualize Cre recombinase activity, we bred *Aldh3-Cre* transgenic mice with the *Rosa26R* reporter strain (Soriano, 1999). Consistent with the endogenous expression of Aldh3 (Davis et al., 2008), apparent β-gal activity was found in CE from PN12-PN14, with a robust increase upon eyelid opening (Fig. S1). At all experimental stages, weak or no β-gal activity was found in limbal epithelial cells (LE) (Fig. S1). To inactivate Pax6 in postnatal CE, *Aldh3-cre* mice were bred with $Pax6^{fl/fl}$ (Klimova and Kozmik, 2014). For the sake of simplicity, we refer to $Pax6^{fl/fl}$ as wild-type and *Aldh3-Cre; Pax6*$^{fl/fl}$ as CE cKO mutant in the text.

To assess the efficiency of *Aldh3-Cre* in Pax6 inactivation, we collected eyeballs from wild-type and CE cKO and analyzed them by Pax6 immunostaining. At PN12 in CE cKO mutant, reduced and patchy Pax6 expression was observed in central CE (Fig. S1). By PN21, very few or no cells expressed Pax6 in the central cornea (Fig. 1A'). At PN28, mosaic expression was observed, with no Pax6 proteins found in the peripheral cornea (Fig. 1D') and a patch of Pax6-positive cells at the central cornea (Fig. 1C'). Pax6 expression was retained in all these stages in LE and at the end of the peripheral cornea (Fig. 1B', D'). High Pax6 protein expression was observed in CE and LE of wild type (Fig. 1A, B, C, D).

To investigate the phenotypic consequences in response to Pax6 inactivation, we performed histological analysis. Hematoxylin and eosin staining revealed no significant difference between wild-type and CE cKO mutant at PN12. (Fig. S1). At PN21, the wild type had 4-6 layered stratified CE with three types of cells; basal, wing, and superficial. Basal cells are cuboidal or columnar with oval nuclei, wing cells are polygonal cells with central rounded nuclei, and superficial cells exhibit flat polygonal morphology and flat nuclei (Fig. 1E and F) (Sridhar, 2018). At the same time, the CE cKO mutant had 2-3 layers lacking any neatly ordered architecture (Fig. 1E', F'). At PN28, the wild type CE had 5-6 layers (Fig. 1G and H), whereas the central CE (which retains Pax6) of CE cKO mutant had 3-4 layers but remained morphologically similar to the wild type (Fig. 1G'). In contrast, the peripheral cornea (with loss of Pax6 expression) showed abnormal epithelial cells (Fig. 1H'). Furthermore, histology revealed disturbed stroma with increased keratocytes at the boundary between the region with and without Pax6 (Fig. S2). The CE did not have mucin-containing goblet cells (Fig. S2), while on the contrary, goblet cells were present in central and peripheral CE in some CE cKO mutants (Fig. S2). Taken together, normal corneal development was disrupted following the onset of Cre expression and depletion/reduction of Pax6 proteins marked by fewer cell layers and abnormal cell morphology.

3.2. Misregulation of differentiation in CE cKO mutants

To further characterize the abnormal corneas, we analyzed the expression of epithelial differentiation markers. Krt12 is a bona fide marker for CE, not for basal limbal and conjunctival epithelial cells (Liu et al., 1994; Moyer et al., 1996). In the wild type, Krt12 is expressed in all layers of CE (Fig. 2A and B). However, by PN21, Krt12 was lost in the entire CE of CE cKO mutants (Fig. 2A', B'). We also examined the expression pattern of Cytokeratin 14 (Krt14), a basal cell marker (Kurpakus et al., 1994). In contrast to wild type CE, where Krt14 is present only in the basal layer (Fig. 2C and D), CE cKO mutants showed strong expression in all existing layers (Fig. 2C', D'). Moreover, there was no change in the expression pattern of Cytokeratin 4 (Krt4) and Cytokeratin

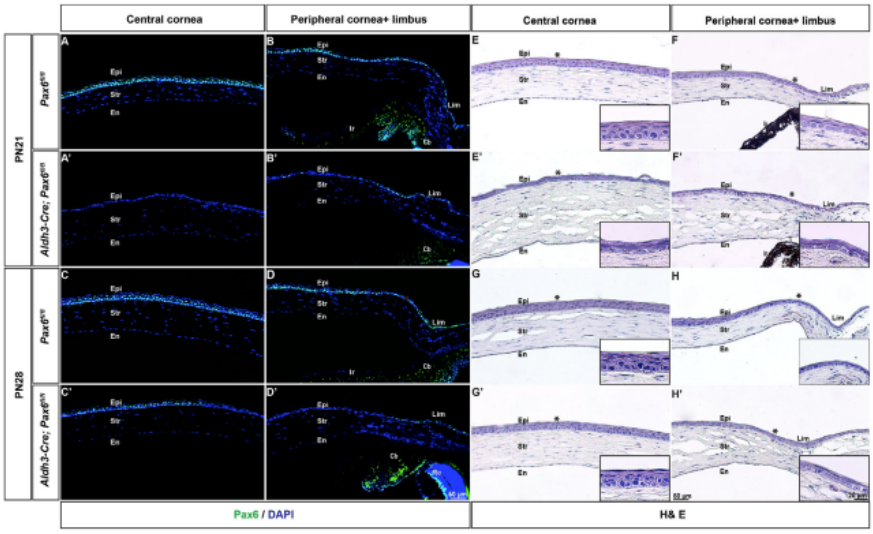

Fig. 1. *Aldh3-Cre*-mediated Pax6 inactivation and morphological consequences in postnatal corneal epithelial cells. **(A-D')** Coronal sections of wild-type ($Pax6^{fl/fl}$) and CE cKO (*Aldh3-Cre;* $Pax6^{fl/fl}$) stained with Pax6 antibody at indicated stages. **(A-B')** At PN21, very few or no active $Pax6^{+}$ cells are found in the CE cKO. At PN28, patchy expression of Pax6 is detected in **(C, C')** central cornea of CE cKO, whereas deletion is observed in **(D, D')** peripheral cornea. **(B', D')** At all stages, Pax6 is retained in LE cells. **(E-H')** Hematoxylin and eosin staining in frontal sections of wild type ($Pax6^{fl/fl}$) and CE cKO (*Aldh3-Cre;* $Pax6^{fl/fl}$) mutant. **(E-F')** At PN21, CE of the CE cKO mutant has a lower number of layers and abnormal stratification. **(G-H')** At PN28, **(G, G')** central CE of CE cKO mutant is slightly thin compared to the age-matched control, but with proper stratification as in wild type. **(H, H')** The peripheral cornea remains thin and with abnormal architecture. Inserts are higher magnification images of the region of interest indicated by asterisks (*). Abbreviations used in this figure and successive images: En, Corneal endothelium; Str, Corneal stroma; Epi, Corneal epithelium; Cb, Ciliary body; Ir, Iris; Lim, Limbal epithelium. Scale bar: **(A-H')** – 50 μm and inserts – 20 μm.

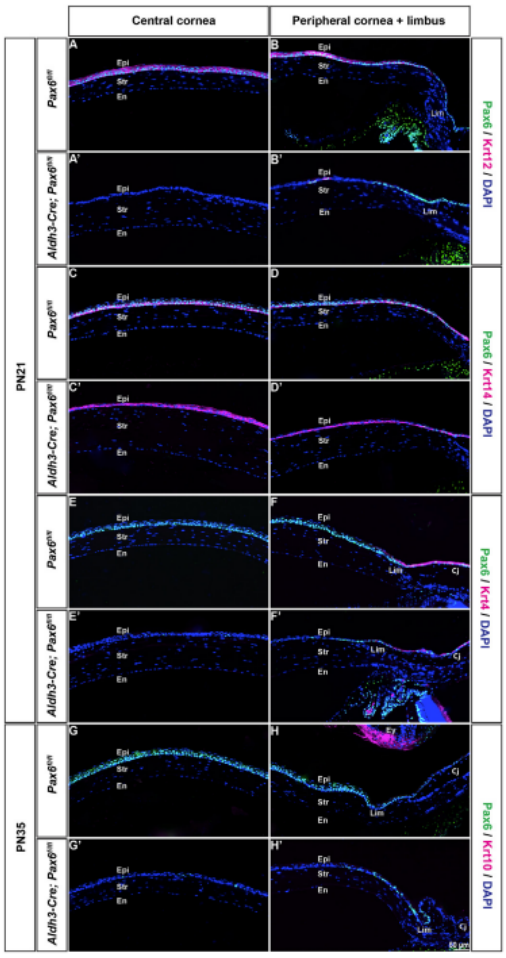

Fig. 2. Altered expression of keratins in corneal epithelium. **(A-H′)** Coronal sections from PN21 and PN35 of wild type (*Pax6*$^{fl/fl}$) and CE cKO mutant (*Aldh3-Cre; Pax6*$^{fl/fl}$) were subjected to immunostaining with antibodies indicated. **(A, B)** Wild-type CE is stained with Krt12, while expression of Krt12 is lost in **(A′, B′)** CE cKO mutant. Expression of Krt14 is seen only in the basal layer of **(C, D)** wild-type cornea, whereas in **(C′, D′)** CE cKO mutant, Krt14 is detected at other layers. **(E–F)** As in the control, conjunctival specific expression of Krt4 was not expanded to the CE in the **(E′-F′)** CE cKO mutant. No immunoreactivity for Krt10 was found in the CE of **(G, H)** wild type and **(G′, H′)** CE cKO mutant. Abbreviations: Cj, Conjunctival epithelium; El, Eyelid, Scale bar: **(A-H′)** – 50 µm.

10 (Krt10), markers of conjunctival epithelial cells (Kurpakus et al., 1994) (Fig. 2E-F′) and skin, respectively (Fig. 2G-H′). Together, these data suggest that upon loss of Pax6 around eyelid opening, CE differentiation is misregulalted.

3.3. Changes in the proliferation potential or apoptotic rate do not accord with fewer layers in CE cKO mutants

Disruption of corneal epithelial differentiation and reduced thickness might be due to changes in the cell proliferation potential. To prove this directly, we investigated the proliferation status of CE at different postnatal development stages by BrdU incorporation for 2 h. The distribution of BrdU$^+$ nuclei was restricted to the basal layer of the CE (Fig. 3B and C). The fraction of proliferating cells was counted by dividing the number of BrdU$^+$ cells by DAPI$^+$ cells in the basal layer. The number of proliferating cells was slightly increased in the CE cKO mutant compared to the wild type at PN12 and PN14 (Fig. S3). Moreover, at PN21 and PN28, only 7.4 ± 1.2%, 5.9 ± 1.7% were BrdU$^+$ in wild-type CE compared with 19.6 ± 2.1%, 20.4 ± 4.2% BrdU$^+$ in CE cKO, respectively (Fig. 3A- F', G). These findings suggest that inactivation of Pax6 results in increased proliferation, although this change in proliferation status does not contribute to the reduced thickness or impaired epithelial differentiation.

Increased cell death could be another possibility for reduced cell layers despite increased cell proliferation. We therefore analyzed apoptosis in corneal epithelium using an antibody against cleaved caspase 3. Nevertheless, we noticed no significant difference in the number of cCaspase3$^+$ cells between the wild type and CE cKO mutants at PN21 and PN28 (Fig. S4). Collectively, variations in the proliferation status or apoptosis do not accord with the decreased number of layers or misregulation in CE differentiation.

3.4. Pax6 activity is required for the proper cell-cell adhesion in postnatal corneal epithelium

Considering the above paradox that proliferation is increased despite the reduced thickness, we next investigated these affected cell populations at the level of cell-cell adhesion. First, we looked at the expression of E-cadherin, a key transmembrane protein of the adherens junction. Immunostaining revealed abundant and proper membrane localization of E-cadherin in wild-type CE (Fig. 4A-B′). In contrast, the CE cKO mutants showed improper membrane localization (Fig. 4C-D′). Next, we analyzed β-catenin, a binding partner of E-cadherin. Similarly to E-cadherin, β-catenin has a plasma membrane localization in wild-type CE (Fig. 4I-J′), whereas its presence sharply decreased in CE cKO mutants (Fig. 4K-L′). Furthermore, we analyzed organization of the F-actin cytoskeleton in CE using fluorescently labeled phalloidin. In contrast to the proper organization in the wild type (Fig. 4E-F′), CE cKO mutants displayed more diffused cytoplasmic localization patterns (Fig. 4G-H′). Finally, we assessed the expression of tight junction protein Zonula occludens-1 (ZO-1), which plays a vital role in the epithelial barrier function of the cornea (Srinivas, 2010; Mandell et al., 2006). In the wild-type cornea, ZO-1 displays robust continuous expression at the cell-cell borders of superficial layers (Fig. 4M, M′), whereas CE cKO mutants had decreased expression at the cell-cell borders (Fig. 4N, N'). These findings suggest a loss of epithelial barrier integrity upon Pax6 depletion. Our aggregate data support the model in which postnatal inactivation of Pax6 results in the loss of proper cell-cell adhesion in CE, which in turn could account for the reduced number of layers.

3.5. Pax6 depletion in the ocular surface ectoderm resulted in thickened epithelia

Next, for conditional inactivation of Pax6 in OSE from embryonic stages, we used *K14-Cre* (Andl et al., 2004), where Cre recombinase activity is controlled by the Krt14 promoter. To visualize the Cre activity, we crossed the *K14-Cre* transgenic mice with the *Rosa26R* reporter strain (Soriano, 1999). X-gal staining revealed weak reporter activity in CE, while modest Cre activity was observed in the presumptive conjunctival epithelium during embryogenesis (Fig. S5).

To generate conditional knockout mutant *K14-Cre; Pax6*$^{fl/fl}$, we crossed *K14-Cre* transgenic mice with *Pax6*$^{fl/fl}$. Hereafter, we refer to *K14-Cre; Pax6*$^{fl/fl}$ as OSE cKO mutant and *Pax6*$^{fl/fl}$ as wild type in the text. To investigate the efficiency of the *K14-Cre* recombinase system in inactivating the Pax6 gene, we performed Pax6 immunohistochemistry. Consistent with Cre expression, patchy Pax6 protein expression was

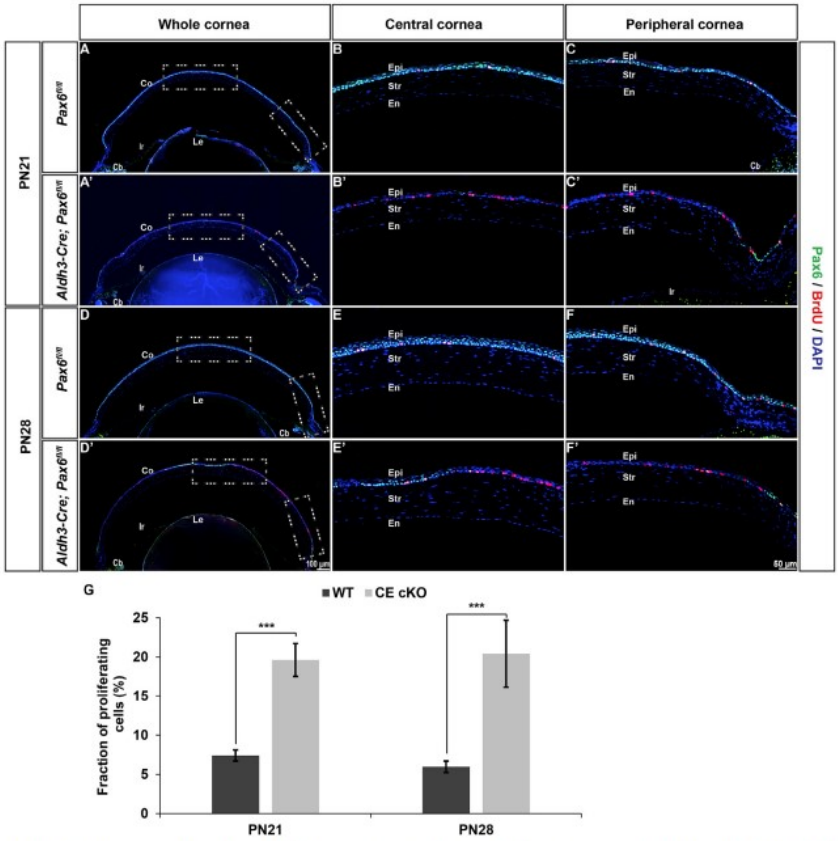

Fig. 3. Increased cell proliferation in corneal epithelium. **(A-F′)** Immunostaining of Pax6 and BrdU in frontal sections of wild type (*Pax6*$^{fl/fl}$) and CE cKO (*Aldh3-Cre; Pax6*$^{fl/fl}$) at PN21 and PN28. CE of **(A′-C′), (D′-F′)** Pax6 CE cKO mutant had an increased number of BrdU^{+} cells compared to the age-matched control at **(A-C)** PN21 and **(D-F)** PN28. **(G)** The fraction of proliferating cells is determined by dividing the number of BrdU^{+} cells by the total number of DAPI^{+}cells in the basal layer. Error bars indicate standard deviation. The p-values are calculated by Student's t-test. ***$p < 0.001$ **(A, A′, D, D′)** The dashed rectangle in the whole cornea indicates the region of interest shown in higher magnification panels. Abbreviations used; Co, Cornea; Le, Lens. Scale bar: 50 µm except for **(A, A′, D, D′)** – 100 µm.

observed in presumptive CE of OSE cKO at E15.5 and E18.5 (Fig. S5). In contrast to E15.5 CE, Pax6 expression was decreased in presumptive conjunctival epithelial cells of the OSE cKO mutant (Fig. S5). At PN2, an asymmetrical deletion pattern was observed in most of the OSE cKO mutants; one periphery had a loss of Pax6^{+} cells, while in contrast, the other periphery and conjunctiva retained Pax6 expression (Fig. 5A–C'). By PN6, very few or no Pax6^{+} cells were found in the entire OSE domain (Fig. 5D–F').

To further characterize the phenotypic changes, we examined morphological and histological changes in OSE cKO mutants and age-matched controls. Hematoxylin and eosin staining at PN2 revealed thickened limbal and conjunctival epithelia in the OSE cKO mutant (Fig. 5H') in contrast to 1–2 layered wild-type epithelia (Fig. 5H and I). Simultaneously, part of the cornea and limbus, which retains Pax6, remained thin (Fig. 5I'). Besides that, no significant change was found in the central CE (Fig. 5G, G′). At PN6, in comparison to wild-type tissue morphology, the corneal, limbal and conjunctival epithelia of the OSE cKO mutants were moderately thickened (Fig. 5J–L'). By PN18, palpebral spaces in OSE cKO mutants were small, with some having eyelashes touching the CE (Fig. S6). By PN23, the eyes of OSE cKO mutants appeared opaque with 20% penetrance (Fig. S6). Histological analysis of opaque eyes at PN23 showed keratinization and extensive thickening of central CE of OSE cKO compared to age-matched control animals (Fig. S6). Collectively, these data show that Pax6 inactivation in OSE during early postnatal stages impairs ocular surface homeostasis.

3.6. Pax6 loss in ocular surface epithelium resulted in corneal epithelium adopting conjunctival keratin expression

Our present histological analysis indicates a switch to epidermal cell fate on the ocular surface. Our hypothesis predicts that loss of Pax6 affects the cell fate decisions in the OSE compartment, and is thus involved in major corneal postnatal developmental processes. To test this hypothesis, we examined the expression of epithelial markers at early postnatal stages (PN1-PN12) prior to eye opening. In contrast to wild-type eyes, Krt12 expression was lost in OSE cKO mutants (Fig. 6A-C'),

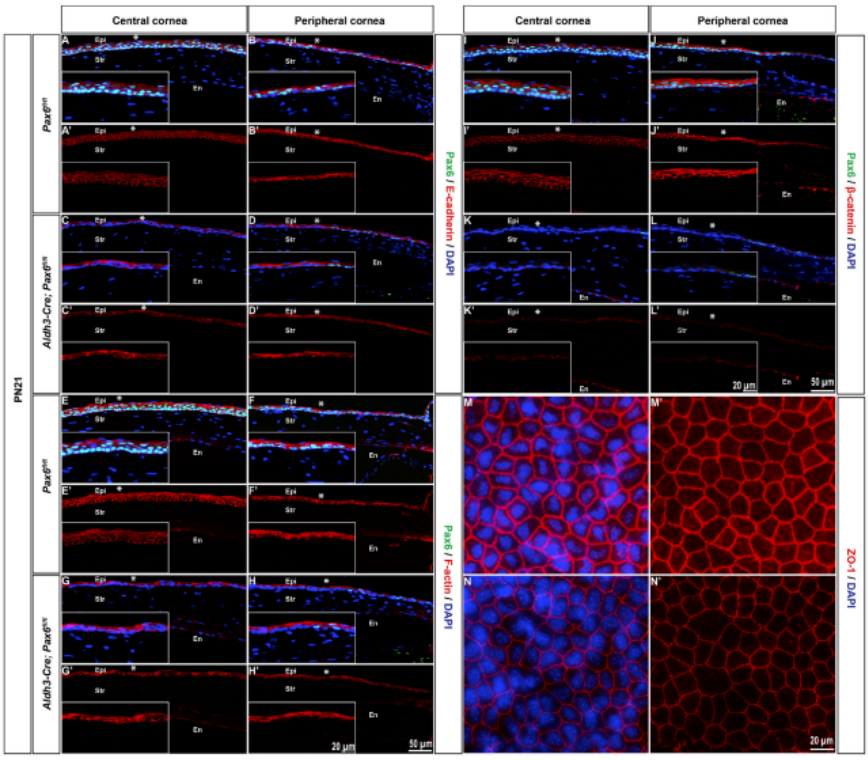

Fig. 4. Cell adhesion and cytoskeletal defects in corneal epithelia. **(A-L′)** Coronal sections from PN21 of control (*Pax6*$^{fl/fl}$) and CE cKO (*Aldh3-Cre; Pax6*$^{fl/fl}$) were subjected to immunostaining with antibodies indicated. **(A-B′)** Proper membranous localization of E-cadherin in CE cells of control eyes **(C-D′)**, while a diffused pattern was observed in CE cKO mutants. **(E-H′)** Diffused expression of F-actin is observed in the CE cKO mutant in contrast to its proper organization in the control. **(I-J′)** Control CE cells have membrane localization of β-catenin, whereas **(K-L′)** the CE cKO mutant has an overall downregulated expression in CE cells. **(M-N′)** Whole-mount immunostaining of ZO-1 in superficial layers of CE at PN21. Inserts are higher magnification images of the region of interest indicated by asterisks **(*)**. Scale bar: **(A-L′)** – 50 μm and inserts – 20 μm, **(M-N′)** – 20 μm.

while expression of Krt14 expanded to all cell layers in the cornea by PN6 (Fig. 6D-F′). These findings demonstrate that corneal epithelial differentiation was impaired upon Pax6 inactivation. In control conjunctiva, Krt14 was expressed in basal and suprabasal cells (Fig. 6D–F), and OSE cKO mutants maintained the same expression pattern even though they had comparatively thicker epithelia (Fig. 6D′-F′).

In most cases, CE of OSE cKO mutants was devoid of Krt10 during early postnatal stages (Fig. 6G-I′). Rarely, some samples with patches of Krt10^{+} cells were observed. These had comparatively no conjunctival sac and more or less direct contact of CE with the thickened conjunctiva (Fig. S7). Keratinization in these samples could be a response to irritations caused by the closeness of thickened conjunctival epithelia and CE. Therefore, we further analyzed the expression of Krt4, which was localized to the conjunctival epithelium in wild-type mice. Krt4 expression expanded into the LE and CE in OSE cKO mutants (Fig. 6J-L′). Based on these data, we infer that the loss of Pax6 in OSE during the early postnatal stages results in the conjunctivalization of CE.

To complete these analyses, we examined the expression of three epithelial markers, Krt12, Krt14 and Krt10, at PN23. The expression of Krt12 was absent in the thickened epithelia of OSE cKO mutants, while the expression of Krt14 was expanded to apical cell layers in OSE cKO mutants in contrast to its basal layer expression in control eyes (Fig. S7). Furthermore, the expression of skin-specific Krt10 was observed in CE with Pax6 loss (Fig. S7). Even though these data indicate the developmental fate change of CE to the epidermis at PN23, we interpret this fate change as a response to irritations happening to the corneal surface, including small palpebral space, infection, and contacts with eyelashes.

4. Discussion and conclusions

This is the first study to define the roles of Pax6 in postnatal mouse corneal development and to integrate these results with previously established critical functions of this transcription factor in early corneal development. These findings are both important for understanding the intricate complexity of corneal development, their maintenance, and the pathology of the cornea in human aniridia patients (Ihnatko et al., 2016; Latta et al., 2021). To accomplish these goals, we employed genetic conditional loss-of-function approaches using two-stage and cell-specific *K14-* and *Aldh3-cre* lines. Previous studies were limited to analysis of various Pax6 haploinsufficiency models (Davis et al., 2003; Mort et al., 2011; Ramaesh et al., 2006); however, in both our *K14* and *Aldh3-cre* models, corneal development proceeds normally until PN1 and PN12-14, respectively. Our data show that Pax6 is important for postnatal development of the cornea and the maintenance of the limbal epithelial identity.

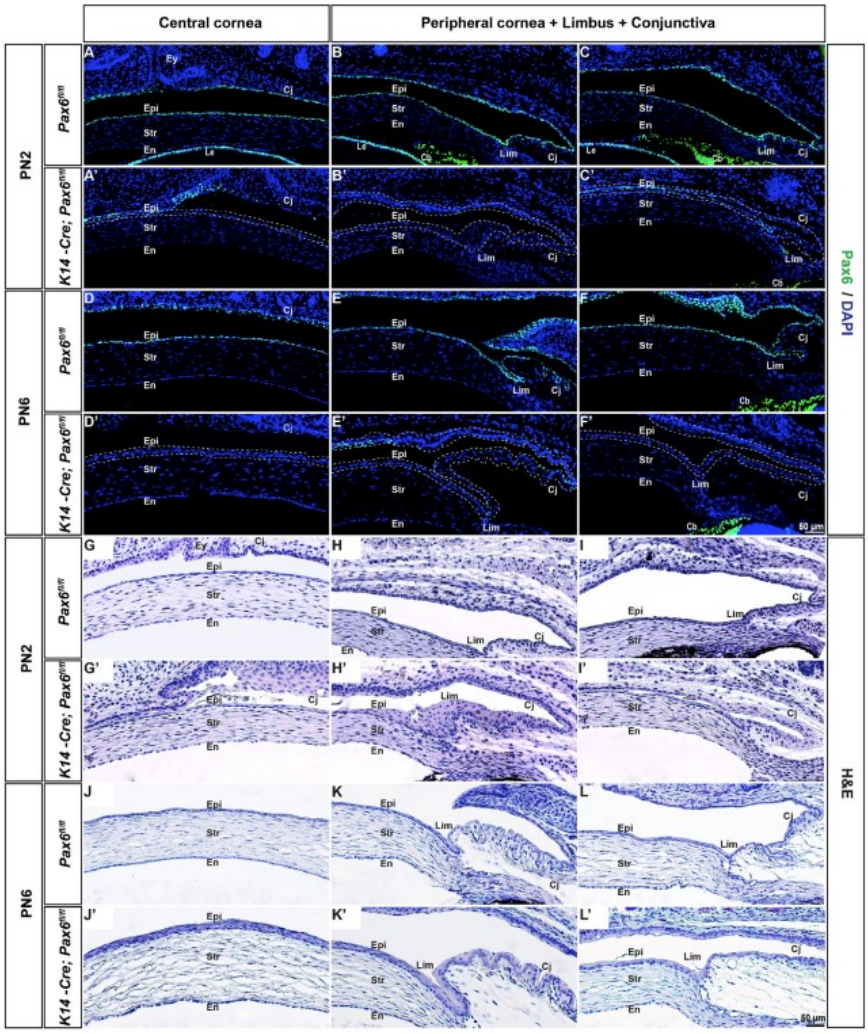

Fig. 5. *K14-Cre*-mediated deletion of Pax6 and histological changes in the ocular surface ectoderm. **(A-L′)** Consecutive frontal sections of control (*Pax6*$^{fl/fl}$) and OSE cKO mutants (*K14-Cre; Pax6*$^{fl/fl}$) were stained with Pax6 and H&E at indicated postnatal stages. **(A-C′)** At PN2, Pax6 expression is retained in one peripheral part of the cornea, while it is deleted in other periphery and central epithelial cells. **(D-F′)** At PN6, Pax6 expression is absent in the central, limbal and conjunctival epithelial cells of OSE cKO mutants. **(G-I′)** At PN2, OSE cKO mutants have thicker LE compared to the control. **(J-L′)** At PN6, the OSE cKO mutant exhibits moderately thickened corneal, limbal and conjunctival epithelium compared to the control epithelium. The dashed line indicates the region of Pax6 deletion. Scale bar: **(A-L′)** – 50 μm.

4.1. Role of Pax6 in corneal epithelium during postnatal development

Selective inactivation of Pax6 in CE concomitant with eye opening leads to the abnormal cornea marked by only 3–4 cell epithelial layers concomitant with altered cell-cell adhesions in the CE of CE cKO compared to control littermates.

Initial analysis of the cornea using chimeric AP-2α wild-type and null cells showed downregulation of E-cadherin in mutated cells (West-Mays et al., 2003). In the follow-up studies, E-cadherin expression was decreased in the lens and CE of AP-2α conditional knockout mutants (Dwivedi et al., 2005). Previous studies have shown that AP-2α, together with Pax6, controls gelatinase B (Mmp9) promoter activity in response to wound healing (Sivak et al., 2004). AP-2α has overlapping expression with Pax6 in both embryonic and adult eyes (West-Mays et al., 1999; Makhani et al., 2007). *In vitro* studies proposed AP-2α-mediated E-cadherin promoter activity (Behrens et al., 1991; Hennig et al., 1996). Corneas of AP-2α conditional knockout mutants exhibit a similar phenotype to Pax6 deficient ones, including adhesion-defective thin epithelium (Davis et al., 2003; Dwivedi et al., 2005). Taken together, these findings raise the possibility of co-operative regulation of E-cadherin expression by Pax6 and AP-2α. Further studies are required to determine whether AP-2α regulates E-cadherin through its co-operative

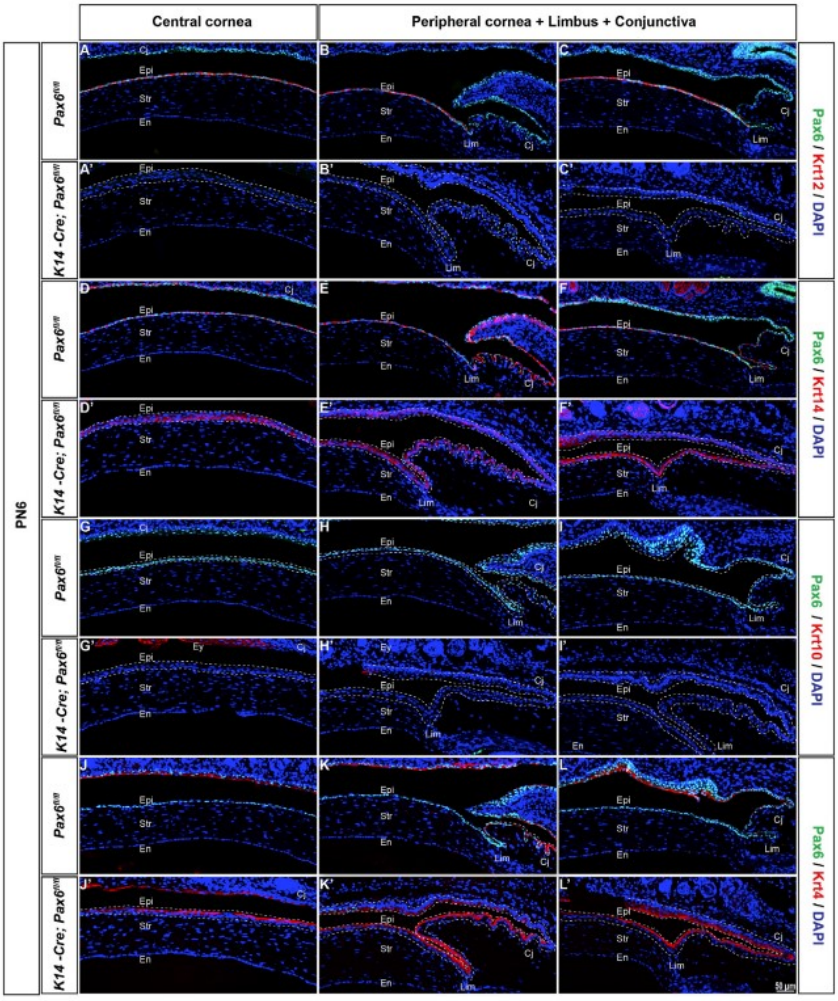

Fig. 6. Corneal epithelium adapts keratin expression pattern in conjunctival epithelium. **(A-L′)** Coronal sections of control (*Pax6*$^{fl/fl}$) and OSE cKO mutants (*K14-Cre; Pax6*$^{fl/fl}$) were stained with indicated antibodies. **(A-C′)** Krt12 expression is lost in CE cells of OSE cKO mutants. **(D-F′)** Krt14 expression is expanded apically to all cell layers in OSE cKO mutants, while it is restricted to the basal cell layer in control CE. **(G-I′)** No immunostaining of Krt10 is observed either in the CE of OSE cKO mutant or control. **(J-L′)** Expansion of Krt4 expression to the CE in the OSE cKO mutant, whereas it is confined to the conjunctival epithelium in the control. Dashed lines indicate OSE with Pax6 loss in OSE cKO mutants. Scale bar: **(A-L′)** – 50 µm.

interaction with Pax6. Interestingly, Pax6 heterozygous corneas showed no change in E-cadherin expression (Davis et al., 2003; Makhani et al., 2007). It is likely that one copy of *Pax6* is sufficient to maintain the promoter activity of E-cadherin (Makhani et al., 2007). It is further supported by the notion that no morphological changes were found upon conditional deletion of one copy of Pax6 in postnatal CE cells using the tamoxifen-inducible Cre model (Dora et al., 2018). However, these models delete the floxed Pax6 allele using the ubiquitous CAG promoter and cell-specific Krt19 at E9.5 and 12 weeks postnatally, respectively (Dora et al., 2018).

Homozygous knockout models in mice (Kao et al., 1996) and mutations in the human Krt12 gene (Nishida et al., 1997) are characterized by corneal fragility. We thus propose that loss of Krt12 in the CE cKO mutant could further deteriorate intercellular adhesion.

Our CE Pax6 cKO data show for the first time that tight junction protein ZO-1 located between the superficial epithelial cells was down-regulated in a *Pax6* gene loss-of-function murine model, consistent with increased fluorescein uptake in corneas of heterozygous Pax6 mutant mice (Davis et al., 2003), which indicates defective tight junctions upon Pax6 loss. The formation of adherens and tight junctions is

interdependent, and the loss of adherens junction components could lead to cells that do not develop tight junctions (Ooshio et al., 2010; Campbell et al., 2017; Capaldo and Macara, 2007; Sugrue and Zieske, 1997). It is plausible that a decrease in adherens junction components could affect other cell-cell junctions and, thus, total cell-cell adhesion.

To further evaluate the possibility of transdifferentiation of CE to the skin-like cells or migration of conjunctival cells, we examined Krt10 and Krt4 expression, respectively. Although earlier studies reported $Krt4^{+}$ cells in the CE of heterozygous Pax6 mutants (Davis et al., 2003), we did not observe any expansion of Krt4 or Krt10 to CE. At the same time, goblet cells were observed in peripheral and Pax6-retaining regions ($Krt12^{+}$) of the central cornea in CE cKO mutants at PN28. The presence of goblet cells in CE is considered a major characteristic of limbal stem cell deficiency (Puangsricharern and Tseng, 1995; Nishida et al., 1995). The stem cells in the limbus cannot maintain epithelial homeostasis, so cells migrate from the conjunctiva into the cornea (Puangsricharern and Tseng, 1995; Nishida et al., 1995). Goblet cells are observed before the limbal stem cells are assumed to be active (Collinson et al., 2002). Hence the ectopic goblet cells cannot be explained as a direct consequence of limbal stem cell deficiency/limbal barrier breach. Incongruent with this, a recent study reported the presence of a compound niche at the limbal-corneal border, which contains a heterogeneous population of cells, including post-mitotic $Krt8^{+}$/$Krt12^{+/}$/$Muc5ac^{+}$ goblet cells. The authors hypothesized that, in the case of wounds in the CE near the limbus, goblet cells increase in number, and they arise from cells in the compound niche, not from bulbar conjunctiva (Pajoohesh-Ganji et al., 2012). We therefore assume that ectopic goblet cells in the CE of CE cKO mutants could be raised from progenitors in the compound niche in response to severe wounding/erosions due to adhesion defects.

Increased proliferation in the CE cKO corneas is consistent with the previous findings from Pax6 heterozygous corneas (Davis et al., 2003; Ramaesh et al., 2005). It is possible that this could be compensation for the cell loss due to adverse adhesion defects (Zieske, 2000). Alternate possibility is that Pax6 directly or indirectly regulates components of cell cycle machinery. For example, Pax6 was found to control cell cycle exit and differentiation into lens fiber cells in ocular lens (Klimova and Kozmik, 2014; Duparc et al., 2007; Estivill-Torrus et al., 2002; Holm et al., 2007).

The development, maturation and maintenance of CE is regulated by a set of transcription factors including Pax6, Ap2-α, EHF and Klf4 (Davis et al., 2003; Dwivedi et al., 2005; Swamynathan et al., 2007; Delp et al., 2015; Tiwari et al., 2017). Pax6 together with Klf4 and Oct4 regulates intermediate filament Krt12 (Swamynathan et al., 2007; Sasamoto et al., 2016; Liu et al., 1999). The expression of Krt12 indicates cornea-specific differentiation, and the loss of Krt12 in CE cKO mutant corneas suggests misregulation of differentiation. This observation is further supported by robust and multilayered expression of basal cell-specific Krt14 in Pax6-deficient CE.

Pax6 is two-fold downregulated in Klf4 conditional knockout mutants. Furthermore, the CE of Klf4 conditional knockout mutants has fewer layers despite the increased proliferation and disrupted cell adhesion, which is remarkably similar to Pax6 CE cKO mutants (Swamynathan et al., 2007, 2008). The Ets transcription factor EHF acts as a regulator for corneal epithelial cell differentiation (Stephens et al., 2013). The Ehf expression is progressively upregulated during development, retained highly in adults and upon ageing. Previous studies suggest the possibility of co-regulation of different set of target genes which promote corneal epithelial differentiation by EHF- PAX6 and EHF –KLF4 (Stephens et al., 2013). But the hierarchical network of these transcriptional regulators in corneal embryonic development and postnatal maturation as well as maintenance is not well established.

The robust expression of Aldh3/Aldh3a1 in CE is directly regulated by Pax6, Oct1/Pou2f1 and p300 (Davis et al., 2008). This explains the repopulation of $Pax6^{+ve}$ central CE by PN28. Even though the central cornea of CE cKO mutants is $Pax6^{+ve}$, we observed fewer layers compared to its age-matched controls. This could be possibly due to the developmental delay resulting from the depletion of Pax6 during stratification initiation. However, somatic depletion of Aldh3 proteins generates structurally normal corneas (Nees et al., 2002), and, thus, we did not investigate further reduction of Aldh3 proteins in our system.

In summary, our data have revealed that Pax6 is required for the proper maintenance of strong intercellular adhesion and differentiation of CE during postnatal development (Fig. 7A).

4.2. Role of Pax6 in the early postnatal ocular surface ectoderm

To unravel the autonomous function of Pax6 in OSE, we *used K14-Cre*, which is controlled by a promoter specific for basal keratinocytes (Andl et al., 2004). Targeted deletion of Pax6 using *K14-Cre* in OSE results (Swamynathan, 2013) in the migration of $Krt4^{+}$ conjunctival cells into the cornea by PN6. In conditions in which the limbus is partially or entirely deleted or lost due to chemical burns, varying degrees of limbal stem cell deficiency (LSCD) arise, which results in conjunctivalization of the cornea (Moyer et al., 1996; Dua and Azuara-Blanco, 2000; Tseng, 1989; Shapiro et al., 1981; Kruse et al., 1990; Koizumi et al., 2000; Lin et al., 2013). While in OSE cKO mutants, migration of conjunctival cells to the cornea occurs prior to limbal stem cell activation (Collinson et al., 2002), it is unlikely to have LSCD in our model. Here, we interpret our phenotype as a loss of limbal epithelial identity, which results in the overgrowth of conjunctival epithelial cells in the cornea.

In the anterior segment of the eye, lens and epithelial components of the eyelid, cornea, limbus, conjunctiva, lacrimal gland, and harderian gland are specified from OSE (Collinson et al., 2004; Chow and Lang, 2001). Spatiotemporal control of Wnt/β-catenin signaling is important for determining these specific fates within OSE. For example, activation of Wnt/β-catenin signaling in the early OSE prevents lens induction, whereas its ablation results in ectopic lens in peripheral SE (Smith et al., 2005; Miller et al., 2006; Kreslova et al., 2007). In addition to this, aberrant expression of β-catenin in presumptive corneal and conjunctival ectoderm disrupts its proper morphogenesis and results in ocular surface squamous metaplasia (Mizoguchi et al., 2015; Zhang et al., 2010). Receptors and ligands of Wnt/β-catenin signaling are consistently expressed throughout the OSE (Liu et al., 2003; Ang et al., 2004). However, active Wnt signaling is detected in early conjunctival epithelium and underlying mesenchyme of the cornea, limbus and conjunctiva, not in the presumptive corneal and limbal ectoderm (Liu et al., 2003; Gage et al., 2008; Zhang et al., 2015). This regional specificity could be necessary for the barrier function of limbal epithelium, which may be maintained by active repression of this pathway at various levels. It is further supported by the wide expression of Wnt inhibitors DKKs and Sfrp1 in the cornea during embryonic and postnatal development (Liu et al., 2003; Ang et al., 2004; Mukhopadhyay et al., 2006). The effect of aberrant Wnt signaling depends on the stage and region of activation; CE could undergo a fate switch to the epidermis (Zhang et al., 2010; Mukhopadhyay et al., 2006; Pearton et al., 2005; Joo et al., 2010; Meng et al., 2014) dedifferentiate to more progenitor-like cells (Zhang et al., 2010; Pearton et al., 2005), proliferate in an unregulated fashion (Mizoguchi et al., 2015; Zhang et al., 2010), or could inhibit stratification of CE cells (Zhang et al., 2015, 2019).

Pax6 directly regulates Wnt inhibitors such as Sfrp1, Sfrp2 and Dkk1 in the lens and central nervous system (Machon et al., 2010; Duparc et al., 2006; Kim et al., 2001). Moreover, elevated mRNA levels of Wnt inhibitors Wif1 and Sfpr2 were found in the cornea with Pax6 overexpression (Davis and Piatigorsky, 2011). Loss of OSE identity and bias towards conjunctival fate was reported for $Dkk2^{-/-}$ mutants similarly to our model. Taken together, we assume that Pax6 regulates the expression of Wnt inhibitor Dkk2 in the cornea. Further research needs to be carried out to see whether Dkk2 is regulated by Pax6 or not.

Finally, as we found keratinization of the cornea by PN23 in OSE cKO mutants, CE of $Dkk2^{-/-}$ mutants also exhibited keratinization and opaque cornea postnatally (Gage et al., 2008). In $Dkk2^{-/-}$ mice, keratinization is assumed as the consequence of irritations caused by ectopic

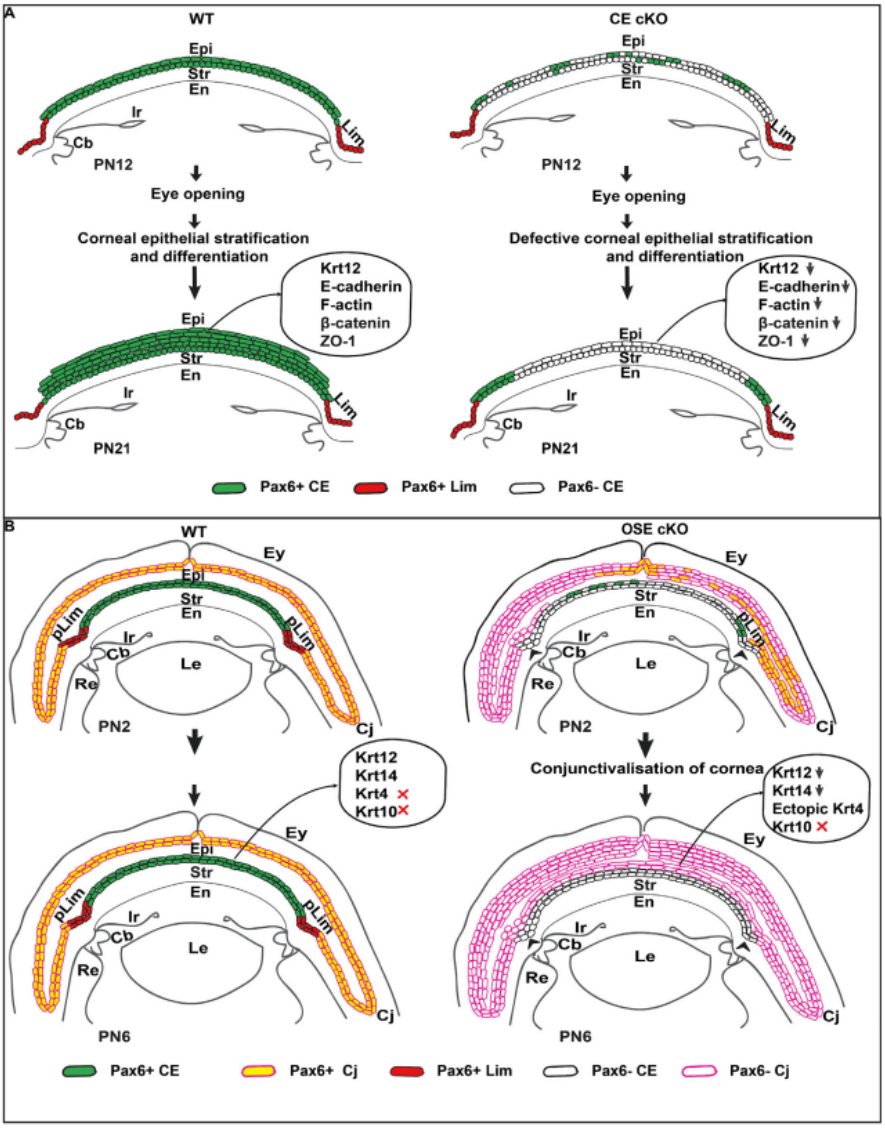

Fig. 7. Schematic summary of the plausible role of Pax6 in the developing cornea. **(A–B)** Schematic summary of the plausible function of Pax6 during mouse corneal development. **(A)** Depletion of Pax6 during postnatal corneal development in CE results in a thinner cornea with adhesion defects. **(B)** Depletion of Pax6 in OSE during early postnatal stages results in conjunctivalization of CE cells. Arrowheads in **(B)** indicate the position of the limbus in OSE cKO mutants.

eyelashes and infections raised due to eyelid defects (Gage et al., 2008). In our study, during early postnatal stages, ectopic Krt10^{+} cells were observed very rarely in OSE, and they exhibited a very narrow conjunctival sac, which could cause rubbing of CE with conjunctival epithelia. We believe that the complete fate switch to the epidermis seen at PN23 in OSE cKO mutants either occurred progressively during development as a disease response to the constant contact of CE with conjunctival epithelium or by chronic irritations by eyelashes after eye opening (Fig. S5).

In conclusion, conditional inactivation of Pax6 in OSE using *K14-Cre* revealed the role of Pax6 in maintaining the epithelial identity of limbal cells. We observed loss of corneal epithelial identity and migration of conjunctival cells to the cornea upon Pax6 loss in OSE (Fig. 7B).

Declaration of competing interest

The authors declare no competing interests.

Data availability

No data was used for the research described in the article.

Acknowledgements

We thank A. Cvekl for critical comments on the manuscript. This work was supported by a grant of the Czech Science Foundation (21–27364S). Mouse costs were partially covered by the Czech Center for Phenogenomics infrastructure supported by LM2018126, OP VaVpI CZ.1.05/2.1.00/19.0395, and CZ.1.05/1.1.00 /02.0109.

Appendix A. Supplementary data

Supplementary data to this article can be found online at https://doi.org/10.1016/j.ydbio.2022.08.006.

References

Ambati, B.K., et al., 2006. Corneal avascularity is due to soluble VEGF receptor-1. Nature 443 (7114), 993–997.
Andl, T., et al., 2004. Epithelial Bmpr1a regulates differentiation and proliferation in postnatal hair follicles and is essential for tooth development. Development 131 (10), 2257–2268.
Ang, S.J., et al., 2004. Spatial and temporal expression of Wnt and Dickkopf genes during murine lens development. Gene Expr. Patterns 4 (3), 289–295.
Antosova, B., et al., 2016. The gene regulatory network of lens induction is wired through meis-dependent shadow enhancers of Pax6. PLoS Genet. 12 (12), e1006441.
Ashery-Padan, R., et al., 2000. Pax6 activity in the lens primordium is required for lens formation and for correct placement of a single retina in the eye. Genes Dev. 14 (21), 2701–2711.
Behrens, J., et al., 1991. The E-cadherin promoter: functional analysis of a G.C-rich region and an epithelial cell-specific palindromic regulatory element. Proc. Natl. Acad. Sci. U. S. A. 88 (24), 11495–11499.
Campbell, H.K., Maiers, J.L., DeMali, K.A., 2017. Interplay between tight junctions & adherens junctions. Exp. Cell Res. 358 (1), 39–44.
Capaldo, C.T., Macara, I.G., 2007. Depletion of E-cadherin disrupts establishment but not maintenance of cell junctions in Madin-Darby canine kidney epithelial cells. Mol. Biol. Cell 18 (1), 189–200.
Chow, R.L., Lang, R.A., 2001. Early eye development in vertebrates. Annu. Rev. Cell Dev. Biol. 17, 255–296.
Collinson, J.M., et al., 2001. Primary defects in the lens underlie complex anterior segment abnormalities of the Pax6 heterozygous eye. Proc. Natl. Acad. Sci. U. S. A. 98 (17), 9688–9693.
Collinson, J.M., et al., 2002. Clonal analysis of patterns of growth, stem cell activity, and cell movement during the development and maintenance of the murine corneal epithelium. Dev. Dynam. 224 (4), 432–440.
Collinson, J.M., et al., 2004. Corneal development, limbal stem cell function, and corneal epithelial cell migration in the Pax6(+/-) mouse. Invest. Ophthalmol. Vis. Sci. 45 (4), 1101–1108.
Cotsarelis, G., et al., 1989. Existence of slow-cycling limbal epithelial basal cells that can be preferentially stimulated to proliferate: implications on epithelial stem cells. Cell 57 (2), 201–209.
Cvekl, A., Callaerts, P., 2017. PAX6: 25th anniversary and more to learn. Exp. Eye Res. 156, 10–21.
Cvekl, A., Tamm, E.R., 2004. Anterior eye development and ocular mesenchyme: new insights from mouse models and human diseases. Bioessays 26 (4), 374–386.
Davis, J., Piatigorsky, J., 2011. Overexpression of Pax6 in mouse cornea directly alters corneal epithelial cells: changes in immune function, vascularization, and differentiation. Invest. Ophthalmol. Vis. Sci. 52 (7), 4158–4168.
Davis, J., et al., 2003. Requirement for Pax6 in corneal morphogenesis: a role in adhesion. J. Cell Sci. 116 (Pt 11), 2157–2167.
Davis, J., et al., 2008. Gene expression of the mouse corneal crystallin Aldh3a1: activation by Pax6, Oct1, and p300. Invest. Ophthalmol. Vis. Sci. 49 (5), 1814–1826.
Delp, E.E., et al., 2015. Spatiotemporally regulated ablation of Klf4 in adult mouse corneal epithelial cells results in altered epithelial cell identity and disrupted homeostasis. Invest. Ophthalmol. Vis. Sci. 56 (6), 3549–3558.
Dhouailly, D., Pearton, D.J., Michon, F., 2014. The vertebrate corneal epithelium: from early specification to constant renewal. Dev. Dynam. 243 (10), 1226–1241.
Dora, N.J., et al., 2018. A conditional Pax6 depletion study with no morphological effect on the adult mouse corneal epithelium. BMC Res. Notes 11 (1), 705.
Douvaras, P., et al., 2013. Increased corneal epithelial turnover contributes to abnormal homeostasis in the Pax6(+/-) mouse model of aniridia. PLoS One 8 (8), e71117.
Dua, H.S., Azuara-Blanco, A., 2000. Limbal stem cells of the corneal epithelium. Surv. Ophthalmol. 44 (5), 415–425.
Duparc, R.H., et al., 2006. Pax6 is required for delta-catenin/neurojugin expression during retinal, cerebellar and cortical development in mice. Dev. Biol. 300 (2), 647–655.
Duparc, R.H., et al., 2007. Pax6 controls the proliferation rate of neuroepithelial progenitors from the mouse optic vesicle. Dev. Biol. 301 (2), 374–387.
Dwivedi, D.J., et al., 2005. Targeted deletion of AP-2alpha leads to disruption in corneal epithelial cell integrity and defects in the corneal stroma. Invest. Ophthalmol. Vis. Sci. 46 (10), 3623–3630.
Estivill-Torrus, G., et al., 2002. Pax6 is required to regulate the cell cycle and the rate of progression from symmetrical to asymmetrical division in mammalian cortical progenitors. Development 129 (2), 455–466.
Gage, P.J., et al., 2008. The canonical Wnt signaling antagonist DKK2 is an essential effector of PITX2 function during normal eye development. Dev. Biol. 317 (1), 310–324.
Genis-Galvez, J.M., 1966. Role of the lens in the morphogenesis of the iris and cornea. Nature 210 (5032), 209–210.
Genis-Galvez, J.M., Santos-Gutierrez, L., Rios-Gonzalez, A., 1967. Causal factors in corneal development: an experimental analysis in the chick embryo. Exp. Eye Res. 6 (1), 48–56.
Hay, E.D., 1980. Development of the vertebrate cornea. Int. Rev. Cytol. 63, 263–322.
Hennig, G., et al., 1996. Mechanisms identified in the transcriptional control of epithelial gene expression. J. Biol. Chem. 271 (1), 595–602.
Hill, R.E., et al., 1991. Mouse small eye results from mutations in a paired-like homeobox-containing gene. Nature 354 (6354), 522–525.
Hingorani, M., Hanson, I., van Heyningen, V., 2012. *Aniridia.* Eur J Hum Genet 20 (10), 1011–1017.
Hogan, B.L., et al., 1986. Small eyes (Sey): a homozygous lethal mutation on chromosome 2 which affects the differentiation of both lens and nasal placodes in the mouse. J. Embryol. Exp. Morphol. 97, 95–110.
Holm, P.C., et al., 2007. Loss- and gain-of-function analyses reveal targets of Pax6 in the developing mouse telencephalon. Mol. Cell. Neurosci. 34 (1), 99–119.
Ihnatko, R., et al., 2016. Congenital aniridia and the ocular surface. Ocul. Surf. 14 (2), 196–206.
Joo, J.H., et al., 2010. Disruption of mouse corneal epithelial differentiation by conditional inactivation of pnn. Invest. Ophthalmol. Vis. Sci. 51 (4), 1927–1934.
Kao, W.W., et al., 1996. Keratin 12-deficient mice have fragile corneal epithelia. Invest. Ophthalmol. Vis. Sci. 37 (13), 2572–2584.
Kim, A.S., et al., 2001. Pax-6 regulates expression of SFRP-2 and Wnt-7b in the developing CNS. J. Neurosci. 21 (5), RC132.
Klimova, L., Kozmik, Z., 2014. Stage-dependent requirement of neuroretinal Pax6 for lens and retina development. Development 141 (6), 1292–1302.
Klintworth, G.K., 2003. The molecular genetics of the corneal dystrophies–current status. Front. Biosci. 8, d687–713.
Koizumi, N., et al., 2000. Amniotic membrane as a substrate for cultivating limbal corneal epithelial cells for autologous transplantation in rabbits. Cornea 19 (1), 65–71.
Koroma, B.M., Yang, J.M., Sundin, O.H., 1997. The Pax-6 homeobox gene is expressed throughout the corneal and conjunctival epithelia. Invest. Ophthalmol. Vis. Sci. 38 (1), 108–120.
Kozmik, Z., 2008. The role of Pax genes in eye evolution. Brain Res. Bull. 75 (2–4), 335–339.
Kreslova, J., et al., 2007. Abnormal lens morphogenesis and ectopic lens formation in the absence of beta-catenin function. Genesis 45 (4), 157–168.
Kruse, F.E., et al., 1990. Conjunctival transdifferentiation is due to the incomplete removal of limbal basal epithelium. Invest. Ophthalmol. Vis. Sci. 31 (9), 1903–1913.
Kurpakus, M.A., Maniaci, M.T., Esco, M., 1994. Expression of keratins K12, K4 and K14 during development of ocular surface epithelium. Curr. Eye Res. 13 (11), 805–814.
Latta, L., et al., 2021. Pathophysiology of aniridia-associated keratopathy: developmental aspects and unanswered questions. Ocul. Surf. 22, 245–266.
Lavker, R.M., et al., 1991. Relative proliferative rates of limbal and corneal epithelia. Implications of corneal epithelial migration, circadian rhythm, and suprabasally located DNA-synthesizing keratinocytes. Invest. Ophthalmol. Vis. Sci. 32 (6), 1864–1875.
Lavker, R.M., et al., 2020. Corneal epithelial biology: lessons stemming from old to new. Exp. Eye Res. 198, 108094.
Leiper, L.J., et al., 2009. Control of patterns of corneal innervation by Pax6. Invest. Ophthalmol. Vis. Sci. 50 (3), 1122–1128.
Li, W., et al., 2007. Niche regulation of corneal epithelial stem cells at the limbus. Cell Res. 17 (1), 26–36.
Lima Cunha, D., et al., 2019. The spectrum of PAX6 mutations and genotype-phenotype correlations in the eye. Genes 10 (12).
Lin, Z., et al., 2013. A mouse model of limbal stem cell deficiency induced by topical medication with the preservative benzalkonium chloride. Invest. Ophthalmol. Vis. Sci. 54 (9), 6314–6325.
Liu, C.Y., et al., 1994. Characterization and chromosomal localization of the cornea-specific murine keratin gene Krt1.12. J. Biol. Chem. 269 (40), 24627–24636.
Liu, J.J., Kao, W.W., Wilson, S.E., 1999. Corneal epithelium-specific mouse keratin K12 promoter. Exp. Eye Res. 68 (3), 295–301.
Liu, H., et al., 2003. Characterization of Wnt signaling components and activation of the Wnt canonical pathway in the murine retina. Dev. Dynam. 227 (3), 323–334.
Lwigale, P.Y., 2015. Corneal development: different cells from a common progenitor. Prog Mol Biol Transl Sci 134, 43–59.
Machon, O., et al., 2010. Lens morphogenesis is dependent on Pax6-mediated inhibition of the canonical Wnt/beta-catenin signaling in the lens surface ectoderm. Genesis 48 (2), 86–95.
Makhani, L.F., Williams, T., West-Mays, J.A., 2007. Genetic analysis indicates that transcription factors AP-2alpha and Pax6 cooperate in the normal patterning and morphogenesis of the lens. Mol. Vis. 13, 1215–1225.
Mandell, K.J., et al., 2006. Antibody blockade of junctional adhesion molecule-A in rabbit corneal endothelial tight junctions produces corneal swelling. Invest. Ophthalmol. Vis. Sci. 47 (6), 2408–2416.

Marquardt, T., et al., 2001. Pax6 is required for the multipotent state of retinal progenitor cells. Cell 105 (1), 43–55.
Masse, K., et al., 2007. Purine-mediated signalling triggers eye development. Nature 449 (7165), 1058–1062.
Meng, Q., et al., 2014. Eyelid closure in embryogenesis is required for ocular adnexa development. Invest. Ophthalmol. Vis. Sci. 55 (11), 7652–7661.
Miller, L.A., et al., 2006. Optic cup and facial patterning defects in ocular ectoderm beta-catenin gain-of-function mice. BMC Dev. Biol. 6, 14.
Mizoguchi, S., et al., 2015. Disruption of eyelid and cornea morphogenesis by epithelial beta-catenin gain-of-function. Mol. Vis. 21, 793–803.
Mort, R.L., et al., 2011. Effects of aberrant Pax6 gene dosage on mouse corneal pathophysiology and corneal epithelial homeostasis. PLoS One 6 (12), e28895.
Moyer, P.D., et al., 1996. Conjunctival epithelial cells can resurface denuded cornea, but do not transdifferentiate to express cornea-specific keratin 12 following removal of limbal epithelium in mouse. Differentiation 60 (1), 31–38.
Mukhopadhyay, M., et al., 2006. Dkk2 plays an essential role in the corneal fate of the ocular surface epithelium. Development 133 (11), 2149–2154.
Nagasaki, T., Zhao, J., 2003. Centripetal movement of corneal epithelial cells in the normal adult mouse. Invest. Ophthalmol. Vis. Sci. 44 (2), 558–566.
Nees, D.W., et al., 2002. Structurally normal corneas in aldehyde dehydrogenase 3a1-deficient mice. Mol. Cell Biol. 22 (3), 849–855.
Nishida, K., et al., 1995. Ocular surface abnormalities in aniridia. Am. J. Ophthalmol. 120 (3), 368–375.
Nishida, K., et al., 1997. Isolation and chromosomal localization of a cornea-specific human keratin 12 gene and detection of four mutations in Meesmann corneal epithelial dystrophy. Am. J. Hum. Genet. 61 (6), 1268–1275.
Ooshio, T., et al., 2010. Involvement of the interaction of afadin with ZO-1 in the formation of tight junctions in Madin-Darby canine kidney cells. J. Biol. Chem. 285 (7), 5003–5012.
Pajoohesh-Ganji, A., et al., 2012. Corneal goblet cells and their niche: implications for corneal stem cell deficiency. Stem Cell. 30 (9), 2032–2043.
Pearton, D.J., Yang, Y., Dhouailly, D., 2005. Transdifferentiation of corneal epithelium into epidermis occurs by means of a multistep process triggered by dermal developmental signals. Proc. Natl. Acad. Sci. U. S. A. 102 (10), 3714–3719.
Puangsricharern, V., Tseng, S.C., 1995. Cytologic evidence of corneal diseases with limbal stem cell deficiency. Ophthalmology 102 (10), 1476–1485.
Ramaesh, T., et al., 2003. Corneal abnormalities in Pax6+/- small eye mice mimic human aniridia-related keratopathy. Invest. Ophthalmol. Vis. Sci. 44 (5), 1871–1878.
Ramaesh, T., et al., 2005. Developmental and cellular factors underlying corneal epithelial dysgenesis in the Pax6+/- mouse model of aniridia. Exp. Eye Res. 81 (2), 224–235.
Ramaesh, T., et al., 2006. Increased apoptosis and abnormal wound-healing responses in the heterozygous Pax6+/- mouse cornea. Invest. Ophthalmol. Vis. Sci. 47 (5), 1911–1917.
Raviv, S., et al., 2014. PAX6 regulates melanogenesis in the retinal pigmented epithelium through feed-forward regulatory interactions with MITF. PLoS Genet. 10 (5), e1004360.
Sasamoto, Y., et al., 2016. PAX6 isoforms, along with reprogramming factors, differentially regulate the induction of cornea-specific genes. Sci. Rep. 6, 20807.
Secker, G.A., Daniels, J.T., 2008. Corneal epithelial stem cells: deficiency and regulation. Stem Cell Rev. 4 (3), 159–168.
Shapiro, M.S., Friend, J., Thoft, R.A., 1981. Corneal re-epithelialization from the conjunctiva. Invest. Ophthalmol. Vis. Sci. 21 (1 Pt 1), 135–142.
Sivak, J.M., et al., 2004. Transcription factors Pax6 and AP-2alpha interact to coordinate corneal epithelial repair by controlling expression of matrix metalloproteinase gelatinase B. Mol. Cell Biol. 24 (1), 245–257.
Smith, A.N., et al., 2005. The duality of beta-catenin function: a requirement in lens morphogenesis and signaling suppression of lens fate in periocular ectoderm. Dev. Biol. 285 (2), 477–489.
Soriano, P., 1999. Generalized lacZ expression with the ROSA26 Cre reporter strain. Nat. Genet. 21 (1), 70–71.
Sridhar, M.S., 2018. Anatomy of cornea and ocular surface. Indian J. Ophthalmol. 66 (2), 190–194.
Srinivas, S.P., 2010. Dynamic regulation of barrier integrity of the corneal endothelium. Optom. Vis. Sci. 87 (4), E239–E254.
Stephens, D.N., et al., 2013. The Ets transcription factor EHF as a regulator of cornea epithelial cell identity. J. Biol. Chem. 288 (48), 34304–34324.
Sugrue, S.P., Zieske, J.D., 1997. ZO1 in corneal epithelium: association to the zonula occludens and adherens junctions. Exp. Eye Res. 64 (1), 11–20.
Sunny, S.S., et al., 2020. Generation and characterization of Aldh3-Cre transgenic mice as a tool for conditional gene deletion in postnatal cornea. Sci. Rep. 10 (1), 9083.
Swamynathan, S.K., 2013. Ocular surface development and gene expression. J Ophthalmol 2013, 103947.
Swamynathan, S.K., et al., 2007. Conditional deletion of the mouse Klf4 gene results in corneal epithelial fragility, stromal edema, and loss of conjunctival goblet cells. Mol. Cell Biol. 27 (1), 182–194.
Swamynathan, S.K., Davis, J., Piatigorsky, J., 2008. Identification of candidate Klf4 target genes reveals the molecular basis of the diverse regulatory roles of Klf4 in the mouse cornea. Invest. Ophthalmol. Vis. Sci. 49 (8), 3360–3370.
Thoft, R.A., Friend, J., 1983. The X, Y, Z hypothesis of corneal epithelial maintenance. Invest. Ophthalmol. Vis. Sci. 24 (10), 1442–1443.
Tiwari, A., et al., 2017. KLF4 plays an essential role in corneal epithelial homeostasis by promoting epithelial cell fate and suppressing epithelial-mesenchymal transition. Invest. Ophthalmol. Vis. Sci. 58 (5), 2785–2795.
Tseng, S.C., 1989. Concept and application of limbal stem cells. Eye 3 (Pt 2), 141–157.
Tseng, S.C.G., et al., 2020. Niche regulation of limbal epithelial stem cells: HC-HA/PTX3 as surrogate matrix niche. Exp. Eye Res. 199, 108181.
van Raamsdonk, C.D., Tilghman, S.M., 2000. Dosage requirement and allelic expression of PAX6 during lens placode formation. Development 127 (24), 5439–5448.
Vincent, A.L., Patel, D.V., McGhee, C.N., 2005. Inherited corneal disease: the evolving molecular, genetic and imaging revolution. Clin. Exp. Ophthalmol. 33 (3), 303–316.
Walker, H., Akula, M., West-Mays, J.A., 2020. Corneal development: role of the periocular mesenchyme and bi-directional signaling. Exp. Eye Res. 201, 108231.
Walther, C., Gruss, P., 1991. Pax-6, a murine paired box gene, is expressed in the developing CNS. Development 113 (4), 1435–1449.
West-Mays, J.A., et al., 1999. AP-2alpha transcription factor is required for early morphogenesis of the lens vesicle. Dev. Biol. 206 (1), 46–62.
West-Mays, J.A., et al., 2003. Positive influence of AP-2alpha transcription factor on cadherin gene expression and differentiation of the ocular surface. Differentiation 71 (3), 206–216.
Zhang, Y., et al., 2010. Aberrant expression of a beta-catenin gain-of-function mutant induces hyperplastic transformation in the mouse cornea. J. Cell Sci. 123 (Pt 8), 1285–1294.
Zhang, Y., et al., 2015. Wnt/beta-catenin signaling modulates corneal epithelium stratification via inhibition of Bmp4 during mouse development. Development 142 (19), 3383–3393.
Zhang, L., et al., 2019. Aberrant expression of a stabilized beta-catenin mutant in keratocytes inhibits mouse corneal epithelial stratification. Sci. Rep. 9 (1), 1919.
Zieske, J.D., 2000. Expression of cyclin-dependent kinase inhibitors during corneal wound repair. Prog. Retin. Eye Res. 19 (3), 257–270.
Zieske, J.D., 2004. Corneal development associated with eyelid opening. Int. J. Dev. Biol. 48 (8–9), 903–911.

Supplementary Information

Multiple roles of Pax6 in corneal limbal epithelial cells and maturing epithelial cell adhesion

Sweetu Susan Sunny[a], Jitka Lachova[a], Naoko Dupacova[a], Zbynek Kozmik[a,*]

[a] Laboratory of Transcriptional Regulation, Institute of Molecular Genetics of the Czech Academy of Sciences, Videnska 1083, Praha 4, 142 20, Czech Republic

[*] Corresponding author: Institute of Molecular Genetics of the Czech Academy of Sciences, Videnska 1083, Praha 4, 142 20, Czech Republic

E-mail: kozmik@img.cas.cz

Phone number: ++420241062146

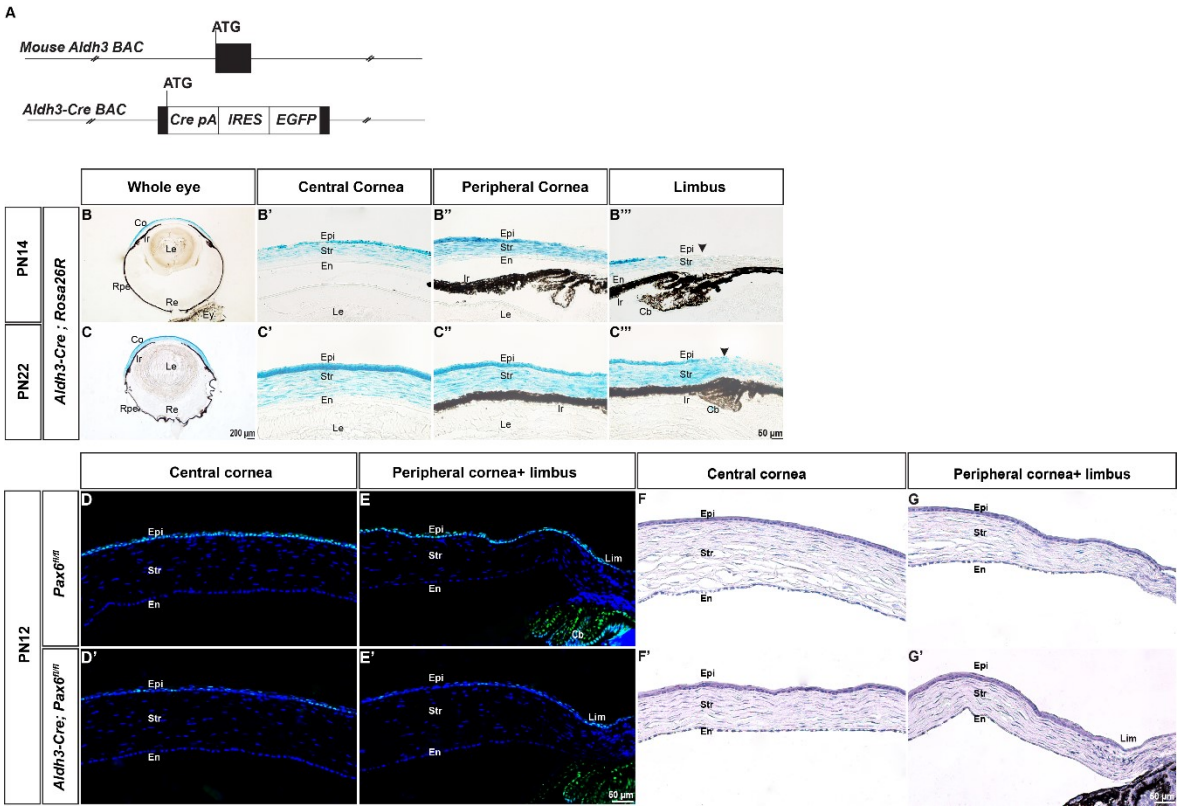

Supplementary Figure 1: Characterization of Cre recombinase activity of *Aldh3-Cre* transgenic mice and Pax6 deletion pattern in the cornea of CE cKO mutants

(A) To generate *Aldh3-Cre,* BAC containing regulatory sequences of the Aldh3 gene was modified by BAC recombineering. A cassette containing *Cre* recombinase (Cre-pA) and *EGFP* linked by Internal ribosomal entry point (*IRES*) sequence was integrated into the first translational start site (ATG) of the *Aldh3* gene. **(B-C”’)**The *Aldh3-Cre* activity was visualized using the *Rosa26R* reporter strain. The β- Gal activity in frontal sections of the eye at **(B-B’’’)** PN14 and **(C-C”’)** PN22. **(D-E’)** Coronal sections of wildtype (*Pax6$^{fl/fl}$*) and CE cKO (*Aldh3-Cre; Pax6$^{fl/fl}$*) stained with Pax6 antibody at PN12. Decreased levels of Pax6 in CE at PN12 **(D’, E’)** in the CE cKO mutant compared to **(D, E)** age-matched control. **(F-G’)** Hematoxylin and eosin staining in frontal sections of wildtype (*Pax6$^{fl/fl}$*) and CE cKO (*Aldh3-Cre; Pax6$^{fl/fl}$*) mutant at PN12. No obvious difference is found in CE morphology. Abbreviations used: Co, Cornea; Le, Lens: Re, Retina; Rpe, Retinal pigment epithelium. En, Corneal endothelium; Str, Corneal stroma; Epi, Corneal epithelium; Cb, Ciliary body; Ir, Iris; Lim, Limbal epithelium Scale bar: **(B, C)** – 200µm **(B’-G’)** – 50µm.

.

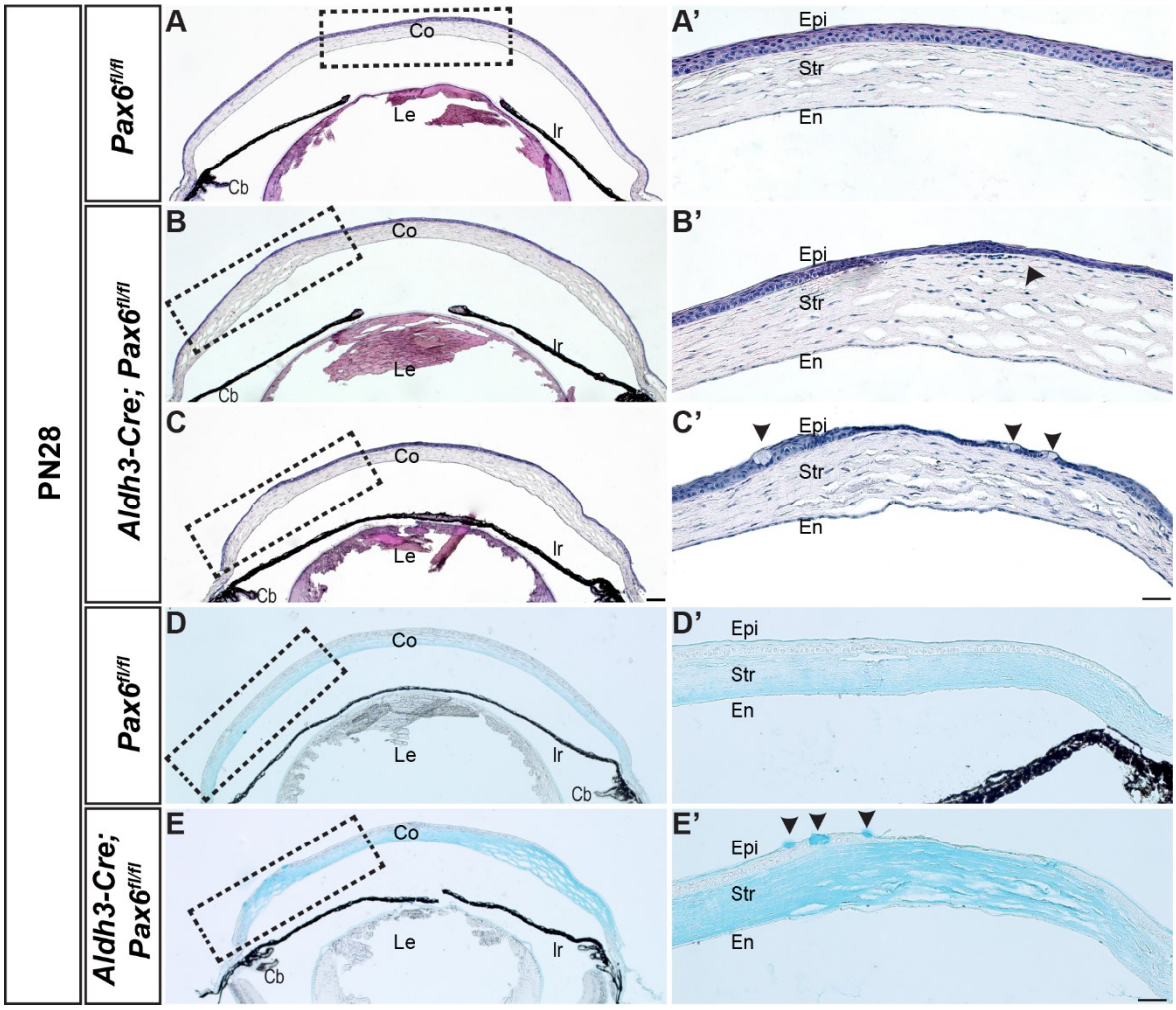

Supplementary Figure 2: Morphological changes in the cornea at PN28

(A-E') Hematoxylin and eosin staining and alcian blue staining of eyes of the control (*Pax6*$^{fl/fl}$) and CE cKO mutant (*Aldh3-Cre; Pax6*$^{fl/fl}$) at PN28. **(A-A')** In contrast to control mice, **(B-B')** the CE cKO mutant has a disturbed stroma with an increased number of keratocytes at regions with the loss of Pax6. **(C-C')** Goblet cells are absent in control CE cells, while the CE cKO mutant has ectopic goblet cells in CE cells. **(D-E')** Presence of globet cells in CE of CE cKO mutants are confirmed by Alcian blue staining **(A, B, C)** Dashed rectangle in the whole cornea indicates the position of the region of interest shown in higher magnification panels. Black arrowheads in **B'** and **C'** indicates keratocytes in the stroma and goblet cells, respectively. Scale bar: **(A, B, C, D, E)** -100µm, **(A', B', C', D', E')** – 50µm.

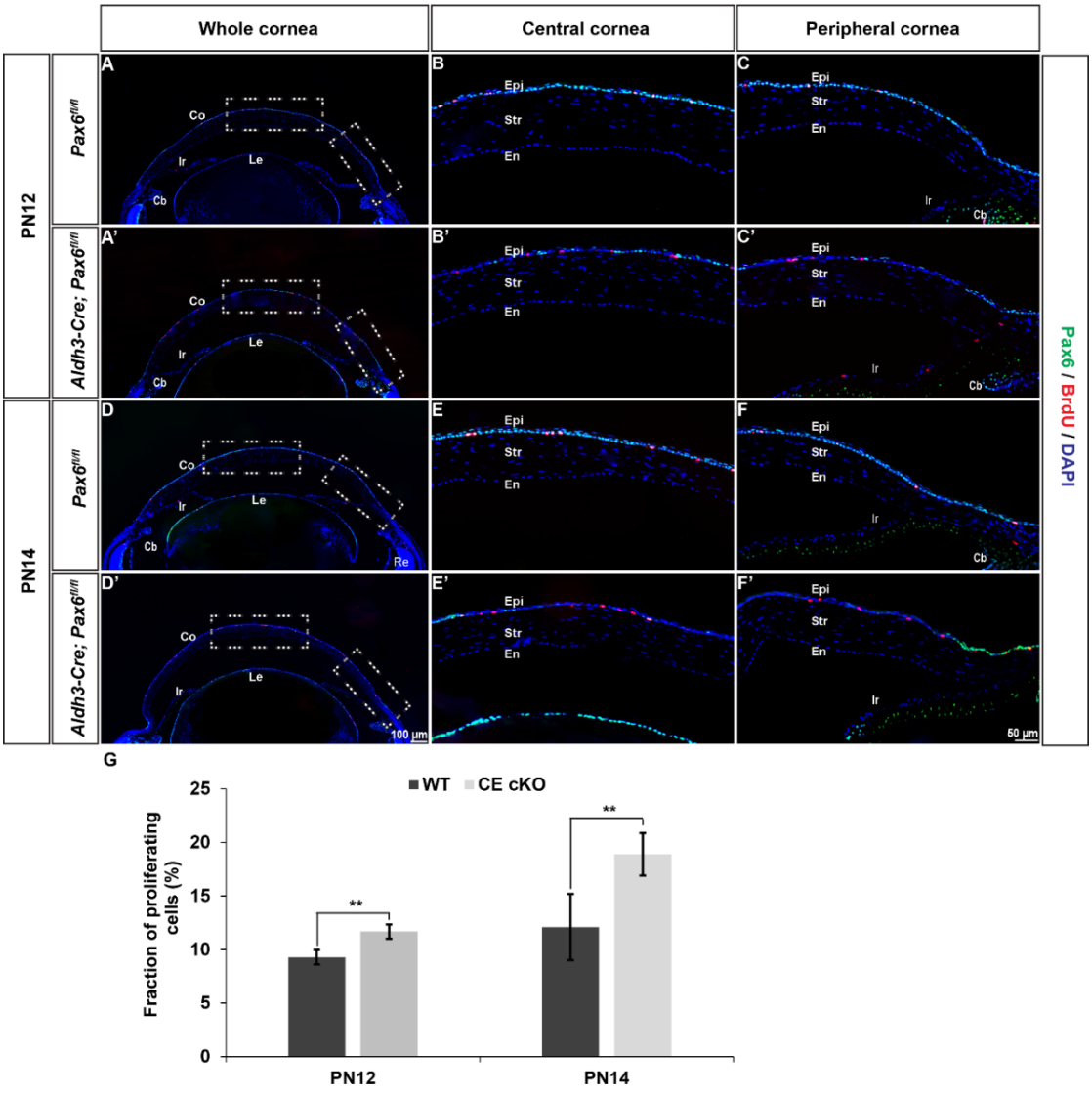

Supplementary Figure 3: Proliferation in CE cKO mutant corneas

(A-F') Coronal sections of control (*Pax6*$^{fl/fl}$) and CE cKO mutants (*Aldh3-Cre; Pax6*$^{fl/fl}$) were stained with Pax6 and BrdU antibodies at PN12 and PN14. CE of CE cKO mutants at **(A-C')** PN12 and **(D-F')** PN14 has a slight increase in the number of BrdU^{+} cells in comparison to control corneas. **(G)** Quantification of S-phase cells determined by the proportion of BrdU^{+} cells against the total number of DAPI^{+} cells in the basal layer. Error bars indicate standard deviation. The p-values are calculated by Student's t-test. ** $p < 0.01$ Scale bar: (**A-F'**) – 50 µm

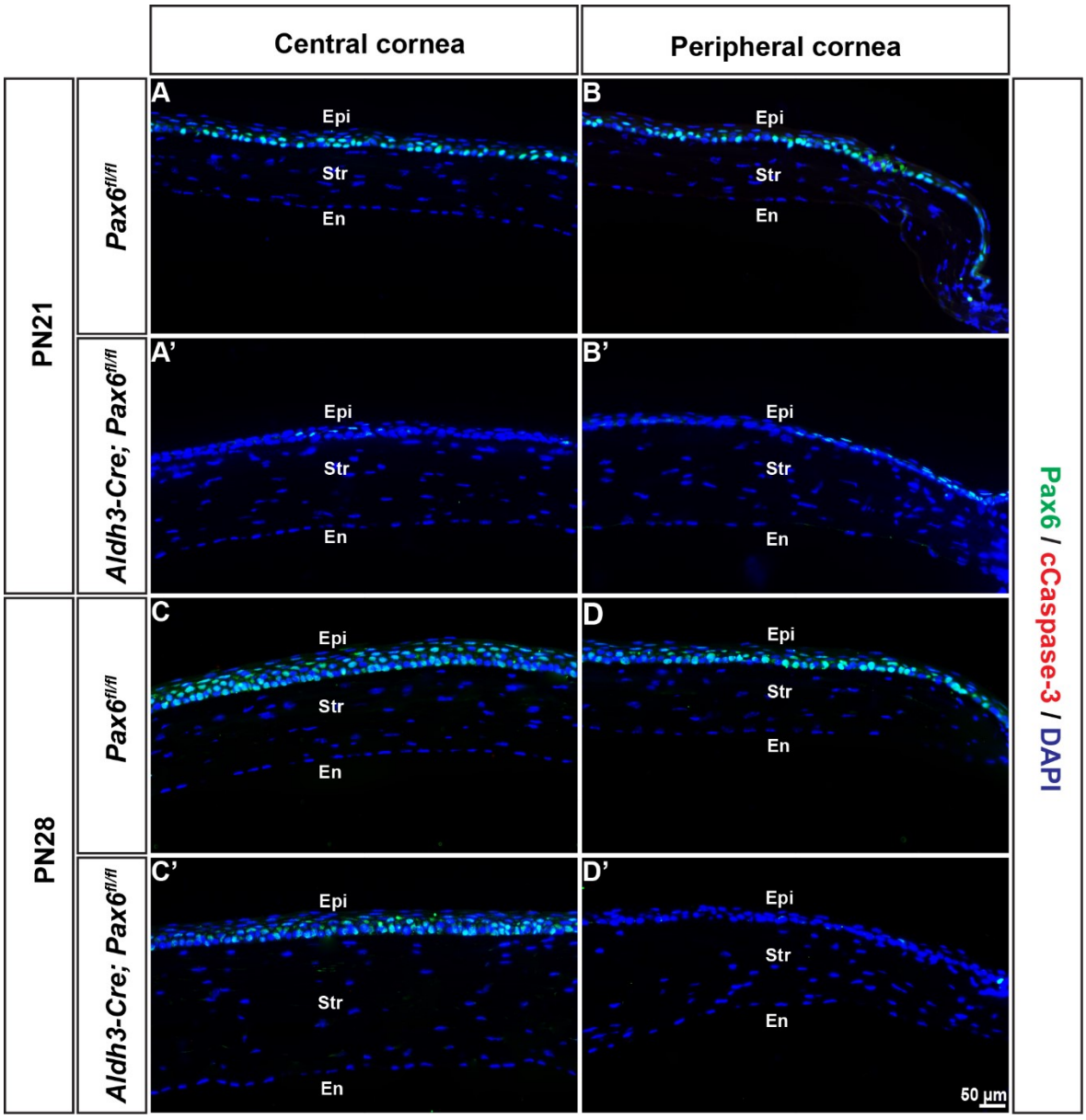

Supplemenatry Figure 4 : Apoptosis in CE cKO mutants

(A-D') Coronal sections of control (*Pax6*$^{fl/fl}$) and OSE cKO mutants (*K14-Cre; Pax6*$^{fl/fl}$) were stained with cCaspase 3 and Pax6 at indicated postnatal stages. No significant changes are found in CE cKO mutants in comparison to controls. Scale bar: (**A-D'**) – 50 µm

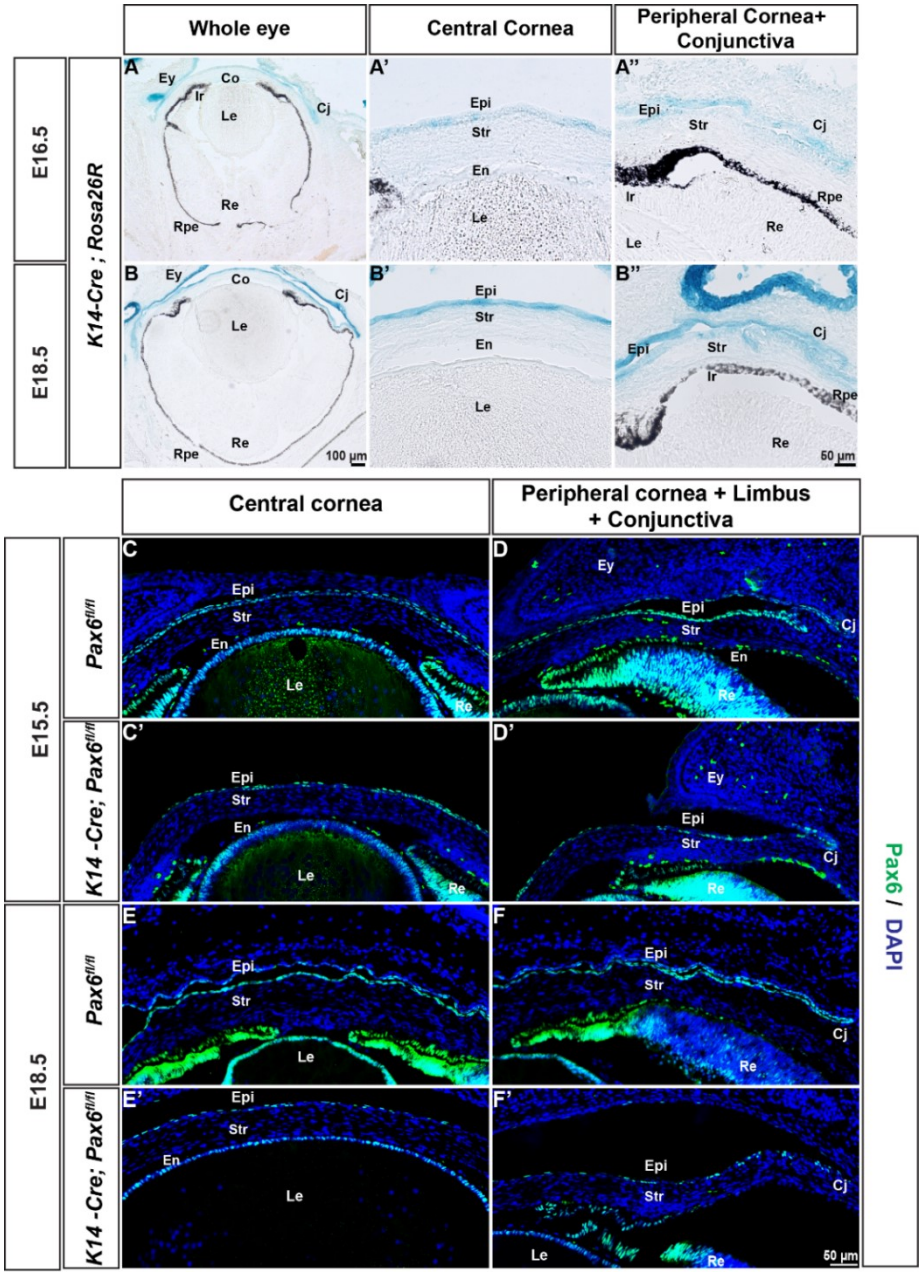

Supplemenatry Figure 5 : Characterization of Cre recombinase activity in *K14-Cre* transgenic mice and Pax6 deletion pattern in the OSE cKO mutants (A-D'') The *K14-Cre* activity was visualized by the *Rosa26R* reporter strain. X-gal staining in coronal sections at **(A-A'')** E14.5, **(B-B")** E16.5, **(C-C'')** E18.5 and **(D-D")** PN2. **(E-H')** Pax6 immunostaining in the eyes of OSE cKO mutants (*K14-Cre; Pax6$^{fl/fl}$*) and age-matched controls (*Pax6$^{fl/fl}$*). **(E, E')** Pax6 staining is retained at E15.5 in CE cells of the OSE cKO mutants **(F, F'),** while it is decreased towards the presumptive conjunctiva compared to the control**. (G, G')** Mosaic expression of Pax6 is observed in CE cells of OSE cKO mutants at E18.5 **(H, H')**, while it is downregulated at presumptive conjunctival epithelial cells. Scale bar: (**A, B, C, D**) – 100 µm, (**A', A'', B', B'', C', C''**) – 50 µm, **(E-H') –** 50 µm.

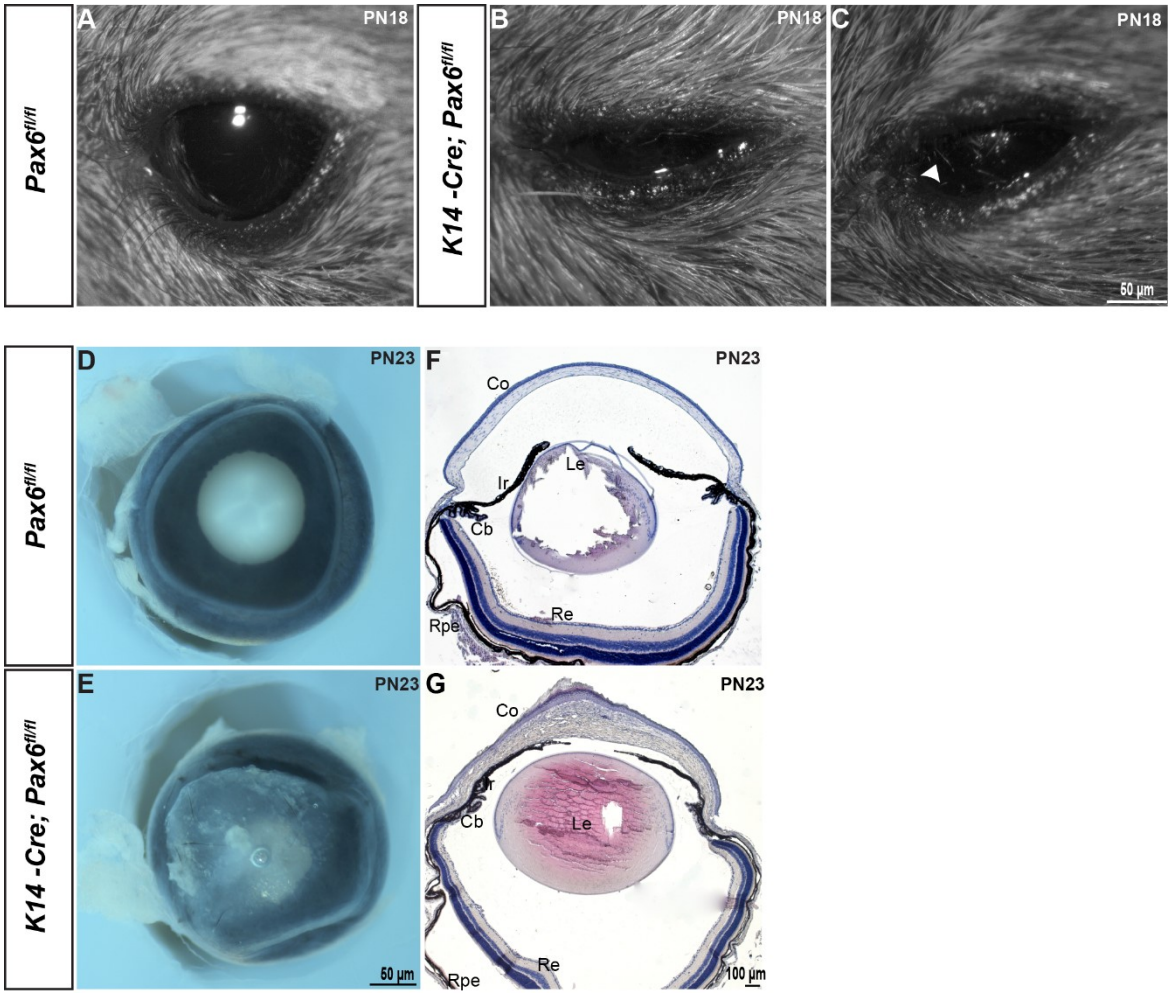

Supplementary Figure 6: Morphological defects in OSE cKO mutants after eye opening

(A) Compared with control (*Pax6*$^{fl/fl}$) eyes, OSE cKO mutants (*K14-Cre; Pax6*$^{fl/fl}$) have **(B, C)** smaller palpebral space and **(C)** eyelashes touching the corneal surface at PN18. **(D, E)** Control eyes at PN23 are transparent, while OSE cKO mutants have opaque eyes. **(F, G)** H&E stained coronal sections of eyes at PN23 of control and OSE cKO mutants. **(G)** In contrast to **(F)** 4-6 stratified layers in the control epithelium, there is extensive thickening and keratinization of central CE in OSE cKO mutants. **(C)** White arrowhead indicates eyelashes touching the ocular surface. Scale bar: **(A, B, C, D, E)** – 50 µm, **(F, G) –** 100 µm.

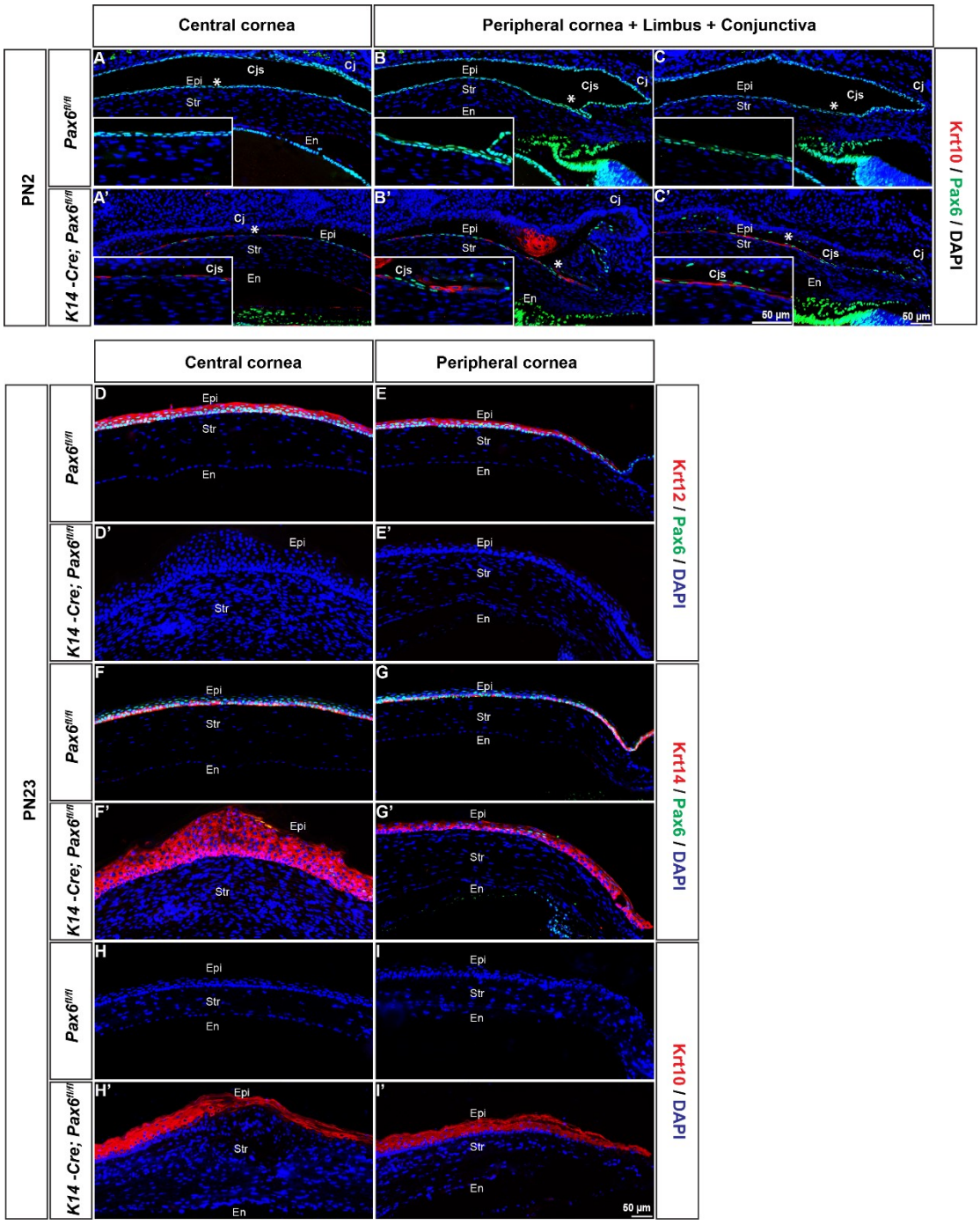

Supplementary Figure 7: Altered keratin expression and switch in developmental fate to epidermis after eye opening

(A-I') Coronal sections of control (*Pax6$^{fl/fl}$*) and OSE cKO mutants (*K14-Cre; Pax6$^{fl/fl}$*) were stained with indicated antibodies at mentioned postnatal stages. (**A-C'**) Krt10^{+} cells in CE and conjunctival epithelium of OSE cKO mutants at PN2. **(D-E')** Krt12 expression is lost in OSE cKO mutants compared to the control. **(F-G')** Krt14 expression is expanded to all layers in OSE cKO mutants. **(H-I')** Ectopic expression of Krt10 in CE cells of OSE cKO mutants. Inserts in (**A-C'**) are higher magnification of (*) indicated positions. Abbreviations used: Cjs, Conjunctival sac Scale bar: **(A-I')** – 50 µm

Antibody	Host	Dilution	Source
Pax6	Rabbit	1:1000	Covance (PRP-278P)
K12	Goat	1:300	Santa Cruz Biotec Inc, sc-17101[1, 2]
K14	Mouse	1:500	Thermo fisher scientific, LL02,MA5-11599
K10	Mouse	1:500	Thermo fisher scientific, DE-K10,MA5-13705
K4	Mouse	1:100	Thermo fisher scientific, 6B10,MA1-35558
E-cadherin	Rat	1:300	Thermo fisher scientific, 13-1900[3, 4]
β-catenin	Rabbit	1:1000	Sigma, C2206[5, 6]
ZO-1	Rabbit	1:250	Thermo fisher scientific, 61-7300[7, 8]

Supplementary Table S1: Primary antibodies used

References

1. Boehlke, C.S., et al., *Cytokeratin 12 in human ocular surface epithelia is the antigen reactive with a commercial anti-Galpha q antibody.* Mol Vis, 2004. **10**: p. 867-73.
2. Dora, N., et al., *PAX6 dosage effects on corneal development, growth, and wound healing.* Dev Dyn, 2008. **237**(5): p. 1295-306.
3. Padmanaban, V., et al., *E-cadherin is required for metastasis in multiple models of breast cancer.* Nature, 2019. **573**(7774): p. 439-444.
4. Oh, J.H., et al., *Circadian Clock Is Involved in Regulation of Hepatobiliary Transport Mediated by Multidrug Resistance-Associated Protein 2.* J Pharm Sci, 2017. **106**(9): p. 2491-2498.
5. Tiwari, A., et al., *KLF4 Plays an Essential Role in Corneal Epithelial Homeostasis by Promoting Epithelial Cell Fate and Suppressing Epithelial-Mesenchymal Transition.* Invest Ophthalmol Vis Sci, 2017. **58**(5): p. 2785-2795.
6. Kumper, S. and A.J. Ridley, *p120ctn and P-cadherin but not E-cadherin regulate cell motility and invasion of DU145 prostate cancer cells.* PLoS One, 2010. **5**(7): p. e11801.
7. Tanaka, K., et al., *Reduced Post-ischemic Brain Injury in Transient Receptor Potential Vanilloid 4 Knockout Mice.* Front Neurosci, 2020. **14**: p. 453.
8. Dodd, W.S., et al., *NLRP3 inhibition attenuates early brain injury and delayed cerebral vasospasm after subarachnoid hemorrhage.* J Neuroinflammation, 2021. **18**(1): p. 163.

6.3 Investigating the effect of the *Ovol2* promoter mutations and their possible association with posterior polymorphous corneal dystrophy (PPCD) 1 in the mouse model.

Corneal dystrophies are a diverse group of inherited disorders with heterogeneous genetic backgrounds. PPCD is a rare, autosomal dominant corneal dystrophy characterized by an abnormal CEn, which leads to corneal opacity, secondary glaucoma and consequently blindness (Evans et al., 2015; Krachmer, 1985; Weiss et al., 2015). PPCD1 is caused by mutations in the evolutionarily conserved promoter region of the *OVOL2* gene causing its upregulation in the CEn (Davidson et al., 2016). Since the disease mechanism leading to PPCD1 phenotypes is not well understood, it is advantageous to model PPCD in an appropriate experimental system.

In an attempt for this, using the CRISPR-Cas9 system, we generated allelic series of mice carrying *Ovol2* promoter mutations, including human PPCD1 pathogenic variant c.-307T>C. Surprisingly, not all mutations resulted in ocular phenotypes in mice, despite of high degree of conservation within the mammals. Four distinct mutations in the distal promoter region did not alter the *Ovol2* mRNA expression as well as did not exhibit any ocular phenotype. Contrary to this, the base substitution of c.-307T>C resulted in the upregulation of (mRNA) *Ovol2* expression in CEn but did not lead to any characteristics of endothelial dystrophy. Similarly, despite increased *Ovol2* mRNA levels, mice carrying a deletion of the Ovol1/Ovol2 binding site located next to the c.-307T>C mutation did not exhibit any signs of endothelial abnormalities. Collectively, even though *Ovol2* mRNA levels are upregulated in CEn of c.-307T>C and c.-307_-320del mutations, the absence of endothelial dystrophy in mice suggest the species-specific variation in CEn genesis. Interestingly, a minority of the c.-307T>C and c.-307_-320del mutants exhibited a myriad of phenotypes including iridocorneal adhesion, persistent hyperplastic primary vitreous (PHPV), and dysplastic retina, implicating the possible role of Ovol2 in early eye development.

My contribution to this work: I generated the majority of the experimental data presented in this study, except for analysis using SD-OCT. I wrote the manuscript prepared for submission, presented on pages 62- 83 of this thesis

Investigating the effect of the *Ovol2* promoter mutations and their possible association with Posterior polymorphous corneal dystrophy (PPCD) 1 in the mouse model.

Sweetu Susan Sunny[a], Jitka Lachova[a], Petr Kasparek[b], Jan Prochazka[b], Radislav Sedlacek[b], Petra Liskova[c], Zbynek Kozmik[a*]

[a] Laboratory of Transcriptional Regulation, Institute of Molecular Genetics of the Czech Academy of Sciences, Videnska 1083, Praha 4, 142 20, Czech Republic

[b] Czech Centre for Phenogenomics and Laboratory of Transgenic Models of Diseases, Institute of Molecular Genetics of the CAS, Vestec, Czech Republic.

[c] Department of Ophthalmology, First Faculty of Medicine, Charles University in Prague and General University Hospital in Prague, U Nemocnice 2, Prague 128 08, Czech Republic

[*] Corresponding author: Institute of Molecular Genetics of the Czech Academy of Sciences, Videnska 1083, Praha 4, 142 20, Czech Republic

E-mail: kozmik@img.cas.cz

Phone number: +420241062146

Abstract

Pathogenic variants in a highly conserved region of the *OVOL2* promoter cause autosomal dominant corneal endothelial dystrophies. The molecular basis of the phenotype appears to be the upregulation of the endothelial *OVOL2* mRNA. Here we produced an allelic series of *Ovol2* promoter mutations in the mouse model including the c.-307T>C mutation present in the affected human PPCD1 individuals. Despite the high evolutionary conservation of the *Ovol2* promoter only some alterations of its sequence resulted in phenotypic consequences in mice. Four independent mutations in the distal part of the mouse *Ovol2* promoter had no significant effect on endothelial *Ovol2* mRNA level and did not produce any ocular phenotype. In contrast, the mutation c.-307T>C resulted in a strong increase of *Ovol2* gene expression in the corneal endothelium, and a small fraction of adult c.-307T>C heterozygotes developed distinct ocular phenotypes such as irido corneal adhesion, corneal opacity and persistent hyperplastic primary vitreous (PHPV). Interestingly, 50% of heterozygotes and 91% of the homozygotes developed phenotypes associated with iris and PHPV already at embryonic stages. We noticed that the c.-307T>C mutation is located next to the Ovol1/Ovol2 transcription factor binding site implicated in Ovol2 autoregulation. Mice carrying an allele with a deletion encompassing the Ovol2 binding site -307_-320del showed significant *Ovol2* gene upregulation in the cornea endothelium and exhibited phenotypes similar to c.-307T>C mutation.

In conclusion, although the mutations c.-307T>C and -307_-320del lead to a comparably strong increase in endothelial *Ovol2* expression as found previously in PPCD1 patients, endothelial dystrophy was not observed in the mouse model, implicating species-specific differences in endothelial cell biology. The emergence of the defined set of dominant ocular phenotypes associated with *Ovol2* promoter mutations in mice nonetheless argues for the possible role of this gene in eye development and/or disease.

Keywords: Eye, Gene, Cornea, PPCD, Ovol2

Introduction

Corneal dystrophies are a group of rare genetic disorders that affects single or several layers of the cornea. Posterior polymorphous corneal dystrophy (PPCD) is an autosomal dominant disorder that is associated primarily with changes in corneal endothelium (CEn). The acuteness and phenotype of PPCD are variable from mild symptoms such as band-like, geographic and vesicular lesions to corneal endothelial failure necessitating surgical intervention /corneal transplantation [1-4]. With PPCD, CEn cells exhibit several epithelial-like characteristics, including the expression of keratin, numerous desmosomes and microvilli. These abnormal endothelial cells can proliferate and migrate through the trabecular meshwork and the peripheral iris surface, which further results in iridocorneal adhesions, iris atrophies and raised intraocular pressure, leading to glaucoma [1, 5-7].

The genetic causation of PPCD is implicated to four different genes. PPCD4 is caused by the mutations in the regulatory region of *GRHL2* gene [8], PPCD3 is arised by the ZEB1 haploinsufficiency due to truncation or deletions of *ZEB1* gene [3, 9-11] and PPCD2 associated with non-synonymous mutations in *COL8A2* gene [12], and PPCD1 with mutations in the promoter region of *OVOL2* gene [4, 13]. Genes that are associated with PPCD encode a group of transcription factors that mediate cell state transitions, such as epithelial-to-mesenchymal transition (EMT) and mesenchymal-to-epithelial transition (MET). ZEB1 (Zinc finger E box binding homeobox 1) promotes EMT and is expressed in human CEn, whereas GRHL2 (Grainy head-like transcription factor 2) and OVOL2 (Ovo–like zinc finger 2) are direct transcriptional repressors of ZEB1 and induces MET [14-19]. Additionally, ZEB1 also suppresses the expression of these genes [15, 20, 21]. Accordingly, the mutations identified in PPCD are causing a shift in OVOL2-ZEB1- GRHL2 axis [4, 8].

Whole genome sequencing analysis of a large British kindred family with PPCD1 identified a heterozygous duplication of 22 bp within the *OVOL2* promoter [4, 6], whereas a c.-370T>C transition was associated with 16 Czech families with PPCD1 [4, 22, 23]. Further screening identified two more mutations in the proximal *OVOL2* promoter region of British families, c.-307T>C and c.-274T>G [4, 13]. Despite this, the OVOL2 expression is not normally found in fetal and adult human CEn. Pathogenic variants of PPCD1 resulted in increased *OVOL2* promoter activity in vitro, which suggested the possibility of its ectopic expression in the CEn [4]. Transcriptomic analysis of RNA-seq data on CEn of PPCD1 patients with c.-307T>C confirmed ectopic expression of *OVOL2* and *GRHL2* and demonstrated decreased expression of *ZEB1*, which indicated the deregulation of OVOL2-ZEB1-GRHL2 axis [24].

Intriguingly, *OVOL2* proximal promoter region encompassing these mutations is highly conserved within mammals [4]. It has been shown that this region has binding sites for multiple transcription factors present in CEn and these mutations are altering their binding sites. Thus it has been hypothesised that the ectopic expression of *OVOL2* is driven by the cryptic cis-regulatory sequence binding site [4]. But the exact mechanism is not clearly understood.

Here, we presented an allelic series of *Ovol2* promoter mutations including pathogenic variant c.-307T>C in mice using the CRISPR-Cas9 approach. Despite a high degree of evolutionary conservation, not all mutations cause ocular abnormalities in mice.

Four distinct mutations in the distal promoter region did not significantly change *Ovol2* mRNA levels and exhibited no ocular phenotype. Nevertheless, our data indicate that similar to human patients, mice carrying c.-307T>C mutation and deletion of the Ovol2/Ovol1 binding site -307_-320del showed increased transcriptional activity of *Ovol2*, but does not lead to endothelial dystrophy, suggesting the species-specific variation in endothelial development. Interestingly, a minority of these mutants showed ocular phenotypes including iridocorneal adhesion, PHPV and dysplastic retina indicating a possible role for Ovol2 in eye development.

Materials and methods

Ethics statement

The housing of the mice and in vivo experiments were performed in agreement with the European Communities Council Directive of 24 November 1986 (86/609/EEC), institutional and national guidelines. Experimental methods and animal care were approved by the Animal Care Committee of the Institute of Molecular Genetics (no. 71/2014). No human subjects are included in this work.

Histology and Immunofluorescence

Eyeballs from appropriate age were isolated, and fixed in 4 % paraformaldehyde in 1x Phosphate buffer saline (PBS) overnight at 4°C. The following day, samples were washed 3 times × 10 minutes in 1x PBS, dehydrated in a series of ethanol, cleared in xylene and then embedded using paraffin wax.

For Hematoxylin and Eosin (H&E) staining, the sections of 6 µm thickness were deparaffinised with xylene and xylene is removed with 100 % ethanol. Then sections are rehydrated with the ethanol series (95% - 80% - 70% - 50% - 25%), dyed with Hematoxylin and eosin and mounted using 70% glycerol.

For immunostaining, deparaffinised and rehydrated sections were treated with sodium citrate buffer (10 mM sodium citrate buffer, 0.05% Tween 20, pH-6.0) for heat-induced epitope retrieval. For preventing nonspecific binding between tissue and primary antibodies, sections were incubated with 10 % BSA (Bovine Serum Albumin) in 0.1% PBT (1x PBS with 0.1% PBT) for 1 hour. Then sections were incubated in primary antibodies in 1% BSA / 0.1% PBT overnight. Next day, sections were washed 4 × 10 minutes with 0.1% PBT, and incubated with secondary antibody for 1 hour, washed 2× 10 minutes with 1x PBS, stained with DAPI (1µg/ml) and mounted using Mowiol. The primary and secondary antibodies utilized in this study are presented in **Table S1**. Stained sections were imaged using Andor Dragonfly 503 (Immunostaining) and Leica DM6000 and Zeis Imager Z2 (H&E staining).

Quantitative RT-PCR (qRT-PCR)

To analyze mRNA expression, CEn cells from PN21 eyes were isolated (each sample = 6 eyes) and total RNA was isolated using Trizol Reagent (Life Technologies/ Invitrogen). Superscript VILO cDNA synthesis kit (Life technologies) was used to generate randomly primed cDNA from 200 ng of total RNA. CEn cells was isolated from at least 6 independent biological replicates. All qRT- PCR experiments were done using a Roche LC480 light cycler and the amplifications are made using SYBR Green I PCR master mix (Roche). The thermal cycling conditions used: Initial denaturation at 95°C for 1 minute followed by 50 cycles at

95°C for 10 seconds, 55°C for 20 seconds, and 72°C for 20 seconds. The experiments were performed with three technical replicates for each biological replicate. The relative quantities are calculated using the $\Delta\Delta C_q$ method [25]. Using this method, we obtained fold changes in gene expression normalized to a housekeeping gene SDHA (Succinate dehydrogenase complex, subunit A).

Sequences of primers used are listed below:

Ovol2_F: GAGCTTCACGACGCCCAA, Ovol2_R: AGAGTTGTCGCATGTGCCG

SDHA_F: AAGGCAAATGCTGGAGAAG, SDHA_R: TGGTTCTGCATCGACTTCTG

Spectral-domain optical coherence tomography (SD-OCT)

Experiments were carried out in 6 wild-type C57Bl/6J and 13 mutant Ovol2 mice of both sexes. Mice were examined at the ages of 12.7 to 13.7 weeks. Animals were housed in individually ventilated cages (Tecniplast, Buguggiate, Italy) under a standard light condition (LD 12:12) at a temperature of 22.5°C and 55% humidity with food and water ad libitum. The measurements were carried out under general anaesthesia (i.m., Tiletamine + Zolazepam, 30 + 30 mg/kg, supplemented with 3.2 mg/kg Xylazine). Anaesthetized mice were kept on a heating pad throughout the experiment, their pupils were dilated with a drop of 0.5% Atropine (Ursapharm, Prague, Czech Republic) and after finishing measurements, the eyes were covered by transparent Vidisic gel (Bausch and Lomb, Berlin, Germany) to prevent eyes from drying. Experiments were approved by the Animal Care and Use Committee of the Czech Academy of Sciences.

For the imaging of the anterior eye segment/cornea, anterior chamber and anterior lens we used a spectral domain– optical coherent tomography (SD-OCT-Heidelberg-Engineering, Heidelberg, Germany) with a special Spectralis anterior segment module (ASM). The mice were positioned with the scanned eye toward the OCT camera so that the eye was displayed in a horizontal view. Volume scan comprising at least 20 A-scans was collected for both eyes with at least 16 frames per A-scan. This setting corresponded to a distance of 69 µm between neighbouring sections. The obtained high-resolution images were used to detect the layers of the cornea in detail.

Results

A mouse model for PPCD1 associated with Family BR3 c.-307T>C shows increased *Ovol2* levels in the corneal endothelium.

Given that the disease-causing mutations associated with PPCD1 are clustered within the 145bp-long evolutionarily conserved promoter region of *OVOL2* **(Fig.1A)**, we generated an allelic series of seven mutations encompassing two areas where PPCD mutations in British and Czech families were previously identified [4]. Four distinct mutations were generated in the distal part of the mouse *Ovol2* promoter region **(Fig.S1)**. To investigate whether these mutations result in some phenotypic consequences in the eye, we performed histological analysis. Hematoxylin and eosin staining displayed no significant difference between wild-type and distal promoter mutants **(Fig.S1)**. Expression of *Ovol2* mRNA in the CEn of wildtype and distal promoter mutants was analyzed via qRT-PCR. Compared to wild-type mice, an apparent decrease (statistically not significant) in *Ovol2* mRNA expression was observed in distal promoter mutants **(Fig.S1)**. Combined, mutations generated by us here in

the distal part of the promoter did not increase the levels of endothelial *Ovol2* (mRNA) and did not result in PPCD or any other conspicuous ocular abnormality.

Next, we generated a mouse model for the pathogenic variant associated with Family BR3, i.e. the base substitution of *c.-307T>C* **(Fig.1A)**. Here on, the mouse allele c.-307T>C will be designated as *Ovol2 307T>C*. To assess whether *Ovol2 307T>C* mutation in mice results in ectopic expression of *Ovol2* mRNA in CEn, we analyzed the expression levels of the *Ovol2* gene by qRT-PCR. Similar to c.-307T>C human patients [24], a 200-fold upregulation was found in *Ovol2 307T>C* heterozygotes in comparison to age-matched wildtype **(Fig.1C)**.

Ocular phenotypes developed in *Ovol2 307T>C* heterozygous mice.

To characterize the phenotypic changes associated with the upregulation of *Ovol2* mRNA in CEn, we examined morphological and histological changes in *Ovol2 307T>C* heterozygotes and age-matched controls. A stereomicroscopic examination revealed an intact cornea with no opacities in 92% of the *Ovol2 307T>C* heterozygous mice **(Fig.2B, Fig.S2)**. Given that, the mouse eye is ~8-10 times smaller than a human eye [26] and the major characteristic of PPCD includes irregular endothelium represented either as vesicular or minute band-like lesions and diffuse or focal edema [4], which suggests the necessity of analyzing the mouse cornea using high-resolution imaging techniques. So here, for further scrutinization of *Ovol2 307T>C* mutants, we performed non-invasive, high-resolution imaging of the anterior segment using SD-OCT followed by hematoxylin and eosin staining on paraffin-embedded sections.

No ocular abnormalities were revealed in the majority of the *Ovol2 307T>C* heterozygous mice **(Fig.2B' F, F').** Interestingly, the remaining 8% of the *Ovol2 307T>C* heterozygotes exhibited a myriad of phenotypes, including irido–corneal adhesions **(Fig.2C, C', G, G')**, iris hypoplasia, corectopia like phenotype, corneal opacity, persistent hyperplastic primary vitreous (PHPV), narrow anterior chamber angle, increased anterior chamber thickness, and a dysplastic retina **(Fig.S2)**.

Clinically, some of the PPCD1 patients show multi-layering of the CEn, which is a sign of MET [4]. To analyze possible MET in the mouse model, we performed immunostaining for MET markers on the cornea of wildtype and *Ovol2 307T>C* heterozygous mice. Corneal epithelial-specific expression of Krt12 is maintained in the corneas with no external phenotype **(Fig.S3)**, although its expression is lost in those corneas that are exhibiting opacity **(Fig.S3)**. However, in none of these cases, the ectopic expression of Krt12 was observed in CEn **(Fig.S3)**. Next, we examined the expression of E-cadherin, a component of the adherens junction and a classical epithelial marker. Similar to wildtype, E-cadherin expression was sustained in the corneal epithelium and no E-cadherin immunostaining was found in the CEn of *Ovol2 307T>C* heterozygotes **(Fig. S3)**. Finally, there was no apparent change in the expression pattern of Zeb1, a mesenchymal marker, which is downregulated in the CEn of PPCD1 patients **(Fig.S3).** Taken together, these data suggest that no MET is occurring in the CEn of *Ovol2 307T>C* heterozygous mice with or without external phenotypes.

We were intrigued by the fact that the frequency of eye phenotype was as low as 8% in *Ovol2 307T>C* heterozygous mice and reasoned that the apparently low penetrance could be at least in part due to lethality in the late embryonic or early postnatal stages. Therefore

we examined whether the correct Mendelian ratio is maintained in the breedings of the *Ovol2 307T>C* strain of mice. A reduced yield of heterozygotes and homozygotes was observed in the adult stages, although the correct Mendelian ratios were obtained for the embryonic stages **(Fig.S4)**, suggesting significant postnatal lethality, especially in the homozygous *Ovol2 307T>C* mutant mice.

Embryonic phenotypes associated with *Ovol2 307T>C* heterozygotes and homozygotes

Since the abnormal Mendelian ratio indicated possible postnatal lethality, we next analyzed *Ovol2 307T>C* heterozygotes and homozygotes at embryonic stages. At E14.5, anatomical examination of wild type **(Fig.3A)** and *Ovol2 307T>C* embryos revealed coloboma **(Fig.3B)** and increased retrolental mass **(Fig.3B')** in *Ovol2 307T>C* heterozygotes (33%), whereas, in addition to coloboma **(Fig.3C)**, the dysplastic retinae **(Fig.3C')** were also found in *Ovol2 307T>C* homozygotes. Further analysis at E18.5, showed the presence of PHPV with increased penetrance in *Ovol2 307T>C* homozygotes (91%) in comparison to heterozygotes (30%) **(Fig. 3E-F)**.

The adult iris and ciliary body are generated from the peripheral part of the retina called the ciliary margin zone (CMZ). Iris morphogenesis starts late embryonically and continues during the first week of postnatal development [27]. Considering the iris phenotypes observed during the adult stages in *Ovol2 307T>C* heterozygotes, we used E18.5 *Ovol2 307T>C* embryos to analyze the expression of CMZ-associated transcription factors Msx1 and FoxP2, water channel Aqp1 and the Shh co-receptor Cdo [28] [29] by immunostaining. A reduction in the number of cells expressing Msx1 was observed in *Ovol2 307T>C* heterozygotes (50%) and homozygotes (66%) as compared to age-matched wildtype mice **(Fig.3G-H)**. In addition to this, the downregulation of Cdo **(Fig.3J-K)**, FoxP2 **(Fig.3M-N)** and Aqp1 **(Fig.3P-Q)** were observed in a significant fraction (~37-50 %) of the *Ovol2 307T>C* heterozygous and homozygotes mice.

Deletion of the Ovol1/Ovol2 binding site recapitulates the ocular phenotype in *Ovol2 307T>C* heterozygotes.

We noticed that a CCGTTA element representing the Ovol1 [30] and Ovol2 [31, 32] consensus binding site **(Fig.4C)** is present next to the c.-307T>C mutation **(Fig.4A)**. Ovol1 and Ovol2 recognize nearly identical consensus sequences for regulating their target genes, proposing the possibility that they may regulate each other or themselves [30, 31].

As a byproduct of the process of generating *Ovol2 307T>C* mice, we obtained two alleles carrying either 5bp or 14bp deletion in the nearby sequence. The 5bp deletion (allele designated as *Ovol2 307_311del*) included a part of the Ovol2 consensus binding site but due to the serendipitous fusion following CRISPR-Cas9 manipulation the Ovol2 consensus binding site was almost completely recreated **(Fig.S5)**. Similar to distal promoter mutants lacking the apparent phenotypes, histological analysis revealed no significant ocular abnormalities in *Ovol2 307_311del* heterozygous mice.

In the allele carrying the deletion of 14bp (further designated here as *Ovol2 307_320del*) the entire Ovol1/2 binding site was eliminated **(Fig.4A)**. To investigate the effect of this deletion on *Ovol2* mRNA levels, we performed qRT-PCR analysis on CEn from *Ovol2 307_320del* heterozygotes and wild type controls. In contrast to the basal level

of expression in wildtype, a 40-fold increase in the expression of *Ovol2* mRNA levels was found on *Ovol2 307_320del* heterozygotes **(Fig.4B)**.

To characterize possible ocular phenotypic, we performed morphological and histological analysis of wildtype and *Ovol2 307_320del* heterozygotes. A 20% of *Ovol2 307_320del* heterozygotes exhibited ocular phenotypes, including corneal opacity **(Fig.4F, F')**, iridocorneal attachment **(Fig.4G, G')**, PHPV **(Fig.4F',G')** and dysplastic retina **(Fig.4F')**, whereas the remaining 80 % of the *Ovol2 307_320del* heterozygotes did not show any ocular phenotype **(Fig.4E, E', E'', Fig.S6)**. Next, we analyzed the expression of CMZ markers by immunostaining at E18.5. In comparison to the wild-type embryos, a decrease in the number of Msx1-positive cells was found in ~50 % of *Ovol2 307_320del* heterozygotes **(Fig.4H-I)**. In addition, a slight decrease in the expression of other CMZ markers, Cdo **(Fig.4J-K),** Aqp1 **(Fig.4L-M)** and FoxP2 **(Fig.4N-O)** were found in *Ovol2 307_320del* heterozygotes. Similar to *Ovol2 307T>C*, a reduced yield of adult heterozygotes was observed in *Ovol2 307_320del* breedings **(Fig.S6)**. In addition, the number of heterozygotes obtained at embryonic stages was also not following the Mendelian law of segregation, which suggests perinatal lethality of the *Ovol2 307_320del* mouse strain **(Fig. S6)**.

Discussion

The genetic cause of PPCD1 is linked to mutations within the evolutionarily conserved promoter region of the *Ovol2* gene [4]. It has been shown that these promoter mutations strongly increase the expression of (mRNA) *Ovol2* in the CEn, which in turn deregulates the OVOL2-ZEB1-GRHL2 axis. An allelic series of seven mutations in mice produced and characterized here, including one of the known pathogenic variants in human PPCD1 patients, c.-307T>C, aimed to create a mouse model of the PPCD disease. We reasoned that given the high evolutionary conservation of the promoter, almost any sequence alteration might de-repress the *Ovol2* promoter in CEn (or elsewhere in the eye) and cause a phenotype. To our surprise, five out of seven mutations for which we were able to establish stable mouse lines did not exhibit an ocular phenotype. It is very well possible that given the dominant nature of *Ovol2* mutations, the CRISPR-Cas9 genome editing in F0 generation counter-selected for phenotypically stronger promoter alterations. It is worth noting that despite repeated efforts we were unable to establish a c.-370T>C stable line of mice corresponding to affected Czech individuals (family C1-14, C25, C30; (**Fig.1A**)).

A similar pattern of ocular phenotypes observed in *Ovol2 307T>C* and *307_311del* mutation suggest that the base pair substitution of T to C could be hindering the binding of Ovol1/Ovol2 to its consensus site or interaction with its hypothetical partner protein(s) and thus preventing repression of *Ovol2* gene transcription [30-32]. This scenario is further supported by the observation that no ocular phenotypes were observed in mouse variant *Ovol2 307_311del* in which the Ovol1/Ovol2 binding site was serendipitously restored. Remarkably, in spite of the fact that a reproducible set of ocular phenotypes was observed in *Ovol2 307T>C* and *307_311del* mice, those abnormalities only occurred in a small fraction of mutants. The reason for the incomplete penetrance is unclear. Although we observed a reduced viability of *Ovol2 307T>C* and *307_311del* mice, this cannot on its own account for low phenotypic penetrance.

Cell fate transitions like MET or EMT are critical for embryonic development and the development of various tissues and organs [33]. The Ovol2 transcription factor is one of the key inducers of MET or a repressor of EMT. It functions by directly repressing EMT by promoting factors like ZEB1, ZEB2, and TWIST and inducing the expression of cell adhesion molecules like E-cadherin [16, 34, 35]. In mice, Ovol2 is indispensable for embryonic development and Ovol2 $^{-/-}$ mice die at E10.5 [36]. Its expression begins during early-mid embryogenesis, especially in inner cell mass and later in ectoderm derivatives of the epiblast. It has also been shown that Ovol2 is required for the efficient migration and survival of neural crest cells [36]. Furthermore, Ovol2 is also expressed in adult epithelial tissues like skin, kidney, cornea, ovary, testis and mammary epithelia [16, 36-39]. Considering the importance of Ovol2 during embryonic development and in organ morphogenesis, we assume that the decreased yield of heterozygotes and homozygotes with phenotypes could be due to perinatal lethality. Even though it is not clear whether Ovol2 regulates the migration and survival of neural crest cells autonomously or non-autonomously [36], the ocular phenotypes we observed are likely associated with defective neural crest [40]. Neural crest cells are important for the development of various structures in the eye such as CEn, corneal keratocytes, trabecular meshwork, iris stroma, and primary vitreous [41-43]. The abnormal migration and differentiation of neural crest cells during embryonic development lead to anterior segment dysgenesis like aniridia, iris hypoplasia, Peters anomaly, congenital hereditary endothelial dystrophy, Axenfeld anomaly and congenital iris ectropion [44-46]. Development of iris hypoplasia, iridocorneal adhesion and absence of CEn in *Ovol2 307T>C* and *Ovol2 307_320del* mutants are thus consistent with abnormal migration, proliferation, or survival of neural crest cells. Furthermore, PHPV-like phenotypes observed in *Ovol2 307T>C* and *Ovol2 307_320del* mutants are known to be caused either by the failed regression of neural crest and mesoderm-derived transient vasculature during post-natal stages [47, 48] or due to the increased migration or proliferation of neural crest cells during embryonic development [40]. Finally, in both *Ovol2 307T>C* and *Ovol2 307_311del* mutants we observed an increased retrolental mass as early as E14.5 which remained persistent throughout postnatal stages. Taken together, these observations strongly suggest that the increased migration or proliferation of neural crest cells, which can be a direct or indirect effect of the deregulation of *Ovol2* expression caused by the engineered promoter mutations, are responsible for the phenotypes described in this study. However, we are currently unable to exclude the possibility that defects in optic fissure closure observed in *Ovol2 307T>C* mutants also significantly contribute to more extensive migration of neural crest cells into the eye cup. We believe that the abnormal lamination of the neural retina located adjacent to the hyperplastic vitreous in the affected *Ovol2* promoter mutants is a secondary phenotype of PHPV, a model proposed previously for human PHPV patients [49].

In conclusion, the pathogenic *Ovol2* promoter mutation c.-307T>C results in strong upregulation of the gene transcription in the cornea endothelium of the mouse model, mirroring the situation in human PPCD1 patients. However, such an upregulation does not trigger phenotypic changes seen in PPCD1 patients suggesting that notable differences exist in corneal endothelial cell biology between humans and mice. The observation of dominant ocular phenotypes in *Ovol2* promoter mutants, potentially associated with defects in the

neural crest, is intriguing. This finding suggests that the *Ovol2* gene may play a significant role in eye development and/or disease. Further studies can help to elucidate the specific role of the *Ovol2* gene in eye development, identify downstream targets or pathways influenced by Ovol2, and potentially uncover its involvement in the development of additional ocular diseases.

Declaration of competing interest

The authors declare no competing interests.

Acknowledgement

This work was supported by a grant of the Czech Science Foundation (21–27364S). Mouse costs were partially covered by the Czech Center for Phenogenomics infrastructure supported by LM2018126, OP VaVpI CZ.1.05/2.1.00/19.0395, and CZ.1.05/1.1.00 /02.0109.

References

1. Krachmer, J.H., *Posterior polymorphous corneal dystrophy: a disease characterized by epithelial-like endothelial cells which influence management and prognosis.* Trans Am Ophthalmol Soc, 1985. **83**: p. 413-75.
2. Weiss, J.S., et al., *IC3D classification of corneal dystrophies--edition 2.* Cornea, 2015. **34**(2): p. 117-59.
3. Evans, C.J., et al., *Identification of six novel mutations in ZEB1 and description of the associated phenotypes in patients with posterior polymorphous corneal dystrophy 3.* Ann Hum Genet, 2015. **79**(1): p. 1-9.
4. Davidson, A.E., et al., *Autosomal-Dominant Corneal Endothelial Dystrophies CHED1 and PPCD1 Are Allelic Disorders Caused by Non-coding Mutations in the Promoter of OVOL2.* Am J Hum Genet, 2016. **98**(1): p. 75-89.
5. Cibis, G.W., et al., *The clinical spectrum of posterior polymorphous dystrophy.* Arch Ophthalmol, 1977. **95**(9): p. 1529-37.
6. Pearce, W.G., R.C. Tripathi, and G. Morgan, *Congenital endothelial corneal dystrophy. Clinical, pathological, and genetic study.* Br J Ophthalmol, 1969. **53**(9): p. 577-91.
7. Yellore, V.S., et al., *Replication and refinement of linkage of posterior polymorphous corneal dystrophy to the posterior polymorphous corneal dystrophy 1 locus on chromosome 20.* Genet Med, 2007. **9**(4): p. 228-34.
8. Liskova, P., et al., *Ectopic GRHL2 Expression Due to Non-coding Mutations Promotes Cell State Transition and Causes Posterior Polymorphous Corneal Dystrophy 4.* Am J Hum Genet, 2018. **102**(3): p. 447-459.
9. Krafchak, C.M., et al., *Mutations in TCF8 cause posterior polymorphous corneal dystrophy and ectopic expression of COL4A3 by corneal endothelial cells.* Am J Hum Genet, 2005. **77**(5): p. 694-708.

10. Liskova, P., et al., *Heterozygous deletions at the ZEB1 locus verify haploinsufficiency as the mechanism of disease for posterior polymorphous corneal dystrophy type 3.* Eur J Hum Genet, 2016. **24**(7): p. 985-91.
11. Liskova, P., et al., *Novel mutations in the ZEB1 gene identified in Czech and British patients with posterior polymorphous corneal dystrophy.* Hum Mutat, 2007. **28**(6): p. 638.
12. Biswas, S., et al., *Missense mutations in COL8A2, the gene encoding the alpha2 chain of type VIII collagen, cause two forms of corneal endothelial dystrophy.* Hum Mol Genet, 2001. **10**(21): p. 2415-23.
13. Chung, D.D., et al., *Confirmation of the OVOL2 Promoter Mutation c.-307T>C in Posterior Polymorphous Corneal Dystrophy 1.* PLoS One, 2017. **12**(1): p. e0169215.
14. Cieply, B., et al., *Suppression of the epithelial-mesenchymal transition by Grainyhead-like-2.* Cancer Res, 2012. **72**(9): p. 2440-53.
15. Hong, T., et al., *An Ovol2-Zeb1 Mutual Inhibitory Circuit Governs Bidirectional and Multi-step Transition between Epithelial and Mesenchymal States.* PLoS Comput Biol, 2015. **11**(11): p. e1004569.
16. Kitazawa, K., et al., *OVOL2 Maintains the Transcriptional Program of Human Corneal Epithelium by Suppressing Epithelial-to-Mesenchymal Transition.* Cell Rep, 2016. **15**(6): p. 1359-68.
17. Liu, J., et al., *Ovol2 induces mesenchymal-epithelial transition via targeting ZEB1 in osteosarcoma.* Onco Targets Ther, 2018. **11**: p. 2963-2973.
18. Pifer, P.M., et al., *Grainyhead-like 2 inhibits the coactivator p300, suppressing tubulogenesis and the epithelial-mesenchymal transition.* Mol Biol Cell, 2016. **27**(15): p. 2479-92.
19. Roca, H., et al., *Transcription factors OVOL1 and OVOL2 induce the mesenchymal to epithelial transition in human cancer.* PLoS One, 2013. **8**(10): p. e76773.
20. Werner, S., et al., *Dual roles of the transcription factor grainyhead-like 2 (GRHL2) in breast cancer.* J Biol Chem, 2013. **288**(32): p. 22993-3008.
21. Cieply, B., et al., *Epithelial-mesenchymal transition and tumor suppression are controlled by a reciprocal feedback loop between ZEB1 and Grainyhead-like-2.* Cancer Res, 2013. **73**(20): p. 6299-309.
22. Gwilliam, R., et al., *Posterior polymorphous corneal dystrophy in Czech families maps to chromosome 20 and excludes the VSX1 gene.* Invest Ophthalmol Vis Sci, 2005. **46**(12): p. 4480-4.
23. Liskova, P., et al., *High prevalence of posterior polymorphous corneal dystrophy in the Czech Republic; linkage disequilibrium mapping and dating an ancestral mutation.* PLoS One, 2012. **7**(9): p. e45495.
24. Chung, D.D., et al., *Alterations in GRHL2-OVOL2-ZEB1 axis and aberrant activation of Wnt signaling lead to altered gene transcription in posterior polymorphous corneal dystrophy.* Exp Eye Res, 2019. **188**: p. 107696.
25. Taylor, S.C., et al., *The Ultimate qPCR Experiment: Producing Publication Quality, Reproducible Data the First Time.* Trends Biotechnol, 2019. **37**(7): p. 761-774.

26. Zhou, X., et al., *A comparative gene expression profile of the whole eye from human, mouse, and guinea pig.* Mol Vis, 2007. **13**: p. 2214-21.
27. Davis-Silberman, N. and R. Ashery-Padan, *Iris development in vertebrates; genetic and molecular considerations.* Brain Res, 2008. **1192**: p. 17-28.
28. Monaghan, A.P., et al., *The Msh-like homeobox genes define domains in the developing vertebrate eye.* Development, 1991. **112**(4): p. 1053-61.
29. Belanger, M.C., B. Robert, and M. Cayouette, *Msx1-Positive Progenitors in the Retinal Ciliary Margin Give Rise to Both Neural and Non-neural Progenies in Mammals.* Dev Cell, 2017. **40**(2): p. 137-150.
30. Teng, A., et al., *Strain-dependent perinatal lethality of Ovol1-deficient mice and identification of Ovol2 as a downstream target of Ovol1 in skin epidermis.* Biochim Biophys Acta, 2007. **1772**(1): p. 89-95.
31. Lee, B., et al., *Transcriptional mechanisms link epithelial plasticity to adhesion and differentiation of epidermal progenitor cells.* Dev Cell, 2014. **29**(1): p. 47-58.
32. Wells, J., et al., *Ovol2 suppresses cell cycling and terminal differentiation of keratinocytes by directly repressing c-Myc and Notch1.* J Biol Chem, 2009. **284**(42): p. 29125-35.
33. Kalcheim, C., *Epithelial-Mesenchymal Transitions during Neural Crest and Somite Development.* J Clin Med, 2015. **5**(1).
34. Aue, A., et al., *A Grainyhead-Like 2/Ovo-Like 2 Pathway Regulates Renal Epithelial Barrier Function and Lumen Expansion.* J Am Soc Nephrol, 2015. **26**(11): p. 2704-15.
35. Watanabe, K., et al., *OVOL2 induces mesenchymal-to-epithelial transition in fibroblasts and enhances cell-state reprogramming towards epithelial lineages.* Sci Rep, 2019. **9**(1): p. 6490.
36. Mackay, D.R., et al., *The mouse Ovol2 gene is required for cranial neural tube development.* Dev Biol, 2006. **291**(1): p. 38-52.
37. Li, B., et al., *Ovol2, a mammalian homolog of Drosophila ovo: gene structure, chromosomal mapping, and aberrant expression in blind-sterile mice.* Genomics, 2002. **80**(3): p. 319-25.
38. Unezaki, S., et al., *Ovol2/Movo, a homologue of Drosophila ovo, is required for angiogenesis, heart formation and placental development in mice.* Genes Cells, 2007. **12**(6): p. 773-85.
39. Watanabe, K., et al., *Mammary morphogenesis and regeneration require the inhibition of EMT at terminal end buds by Ovol2 transcriptional repressor.* Dev Cell, 2014. **29**(1): p. 59-74.
40. Lin, S., et al., *Neogenin-loss in neural crest cells results in persistent hyperplastic primary vitreous formation.* J Mol Cell Biol, 2020. **12**(1): p. 17-31.
41. Bahn, C.F., et al., *Classification of corneal endothelial disorders based on neural crest origin.* Ophthalmology, 1984. **91**(6): p. 558-63.
42. Beauchamp, G.R. and P.A. Knepper, *Role of the neural crest in anterior segment development and disease.* J Pediatr Ophthalmol Strabismus, 1984. **21**(6): p. 209-14.

43. Tripathi, B.J. and R.C. Tripathi, *Neural crest origin of human trabecular meshwork and its implications for the pathogenesis of glaucoma.* Am J Ophthalmol, 1989. **107**(6): p. 583-90.
44. Sridhar, U. and K. Tripathy, *Iris Ectropion Syndrome*, in *StatPearls*. 2023: Treasure Island (FL).
45. Churchill, A. and A. Booth, *Genetics of aniridia and anterior segment dysgenesis.* Br J Ophthalmol, 1996. **80**(7): p. 669-73.
46. Jat, N.S. and K. Tripathy, *Peters Anomaly*, in *StatPearls*. 2023: Treasure Island (FL).
47. Pollard, Z.F., *Persistent hyperplastic primary vitreous: diagnosis, treatment and results.* Trans Am Ophthalmol Soc, 1997. **95**: p. 487-549.
48. Shastry, B.S., *Persistent hyperplastic primary vitreous: congenital malformation of the eye.* Clin Exp Ophthalmol, 2009. **37**(9): p. 884-90.
49. Hunt, A., et al., *Outcomes in persistent hyperplastic primary vitreous.* Br J Ophthalmol, 2005. **89**(7): p. 859-63.

Figures

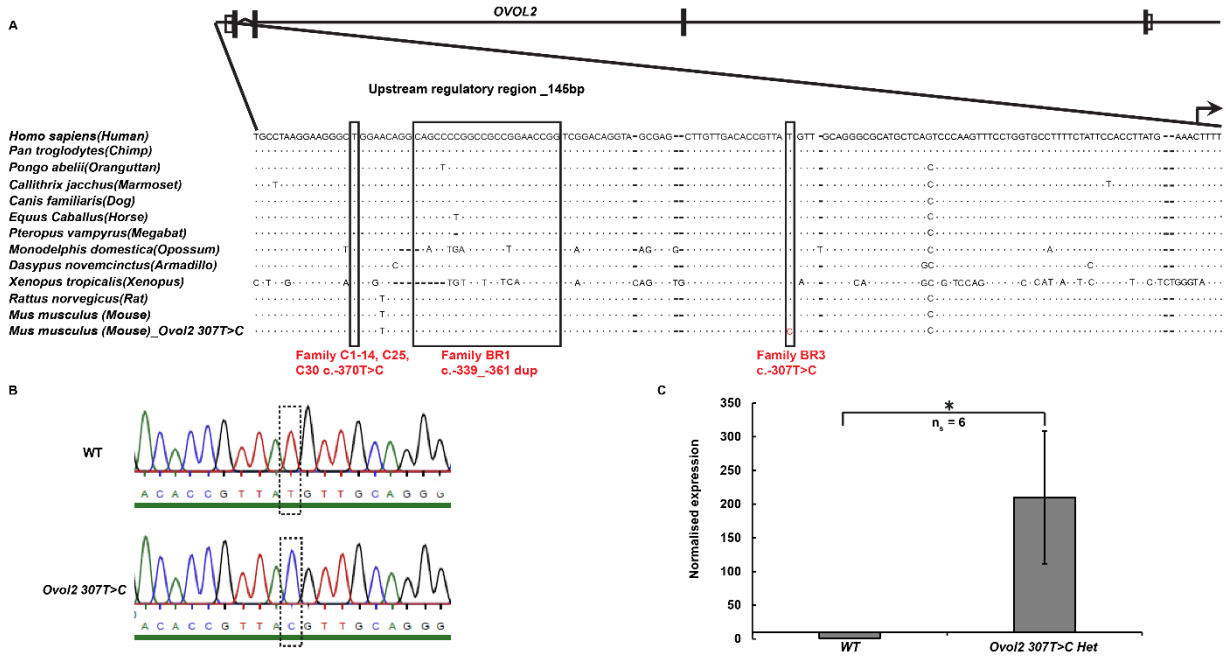

Figure 1: Generation and validation of mouse model for PPCD1 associated with Family BR3 c.-307T>C. **(A)** Schematic representation of sequence conservation of 145 bp long promoter region of *Ovol2* among mammals (Adapted from [4]). The black box indicates the position of pathogenic variants, red letter 'C in the alignment indicates base pair substitution generated in mice using CRISPR-Cas 9 system (*Ovol2 307T>C*). The arrow indicates the transcription start site. **(B)** Representation of sequencing results validating the base substitution of c.-307T>C in mice. **(C)** Quantitative qRT-PCR levels of *Ovol2* mRNA in the corneal endothelium of *Ovol2 307T>C* mutant and wild type. A 200-fold increase in the expression levels of (mRNA) *Ovol2* in *Ovol2 307T>C* mutant compared to the wild type. The error bar indicates standard error. The p values are calculated using the student's t-test, *$p < 0.01$. n_s represents the number of samples used.

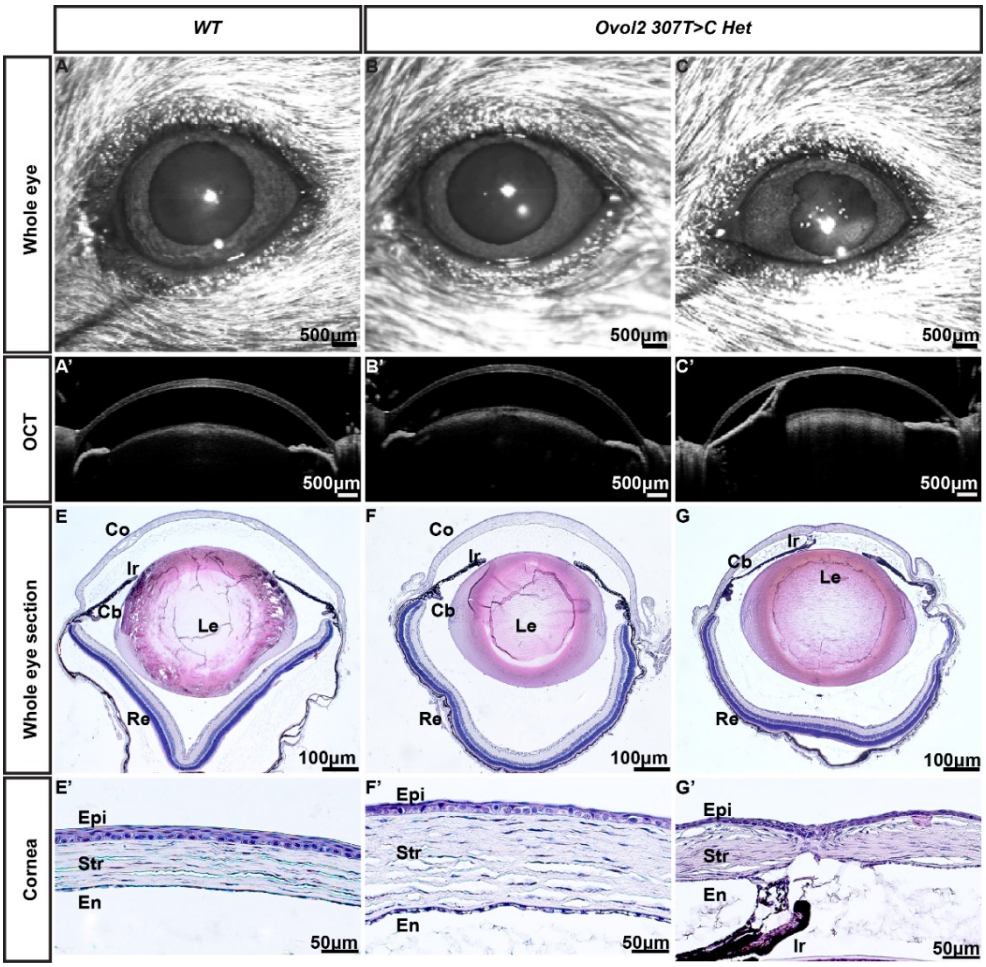

Figure 2: Occular phenotypes in *Ovol2 307T>C* heterozygous mice. (A-L) Representative examples of in vivo anterior segment images recorded using spectral domain optical coherence tomography (SD-OCT) of 4 months old *Ovol2 307T>C* heterozygotes and wildtype mice and Hematoxylin and Eosin staining on paraffin-embedded sections. **(A-C)** An aEn face view of the mouse eye **(A'-C')** indicates the SD-OCT images of the anterior segment of the eye. **(B, B', F, F')** Representative image of *Ovol2 307T>C* heterozygote eye showing no significant difference compared to **(A, A', E, E')** age-matched control whereas **(C, C' G, G')** represents *Ovol2 307T>C* heterozygote eye with an irido-corneal adhesion**.** Abbreviations used: Co, Cornea; Ir, Iris; Cb, Ciliary body; Le, lens; Re, Retina; Epi, Corneal epithelium; Str, Corneal Stroma; En, Corneal endothelium. Scale bar: **(A-C')**-500µm**, (E-G) -**100µm, **(E'-G') -** 50µm

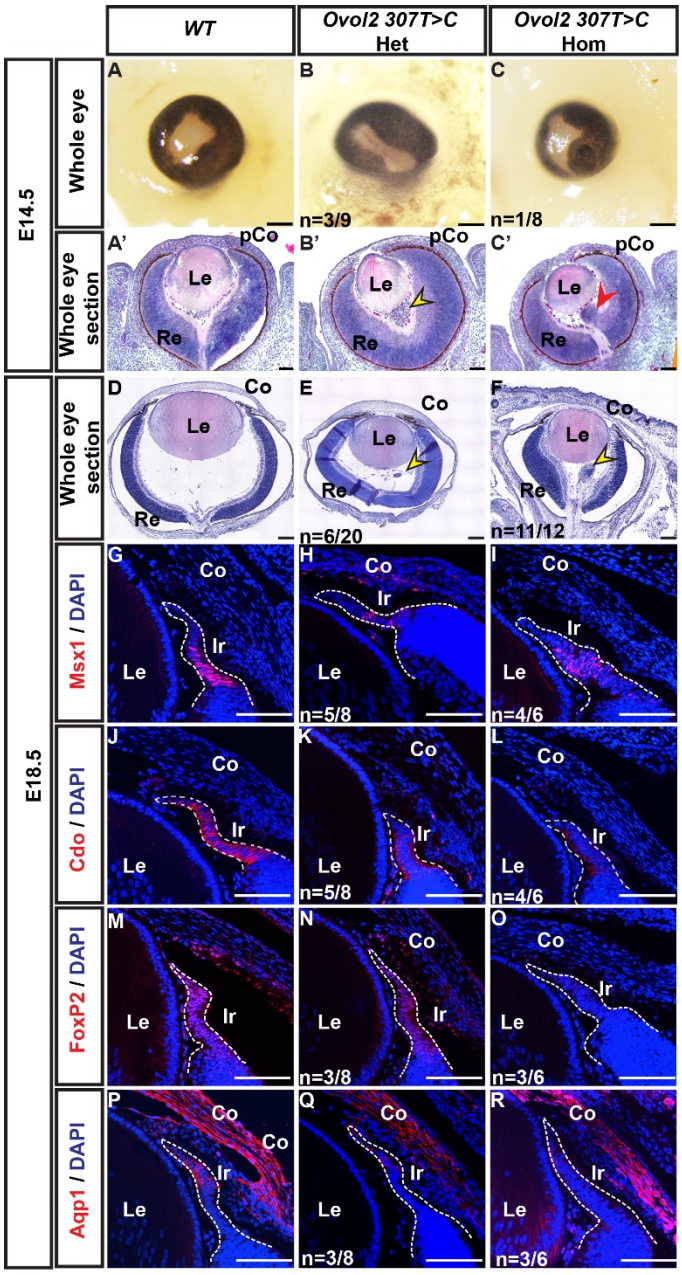

Figure 3: Ocular phenotypes observed during embryonic stages in *Ovol2 307T>C* mutant mice. (A-C) Eye at E14.5 in control, *Ovol2 307T>C* heterozygotes and *Ovol2 307T>C* homozygotes. **(B, C)** The coloboma was observed in some of the *Ovol2 307T>C* heterozygotes and homozygotes. **(A'-C')** H & E staining illustrates the presence of retrolental mass (yellow arrowhead) in *Ovol2 307T>C* heterozygous mutants and deformed retina (red arrowhead) in *Ovol2 307T>C* homozygous mutants. **(D-F)** Presence of retrolental mass/persistent hyperplastic primary vitreous (yellow arrowheads) in heterozygotes and homozygotes of *Ovol2 307T>C* mutants. n: indicates the number of mice analyzed. **(G-R)** Coronal sections from E18.5 of wild type, *Ovol2 307T>C* heterozygotes and homozygotes, were subjected to immunostaining with antibodies indicated. In contrast to CMZ-specific expression of Msx1, Cdo, FoxP2, and Aqp1in wildtype**,** decreased expression was observed in *Ovol2 307T>C* heterozygotes and homozygotes. The dotted line represents the CMZ region. Other abbreviations used: pCo, Presumptive cornea. Scale bar: **(A-C)** - 200µm, **(A'-F)** - 100µm, **(G-R)** - 5µm

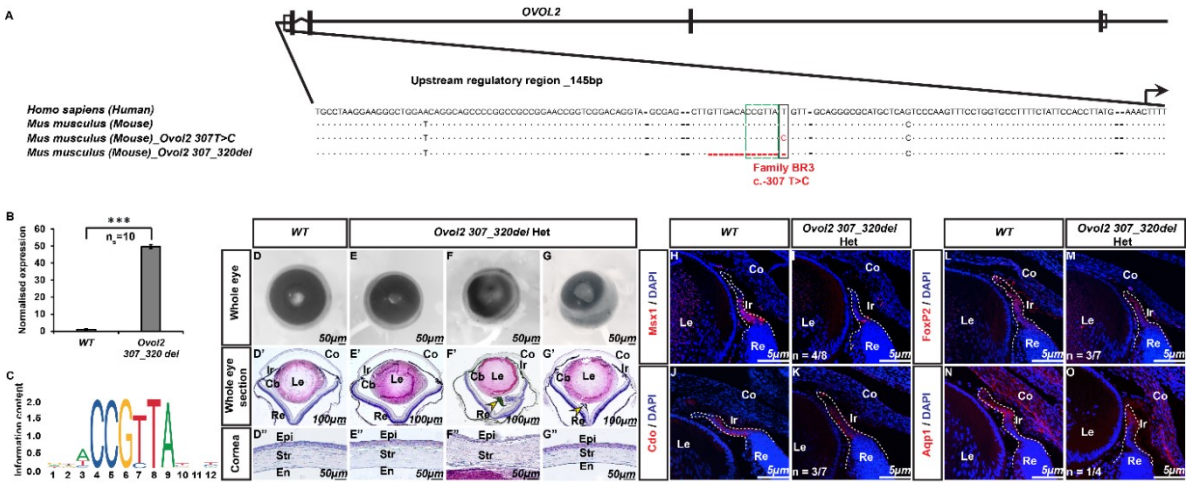

Figure 4: Ocular phenotypes associated with *Ovol2 307_320del* heterozygotes. (A) Schematic representation of 14bp deletion (-307_-320del), including Ovol2 binding site in the highly conserved 145bp long promoter region of mouse *Ovol2* gene (*Ovol2 307_320del).* The green and black box indicates Ovol2 binding site and pathogenic variant c.-307T>C in Family BR3 respectively. Red letters and hyphens depict base pair substitution and deletion respectively. **(B)** Quantitative qRT-PCR levels of *Ovol2* mRNA in the corneal endothelium of wild type and *Ovol2 307_320del* heterozygous mutants. A 40-fold increase in the expression levels of (mRNA) *Ovol2* is observed in *Ovol2 307_320del* heterozygotes compared to the wild type. The error bar indicates standard error. The p values are calculated using the student's t-test, ***$p < 0.001$. n_s: represents the number of samples used and each sample consists of corneal endothelium from 6 eyes of 3 weeks old mice. **(C)** The binding sequence of human transcription factor Ovol2 derived from JASPER. **(D-G'')** Representative images of whole eye and Hematoxylin and Eosin staining in coronal sections of 3 weeks old wildtype and *Ovol2 307_320del* heterozygous mutants. **(E, E', E'')** In contrast to 80% of the *Ovol2 307_320del* heterozygous mutants which show no histologic abnormalities, **(F-G'')** 20% of the mutants exhibit ocular phenotypes including **(F)** opaque cornea, **(G)** iridocorneal adhesion, **(F')** Persistent hyperplastic primary vitreous (Arrowhead), **(F'')** absence of corneal endothelium. **(H-O)** Frontal sections from E18.5 of wildtype and *Ovol2 307_320del* heterozygotes were subjected to H&E staining and antibodies indicated. Decreased expression of CMZ markers was observed in *Ovol2 307_320del* heterozygous mutants in comparison to controls. n: indicates the number of mice. The dotted lines represent the CMZ region. n indicates the number of mice analyzed. Scale bar: **(D-G)**-50 µm, **(D'-G')** - 100 µm**, (D''-G'')** -50 µm, **(H-O** -5 µm

Supplementary Information

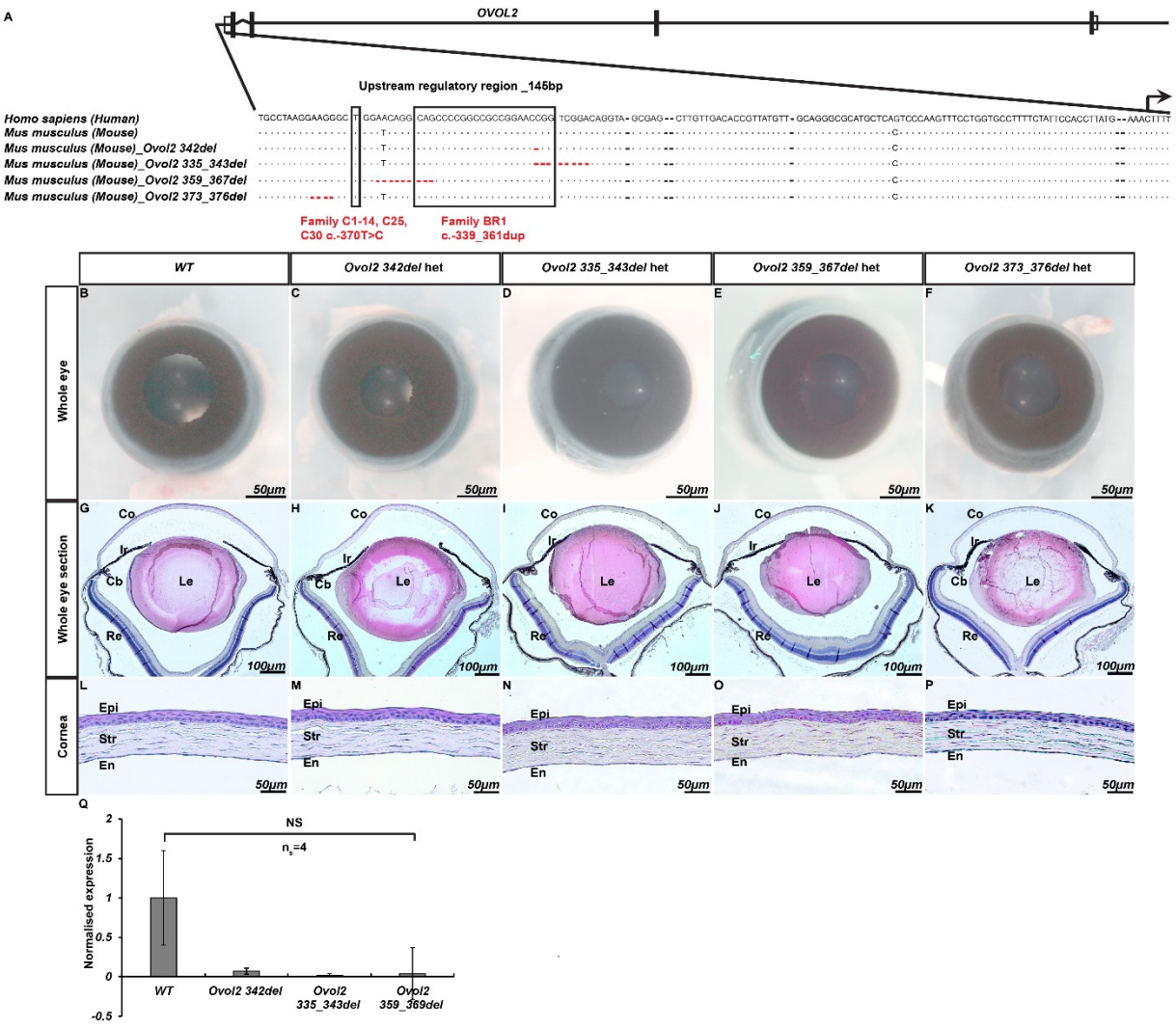

Supplementary Figure 1: No phenotypic consequences are observed in mutants carrying distinct deletions at the distal promoter region of *Ovol2 gene* **(A)** Schematic depiction of four different deletions generated in mice using CRISPR-Cas9 technology in the distal part of highly conserved 145bp long *Ovol2* promoter region. The black box indicates the position of pathogenic variants known in humans. Red hyphens represent the deletion of base pairs (-342del, -335_-343del, -359_-367del,-373_-376del). Arrow indicates the transcription start site. **(B-P)** Representative images of isolated eyeballs and H& E staining on paraffin-embedded sections from wildtype and *Ovol2 342del*, *Ovol2 335_343del*, *Ovol2 359_367del*, and *Ovol2 373_376del* heterozygotes. No morphological or histological abnormalities were observed in these mutants. **(Q)** Quantification of *Ovol2* mRNA levels in corneal endothelium by qRT-PCR indicates decreased *Ovol2* mRNA expression in mutants compared to that of control. *Ovol2* mRNA levels are normalized to SDHA expression. The error bar indicates standard error. The p-value is calculated using the student's t–test and NS represents the data which is not statistically significant. Abbreviations used: Co, Cornea; Ir, Iris; Cb, Ciliary body; Le, lens; Re, Retina; Epi, Corneal epithelium; Str, Corneal Stroma; En, Corneal endothelium. Scale bar: **(B-F), (L- P)** -50 µm, **(G-K)** - 100µm

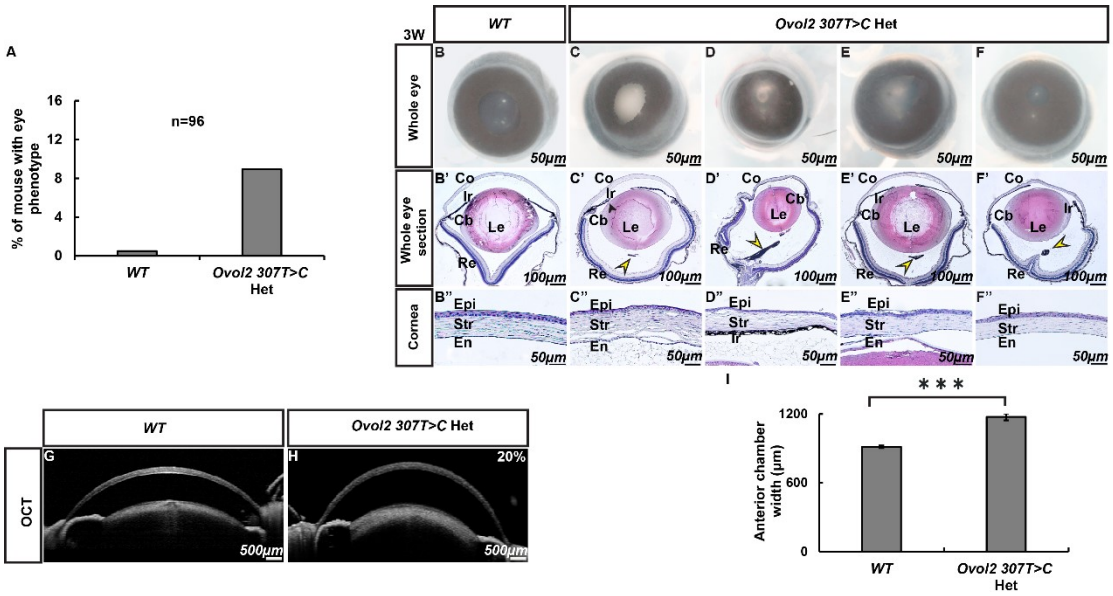

Supplementary Figure 2: Other phenotypic consequences in *Ovol2 307 T>C het*erozygotes. (A) Frequency of eye phenotype in *Ovol2 307T>C* heterozygotes at postnatal stages**. (B-F'') ** Representative images of eyeballs and H&E staining from 3 weeks old wildtype and *Ovol2 307T>C het*erozygous mutants. **(C-C'')** represents a mutant with iris hypoplasia and no significant changes were found in the architecture of the cornea. **(D-D'')** represents mutants with an opaque cornea, iridocorneal attachment, persistent hyperplastic primary vitreous (PHPV), absence of anterior chamber angle, and corneal endothelium. **(E-E'')** depicts a mutant eye with iris hypoplasia, attachment of the lens to the corneal endothelium and PHPV. **(F-F'')** illustrates a mutant eye with PHPV, narrow anterior chamber angle. **(G-H)** Representative SD-OCT anterior segment image showing increased anterior chamber thickness. **(I)** Measurement of anterior chamber width shows a significant increase in *Ovol2 307T>C* heterozygous mutants in comparison to age-matched control. The error bar indicates standard error. The p values are calculated using the student's t-test. ***p < 0.0001. Arrowheads indicate PHPV. Scale bar: **(B-F), (B''-F'') -** 50 µm, **(B'- F')** - 100 µm, **(G-H)** -500µm

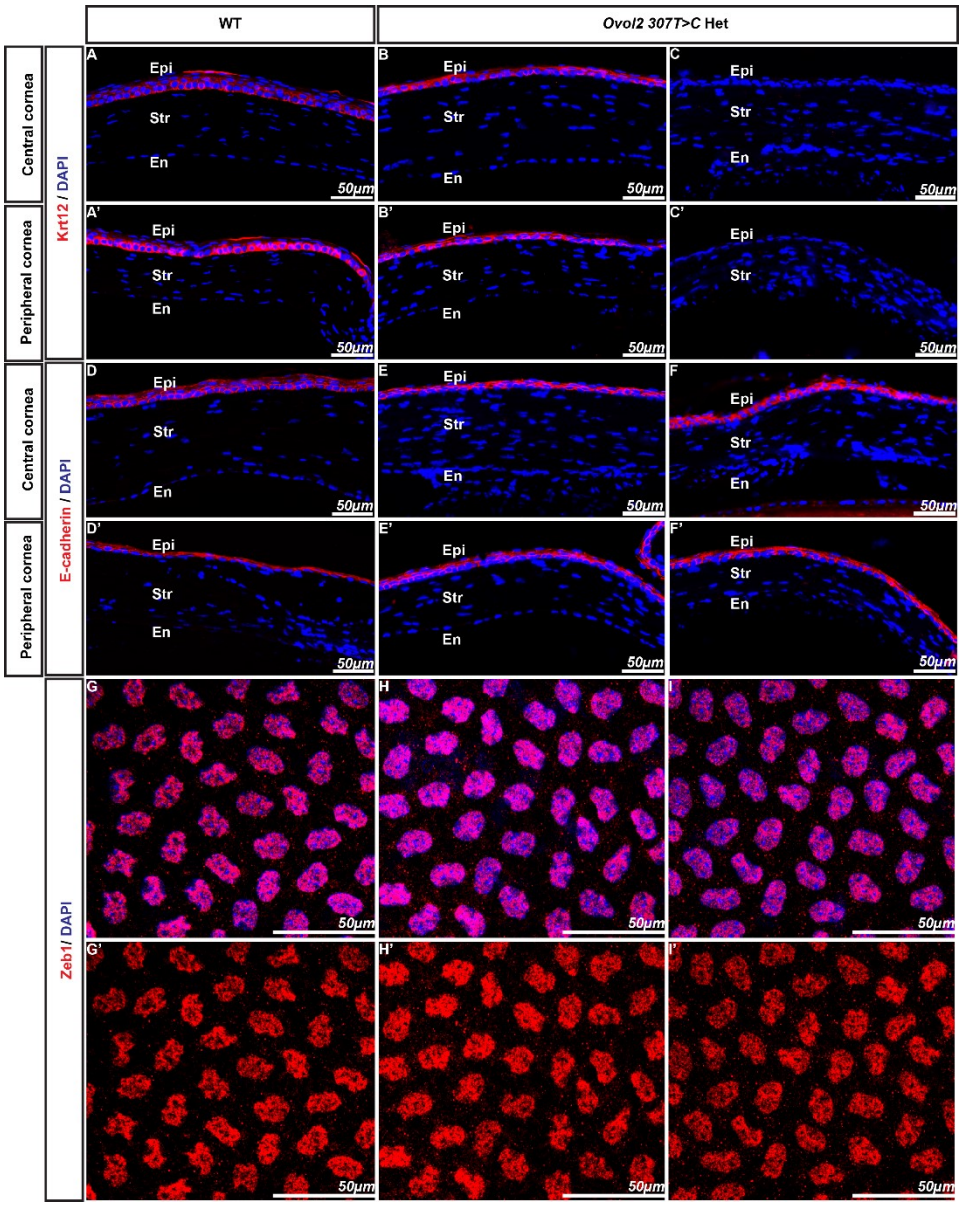

Supplementary Figure 3: No mesenchymal to epithelial transition is observed in the corneal endothelium of *Ovol2 307T>C het*erozygote mice. (A-F') Immunostaining of Krt12 and E-cadherin in frontal sections of wildtype and *Ovol2 307T>C* het mutants. **(A, A')** As in the control, corneal epithelial-specific expression of Krt12 is maintained in **(B, B')** *Ovol2 307T >C* het mutants (Corresponds to **(D, E)** in **Fig. S2**), while Krt12 expression is lost in **(C, C')** (corresponds to **Fig.2C**). Nevertheless, Krt12 has not been detected in the corneal endothelium of *Ovol2 307T>C* het mutants. **(D-F')** E-cadherin is expressed in the corneal epithelium of wild type and its expression pattern remains similar in *Ovol2 307T>C* het mutants. In addition, no ectopic E-cadherin expression was observed in the corneal endothelium of the mutants. **(G-I')** Whole-mount immunostaining of Zeb1 in the corneal endothelium at 4 weeks. The expression pattern of Zeb1 remains the same in *Ovol2 307T>C* het mutants in comparison to the wild type. Scale bar: **(A-F') (G-I')** - 50µm.

A

Ovol2 307T>C Het × WT *(n=74)*		
Genotype	WT	*Ovol2 307T>C* Het
Born number (%)	61	39
Expected number (%)	50	50
Ovol2 307T>C Het × *Ovol2 307T>C* Het*(n=37)*		
Genotype	WT	*Ovol2 307T>C* Het
Born number (%)	24	44
Expected number (%)	25	50
Genotype	*Ovol2 307T>C* Hom	Preweaning loss
Born number (%)	6	26
Expected number (%)	25	0

B

Ovol2 307T>C Het × WT *(n=64)*		
Genotype	WT	*Ovol2 307T>C* Het
Number of embryo's (%)	50	50
Expected number (%)	50	50
Ovol2 307T>C Hom × *Ovol2 307T>C* Het *(n=18)*		
Genotype	*Ovol2 307T>C* Het	*Ovol2 307T>C* Hom
Number of embryo's (%)	50	50
Expected number (%)	50	50

Supplementary Figure 4: Abnormal Mendelian ratio in *Ovol2 307T>C* mutants (A) Summary of viable offspring derived postnatally from indicated crossings. According to Mendel's law of segregation, a reduced yield of heterozygotes and homozygotes was observed. **(B)** Summary on offspring derived embryonically from indicated breedings. The proper genotypic ratio of wild type, heterozygotes and homozygotes in accordance with Mendel's law of segregation. n indicates the number of mice analyzed.

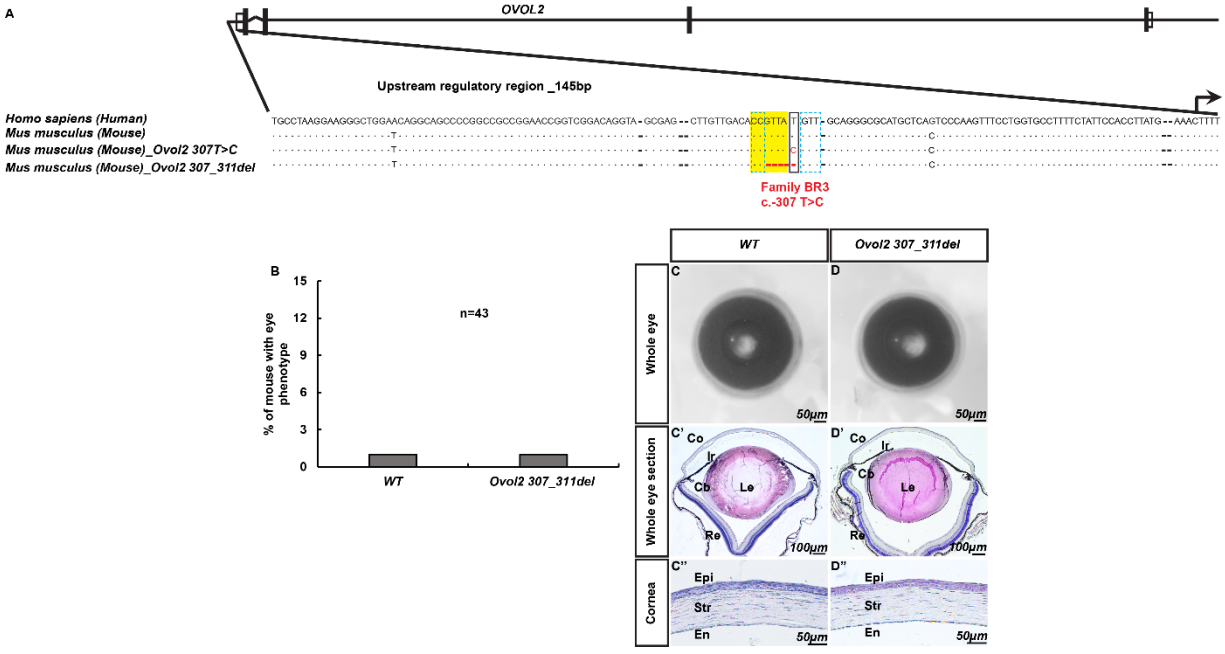

Supplementary Figure 5: **No phenotypic consequences are observed in *Ovol2 307_311del* heterozygote mice. (A)** Schematic representation of 5bp deletion c.-307_-311del, including parts of Ovol2 binding site in the highly conserved 145 bp long promoter region of mouse *Ovol2* gene (*Ovol2 307_311del*). The yellow highlights indicates Ovol2 binding site and the black box illustrates the pathogenic variant found in Family BR3. The blue box demonstrates the restored Ovol2 binding site, despite the deletion and red hyphens highlights 5bp deletion. **(B)** Frequency of mouse with eye phenotype postnatally. **(C)** Eyeballs and H &E staining of paraffin-embedded sections from wildtype and *Ovol2 307_311del* het mutants. As in control, no

phenotypic consequences were observed in *Ovol2 307_311del* het mutants. n - represents the number of mice analyzed. Scale bar: **(C-H)**-50 µm

Supplementary Figure 6: Abnormal Mendelian ration was observed in *Ovol2 307_320del* mutants. (A)

A

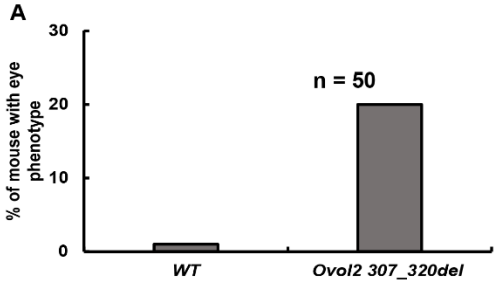

B

Ovol2 307_320del Het × WT *(n=55)*			
Genotype	WT	*Ovol2 307_320del* Het	Preweaning loss
Born number (%)	53	40	7
Expected number (%)	50	50	0

C

Ovol2 307_320del Het × WT *(n=59)*		
Genotype	WT	*Ovol2 307_320del* Het
Number of embryo's (%)	75	25
Expected number (%)	50	50

Frequency of ocular phenotype in *Ovol2 307_320del* mutants during postnatal stages. **(B)** Summary on viable mouse-derived postnatally from indicated crossings. **(C)** Summary of embryos derived from the indicated breedings. n: denotes the number of mice analyzed.

Antibody	Source
Goat polyclonal anti-Cdo (1:600)	R & D systems, Cat#AF2429
Goat polyclonal anti-Msx1 (1:300)	R & D systems, Cat#AF5045
Rabbit polyclonal anti-Aqp1(1:500)	Millipore, Cat#178611
Rabbit polyclonal anti-FoxP2 (1:1000)	Abcam, Cat#ab16046
Rabbit polyclonal anti-Zeb1 (1:1000)	Novus Biologicals, Cat #NBP18845
Rat monoclonal anti-Ecadherin(1:300)	Thermo fisher scientific, Cat#13-1900
Goat polyclonal anti-K12(1:300)	Santa Cruz Biotec Inc, Cat# sc-17101
Donkey anti-rabbit secondary antibody , Alexa Fluor 594(1:500)	Thermofisher scientific , Cat#A-21207
Donkey anti-Goat secondary antibody, Alexa Fluor 594 (1:500)	Thermofisher scientific , Cat# A11058
Donkey anti-rat secondary antibody, Alexa Fluor 594 (1:500)	Thermofisher scientific , Cat# A21209

Table S1: Primary and secondary antibodies used

6.4 Chromatin remodelling enzyme Snf2h is essential for retinal cell proliferation and photoreceptor maintenance

Chromatin remodeling complexes are crucial regulatory factors involved in various nuclear processes, including transcription, DNA replication, and DNA repair. These complexes play a vital role in modulating the structure and accessibility of chromatin, which is the combination of DNA and proteins in the nucleus (Magana-Acosta and Valadez-Graham, 2020). There are several classes of chromatin remodeling complexes, each characterized by specific subunit composition and enzymatic activities. The ISWI (Imitation Switch) family of ATP-dependent chromatin remodelling factors, including yeast Isw1/Isw2 and their vertebrate counterparts sucrose nonfermenting protein 2 homolog (SNF2H) and sucrose nonfermenting 2-like protein (SNF2L), are highly conserved and play diverse roles in chromatin organization (Magana-Acosta and Valadez-Graham, 2020). Yet, the function of these complexes in a tissue-specific manner is less understood.

The mature vertebrate retina has a laminar organisation formed by six major classes of neurons and one class of glia. These cells are derived from multipotent retinal progenitor cells in a sequential yet overlapping order (Cepko, 2014; Livesey and Cepko, 2001). A proper balance of proliferation and differentiation of multipotent progenitor cells is essential for the development and maintenance of the retina (Dyer and Cepko, 2001; Hardwick et al., 2015). Studies have shown that, in addition to environmental cues, these processes are regulated by intrinsic factors such as transcription factors, chromatin modifiers and remodelers (Fujimura et al., 2018; Merbs et al., 2012; Popova et al., 2014; Popova et al., 2013; Zhang et al., 2015). Nonetheless, the role of Snf2h during the development of the retina is not studied. Our results show that Snf2h expression is observed in RPC and postnatal retinal cells. Here, we conditionally depleted the Snf2h in retinal progenitor cells using *mRx-Cre* transgenic mice. We show that, in the absence of the Snf2h, the overall thickness of the retina was significantly reduced and the complete absence of the outer nuclear layer consisting of photoreceptors. Interestingly, the depletion of the Snf2h did not affect the ability of RPC to specify different cell types. But Snf2h depleted retina exhibited defective cell-cycle defects and increased apoptosis, which ultimately lead to abnormal retinal lamination and the destruction of the photoreceptor layer.

My contribution to this work: I have performed the analysis of qRT-PCR data presented in Figure 8 of the published paper *Kuzelova A et al 2023*, (presented on pages 85-113 of this thesis)

cells

MDPI

Article

Chromatin Remodeling Enzyme Snf2h Is Essential for Retinal Cell Proliferation and Photoreceptor Maintenance

Andrea Kuzelova [1], Naoko Dupacova [1], Barbora Antosova [1], Sweetu Susan Sunny [1], Zbynek Kozmik, Jr. [2], Jan Paces [2], Arthur I. Skoultchi [3], Tomas Stopka [4] and Zbynek Kozmik [1,5,*]

1 Laboratory of Transcriptional Regulation, Institute of Molecular Genetics of the Czech Academy of Sciences, 142 20 Prague, Czech Republic
2 Laboratory of Genomics and Bioinformatics, Institute of Molecular Genetics of the Czech Academy of Sciences, Videnska 1083, 142 20 Prague, Czech Republic
3 Department of Cell Biology, Albert Einstein College of Medicine, 1300 Morris Park Ave., Bronx, NY 10461, USA
4 Biocev, First Faculty of Medicine, Charles University, Prumyslova 595, 252 50 Vestec, Czech Republic
5 Research Unit for Rare Diseases, Department of Paediatrics and Inherited Metabolic Disorders, First Faculty of Medicine, Charles University and General University Hospital in Prague, 128 08 Prague, Czech Republic
* Correspondence: kozmik@img.cas.cz; Tel.: +420-241-062-100; Fax: +420-224-310-955

Abstract: Chromatin remodeling complexes are required for many distinct nuclear processes such as transcription, DNA replication, and DNA repair. However, the contribution of these complexes to the development of complex tissues within an organism is poorly characterized. Imitation switch (ISWI) proteins are among the most evolutionarily conserved ATP-dependent chromatin remodeling factors and are represented by yeast Isw1/Isw2, and their vertebrate counterparts Snf2h (Smarca5) and Snf2l (Smarca1). In this study, we focused on the role of the *Snf2h* gene during the development of the mammalian retina. We show that *Snf2h* is expressed in both retinal progenitors and post-mitotic retinal cells. Using *Snf2h* conditional knockout mice (*Snf2h* cKO), we found that when *Snf2h* is deleted, the laminar structure of the adult retina is not retained, the overall thickness of the retina is significantly reduced compared with controls, and the outer nuclear layer (ONL) is completely missing. The depletion of Snf2h did not influence the ability of retinal progenitors to generate all the differentiated retinal cell types. Instead, the Snf2h function is critical for the proliferation of retinal progenitor cells. Cells lacking Snf2h have a defective S-phase, leading to the entire cell division process impairments. Although all retinal cell types appear to be specified in the absence of the Snf2h function, cell-cycle defects and concomitantly increased apoptosis in *Snf2h* cKO result in abnormal retina lamination, complete destruction of the photoreceptor layer, and consequently, a physiologically non-functional retina.

Keywords: Snf2h; Smarca5; retina; photoreceptors; cell cycle; apoptosis

Citation: Kuzelova, A.; Dupacova, N.; Antosova, B.; Sunny, S.S.; Kozmik, Z., Jr.; Paces, J.; Skoultchi, A.I.; Stopka, T.; Kozmik, Z. Chromatin Remodeling Enzyme Snf2h Is Essential for Retinal Cell Proliferation and Photoreceptor Maintenance. *Cells* **2023**, *12*, 1035. https://doi.org/10.3390/cells12071035

Academic Editor: Paola Bagnoli

Received: 14 February 2023
Revised: 22 March 2023
Accepted: 23 March 2023
Published: 28 March 2023

1. Introduction

In eukaryotes, the chromosomal DNA is compacted in a highly organized nucleoprotein structure called chromatin that presents a barrier to most cellular processes [1]. The nucleosome is the basic structural unit of chromatin and is composed of four histone cores (H2A, H2B, H3, and H4) around which 147 bp of DNA are wrapped [1]. Various ATP-dependent chromatin remodeling complexes can reposition nucleosomes through the energy released via ATP hydrolysis [2,3]. Among the chromatin remodeling ATPases, the imitation switch (ISWI) family is highly conserved during evolution [4–7]. Mammals have two ISWI homologs—Snf2h (sucrose nonfermenting 2 homolog; also known as Smarca 5) and Snf2l (sucrose nonfermenting 2-like; also known as Smarca 1). Both proteins are present in complexes with a diverse array of noncatalytic subunits and are therefore able to promote many biological functions, including DNA replication, DNA repair, transcriptional repression or activation, and maintenance of chromosome structure [8–14].

Snf2h is known to function as the catalytic ATPase in at least five distinct complexes in mammalian cells, including WICH, CHRAC, ACF, RSF, and NoRC (reviewed in [3,15]). The presence of Snf2h within these complexes and the interactions of these complexes with other partners result in the targeting of Snf2h for particular biological functions in chromatin. For example, Snf2h is recruited to double-strand breaks by sirtuin protein SIRT6 to promote DNA break repair [10]. The lack of SIRT6 and Snf2h impairs chromatin remodeling, increasing sensitivity to genotoxic damage and recruitment of downstream factors such as 53BP1 [10]. Snf2h also plays a major role in organizing arrays of nucleosomes adjacent to the binding sites for the architectural chromatin factor CTCF and acts to promote CTCF binding on DNA [8]. Several studies have focused on the in vivo function of Snf2h ATPases and ISWI-containing complexes [6,7,16–23]. However, the simultaneous presence of Snf2h in distinct multicomponent complexes dedicated to unrelated nuclear functions makes it harder to interpret the molecular mechanisms underlying the observed pathological states in the context of a tissue or organism [17,22,24].

There are seven major cell types in the mammalian retina that are generated from a common pool of multipotent retinal progenitor cells (RPCs) [25–27]. Each cell type is born in a defined order [26,28–30] and plays a specific role in visual perception [31,32]. Ganglion cells (GCs) arise first, around embryonic day 11 (E11) in mice, and are the only retinal type whose axons project to the brain [31,33,34]. Simultaneously, the propagation of other early-born retinal neurons occurs. Horizontal cells (HCs), amacrine cells (ACs), and cone photoreceptors are produced with the highest peak at E14 [35–38]. Thereafter, later-born cells begin to form, namely, bipolar cells (BCs), Müller glia cells (MCs), and rod photoreceptors, whose generation increases shortly after birth [26,36,38,39]. The process of retinal differentiation in mice is finished at postnatal day 14 (P14) when the eyes open [40]. Mature retinal neurons and glia are arranged in three main layers—ganglion cell layer (GCL), inner nuclear layer (INL), and outer nuclear layer (ONL) [27]. With respect to the entire eye, the GCL is located closest to the lens and is particularly occupied by GCs [36]. The interneurons (HCs, ACs, and BCs), primarily associated with the transmission of information throughout the retina, are placed together with MCs, ensuring retinal homeostasis, in the INL [27,36,41]. The ONL, the outermost retinal region, is formed by photoreceptors [36]. Cones and rods are specialized sensory neurons that absorb photons of light and activate the process of photo-transduction [42]. Postnatally, murine photoreceptors express different types of opsin proteins—rhodopsin gene expression is characteristic of rod photoreceptors, while S-opsin (short-wavelength opsins) and M-opsin (medium-wavelength opsins) expression characterize cone photoreceptors. Photoreceptors are highly metabolically active and require a stable cellular environment; otherwise, the cell morphology or physiology is disrupted [43,44]. A number of studies investigated the role of transcription factors in photoreceptor development [45–56]. In contrast, the regulatory molecules affecting photoreceptor cell maintenance during embryonic and postnatal stages remain largely unknown. It is well established that in order to generate retinal diversity, while maintaining appropriate cell numbers, a proper balance between cell proliferation and differentiation of progenitor cells is required [57,58]. These events are regulated by various extrinsic and intrinsic cues, from which the transcription factors seem to be the most relevant (reviewed in [58,59]). Recent epigenetic studies show that the chromatin-modifying or remodeling mechanisms are also important for retina development and maintenance; however, it is unknown how Snf2h, a key component in chromatin remodeling complexes, is involved in the process [60–65]. Here, we studied the role of the Snf2h during mouse retinal development and differentiation. Since *Snf2h*-deficient mice die at the peri-implantation stage due to the growth arrest of trophectoderm and inner cell mass [22], we performed conditional gene targeting using the floxed allele of *Snf2h* [17] and mRx-Cre active in RPCs from E9.0 onwards [66].

2. Materials and Methods

2.1. Mouse Lines

For the retina-specific inactivation of *Snf2h*, mRx-Cre [66] and Snf2h$^{fl/fl}$ [17] mice were used.

2.2. Tissue Collection and Histology

Mouse embryos were harvested from timed pregnant females. The morning of the vaginal plug was determined as embryonic day 0.5 (E0.5). The embryos and eyes of postnatal mice were fixed in 4% formaldehyde in PBS (*w*/*v*) overnight at 4 °C. The next day samples were washed with cold PBS and incubated in 70% ethanol. Subsequently, samples were dehydrated, embedded in paraffin blocks, and sectioned. Horizontal sections of 5 µm were prepared, stored at 4 °C, and used for up to one month.

2.3. Immunohistochemistry

Paraffin sections were deparaffinized and rehydrated. The epitope retrieval was performed for 20 min in a citrate buffer (10 mM, pH 6.0) at 98 °C in a pressure cooker. For immunofluorescent analysis, the sections were washed three times in PBT, blocked with 10% BSA in PBT (*w*/*v*) for one hour, and incubated overnight with primary antibody at 4 °C (diluted in 1% BSA/PBT). The sections were washed three times in PBT, incubated for 45 min at room temperature with a secondary antibody, washed three times with PBT, and covered with DAPI/PBS (1 µg/mL) for 10 min. After washing in PBT, the sections were mounted into Mowiol (488; Sigma, Munich, Germany). For the immunohistological analysis, the dewaxed sections were washed three times in PBT, treated with 1.5% H_2O_2 in 10% methanol in PBS for 25 min, washed again with PBT, blocked with 10% BSA/PBT for one hour, and incubated with primary antibody overnight at 4 °C. The applied primary antibody was detected with a biotinylated secondary antibody (Vector Laboratories, Burlingame, CA, USA) and visualized with Vectastain ABC Elite kit and ImmPACT DAB substrate (all Vector Laboratories). The primary antibodies used for immunohistochemistry are listed in Table S1. The standard histological staining of paraffin sections using hematoxylin and eosin (H&E) was also performed. At least three different embryos from at least two different litters were analyzed with each staining.

2.4. EdU Incorporation

Timed pregnant females were injected intraperitoneally with 13 µg per g body weight of 5-ethynyl-2′-deoxyuridine (Edu; Thermo Fisher Scientific, Waltham, MA, USA) and sacrificed after 1 h or 24 h. Whole embryos were processed identically as described above. The acquired paraffin sections were deparaffinized, rehydrated, and washed three times in PBT. The sections were incubated in proteinase K/TE buffer (20 µg/mL) at 37 °C for 10 min and washed with PBT. The sections were treated with 0.3% H_2O_2 in methanol for 20 min at room temperature and washed three times in PBT and incubated with Click-iT Edu Imaging kit (AlexaFluor azide, Click-iT Edu reaction buffer; $CuSO_4$, Click-iT Edu buffer additive) for 1 h. After rinsing, the sections were incubated with DAPI/PBS (1 µg/mL) for 10 min, washed in PBT, and mounted into Mowiol (4–88; Sigma-Aldrich, Munich, Germany).

2.5. Quantification of Marker-Positive Cells

The quantification analysis of different retinal cell types, including apoptotic cells and cell-cycle analysis, was performed via the manual counting of marker-positive cells per central retinal section. In case an eye was removed from the individual (postnatal stages), the eye was precisely oriented into the paraffin block, and the central region was verified using a magnifier. Only those sections that were cut through the optic nerve were taken into account. The number of marker-positive cells per whole retinal section (GCs and HCs) or per defined retinal area in the central retinal part (ACs, BCs, MCs, rods, cones, apoptotic cells, and proliferating cells) was counted and normalized to wild-type controls. For a

single eye, a minimum of six sections was used; for each genotype, a minimum of four individual retinae was analyzed. Statistical significance was assessed using Student's *t*-test.

2.6. Quantitative RT-PCR (qRT-PCR)

Differentially expressed genes related to the p53 pathway in wild-type and *Snf2h* deficient retinal cells were established in P0 eyes. Postnatal retinae were dissected from the eye, separately from retinal pigment epithelium (RPE) and lens. Total RNA was isolated with a Trizol Reagent (Life Technologies, Carlsbad, CA, USA). Random-primed cDNA was generated from 500 ng total RNA using a SuperScript VILO cDNA Synthesis Kit (Life Technologies). Six different individuals originating from three litters were used for tissue dissection and subsequent analysis, for both wild-type and *Snf2h*-deficient cells. qRT-PCR reactions were run in a LightCycler 480 Instrument (Roche, Basel, Switzerland) using a 5 µL reaction mixture of DNA SYBR Green I Master (Roche) according to the standard manufacturer's protocol. Analysis was performed on the replicates of six different individual samples per genotype, run in triplicate. Crossing point (Cp) values were calculated with LightCycler 480 Software (Roche) using the second-derivate maximum algorithm. The average Cp values of all the biological and technical replicates were normalized using the Cp values of housekeeping genes *Gapdh*, *Ubb*, and *Actb*. The statistical significance of the change in mRNA expression was calculated using a two-tailed Student's-test in Microsoft Excel. Finally, the change in mRNA expression was presented as the ratio of mRx-Cre; $Snf2h^{fl/fl}$ to wild-type retinae on a log2 scale. Primer sequences are listed in Table S2.

2.7. RNA-Seq

Raw data were obtained from Gene Expression Omnibus (GEO) under accession number GSE87064 and used for re-analysis [67]. RNA-seq reads were preprocessed with FASTX tool kit v0.0.11 to remove short and low-quality reads. The reads were aligned to the mm10 genome using HISAT2 V2.1.0 [68].

3. Results

3.1. Conditional Deletion of Snf2h Disrupts Retinal Morphology

To determine *Snf2h* expression during mouse retinal development, we performed immunohistochemistry staining stages E9.5 to P18. Snf2h was detected in all RPCs of the optic cup at E9.5 and subsequently in all RPCs and differentiated retinal cells during the later embryonic stages (Figure 1A–D). After birth, strong *Snf2h* expression was detectable throughout the entire retina, independently of the cell type (Figure 1I–L). Snf2h functions in multiple protein complexes [69]. We, therefore, examined gene expression changes in Snf2h and its interacting partners during retinal development with publicly available RNA-seq data [67]. The CORUM database was used to identify the components of the complexes [70]. *Snf2h* was remarkably upregulated during P0 and P3 (Figure S1). Interestingly, the expression of genes encoding ACF, CHRAC, WICH, B-WICH, cohesin, All-1, and Dnmt3b including complex members was also increased (Figures S1–S3).

In order to investigate the function of the *Snf2h* gene during retinal development, we conditionally inactivated *Snf2h* in RPCs and their progeny by crossing mRx-Cre mice with $Snf2h^{fl/fl}$ mice. The mRx-Cre retinal driver is active in RPCs from E9.0 onwards [66], which corresponds with the onset of retinal neurogenesis. We analyzed the extent of Snf2h depletion in the retina of mRx-Cre $Snf2h^{fl/fl}$ mice (referred to as *Snf2h* cKO) via immunohistochemistry. The first conspicuous reduction in Snf2h immunoreactivity was observed at E12.5 (Figure 1F), i.e., at a time when the early-born retinal cell types are already being generated [36]. It is therefore likely that many GCs, HCs, ACs, and cones are established in the presence of functional Snf2h protein in the *Snf2h* cKO embryo. During the following embryonic stages examined, the number of retinal cells expressing Snf2h rapidly decreased, and from E15.5 onwards, almost all the remaining cells lacked the Snf2h protein (Figure 1G,H,M–P). Therefore, some early-born and almost all late-born retinal cells

developed in the absence of the Snf2h function. To investigate the phenotypic consequences of Snf2h deficiency, we first analyzed the retinal morphology with hematoxylin–eosin (H&E) staining. We did not find any obvious difference between wild-type and *Snf2h* cKO mice in the early embryonic stages (E9.5–E15.5). The retinal thickness of *Snf2h* cKO was comparable to wild-type control at E16.5 (Figure 2A,D), and no significant difference was observed until E18.5 (Figure 2G). After birth, the thickness of the *Snf2h*-deficient retina gradually decreased, and at P18, the retina was reduced by 60% compared with the wild-type control (Figure 2G). In contrast, *Snf2h* heterozygote mice (genotype mRx-Cre;Snf2h$^{fl/+}$) had normal retinal thickness and morphology even at postnatal week 50 (PW 50, Figure S4), indicating that a single functional allele of *Snf2h* is sufficient for normal retina development. The reduction in retinal thickness in *Snf2h* cKO was accompanied by the selective loss of the outer retinal segment, including ONL and the outer plexiform layer (OPL) (Figure 2F). It is of note that retinal lamination was preserved until P16, although the ONL was poorly distinguishable (Figure 2E). The GCL and INL, along with the inner plexiform layer (IPL), were retained but were thinner than the wild-type control (Figure 2C,F).

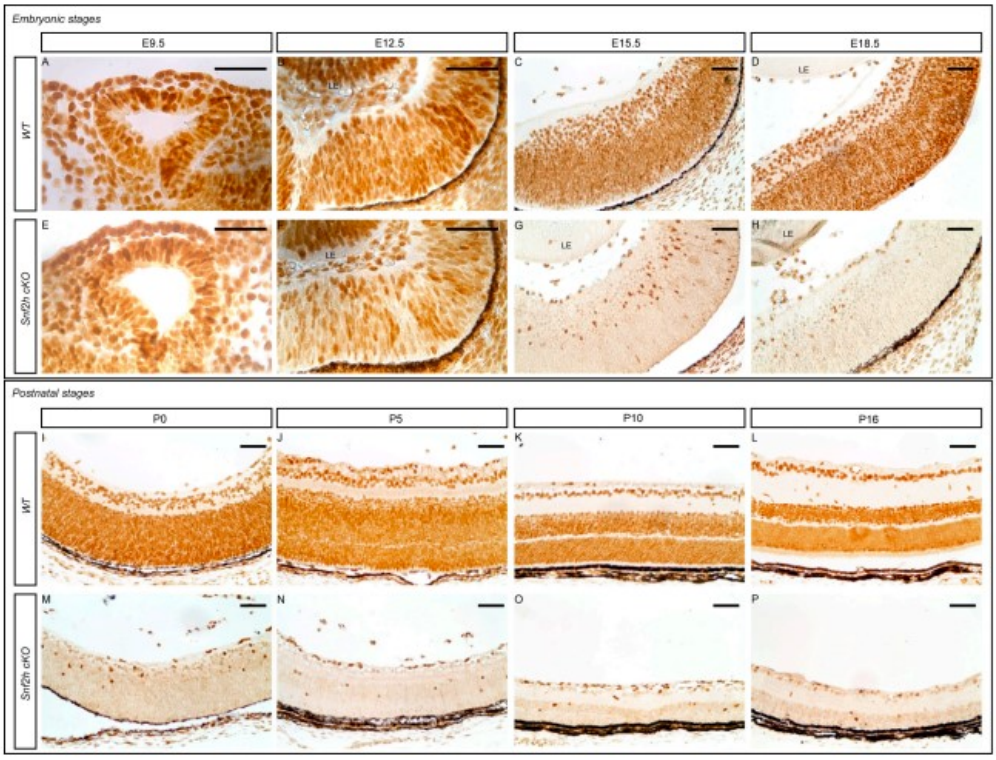

Figure 1. *Snf2h* expression during retina development. Immunohistochemistry staining of wild-type and mRx-Cre; Snf2h$^{fl/fl}$ (*Snf2h* cKO) mice was carried out with anti-Snf2h specific antibodies in different embryonic and postnatal stages. *Snf2h* started to be expressed in early embryonic stages and was maintained in wild-type individuals throughout embryonic development, and in adulthood in both retinal progenitors and differentiated retinal cells (**A**–**D**,**I**–**L**). A decrease in Snf2h levels was first observed in E12.5 conditionally mutant retinae (**A**,**B**,**E**,**F**). During the following embryonic stages, a rapid reduction in Snf2h-positive cells in *Snf2h* cKO eye sections occurred (**G**,**H**), and only a few Snf2h-positive cells were found in *Snf2h* cKO at the postnatal stage (**M**–**P**). LE–lens. Scale bars: 50 µm.

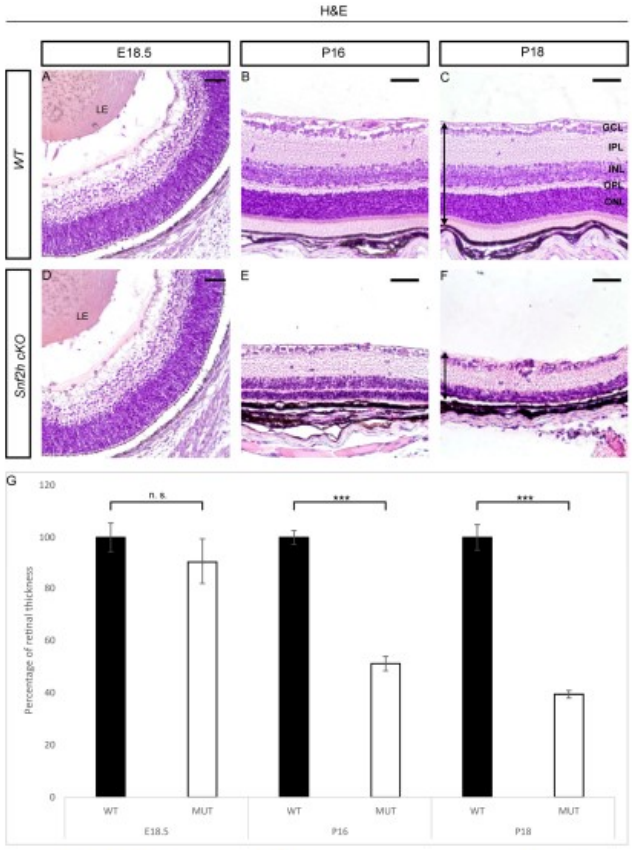

Figure 2. Morphology of *Snf2h*-deficient retina. Hematoxylin and eosin staining of embryonic and postnatal retinal sections of wild-type and *Snf2h* cKO was performed to display the retinal morphology. At the time of fully differentiated retinal cell types (P18), *Snf2h* cKO had dramatically reduced retinal thickness compared with controls (**C**,**F**). The outer retinal segment of *Snf2h* cKO mice was completely missing at P18 (**F**). *Snf2h*-deficient mice maintained the appropriate retinal structure until P16, although the outer nuclear layer (ONL) was almost indistinguishable (**B**,**E**). Differences in the thickness of the retina were not significant until birth (**A**,**D**,**G**). The time course of the retinal thinning is shown in the graph (**G**). The arrows show the range from where the retinal thickness was measured (**C**,**F**). GCL—ganglion cell layer, INL—inner nuclear layer, ONL—outer nuclear layer, IPL—inner plexiform layer, OPL—outer plexiform layer, and LE—lens. Error bars indicate standard derivation; *p*-values were calculated using Student's *t*-test ($n = 3$). *** $p < 0.001$, n.s. = not significant. Scale bars: 50 µm.

3.2. Snf2h Is Required for Photoreceptor Maintenance and Visual Perception of Mice

Considering that the outermost layer of the retina, which is missing in adult *Snf2h*-deficient mice, is formed by photoreceptors, we analyzed differentiation of cones and rods in *Snf2h* cKO mice during embryonic and postnatal stages. To follow photoreceptor specification and maturation, a set of antibodies directed against Otx2, Crx, and Rxrγ was used for photoreceptor mapping during embryonic stages. No significant differences in the immunoreactivity for these photoreceptor markers were observed in *Snf2h* cKO at E18.5 compared with controls (Figure 3A–F). At P0, we observed an approximately 25% reduction in photoreceptors in *Snf2h* cKO (Figure 3G–N).

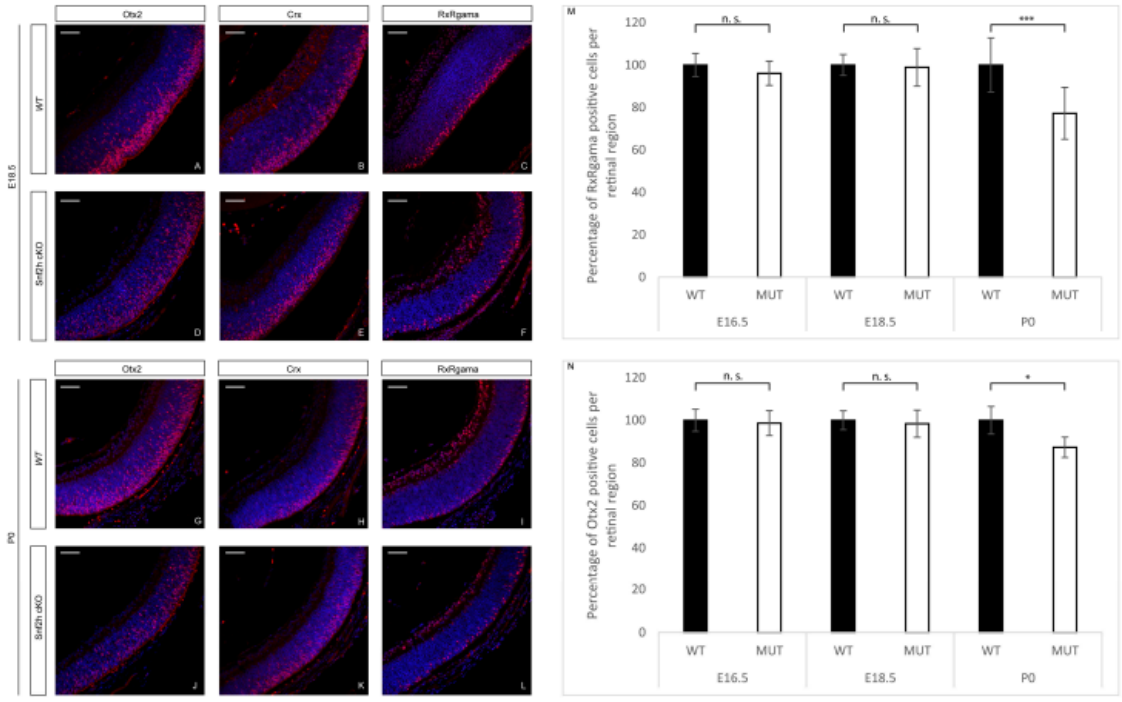

Figure 3. Photoreceptor specification in *Snf2h* cKO. To screen the photoreceptor development, a variety of different photoreceptor-specific markers were used; among them, Otx2, Crx, and Rxrγ were chosen for the embryonic immunofluorescent analysis. The immunostained retinal sections showed no significant differences between *Snf2h* cKO mice and controls at E18.5 (**A**–**F**). However, there was a rapid decrease in Rxrγ- and Otx2-positive cells in *Snf2h*-deficient mice immediately after birth (**G**–**N**). Error bars indicate standard derivation; *p*-values were calculated using Student's *t*-test ($n = 3$). * $p < 0.05$, *** $p < 0.001$, n.s. = not significant. Scale bars: 50 µm.

At postnatal stages, we used different opsin markers specific for cones or rods to follow photoreceptor maturation based on their onset, the level of expression, and subcellular localization. Rhodopsins are expressed throughout the entire length of the outer retinal segment, whereas M-opsins are preferentially located dorsally, and S-opsins are located ventrally [55,71]. Since the mouse retina is rod-dominated, the prevailing opsin is rhodopsin, which was first detectable in control mice at P5 (Figure 4A). In *Snf2h* cKO mice, the process of rod photoreceptor maturation appeared to occur normally, although the signal strength of immunostaining was weaker than wild-type controls (Figure 4D). An approximately normal level of rhodopsin expression was detected in *Snf2h*-deficient retina even at P10 (Figure 4E). Shortly thereafter, the expression of rhodopsin was extinguished, and only sparse rhodopsin-positive cell residues were present at P18 (Figure 4F). A similar result was obtained via immunostaining for cone photoreceptors. We used two mouse cone-opsin-specific markers, S-opsin (short wavelength) and M-opsin (medium wavelength). At P5, the expression of S-opsin was weaker in *Snf2h* cKO mice compared with controls (Figure 4G,J). At P10, the *Snf2h* deficient retina still retained some S-opsin-positive cells, but compared with wild-type, their numbers were reduced (Figure 4H,K). Finally, at P18, the *Snf2h*-deficient cones lacked their characteristic shape and S-opsin positive residues were accumulated just below the INL (Figure 4I,L). The M-opsin staining at P18 showed a pattern overall similar to that of S-opsin (Figure 4R). Since the main decline in photoreceptor development occurred between P10 and P18, we hypothesized that the key event leading to

photoreceptor damage is the opening of the eye at P14. The animals were analyzed at P13, when the eyes are still closed, and at P14, after eye opening. A noticeable difference in the thickness of *Snf2h* cKO retinas between the P13 and P14 stages was observed (Figure S5). Immunodetection for rhodopsin, M- and S-opsin confirmed the significant deterioration of the morphology of the outer photoreceptor segment between stages P13 (Figure S6) and P14 (Figure S7) in *Snf2h* cKO mice. The outer photoreceptor segments were extremely shortened, lost their orientation, and spread within the outermost retinal layer. Our data, therefore, suggest that an excess of light at the eye-opening stage is not a leading factor of photoreceptor damage in *Snf2h* cKO. Instead, the loss of photoreceptors is regulated by intrinsic cues and is gradual.

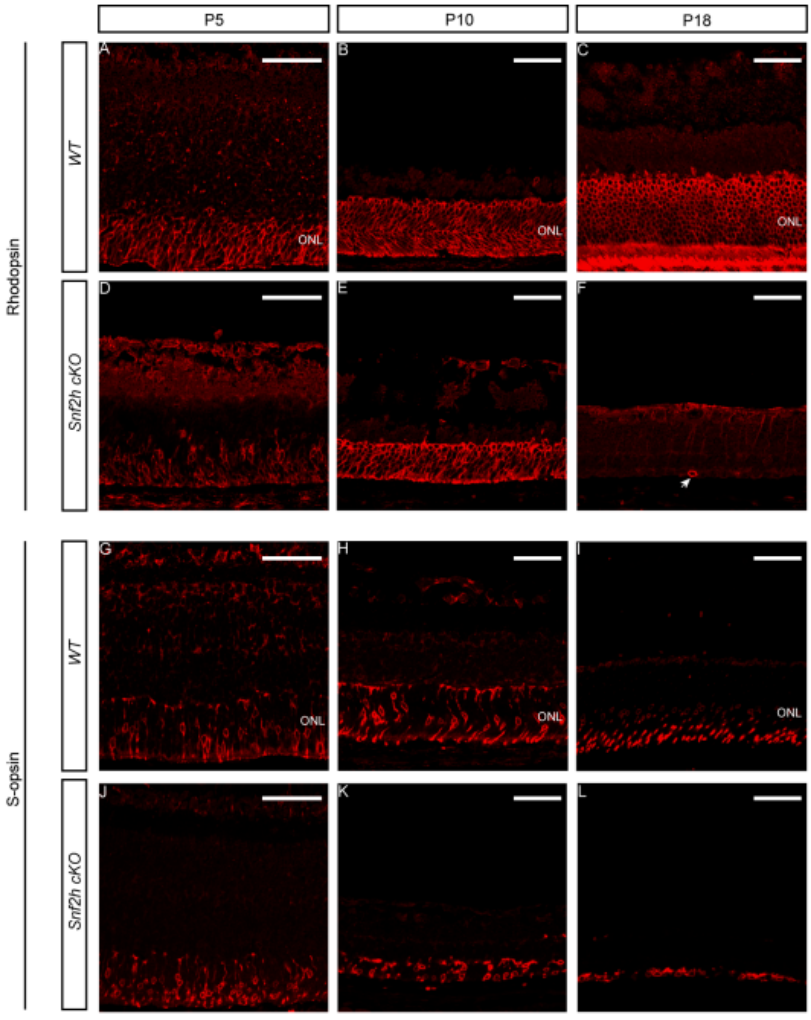

Figure 4. *Cont.*

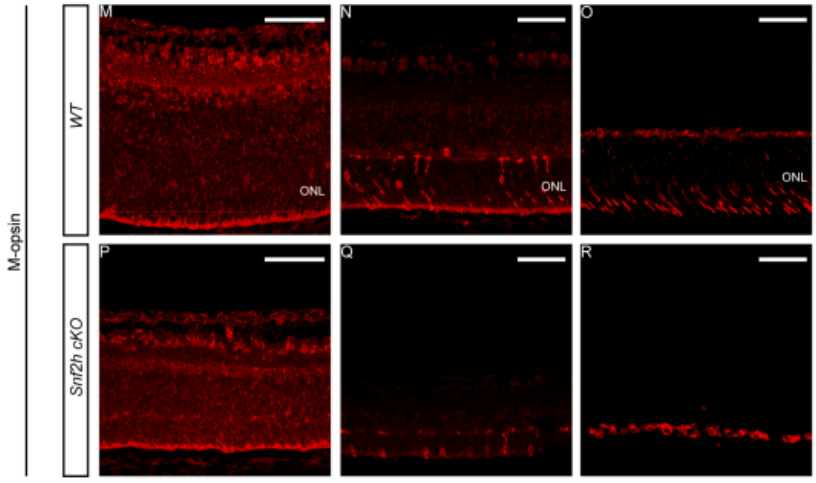

Figure 4. Photoreceptor maintenance in *Snf2h* cKO during postnatal stages. Specific opsin markers were used to determine the photoreceptor state in *Snf2h* cKO after birth. Rhodopsin detects the rod photoreceptors S-opsin (the short-wavelength cone photoreceptors) and M-opsin (the medium-wavelength cones). Except for M-opsin, which was not expressed until P8, opsin expression was mapped from P5 to P18 (**A**–**R**). At P10, all opsins were expressed in *Snf2h*-deficient retinae, although the ONL layer was significantly reduced in thickness compared with controls (**B**,**E**,**H**,**K**,**N**,**Q**). At P18, no rhodopsin-positive photoreceptors were present in *Snf2h* cKO, and only scattered rhodopsin-positive residues were identified in the entire retinal section (**F**, indicated by an arrow). At P18, the differences between *Snf2h* cKO and controls in S-opsin (**I**,**L**) and M-opsin (**O**,**R**) expression were conspicuous, but not as pronounced as the loss of rhodopsin expression. Nevertheless, the shape of cone photoreceptors appeared abnormal. Scale bars: 50 µm.

3.3. All Other Retinal Cell Types Are Specified in the Absence of Snf2h Function

To investigate whether the Snf2h function is not restricted to photoreceptors but is also required for the generation and/or maintenance of other retinal cell types, we performed immunohistochemistry labeling for specific retinal markers of each cell type. We found that GCs (Brn3a-positive cells, Figure 5A,F), HCs (Oc2-positive cells, Figure 5B,G), ACs (Pax6-positive cells, Figure 5C,H), BCs (Chx10-positive cells, Figure 5D,I), and MCs (Lhx2-positive cells, Figure 5E,J) were present in Snf2h-deficient retina. Combined, our data indicate that *Snf2h* is not necessary for the specification of these cell types in the mature mouse retina.

3.4. Loss of Snf2h Causes Cell-Cycle Defects and Increased Apoptosis

Next, we sought to determine whether the decreased retinal cell numbers were due to poor RPC expansion or the initiation of intense apoptosis, or both. To analyze retinal cell proliferation, we examined EdU incorporation during embryonic retina development following a 24 h chase period. The EdU incorporation at P0 revealed a dramatic reduction in the number of EdU-positive cells in *Snf2h* cKO—almost no EdU^+ cells were detectable in contrast to controls, where the proliferation was still high and concentrated in the INL (Figure 6D,H,I). Such an extreme loss of proliferating cells explains the sharp reduction in retinal thickness after birth. A major proliferation defect was already observed during embryonic development. The EdU labeling of wild-type and *Snf2h* cKO retinae significantly differed at E16.5, and the difference increased with each consecutive embryonic day (Figure 6A–H,I). The reduction in EdU-positive cells in the *Snf2h*-deficient retina was already detectable at E15.5 following a brief 1 h pulse (Figure 6J–L). Very similar data were obtained using cyclin D1 immunofluorescent labeling (Figure S8), which not only reflected the S-phase but also the G1/S transition. Combined, these results indicate that

Snf2h is necessary for the proper initiation and progress of DNA replication in retinal cells, which is consistent with previous in vitro studies [72–75]. Next, we used an anti-CENP-A (centromere protein A) antibody recognizing the H3 histone variant that is incorporated into centromeric nucleosomes and is essential for centromere localization and chromosomal segregation. The overall signal was substantially decreased in *Snf2h* cKO mice, in contrast with wild-type animals at E17.5 (Figure 6M,N).

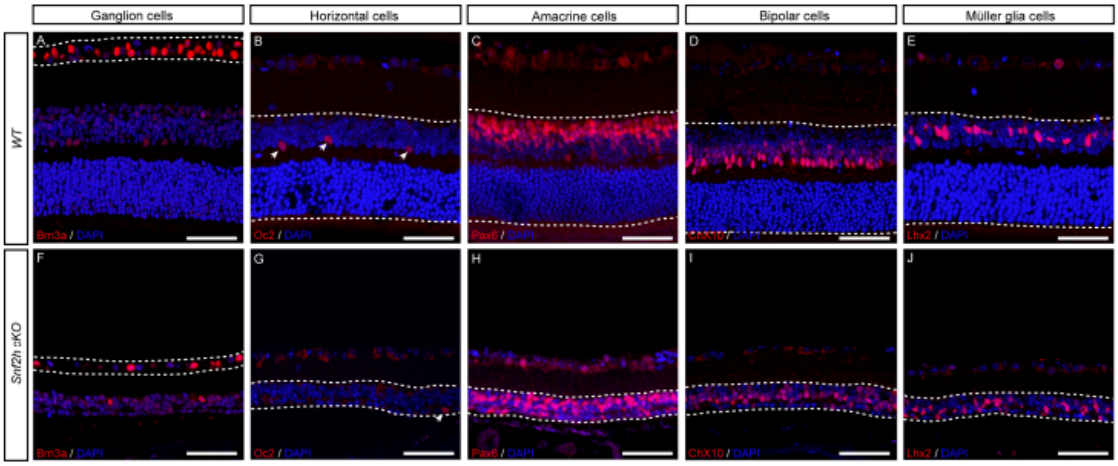

Figure 5. All cell types in GCL and INL are present in the *Snf2h*-deficient retina. GCs in the GCL were detected using anti-Brn3a antibodies in the P18 retina (**A**,**F**). The interneurons in INL of P18 (**B**,**D**,**E**,**G**,**I**,**J**) or P22 (**C**,**H**) were identified by the following molecular markers: Oc2 (HCs), Pax6 (ACs), Chx10 (BCs), and Lhx2 (MCs). Scale bars: 50 µm.

This result suggests that in *Snf2h* cKO retinal cells, the chromosomes are not able to attach to the spindle apparatus and are therefore not separated. Next, we investigated whether the dramatic decrease in retinal cell numbers was also partly due to increased apoptosis. It was indeed likely that the DNA damage in *Snf2h* cKO led to chromosomal instability and an increased rate of programmed cell death. We first analyzed the apoptosis using an anti-cleaved caspase-3 (cCas3) antibody at E16.5, and in correlation with pronounced proliferation defects, the number of apoptotic cells also increased (Figure 7A,I). A dramatic increase in cCas3-positive cells was observed in *Snf2h* cKO compared with controls at P0 (Figure 7D,H,I). It should be noted that both poor replication and an increase in apoptosis were not unique to any specific retinal layer but observed in almost the entire retina. The p53 pathway is often activated upon DNA damage, leading to increased apoptosis. To determine whether the p53 pathway was activated in *Snf2h*-deficient retinae, we analyzed the expression of the pathway-related genes using qRT-PCR (Figure 8). We focused on genes directly controlled by p53, namely *Cdkn1a* (p21), *Cdkn2a* (Arf), *Atm*, *Atr*, *Mdm2*, *Ptf1a* (p48), *Casp3*, *Casp9*, *Ccna2* (cyclin A), *Ccnb1* (cyclin B), *Ccne1* (cyclin E), and *Ccng1* (cyclin G). These genes encode the proteins involved in various functions: Some are necessary for entering the next cell-cycle phase, some act as checkpoints, and others change their expression levels upon the programmed cell death or directly inhibit p53 function. The qRT-PCR confirmed the increased expression of the *Trp53* gene (p53) in *Snf2h* cKO retinae. In addition, the levels of cyclin inhibitor p21 were elevated. This result suggests that the *Snf2h*-depleted retinal cells are arrested in the G1-phase of the cell cycle. The altered levels of cyclin E and cyclin B furthermore indicated possible irregularities during S-phase progression, whereas the reduced levels of both Atm and Atr mRNAs in *Snf2h* cKO retinae showed impairment in cell-cycle checkpoints. Severe downregulation of cyclin G mRNA levels in *Snf2h*-deficient retinae indicated impaired p53 negative feedback loop, a condition

that may result in the constitutive activation of the p53 pathway. Finally, we compared the expression levels of caspase-3 and caspase-9 genes in wild-type and *Snf2h* cKO. Although both genes are expressed during apoptosis, only caspase-3 mRNA levels were upregulated in the mutant retinae.

Taken together, our analyses demonstrate cell-cycle defects, the activation of the p53 pathway mRNA targets, and increased apoptosis in *Snf2h* cKO retinae.

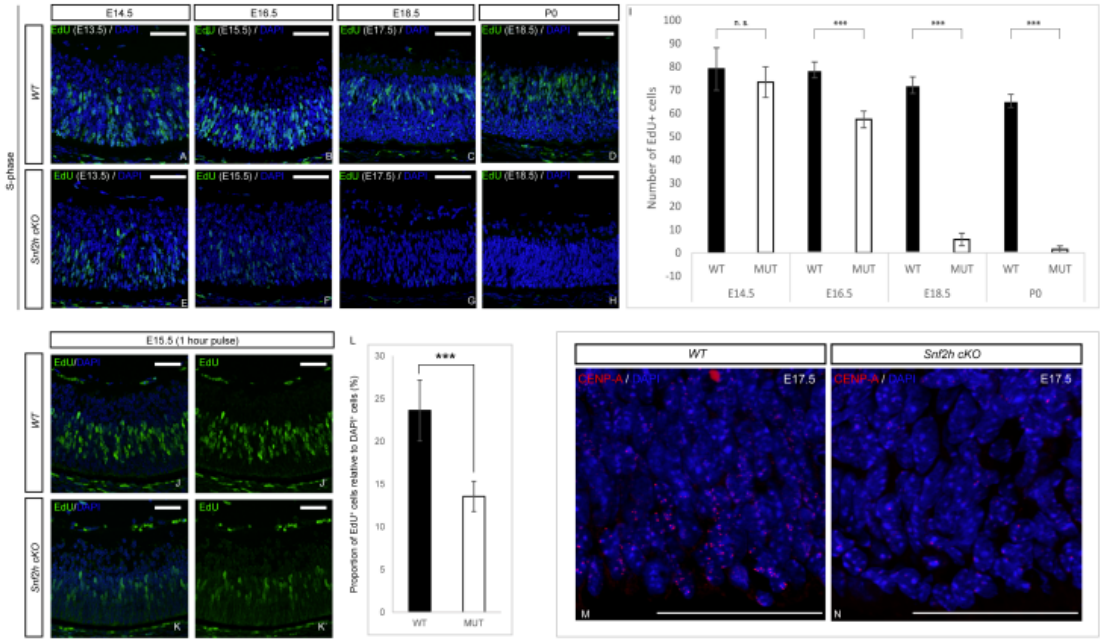

Figure 6. Cell-cycle analysis of *Snf2h*-deficient retinal cells. The retinal proliferation was analyzed via EdU incorporation. Pregnant females were intraperitonally injected with EdU 24 h prior to sacrifice at indicated stages. The number of EdU$^+$ cells in wild-type and *Snf2h* cKO mice was comparable until E14.5. The differences first appeared at E16.5—the number of EdU$^+$ cells was decreased by ~25% in *Snf2h*-deficient mice compared with controls. Subsequently, at E18.5 and after birth, almost no EdU$^+$ cells were detectable in *Snf2h* cKO, in contrast with the massive proliferation rate in wild-type retinae (**A**–**I**). Pregnant females were injected with EdU one hour prior to sacrifice. The proportion of EdU$^+$ cells/DAPI$^+$ cells was reduced in *Snf2h*-deficient retina at E15.5 (**J**, **J′**,**K**, **K′**,**L**). Expression of CENP-A (centromere protein A) at E17.5. CENP-A is essential for centromere localization and proper chromosomal segregation. The CENP-A antibody staining was widespread in wild-type retinae at E17.5 (**M**), whereas in *Snf2h*-depleted retinae, only a few CENP-A-positive cells were found (**N**), indicating impaired chromosomal segregation in *Snf2h* cKO retinal cells. Error bars indicate standard derivation; *p*-values were calculated using Student's *t*-test ($n = 4$). *** $p < 0.001$, n.s. = not significant. Scale bars: 50 µm.

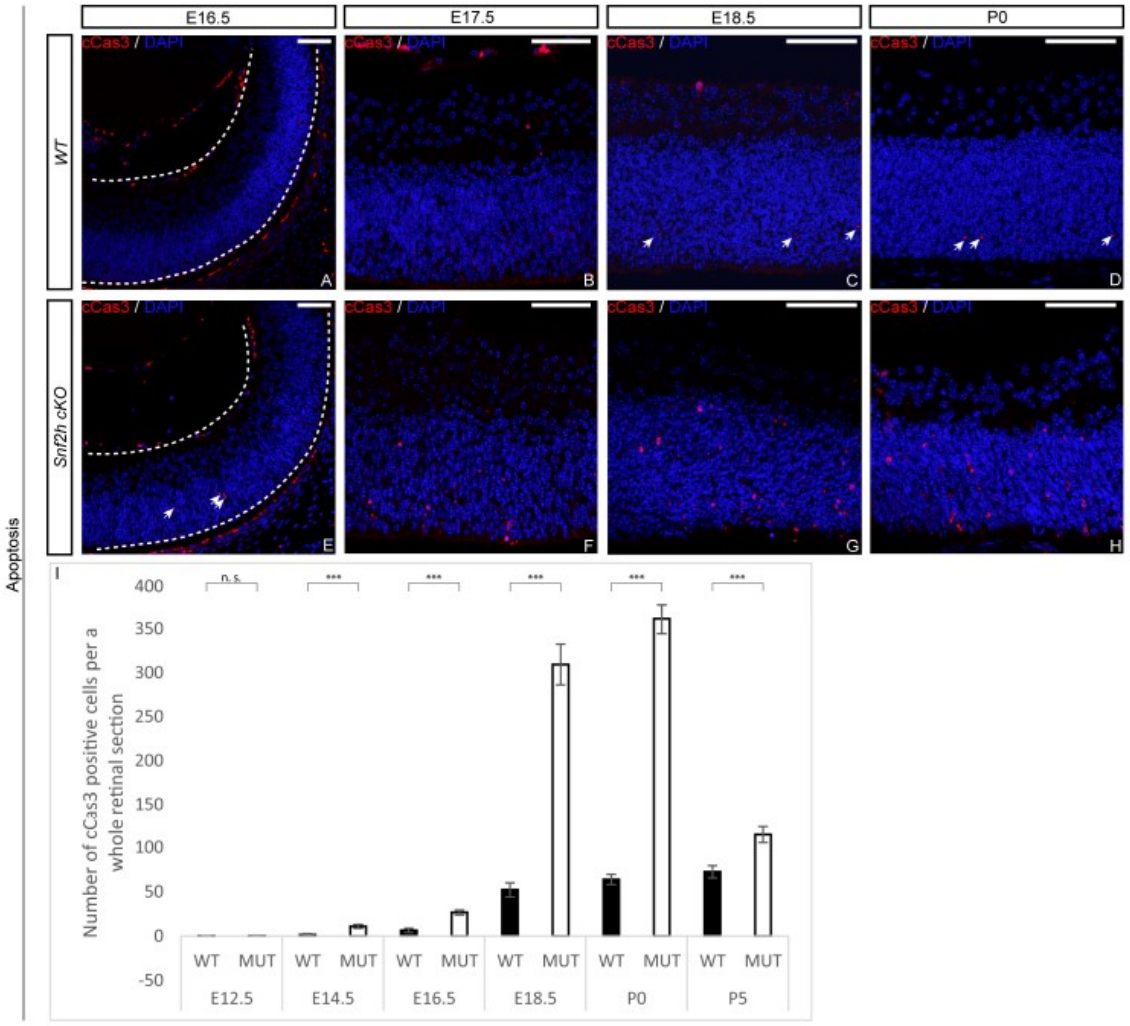

Figure 7. Loss of Snf2h in developing retina is accompanied by massive apoptosis. The number of apoptotic cells in embryonic and postnatal retinae was detected using the anti-cleaved caspase-3 (cCas3) antibody. The differences between *Snf2h* cKO and controls first appeared at E14.5 (**I**) and gradually increased during later embryonic stages (**A**–**C**,**E**–**G**,**I**). The peak of apoptosis in *Snf2h*-deficient mice was at P0 (**D**,**H**,**I**). The number of cCas3-positive cells in *Snf2h*-deficient retinae decreased during the postnatal stages; nevertheless, it remained significantly higher at P5 compared with wild-type controls (**I**). Error bars indicate standard derivation; *p*-values were calculated using Student's *t*-test ($n = 4$). *** $p < 0.001$, n.s. = not significant. White arrows indicate cCas3-positive cells. Scale bars: 50 m.

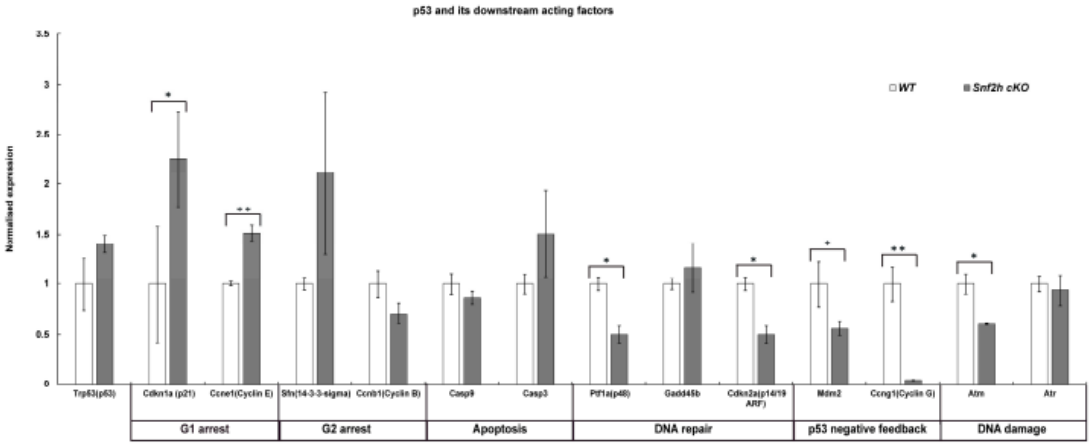

Figure 8. Quantification of mRNA expression of p53 downstream acting factors at P0 assessed with qRT-PCR. Whole retinae from P0 wild-type and *Snf2h* cKO eyes were dissected, subjected to RNA isolation, and processed using qRT-PCR. A total of 3 retinas were tested. Error bars indicate standard derivation; *p*-values were calculated using Student's *t*-test ($n = 3$). * $p < 0.05$, ** $p < 0.01$.

4. Discussion

The Snf2h protein acts as a chromatin remodeler. Here, through conditional gene targeting and detailed phenotypic analysis, we elucidated the function of the *Snf2h* gene during the development, differentiation, and maturation of the mouse retina. Considering that Snf2h serves as a catalytic subunit (ATPase) and is incorporated into several distinct ISWI chromatin remodeling complexes (ACF, WICH, CHRAC, RSF, and NoRC), the loss of Snf2h likely results in broad impairment of the chromatin dynamics and organization. Snf2h acts as the main executive component of these complexes, whereas the other subunits enhance and direct diverse processes such as DNA replication, DNA repair, recombination, and transcription [15,76,77]. Defects observed here in *Snf2h* cKO might be due to the Snf2h function in any of these processes alone or due to a combination of defects in several of them. Our data indicated that the *Snf2h*-deficient retina exhibited impaired progenitor cell expansion. Based on EdU incorporation and the immunofluorescent staining of proliferation markers, we identified a dominant defect in the S-phase of the cell cycle (the process of DNA replication). When *Snf2h* cKO mice were compared with controls, the first remarkable decline in S-phase progression manifested itself at E16.5, i.e., soon after the common peak of production of early-born retinal cells [35–38]. During later embryonic development, the replication activity gradually decreased in *Snf2h* cKO and was minimal at birth. In contrast, in wild-type retinae, proliferation continued approximately up to P8 [30,78,79]. Such a rapid loss of DNA replication was previously observed in the *Snf2h*-depleted Purkinje cells of the mouse cerebellum [17]. Our qRT-PCR results provided further support for aberrant S-phase progression and specifically pointed to the G1/S transition. The increased levels of p21 and cyclin E mRNAs in *Snf2h*-depleted retinal cells indicated cell-cycle arrest in G1. It is therefore likely that the extremely rapid decline in DNA replication in embryonic retinal cells is due to the combination of both factors. The importance of Snf2h for DNA replication during the cell cycle was previously shown by several in vitro studies [72–75]. These studies were focused on the specific aspects of the S-phase, and all established the key role of Snf2h-containing complexes during heterochromatin replication. In addition, the Snf2h function is required in the early S-phase [75], in which the actively transcribed genes within euchromatin are replicated [80]. We propose that the process of cell division is impaired in the *Snf2h* cKO retinae. Heterochromatin, whose replication is primarily disrupted, is incorporated into the pericentromeric region. This region is

characterized as a condensed, transcriptionally repressed chromatin part, necessary for genome stability, chromosome pairing, and segregation [81–83]. Perpelescu et al. [84] established a key role for the RSF complex, composed of Rsf1 (remodeling and spacing factor 1) and Snf2h, in maintaining a proper centromere structure via the stabilization of the centromere protein A histone variant (CENPA). Our CENP-A analysis indicates that the *Snf2h*-depleted mitotic chromosomes do not contain functional centromeres. It is interesting that Alvarez-Saavedra et al. [17] listed *HJURP* (Holliday junction recognition protein) as a gene downregulated in the *Snf2h*-deficient cerebellum. HJURP was recently identified as a protein involved in the localization of CENP-A into the centromere and thereby is critical for centromere formation and maintenance [85–88]. If the division of the cell nucleus is indeed not properly carried out, then the *Snf2h*-deficient retinal cells likely carry an abnormal number of chromosomes. Hereby, we can conclude that the *Snf2h* gene is required for the proliferation of RPCs. In the absence of the Snf2h function, several cell-cycle processes occur incorrectly.

The loss of Snf2h in the retina leads to massive apoptosis demonstrated by an increased number of cleaved caspase-3-positive cells from E16.5 onwards, with the highest peak at P0. Caspase-3 activates the extrinsic apoptotic pathway, whereas caspase-9, whose levels were not significantly changed in the *Snf2h* cKO retinae, activates the intrinsic apoptotic pathway. We speculate that the loss of Snf2h and the activation of the p53 pathway influences only the extrinsic apoptotic pathway whose effector caspase is caspase-3.

Given that all retinal cell types are developed from a common pool of retinal progenitor cells, the population of which depletes with proceeding retinogenesis, it is not surprising that the proliferation defects in *Snf2h* cKO cause retina abnormalities in young adult mice. More remarkable is, however, that the degeneration predominantly affects photoreceptor cells. The reason for this is currently unclear. Cones and rods occupy the outermost layer of the retina, and their basic function and morphology are similar despite their different birth order during retinogenesis. Cones are generated along with the early-born retinal neurons, whereas rods are classified as later-born cells [36].

The Cre driver used here, the mRx-Cre BAC transgenic line, is an early retina-specific deleter active from E9.0 [66]. In our previous study using this Cre line, we were able to efficiently deplete Pax6 already by E10.5 [89] and Meis1/Meis2 by E14.5 [90]. However, due to the Snf2h protein stability, the conspicuous depletion of the Snf2h protein was observed by E12.5, and little to no Snf2h immunoreactivity was present only by E15.5, which is still much earlier than the P0 stage by which we observed the elimination of the extremely stable polycomb proteins [65]. Considering that the Snf2h depletion in *Snf2h* cKO started at E12.5, many cones were still generated in the presence of Snf2h. This was, however, not the case for late-born rods. Originally, we hypothesized that the birth order of each retinal cell type would play a role in the resulting phenotype of *Snf2h* cKO mice. We assumed that the late-born cell types that develop in the absence of the Snf2h function (BCs, MGs, and rod photoreceptors) would be much more affected than the early-born neurons. Our results indicated, however, that the birth order did not generally correlate with the magnitude of the loss of a particular retinal cell type. GCs, ACs, MGs, and BCs were present in adult mice, whereas the photoreceptors had a tendency to disappear completely. Based on marker analysis during embryonic stages (Otx, Crx, Blimp, and Rxrγ immunoreactivity), we concluded that the photoreceptors in *Snf2h* cKO were correctly specified and were generated in numbers comparable to wild-type controls. The small loss in photoreceptor numbers occurring before birth was associated with insufficient proliferation and increased apoptosis. Overall, the process of photoreceptor degeneration appeared to be gradual and not directly triggered by external stimuli such as light. Moreover, on closer observation, we found that the photoreceptor collapse could also be caused by damage in synaptogenesis. In the case in which the photoreceptor cells lose contact with either interneurons or retinal pigment epithelium, a subsequent degenerative process is initiated [91–94]. In the case of *Snf2h* cKO, retinal degeneration occurs early and is fairly rapid. When retinal degeneration occurs, MCs can activate a gliosis process, which leads to the formation of a glial scar

containing a range of auxiliary materials [95,96]. This in turn acts as a protection against further neuronal deprivation [97,98]. Such a protective mechanism in the *Snf2h*-deficient retina could perhaps contribute to the maintenance of GCL and INL, including the relevant cell types, even in aging mice (at PW 50).

5. Conclusions

Our analysis of *Snf2h*-deficient mice revealed that Snf2h controls the expansion of the pool of RPCs by safeguarding the cell-cycle progress. In addition, Snf2h appears to be critically required for photoreceptor maintenance in the postnatal mouse retina. Since at the molecular level, Snf2h is a catalytic subunit of several distinct multicomponent complexes dedicated to unrelated nuclear processes, it is unlikely that all the defects observed in *Snf2h* cKO are due to a single Snf2h complex. Further studies aimed at the functional characterization of other components of Snf2h-containing complexes are needed in order to dissect their specific roles in retina growth, maturation, and maintenance.

Supplementary Materials: The following supporting information can be downloaded at: https://www.mdpi.com/article/10.3390/cells12071035/s1. Figure S1: Expression of Snf2h and its interacting partners during retinal development; Figure S2: Expression of components of ALL-1 supercomplex and PRC1 complex during retinal development. Figure S3: Expression of centromere complex components during retinal Development; Figure S4: Morphology of heterozygous mice at postnatal week 50 (PW50); Figure S5: Retinal morphology of Snf2h cKO at P13 and P14; Figure S6: Photoreceptor characterization at P13 (before eye opening); Figure S7: Photoreceptor characterization at P14 (after eye opening); Figure S8: Expression of cyclin D1 in Snf2h cKO during embryonic and postnatal stages; Table S1. List of primary antibodies used for immunohistochemistry; Table S2: List of primers used for qRT-PCR.

Author Contributions: A.K., N.D. and Z.K.: conception and project design, acquisition of data, analysis and interpretation of data, drafting and revising the manuscript. B.A., S.S.S., Z.K.J. and J.P.: analysis and interpretation of data. A.I.S. and T.S.: provision of Snf2h-floxed mouse strain. All authors have read and agreed to the published version of the manuscript.

Funding: This work was supported by a grant from the Czech Science Foundation (21–27364S) to Z.K. Portions of this work were supported by national funds from the Ministry of Education, Youth and Sports of the Czech Republic under the European Joint Programme on Rare Diseases (Solve-RET 8F20004), by a grant from the National Institutes of Health (GM116143) to A.I.S., and by AZV NU22-05-00374, Programme EXCELES LX22NPO5102, University Center UNCE/MED/016, and COOPERATIO 207020 Biology to T.S.

Institutional Review Board Statement: The housing of mice and in vivo experiments were performed in compliance with the European Communities Council Directive of 24 November 1986 (86/609/EEC) and national and institutional guidelines. Animal care and experimental procedures were approved by the Animal Care Committee of the Institute of Molecular Genetics (no. 71/2014). This work did not include human subjects.

Informed Consent Statement: Not applicable.

Data Availability Statement: The data presented in this study are available on request from the corresponding author.

Acknowledgments: We would like to thank Veronika Noskova, Anna Zitova, Jitka Lachova, and Jindra Pohorela for their technical assistance. We are grateful to Ales Cvekl for valuable discussions and Sarka Takacova for proofreading the manuscript. We acknowledge the Light Microscopy Core Facility, IMG CAS, Prague, Czech Republic, supported by MEYS (LM2018129, CZ.02.1.01/0.0/0.0/18_046/0016045) and RVO: 68378050-KAV-NPUI, for their support with the light sheet microscopy presented herein.

Conflicts of Interest: The authors declare no conflict of interest.

References

1. Richmond, T.J.; Davey, C.A. The structure of DNA in the nucleosome core. *Nature* **2003**, *423*, 145–150. [CrossRef] [PubMed]
2. Narlikar, G.J.; Fan, H.Y.; Kingston, R.E. Cooperation between complexes that regulate chromatin structure and transcription. *Cell* **2002**, *108*, 475–487. [CrossRef] [PubMed]
3. Jiang, D.; Li, T.; Guo, C.; Tang, T.S.; Liu, H. Small molecule modulators of chromatin remodeling: From neurodevelopment to neurodegeneration. *Cell Biosci.* **2023**, *13*, 10. [CrossRef] [PubMed]
4. Flaus, A.; Owen-Hughes, T. Mechanisms for ATP-dependent chromatin remodelling: The means to the end. *FEBS J.* **2011**, *278*, 3579–3595. [CrossRef]
5. Corona, D.F.; Tamkun, J.W. Multiple roles for ISWI in transcription, chromosome organization and DNA replication. *Biochim. Biophys. Acta* **2004**, *1677*, 113–119. [CrossRef]
6. Lazzaro, M.A.; Picketts, D.J. Cloning and characterization of the murine Imitation Switch (ISWI) genes: Differential expression patterns suggest distinct developmental roles for Snf2h and Snf2l. *J. Neurochem.* **2001**, *77*, 1145–1156. [CrossRef]
7. Kent, N.A.; Karabetsou, N.; Politis, P.K.; Mellor, J. In vivo chromatin remodeling by yeast ISWI homologs Isw1p and Isw2p. *Genes Dev.* **2001**, *15*, 619–626. [CrossRef]
8. Wiechens, N.; Singh, V.; Gkikopoulos, T.; Schofield, P.; Rocha, S.; Owen-Hughes, T. The Chromatin Remodelling Enzymes SNF2H and SNF2L Position Nucleosomes adjacent to CTCF and Other Transcription Factors. *PLoS Genet.* **2016**, *12*, e1005940. [CrossRef]
9. Atsumi, Y.; Minakawa, Y.; Ono, M.; Dobashi, S.; Shinohe, K.; Shinohara, A.; Takeda, S.; Takagi, M.; Takamatsu, N.; Nakagama, H.; et al. ATM and SIRT6/SNF2H Mediate Transient H2AX Stabilization When DSBs Form by Blocking HUWE1 to Allow Efficient gammaH2AX Foci Formation. *Cell Rep.* **2015**, *13*, 2728–2740. [CrossRef]
10. Toiber, D.; Erdel, F.; Bouazoune, K.; Silberman, D.M.; Zhong, L.; Mulligan, P.; Sebastian, C.; Cosentino, C.; Martinez-Pastor, B.; Giacosa, S.; et al. SIRT6 recruits SNF2H to DNA break sites, preventing genomic instability through chromatin remodeling. *Mol. Cell* **2013**, *51*, 454–468. [CrossRef]
11. Eberharter, A.; Becker, P.B. ATP-dependent nucleosome remodelling: Factors and functions. *J. Cell Sci.* **2004**, *117*, 3707–3711. [CrossRef]
12. Kadam, S.; Emerson, B.M. Mechanisms of chromatin assembly and transcription. *Curr. Opin. Cell Biol.* **2002**, *14*, 262–268. [CrossRef]
13. Langst, G.; Becker, P.B. Nucleosome mobilization and positioning by ISWI-containing chromatin-remodeling factors. *J. Cell Sci.* **2001**, *114*, 2561–2568. [CrossRef]
14. Reyes, A.A.; Marcum, R.D.; He, Y. Structure and Function of Chromatin Remodelers. *J. Mol. Biol.* **2021**, *433*, 166929. [CrossRef]
15. Erdel, F.; Rippe, K. Chromatin remodelling in mammalian cells by ISWI-type complexes–where, when and why? *FEBS J.* **2011**, *278*, 3608–3618. [CrossRef]
16. Acemel, R.D.; Tena, J.J.; Irastorza-Azcarate, I.; Marletaz, F.; Gomez-Marin, C.; de la Calle-Mustienes, E.; Bertrand, S.; Diaz, S.G.; Aldea, D.; Aury, J.M.; et al. A single three-dimensional chromatin compartment in amphioxus indicates a stepwise evolution of vertebrate Hox bimodal regulation. *Nat. Genet.* **2016**, *48*, 336–341. [CrossRef]
17. Alvarez-Saavedra, M.; De Repentigny, Y.; Lagali, P.S.; Raghu Ram, E.V.; Yan, K.; Hashem, E.; Ivanochko, D.; Huh, M.S.; Yang, D.; Mears, A.J.; et al. Snf2h-mediated chromatin organization and histone H1 dynamics govern cerebellar morphogenesis and neural maturation. *Nat. Commun.* **2014**, *5*, 4181. [CrossRef]
18. Pessina, F.; Lowndes, N.F. The RSF1 histone-remodelling factor facilitates DNA double-strand break repair by recruiting centromeric and Fanconi Anaemia proteins. *PLoS Biol.* **2014**, *12*, e1001856. [CrossRef]
19. Sala, A.; Toto, M.; Pinello, L.; Gabriele, A.; Di Benedetto, V.; Ingrassia, A.M.; Lo Bosco, G.; Di Gesu, V.; Giancarlo, R.; Corona, D.F. Genome-wide characterization of chromatin binding and nucleosome spacing activity of the nucleosome remodelling ATPase ISWI. *EMBO J.* **2011**, *30*, 1766–1777. [CrossRef]
20. Alenghat, T.; Yu, J.; Lazar, M.A. The N-CoR complex enables chromatin remodeler SNF2H to enhance repression by thyroid hormone receptor. *EMBO J.* **2006**, *25*, 3966–3974. [CrossRef]
21. Dirscherl, S.S.; Henry, J.J.; Krebs, J.E. Neural and eye-specific defects associated with loss of the imitation switch (ISWI) chromatin remodeler in Xenopus laevis. *Mech. Dev.* **2005**, *122*, 1157–1170. [CrossRef] [PubMed]
22. Stopka, T.; Skoultchi, A.I. The ISWI ATPase Snf2h is required for early mouse development. *Proc. Natl. Acad. Sci. USA* **2003**, *100*, 14097–14102. [CrossRef] [PubMed]
23. Deuring, R.; Fanti, L.; Armstrong, J.A.; Sarte, M.; Papoulas, O.; Prestel, M.; Daubresse, G.; Verardo, M.; Moseley, S.L.; Berloco, M.; et al. The ISWI chromatin-remodeling protein is required for gene expression and the maintenance of higher order chromatin structure in vivo. *Mol. Cell* **2000**, *5*, 355–365. [CrossRef] [PubMed]
24. He, S.; Limi, S.; McGreal, R.S.; Xie, Q.; Brennan, L.A.; Kantorow, W.L.; Kokavec, J.; Majumdar, R.; Hou, H., Jr.; Edelmann, W.; et al. Chromatin remodeling enzyme Snf2h regulates embryonic lens differentiation and denucleation. *Development* **2016**, *143*, 1937–1947. [CrossRef]
25. Cepko, C.L. The patterning and onset of opsin expression in vertebrate retinae. *Curr. Opin. Neurobiol.* **1996**, *6*, 542–546. [CrossRef]
26. Turner, D.L.; Cepko, C.L. A common progenitor for neurons and glia persists in rat retina late in development. *Nature* **1987**, *328*, 131–136. [CrossRef]
27. Turner, D.L.; Snyder, E.Y.; Cepko, C.L. Lineage-independent determination of cell type in the embryonic mouse retina. *Neuron* **1990**, *4*, 833–845. [CrossRef]

28. Rapaport, D.H.; Wong, L.L.; Wood, E.D.; Yasumura, D.; LaVail, M.M. Timing and topography of cell genesis in the rat retina. *J. Comp. Neurol.* **2004**, *474*, 304–324. [CrossRef]
29. Young, R.W. Cell differentiation in the retina of the mouse. *Anat. Rec.* **1985**, *212*, 199–205. [CrossRef]
30. Young, R.W. Cell proliferation during postnatal development of the retina in the mouse. *Brain Res.* **1985**, *353*, 229–239. [CrossRef]
31. Masland, R.H. Neuronal diversity in the retina. *Curr. Opin. Neurobiol.* **2001**, *11*, 431–436. [CrossRef]
32. Wassle, H.; Boycott, B.B. Functional architecture of the mammalian retina. *Physiol. Rev.* **1991**, *71*, 447–480. [CrossRef]
33. Zagozewski, J.L.; Zhang, Q.; Eisenstat, D.D. Genetic regulation of vertebrate eye development. *Clin. Genet.* **2014**, *86*, 453–460. [CrossRef]
34. Hong, Y.K.; Kim, I.J.; Sanes, J.R. Stereotyped axonal arbors of retinal ganglion cell subsets in the mouse superior colliculus. *J. Comp. Neurol.* **2011**, *519*, 1691–1711. [CrossRef]
35. Cherry, T.J.; Trimarchi, J.M.; Stadler, M.B.; Cepko, C.L. Development and diversification of retinal amacrine interneurons at single cell resolution. *Proc. Natl. Acad. Sci. USA* **2009**, *106*, 9495–9500. [CrossRef]
36. Livesey, F.J.; Cepko, C.L. Vertebrate neural cell-fate determination: Lessons from the retina. *Nat. Rev. Neurosci.* **2001**, *2*, 109–118. [CrossRef]
37. Brown, N.L.; Kanekar, S.; Vetter, M.L.; Tucker, P.K.; Gemza, D.L.; Glaser, T. Math5 encodes a murine basic helix-loop-helix transcription factor expressed during early stages of retinal neurogenesis. *Development* **1998**, *125*, 4821–4833. [CrossRef]
38. Cepko, C.L.; Austin, C.P.; Yang, X.; Alexiades, M.; Ezzeddine, D. Cell fate determination in the vertebrate retina. *Proc. Natl. Acad. Sci. USA* **1996**, *93*, 589–595. [CrossRef]
39. Carter-Dawson, L.D.; LaVail, M.M. Rods and cones in the mouse retina. I. Structural analysis using light and electron microscopy. *J. Comp. Neurol.* **1979**, *188*, 245–262. [CrossRef]
40. Ohsawa, R.; Kageyama, R. Regulation of retinal cell fate specification by multiple transcription factors. *Brain Res.* **2008**, *1192*, 90–98. [CrossRef]
41. Bringmann, A.; Iandiev, I.; Pannicke, T.; Wurm, A.; Hollborn, M.; Wiedemann, P.; Osborne, N.N.; Reichenbach, A. Cellular signaling and factors involved in Muller cell gliosis: Neuroprotective and detrimental effects. *Prog. Retin. Eye Res.* **2009**, *28*, 423–451. [CrossRef] [PubMed]
42. Fu, Y.; Yau, K.W. Phototransduction in mouse rods and cones. *Pflug. Arch. Eur. J. Physiol.* **2007**, *454*, 805–819. [CrossRef] [PubMed]
43. Brzezinski, J.A.; Reh, T.A. Photoreceptor cell fate specification in vertebrates. *Development* **2015**, *142*, 3263–3273. [CrossRef] [PubMed]
44. Du, J.; Rountree, A.; Cleghorn, W.M.; Contreras, L.; Lindsay, K.J.; Sadilek, M.; Gu, H.; Djukovic, D.; Raftery, D.; Satrustegui, J.; et al. Phototransduction Influences Metabolic Flux and Nucleotide Metabolism in Mouse Retina. *J. Biol. Chem.* **2016**, *291*, 4698–4710. [CrossRef] [PubMed]
45. Brzezinski, J.A.T.; Kim, E.J.; Johnson, J.E.; Reh, T.A. Ascl1 expression defines a subpopulation of lineage-restricted progenitors in the mammalian retina. *Development* **2011**, *138*, 3519–3531. [CrossRef]
46. Brzezinski, J.A.T.; Lamba, D.A.; Reh, T.A. Blimp1 controls photoreceptor versus bipolar cell fate choice during retinal development. *Development* **2010**, *137*, 619–629. [CrossRef]
47. Katoh, K.; Omori, Y.; Onishi, A.; Sato, S.; Kondo, M.; Furukawa, T. Blimp1 suppresses Chx10 expression in differentiating retinal photoreceptor precursors to ensure proper photoreceptor development. *J. Neurosci. Off. J. Soc. Neurosci.* **2010**, *30*, 6515–6526. [CrossRef]
48. Liu, H.; Etter, P.; Hayes, S.; Jones, I.; Nelson, B.; Hartman, B.; Forrest, D.; Reh, T.A. NeuroD1 regulates expression of thyroid hormone receptor 2 and cone opsins in the developing mouse retina. *J. Neurosci. Off. J. Soc. Neurosci.* **2008**, *28*, 749–756. [CrossRef]
49. Livne-Bar, I.; Pacal, M.; Cheung, M.C.; Hankin, M.; Trogadis, J.; Chen, D.; Dorval, K.M.; Bremner, R. Chx10 is required to block photoreceptor differentiation but is dispensable for progenitor proliferation in the postnatal retina. *Proc. Natl. Acad. Sci. USA* **2006**, *103*, 4988–4993. [CrossRef]
50. Nishida, A.; Furukawa, A.; Koike, C.; Tano, Y.; Aizawa, S.; Matsuo, I.; Furukawa, T. Otx2 homeobox gene controls retinal photoreceptor cell fate and pineal gland development. *Nat. Neurosci.* **2003**, *6*, 1255–1263. [CrossRef]
51. Bessant, D.A.; Payne, A.M.; Mitton, K.P.; Wang, Q.L.; Swain, P.K.; Plant, C.; Bird, A.C.; Zack, D.J.; Swaroop, A.; Bhattacharya, S.S. A mutation in NRL is associated with autosomal dominant retinitis pigmentosa. *Nat. Genet.* **1999**, *21*, 355–356. [CrossRef]
52. Rehemtulla, A.; Warwar, R.; Kumar, R.; Ji, X.; Zack, D.J.; Swaroop, A. The basic motif-leucine zipper transcription factor Nrl can positively regulate rhodopsin gene expression. *Proc. Natl. Acad. Sci. USA* **1996**, *93*, 191–195. [CrossRef]
53. Mears, A.J.; Kondo, M.; Swain, P.K.; Takada, Y.; Bush, R.A.; Saunders, T.L.; Sieving, P.A.; Swaroop, A. Nrl is required for rod photoreceptor development. *Nat. Genet.* **2001**, *29*, 447–452. [CrossRef]
54. Swaroop, A.; Xu, J.Z.; Pawar, H.; Jackson, A.; Skolnick, C.; Agarwal, N. A conserved retina-specific gene encodes a basic motif/leucine zipper domain. *Proc. Natl. Acad. Sci. USA* **1992**, *89*, 266–270. [CrossRef]
55. Swaroop, A.; Kim, D.; Forrest, D. Transcriptional regulation of photoreceptor development and homeostasis in the mammalian retina. *Nat. Rev. Neurosci.* **2010**, *11*, 563–576. [CrossRef]
56. Swain, P.K.; Chen, S.; Wang, Q.L.; Affatigato, L.M.; Coats, C.L.; Brady, K.D.; Fishman, G.A.; Jacobson, S.G.; Swaroop, A.; Stone, E.; et al. Mutations in the cone-rod homeobox gene are associated with the cone-rod dystrophy photoreceptor degeneration. *Neuron* **1997**, *19*, 1329–1336. [CrossRef]

57. Hardwick, L.J.; Ali, F.R.; Azzarelli, R.; Philpott, A. Cell cycle regulation of proliferation versus differentiation in the central nervous system. *Cell Tissue Res.* **2015**, *359*, 187–200. [CrossRef]
58. Dyer, M.A.; Cepko, C.L. Regulating proliferation during retinal development. *Nat. Rev. Neurosci.* **2001**, *2*, 333–342. [CrossRef]
59. Diacou, R.; Nandigrami, P.; Fiser, A.; Liu, W.; Ashery-Padan, R.; Cvekl, A. Cell fate decisions, transcription factors and signaling during early retinal development. *Prog. Retin. Eye Res.* **2022**, *91*, 101093. [CrossRef]
60. Zhang, J.; Taylor, R.J.; La Torre, A.; Wilken, M.S.; Cox, K.E.; Reh, T.A.; Vetter, M.L. Ezh2 maintains retinal progenitor proliferation, transcriptional integrity, and the timing of late differentiation. *Dev. Biol.* **2015**, *403*, 128–138. [CrossRef]
61. Popova, E.Y.; Grigoryev, S.A.; Fan, Y.; Skoultchi, A.I.; Zhang, S.S.; Barnstable, C.J. Developmentally regulated linker histone H1c promotes heterochromatin condensation and mediates structural integrity of rod photoreceptors in mouse retina. *J. Biol. Chem.* **2013**, *288*, 17895–17907. [CrossRef] [PubMed]
62. Popova, E.Y.; Barnstable, C.J.; Zhang, S.S. Cell type-specific epigenetic signatures accompany late stages of mouse retina development. *Adv. Exp. Med. Biol.* **2014**, *801*, 3–8. [CrossRef] [PubMed]
63. Merbs, S.L.; Khan, M.A.; Hackler, L., Jr.; Oliver, V.F.; Wan, J.; Qian, J.; Zack, D.J. Cell-specific DNA methylation patterns of retina-specific genes. *PLoS ONE* **2012**, *7*, e32602. [CrossRef] [PubMed]
64. Lagali, P.S.; Picketts, D.J. Matters of life and death: The role of chromatin remodeling proteins in retinal neuron survival. *J. Ocul. Biol. Dis. Inform.* **2011**, *4*, 111–120. [CrossRef]
65. Fujimura, N.; Kuzelova, A.; Ebert, A.; Strnad, H.; Lachova, J.; Machon, O.; Busslinger, M.; Kozmik, Z. Polycomb repression complex 2 is required for the maintenance of retinal progenitor cells and balanced retinal differentiation. *Dev. Biol.* **2018**, *433*, 47–60. [CrossRef]
66. Klimova, L.; Lachova, J.; Machon, O.; Sedlacek, R.; Kozmik, Z. Generation of mRx-Cre transgenic mouse line for efficient conditional gene deletion in early retinal progenitors. *PLoS ONE* **2013**, *8*, e63029. [CrossRef]
67. Aldiri, I.; Xu, B.; Wang, L.; Chen, X.; Hiler, D.; Griffiths, L.; Valentine, M.; Shirinifard, A.; Thiagarajan, S.; Sablauer, A.; et al. The Dynamic Epigenetic Landscape of the Retina During Development, Reprogramming, and Tumorigenesis. *Neuron* **2017**, *94*, 550–568. [CrossRef]
68. Kim, D.; Paggi, J.M.; Park, C.; Bennett, C.; Salzberg, S.L. Graph-based genome alignment and genotyping with HISAT2 and HISAT-genotype. *Nat. Biotechnol.* **2019**, *37*, 907–915. [CrossRef]
69. Goodwin, L.R.; Picketts, D.J. The role of ISWI chromatin remodeling complexes in brain development and neurodevelopmental disorders. *Mol. Cell Neurosci.* **2018**, *87*, 55–64. [CrossRef]
70. Tsitsiridis, G.; Steinkamp, R.; Giurgiu, M.; Brauner, B.; Fobo, G.; Frishman, G.; Montrone, C.; Ruepp, A. CORUM: The comprehensive resource of mammalian protein complexes—2022. *Nucleic Acids Res.* **2023**, *51*, D539–D545. [CrossRef]
71. Applebury, M.L.; Antoch, M.P.; Baxter, L.C.; Chun, L.L.; Falk, J.D.; Farhangfar, F.; Kage, K.; Krzystolik, M.G.; Lyass, L.A.; Robbins, J.T. The murine cone photoreceptor: A single cone type expresses both S and M opsins with retinal spatial patterning. *Neuron* **2000**, *27*, 513–523. [CrossRef]
72. Poot, R.A.; Bozhenok, L.; van den Berg, D.L.; Steffensen, S.; Ferreira, F.; Grimaldi, M.; Gilbert, N.; Ferreira, J.; Varga-Weisz, P.D. The Williams syndrome transcription factor interacts with PCNA to target chromatin remodelling by ISWI to replication foci. *Nat. Cell Biol.* **2004**, *6*, 1236–1244. [CrossRef]
73. Poot, R.A.; Dellaire, G.; Hulsmann, B.B.; Grimaldi, M.A.; Corona, D.F.; Becker, P.B.; Bickmore, W.A.; Varga-Weisz, P.D. HuCHRAC, a human ISWI chromatin remodelling complex contains hACF1 and two novel histone-fold proteins. *EMBO J.* **2000**, *19*, 3377–3387. [CrossRef]
74. Bozhenok, L.; Wade, P.A.; Varga-Weisz, P. WSTF-ISWI chromatin remodeling complex targets heterochromatic replication foci. *EMBO J.* **2002**, *21*, 2231–2241. [CrossRef]
75. Collins, N.; Poot, R.A.; Kukimoto, I.; Garcia-Jimenez, C.; Dellaire, G.; Varga-Weisz, P.D. An ACF1-ISWI chromatin-remodeling complex is required for DNA replication through heterochromatin. *Nat. Genet.* **2002**, *32*, 627–632. [CrossRef]
76. Eberharter, A.; Ferrari, S.; Langst, G.; Straub, T.; Imhof, A.; Varga-Weisz, P.; Wilm, M.; Becker, P.B. Acf1, the largest subunit of CHRAC, regulates ISWI-induced nucleosome remodelling. *EMBO J.* **2001**, *20*, 3781–3788. [CrossRef]
77. Ito, T.; Levenstein, M.E.; Fyodorov, D.V.; Kutach, A.K.; Kobayashi, R.; Kadonaga, J.T. ACF consists of two subunits, Acf1 and ISWI, that function cooperatively in the ATP-dependent catalysis of chromatin assembly. *Genes Dev.* **1999**, *13*, 1529–1539. [CrossRef]
78. Zhang, J.; Gray, J.; Wu, L.; Leone, G.; Rowan, S.; Cepko, C.L.; Zhu, X.; Craft, C.M.; Dyer, M.A. Rb regulates proliferation and rod photoreceptor development in the mouse retina. *Nat. Genet.* **2004**, *36*, 351–360. [CrossRef]
79. Alexiades, M.R.; Cepko, C. Quantitative analysis of proliferation and cell cycle length during development of the rat retina. *Dev. Dyn. Off. Publ. Am. Assoc. Anat.* **1996**, *205*, 293–307. [CrossRef]
80. O'Keefe, R.T.; Henderson, S.C.; Spector, D.L. Dynamic organization of DNA replication in mammalian cell nuclei: Spatially and temporally defined replication of chromosome-specific alpha-satellite DNA sequences. *J. Cell Biol.* **1992**, *116*, 1095–1110. [CrossRef]
81. Bernard, P.; Allshire, R. Centromeres become unstuck without heterochromatin. *Trends Cell Biol.* **2002**, *12*, 419–424. [CrossRef] [PubMed]
82. Taddei, A.; Maison, C.; Roche, D.; Almouzni, G. Reversible disruption of pericentric heterochromatin and centromere function by inhibiting deacetylases. *Nat. Cell Biol.* **2001**, *3*, 114–120. [CrossRef] [PubMed]
83. Wallrath, L.L. Unfolding the mysteries of heterochromatin. *Curr. Opin. Genet. Dev.* **1998**, *8*, 147–153. [CrossRef] [PubMed]

84. Perpelescu, M.; Nozaki, N.; Obuse, C.; Yang, H.; Yoda, K. Active establishment of centromeric CENP-A chromatin by RSF complex. *J. Cell Biol.* **2009**, *185*, 397–407. [CrossRef]
85. Perpelescu, M.; Hori, T.; Toyoda, A.; Misu, S.; Monma, N.; Ikeo, K.; Obuse, C.; Fujiyama, A.; Fukagawa, T. HJURP is involved in the expansion of centromeric chromatin. *Mol. Biol. Cell* **2015**, *26*, 2742–2754. [CrossRef]
86. Tachiwana, H.; Muller, S.; Blumer, J.; Klare, K.; Musacchio, A.; Almouzni, G. HJURP involvement in de novo CenH3(CENP-A) and CENP-C recruitment. *Cell Rep.* **2015**, *11*, 22–32. [CrossRef]
87. Bassett, E.A.; DeNizio, J.; Barnhart-Dailey, M.C.; Panchenko, T.; Sekulic, N.; Rogers, D.J.; Foltz, D.R.; Black, B.E. HJURP uses distinct CENP-A surfaces to recognize and to stabilize CENP-A/histone H4 for centromere assembly. *Dev. Cell* **2012**, *22*, 749–762. [CrossRef]
88. Foltz, D.R.; Jansen, L.E.; Bailey, A.O.; Yates, J.R., 3rd; Bassett, E.A.; Wood, S.; Black, B.E.; Cleveland, D.W. Centromere-specific assembly of CENP-a nucleosomes is mediated by HJURP. *Cell* **2009**, *137*, 472–484. [CrossRef]
89. Klimova, L.; Kozmik, Z. Stage-dependent requirement of neuroretinal Pax6 for lens and retina development. *Development* **2014**, *141*, 1292–1302. [CrossRef]
90. Dupacova, N.; Antosova, B.; Paces, J.; Kozmik, Z. Meis homeobox genes control progenitor competence in the retina. *Proc. Natl. Acad. Sci. USA* **2021**, *118*, e2013136118. [CrossRef]
91. Housset, M.; Samuel, A.; Ettaiche, M.; Bemelmans, A.; Beby, F.; Billon, N.; Lamonerie, T. Loss of Otx2 in the adult retina disrupts retinal pigment epithelium function, causing photoreceptor degeneration. *J. Neurosci. Off. J. Soc. Neurosci.* **2013**, *33*, 9890–9904. [CrossRef]
92. Sonntag, S.; Dedek, K.; Dorgau, B.; Schultz, K.; Schmidt, K.F.; Cimiotti, K.; Weiler, R.; Lowel, S.; Willecke, K.; Janssen-Bienhold, U. Ablation of retinal horizontal cells from adult mice leads to rod degeneration and remodeling in the outer retina. *J. Neurosci. Off. J. Soc. Neurosci.* **2012**, *32*, 10713–10724. [CrossRef]
93. Pacione, L.R.; Szego, M.J.; Ikeda, S.; Nishina, P.M.; McInnes, R.R. Progress toward understanding the genetic and biochemical mechanisms of inherited photoreceptor degenerations. *Annu. Rev. Neurosci.* **2003**, *26*, 657–700. [CrossRef]
94. Blanks, J.C.; Adinolfi, A.M.; Lolley, R.N. Photoreceptor degeneration and synaptogenesis in retinal-degenerative (rd) mice. *J. Comp. Neurol.* **1974**, *156*, 95–106. [CrossRef]
95. Jones, B.W.; Watt, C.B.; Frederick, J.M.; Baehr, W.; Chen, C.K.; Levine, E.M.; Milam, A.H.; Lavail, M.M.; Marc, R.E. Retinal remodeling triggered by photoreceptor degenerations. *J. Comp. Neurol.* **2003**, *464*, 1–16. [CrossRef]
96. Jones, B.W.; Marc, R.E. Retinal remodeling during retinal degeneration. *Exp. Eye Res.* **2005**, *81*, 123–137. [CrossRef]
97. Escher, P.; Cottet, S.; Aono, S.; Oohira, A.; Schorderet, D.F. Differential neuroglycan C expression during retinal degeneration in Rpe65-/- mice. *Mol. Vis.* **2008**, *14*, 2126–2135.
98. Inatani, M.; Honjo, M.; Otori, Y.; Oohira, A.; Kido, N.; Tano, Y.; Honda, Y.; Tanihara, H. Inhibitory effects of neurocan and phosphacan on neurite outgrowth from retinal ganglion cells in culture. *Investig. Ophthalmol. Vis. Sci.* **2001**, *42*, 1930–1938.

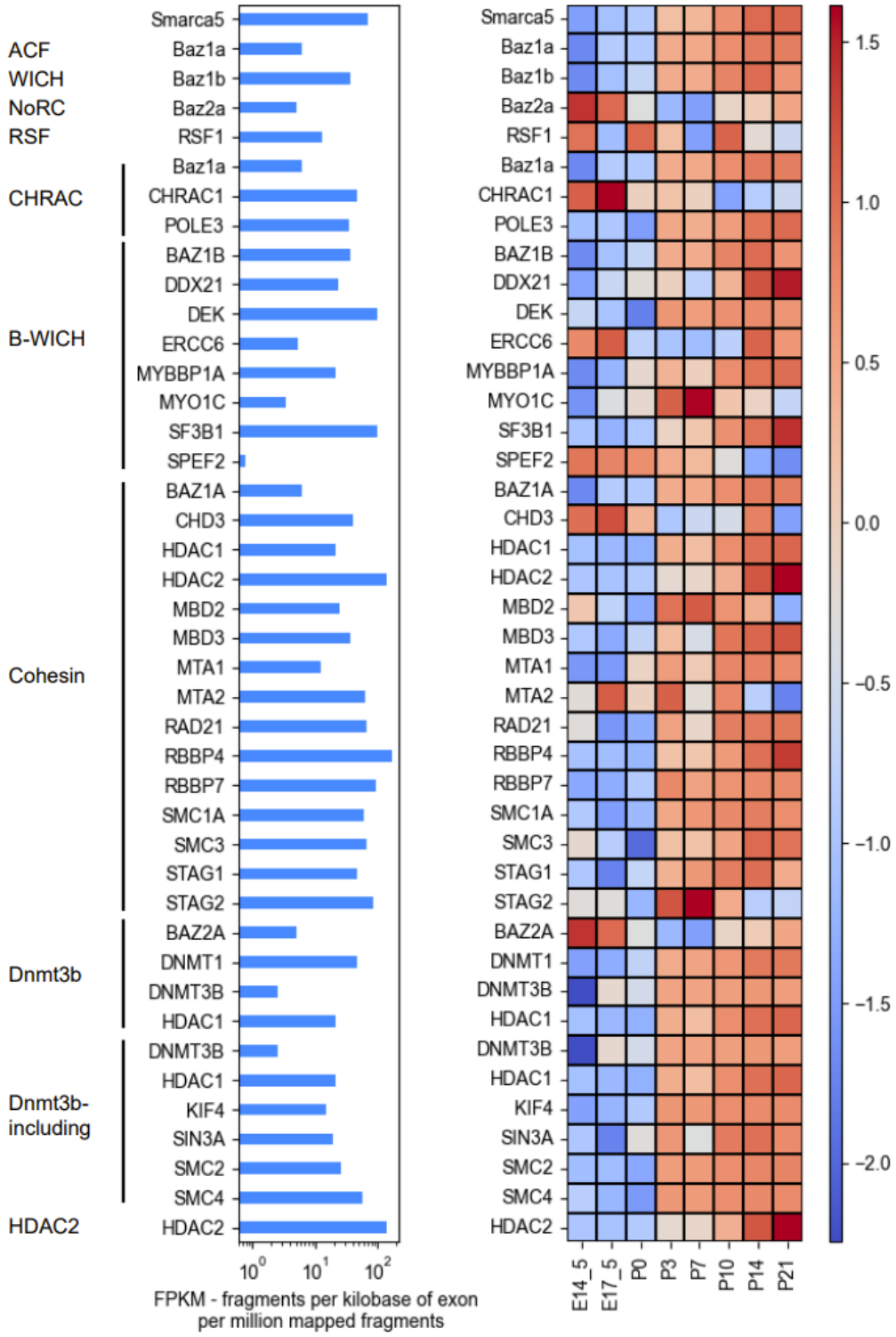

Supplementary Figure S1. Expression of Snf2h and its interacting partners during retinal development.

Heatmap showing expression of components of ACF,WICH,NoRC, RSF, CHRAC, B-WICH, Cohesin, Dnmt3b, Dnmt3b-including, and HDAC2 complexes in retina at E14.5, E17.5, P0, P3, P7, P10, P14, and P21 (GSE87064 (Aldiri et al., 2017)). The left graph indicates FPKM.

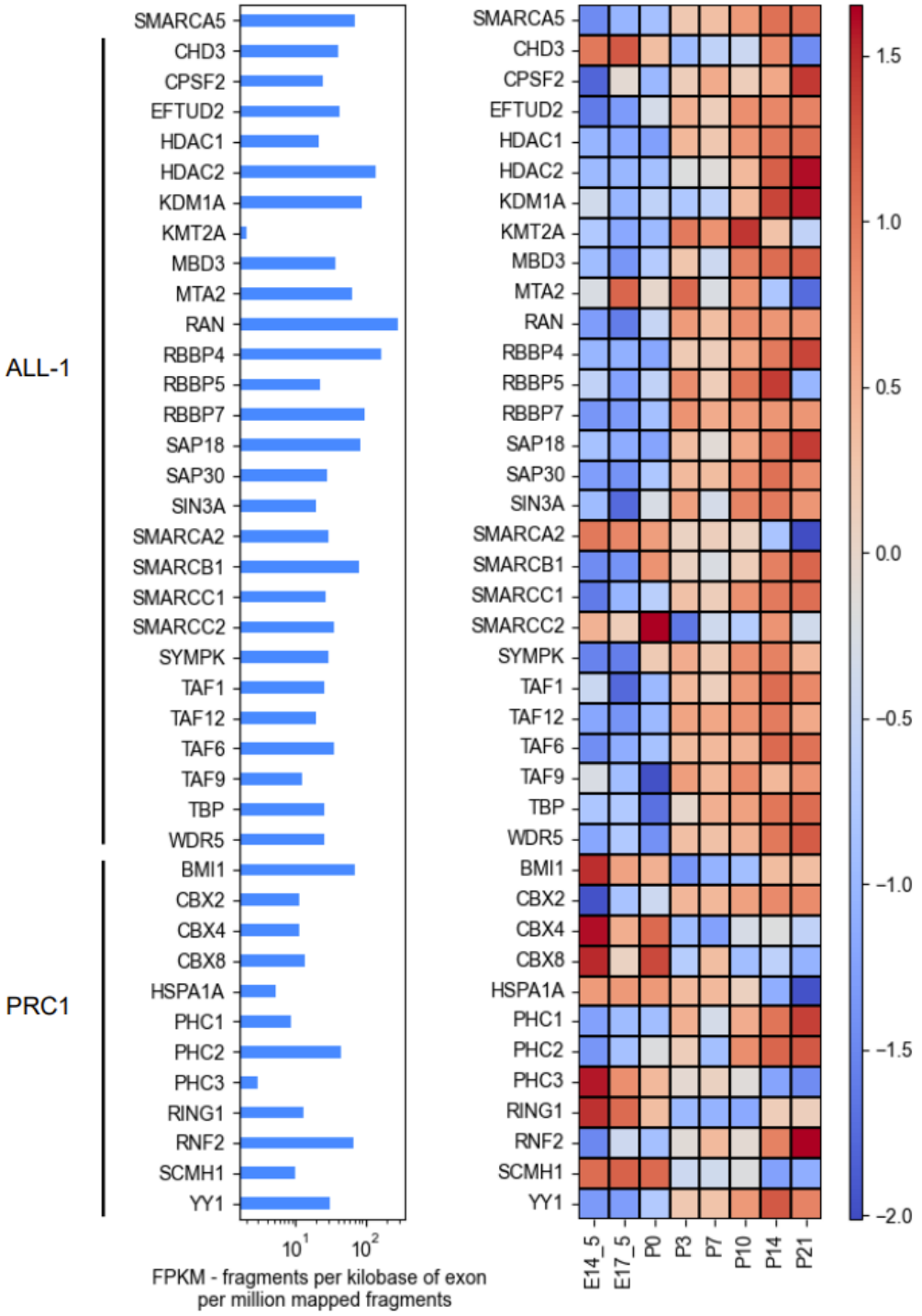

Supplementary Figure S2. Expression of components of ALL-1 supercomplex and PRC1 complex during retinal development.
Heatmap showing expression of components of ALL-1 supercomplex and PRC1 complex in retina at E14.5, E17.5, P0, P3, P7, P10, P14, and P21 (GSE87064 (Aldiri et al., 2017)). The left graphindicates FPKM.

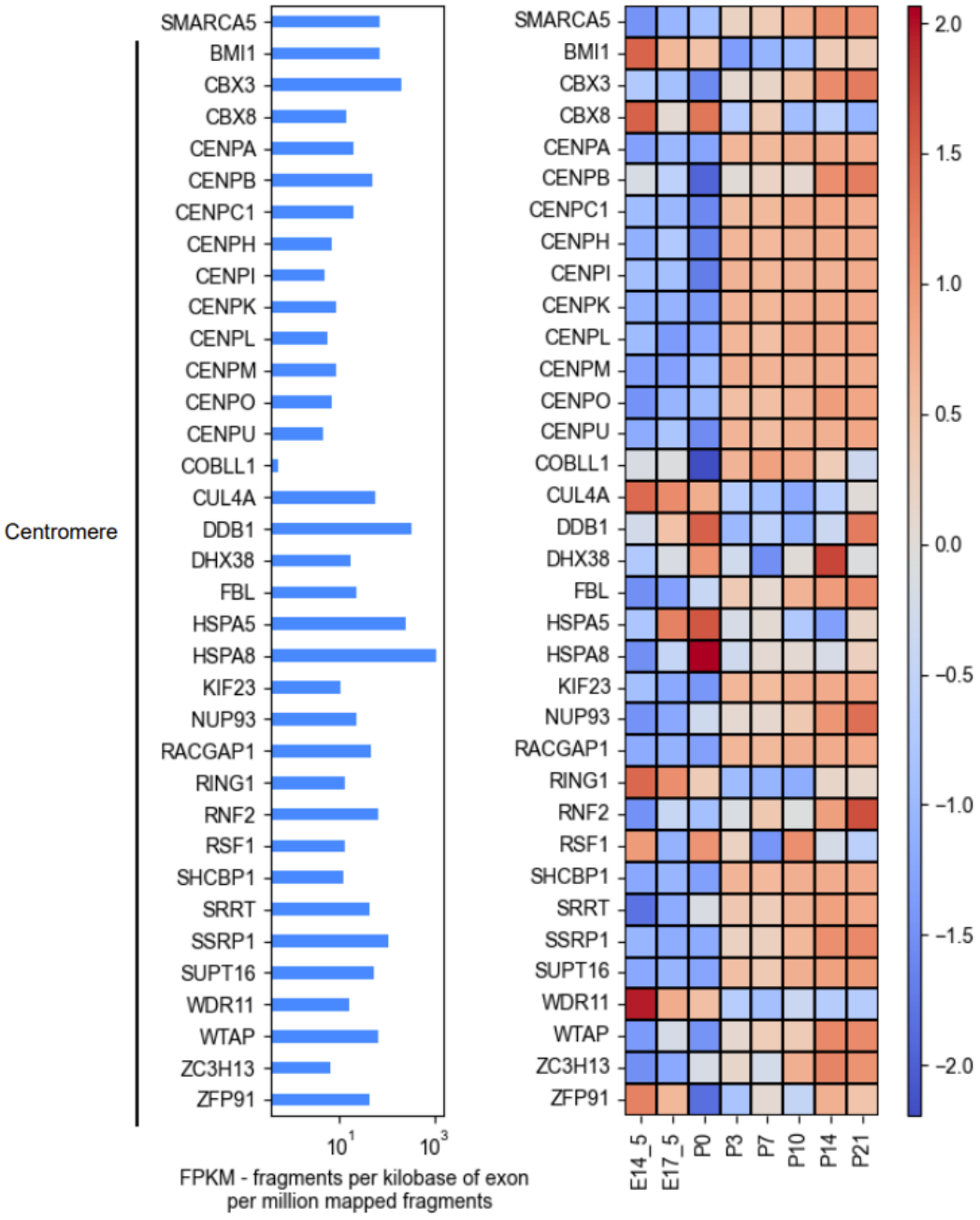

Supplementary Figure S 3. Expression of centromere complex components during retinal development.
Heatmap showing expression of components of centromere complex in retina at E14.5, E17.5, P0, P3, P7, P10, P14, and P21 (GSE87064 (Aldiri et al., 2017)). The left graph indicates FPKM.

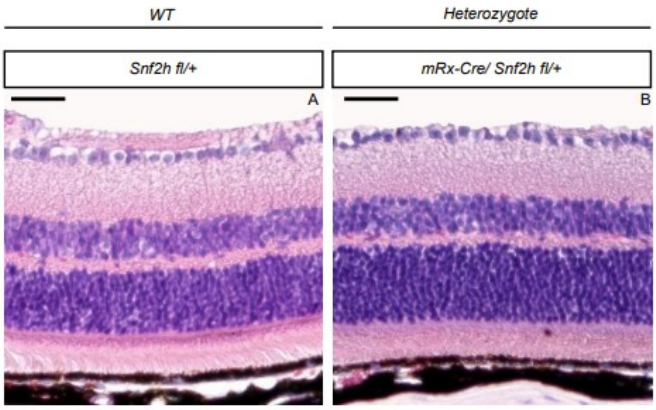

Supplementary Figure S4. Morphology of heterozygous mice at postnatal week 50 (PW50).

Hematoxylin and eosin staining of wild-type (A) and mRx-Cre/ $Snf2h^{fl/+}$ (B) mice did not manifest obvious differences between the two genotypes. One active allele of the Snf2h gene is thus sufficient for the maintenance of an apparently normal gross retinal morphology.

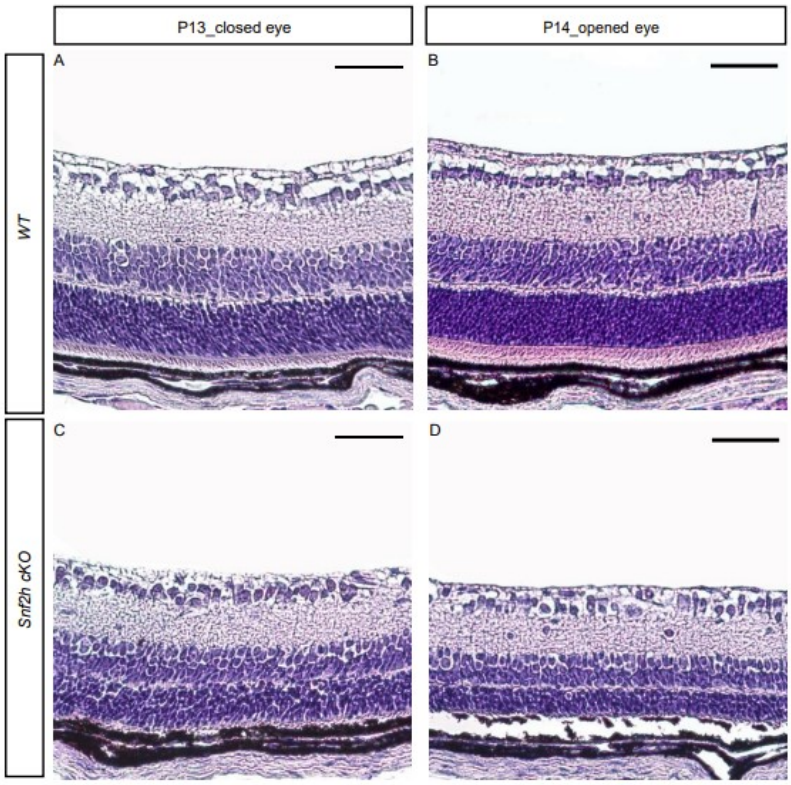

Supplementary Figure S5. Retinal morphology of Snf2h cKO at P13 and P14.

Hematoxylin-eosin staining of postnatal retinal sections at postnatal day 13 (P13) and day 14 (P14) of wild-type and Snf2h cKO. The retinal section of Snf2h cKO at P14 (D) was clearly thinner compared with the same genotype at P13 (C).

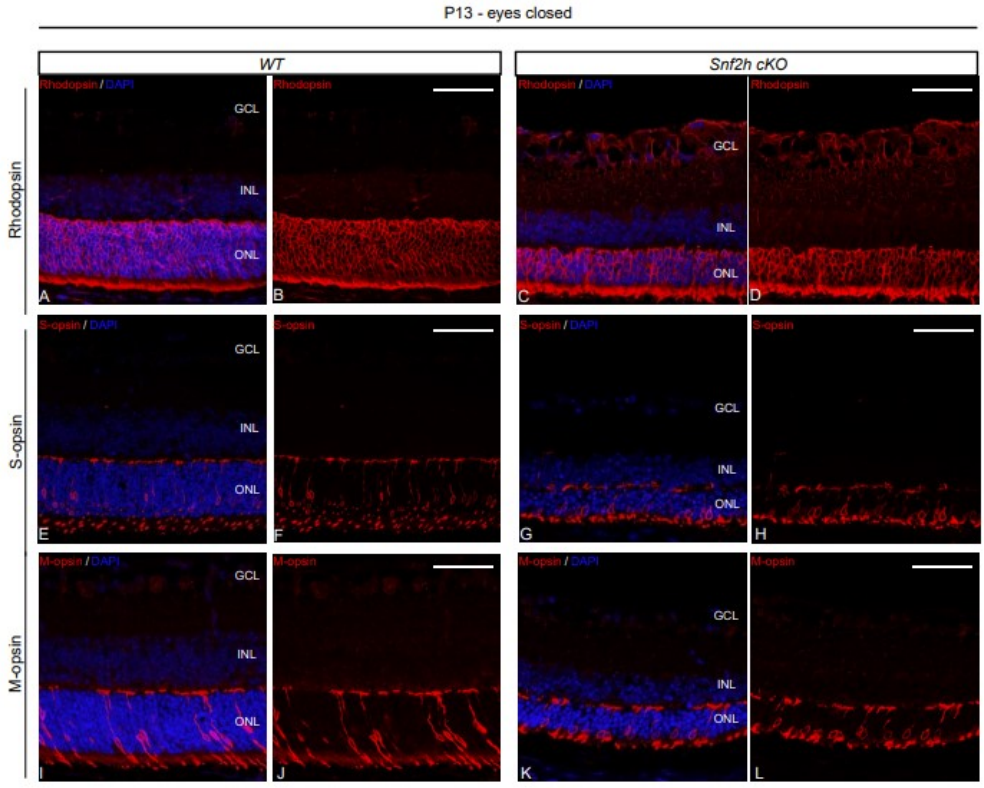

Supplementary Figure S6. Photoreceptor characterization at P13 (before eye opening).

Rod photoreceptors in the wild-type retina (A, B). The rod photoreceptors in Snf2h cKO were present (C, D). Although the number of rods was reduced, their cell shape and positioning was comparable with the wild-type controls. The same result was obtained with cone photoreceptor staining (E-H, I-L).

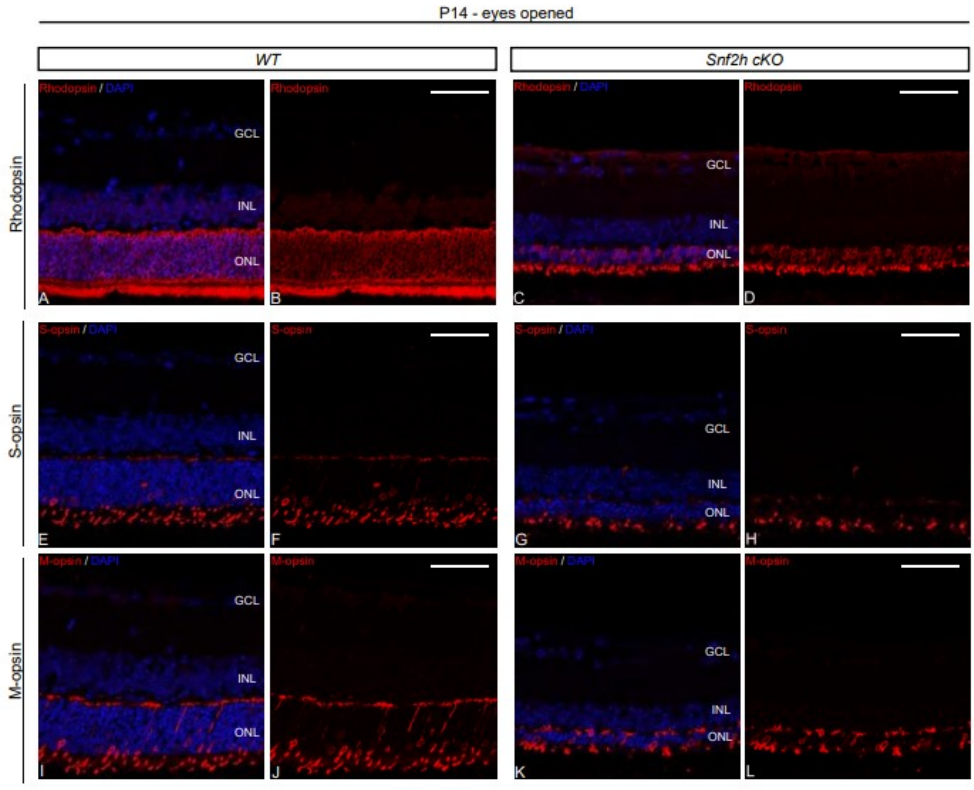

Supplementary Figure S7. Photoreceptor characterization at P14 (after eye opening).

The rod photoreceptors in Snf2h cKO were preserved, but their length was reduced by about a half compared with control, which was associated with reduced thickness of the ONL in Snf2h cKO (A-D). The cone photoreceptors exhibited an abnormal shape, the outer segments were reduced, and the photoreceptor protrusions detected in wild-type animals inside the OPL were missing in Snf2h cKO (E-H, I-L).

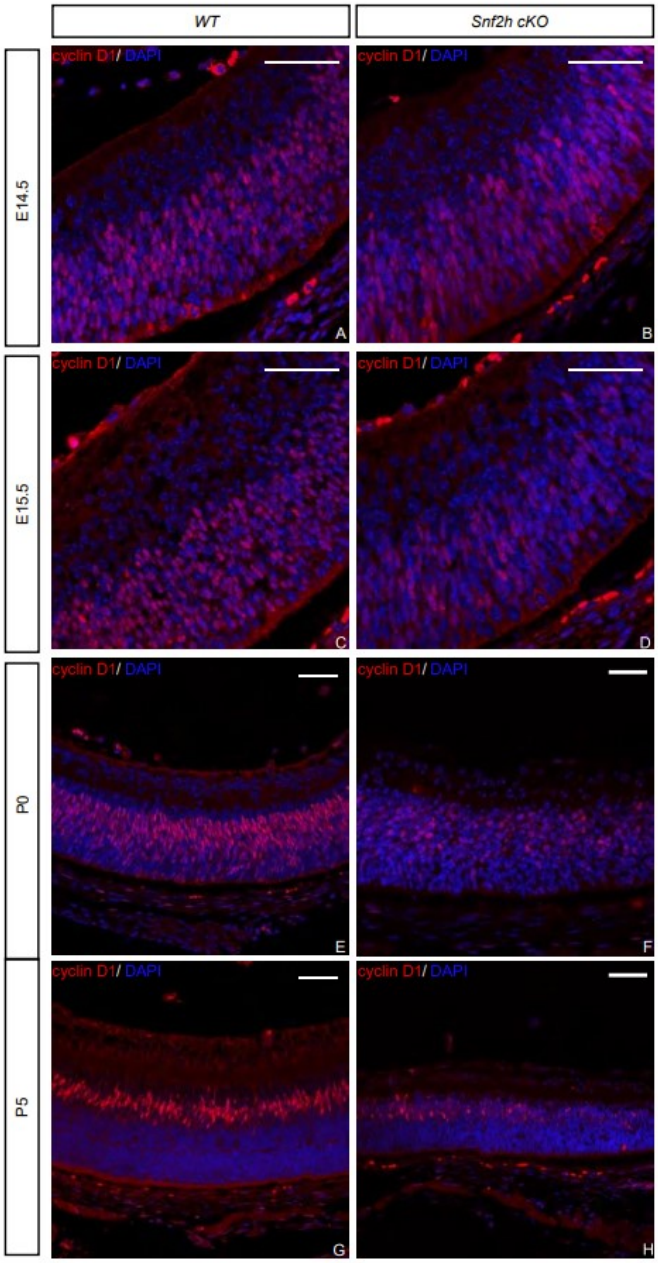

Supplementary Figre S8. Expression of cyclin D1 in Snf2h cKO during embryonic and postnatal stages.

Immunostaining for cyclin D1, required for G1/S transition during the cell cycle, in wild-type and Snf2h cKO. Differences in cyclin D1 immunoreactivity appeared already during embryonic development (A-D). A dramatic decrease in cyclin D1-positive cells and cyclin D1 expression level in Snf2h cKO compared with wild-type controls was observed at birth (E, F) and at P5 (G, H).

Supplementary Table S1. List of primary antibodies used for immunohistochemistry

Antigen	Host	Dilution	Retinal cell types	stage
Snf2h (Abcam)	Rabbit	1:500		Adult
Rhodopsin (Chemicon)	Mouse	1:200	Cone photoreceptor cells	Adult
S-opsin (Santa Cruz)	Goat	1:500	Cone photoreceptor cells	Adult
M-opsin (Santa Cruz)	Rabbit	1:500	Cone photoreceptor cells	Adult
Lhx2 (Santa Cruz)	Goat	1:1000	Müller glial cells	Adult
Chx10 (ThermoFisher Scientific)	Sheep	1:500	Bipolar cells	Adult
Oc2 (R&D Systems)	Sheep	1:500	Horizontal cells	Adult
Pax6 (Covance)	Rabbit	1:500	Amacrine cells	Adult
Brn3a (Dr. E. Turner)	Rabbit	1:4000	Retinal ganglion cells	Adult
Tbr2 (Abcam)	Rabbit	1:500	Retinal ganglion cells	Adult
Otx2 (Dr. Vaccarino)	Rabbit	1:500	Photoreceptor cells	Embryo
Crx (Santa Cruz)	Rabbit	1:100	Photoreceptor cells	Embryo
Blimp1 (Santa Cruz)	Rat	1:300	Photoreceptor cells	Embryo
Rxrγ (Santa Cruz)	Rabbit	1:3000	Photoreceptor cells	Embryo
cCas3 (Cell Signaling)	Rabbit	1:500		Embryo
Cyclin D1 (Santa Cruz)	Mouse	1:300		Embryo
pH3 (Santa Cruz)	Rabbit	1:800		Embryo
CENP-A (Cell Signaling)	Rabbit	1:500		Embryo

Supplementary Table S2. List of primers used for qRT-PCR	
Name	**Sequence (5'→3')**
Atm-F	CCAGGGGAAGATGATGAAGA
Atm-R	TCGGCAGCTAAAGGACTCAT
Atr-F	GCTGTAGCGTCCTTTCGTTC
Atr-R	GGCTCATGCATAGCAGCATA
Casp3-F	GAGATGGCTTGCCAGAAGAT
Casp3-R	CCGTCCTTTGAATTTCTCCA
Casp9-F	GATGCTGTCCCCTATCAGGA
Casp9-R	CAGAATGCCATCCAAGGTCT
Cdkn2a-F	GCTCTGGCTTTCGTGAACAT
Cdkn2a-R	CGAATCTGCACCGTAGTTGA
CyclinA-F	CTGTCTCTTTACCCGGAGCA
CyclinA-R	AACGTTCACTGGCTTGTCTTC
CyclinB-F	GAGAAGGTGCCTGTGTGTGA
CyclinB-R	GGCTTGGAGAGGGATTATCA
CyclinE-F	CGTTACATGGCATCACAACA
CyclinE-R	GGTGCAACTTTGGAGGGTAG
CyclinG-F	GGCTTTGACACGGAGACATT
CyclinG-R	AGTCGCTTTCACAGCCAAAT
Mdm2-F	TGTGTGAGCTGAGGGAGATG
Mdm2-R	ATCCTGATCCAGGCAATCAC
p21-F	GTACTTCCTCTGCCCTGCTG
p21-R	TCTGCGCTTGGAGTGATAGA
p48-F	AACCAGGCCCAGAAGGTTAT
p48-R	CCTCTGGGGTCCACACTTTA
p53-F	CTAGCATTCAGGCCCTCATC
p53-R	ACTCCTCCATGGCAGTCATC
Gadd45b-F	CACCCTGATCCAGTCGTTCT
Gadd45b-R	TTGGCTTTTCCAGGAATCTG
Sfn-F	TGGCCCTGAACTTTTCAGTC
Sfn-R	GATGAGGGTGCTGTCCTTGT
UBB-F	ATGTGAAGGCCAAGATCCAG
UBB-R	TAATAGCCACCCCTCAGACG
Actb-F	GTCCACACCCGCCACCAGTTC
Actb-R	TTCTCCATGTCGTCCCAGTTG
Ubb-F	ATGTGAAGGCCAAGATCCAG
Ubb-R	TAATAGCCACCCCTCAGACG
Sdha-F	AAGGCAAATGCTGGAGAAGA
Sdha-R	TGGTTCTGCATCGACTTCTG
Gapdh-F	AACTTTGGCATTGTGGAAGG
Gapdh-R	ATCCACAGTCTTCTGGGTGG

7. Discussion

The cornea, a transparent tissue at the front of the eye, plays a crucial role in visual function by refracting light onto the retina. Its integrity and clarity are essential for maintaining optimal vision. The development of the cornea is a complex process involving precise spatiotemporal regulation of gene expression and intricate cellular interactions. Transcription factors, as key regulators of gene expression, are known to orchestrate the intricate molecular events underlying tissue development. Advancements in the field of transgenic and knockout technologies have provided valuable insights into the role of various transcription factors in corneal morphogenesis and disease progression (Collinson et al., 2004; Dwivedi et al., 2005; Kenchegowda et al., 2011; Loughner et al., 2017; Swamynathan et al., 2007). Interestingly, the human corneal disorders coupled with mutations in genes encoding these transcription factors are in tune with their conserved function in eye development across different species (Hanson et al., 1993; Hill et al., 1991; Jordan et al., 1992; Liskova et al., 2016; Yu et al., 2022). Hence understanding the precise role of these transcription factors in corneal development and homeostasis using a proper model system is advantageous.

Results presented in section 6 of this thesis are mainly focused on the

(i) Generation and characterization of a transgenic Cre driver line for postnatal corneal studies

(ii) Role of transcription factor Pax6 in corneal development

(iii) Distinct set of ocular phenotypes are associated with *Ovol2* promoter mutations in the mouse model

7.1 Generation and characterization of a transgenic Cre driver line for postnatal corneal studies

Conventional gene knockout mouse has been an excellent tool to understand gene function in vivo (Hill et al., 1991; Hogan et al., 1986). However, developmental arrest or embryonic lethality restricts us from studying gene function postnatally. This limitation was circumvented by the generation of cKO models by the Cre-*loxP* system (Gu et al., 1994; Gu et al., 1993). Several Cre driver lines are used for the conditional deletion of genes of interest in the ocular surface. But, Cre recombinase activity begins during embryonic development in these lines (Joo et al., 2010; Kokado et al., 2018; Lu et al., 2012; Swamynathan et al., 2007; Tanifuji-Terai et al., 2006; Weng et al., 2008). As a result, it is challenging to elucidate the postnatal function of genes such as Pax6, which is expressed throughout the CE development and maintained in adult CE.

In order to establish a Cre driver line, in which Cre-mediated recombination starts coincident with postnatal CE stratification, we choose *Aldh3* as a candidate gene. Aldh3 starts its endogenous activity in CE at PN9 and increases strongly by PN13 (Abedinia et al., 1990; Davis et al., 2008). In our study, we used a BAC construct containing the regulatory sequence of the *Aldh3* gene to generate an *Aldh3-Cre* transgenic line. We visualised the specificity of Cre-mediated recombination in *Aldh3-Cre*, by breeding them with *Rosa26R* (Soriano,

1999). Our data showed that Cre recombinase activity is observed in corneal stroma from E15.5, but not in presumptive CE or postnatal CE, till PN9 and it increased from PN12 to PN28. Additionally, no Cre activity was observed in limbal epithelial cells, whereas X-gal staining was also found in conjunctival epithelial cells from PN9. This change in Cre activity compared to its known endogenous expression could plausibly be due to the absence of some of the regulatory elements associated with the *Aldh3* gene in our BAC construct.

Furthermore, we showed the efficiency of the *Aldh3-Cre* transgenic line by breeding them with *Ctnnb1*$^{lox\ (ex3)\ /+}$ (Harada et al., 1999) and *Ctnnb1*$^{lox\ (ex2\text{-}6)/\ lox\ (ex2\text{-}6)}$ (Brault et al., 2001) resulted in gain and loss of function of β-catenin respectively in the ocular surface. The phenotypes observed in these gain and loss of function mutants are in agreement with previous findings, suggesting as our *Aldh3-Cre* efficiently inactivates the gene of interest in the regions of Cre activity. β-catenin is expressed in CE as well as in corneal stroma. Conditional deletion of β-catenin in corneal stromal keratocytes results in precocious stratification of CE (Zhang et al., 2015) as observed in *Ctnnb1*$^{lox\ (ex2\text{-}6/lox\ (ex2\text{-}6)}$. This makes it difficult to distinguish whether the phenotypes observed on CE are due to its loss of function in CE or the stroma. Regardless of this, *Aldh3-Cre* is an excellent tool for the inactivation of genes which are specifically expressed in CE or conjunctival epithelium in postnatal stages.

7.2 The role of Pax6 in corneal development

Pax6 is regarded as the master regulator gene in eye development, due to its highly conserved role in morphogenesis and maintenance of eyes (Gehring, 2004). In mice, Pax6 is detected in SE and OV from a very early stage and during mid-gestation in developing NR, RPE and all SE-derived parts lens, cornea, limbus and conjunctiva. Unlike in other tissues, where Pax6 expression is reduced in the adult, it remained strong in the epithelia of the adult cornea, limbus and conjunctiva (Koroma et al., 1997; Walther and Gruss, 1991), suggesting its possible role in postnatal corneal development. Homozygous (*Pax6*$^{-/-}$) mutants are embryonically lethal (Hogan et al., 1986) and heterozygous (*Pax6*$^{+/-}$) mutants exhibit a myriad of corneal phenotypes such as the thin cornea, hypocellular stroma, corneal neovascularisation, epithelial erosions, presence of globet cells, and corneal opacity (Collinson et al., 2001; Davis et al., 2003; Hill et al., 1991; Ramaesh et al., 2003; Ramaesh et al., 2005; van Raamsdonk and Tilghman, 2000). Despite numerous studies describing corneal defects in *Pax6*$^{+/-}$ mutants, it was unclear if these traits resulted from defective postnatal development or its function during embryonic development. In our study, we used two specific Cre drivers for the inactivation of Pax6 in postnatal CE and OSE.

Postnatal depletion of Pax6 in CE using *Aldh3-Cre* reveals abnormal thin CE with cell-cell adhesion defects. Increased proliferation was found in the CE of cKO mutants, suggesting that Pax6 directly or indirectly regulates components involved in the epithelial cell cycle (Davis et al., 2003; Ramaesh et al., 2005). An alternative possibility is reparation for the cell loss due to cell-cell adhesion defects (Zieske, 2000).

Adherens junctions are multi-protein complexes essential during development and tissue morphogenesis (Gumbiner, 2005; Nishimura and Takeichi, 2009). E-cadherin is a transmembrane protein, a core component of adherens junctions (Takeichi, 1988a, b; Xu et al., 2002). The cytoplasmic tail of cadherin interacts with catenin proteins which further

links cadherins to the actin cytoskeleton (Hartsock and Nelson, 2008; Perez-Moreno and Fuchs, 2006; Pokutta and Weis, 2007). The CE has E-cadherin expression in all layers and is known to be vital for the maintenance of its structural integrity (Mohan et al., 1995; Xu et al., 2002). Our study found that abundant and proper membrane localisation of E-cadherin in CE is lost in CE cKO mutants. A similar diffused pattern of expression is observed for F-actin and β- catenin. This suggests that adherens junctions are aberrant in CE upon Pax6 loss, accounting for the reduced number of cell layers.

Tight junction protein Zo-1, which is expressed in the superficial CE is downregulated in CE cKO mutants. This observation is consistent with higher fluorescein uptake in corneas of *Pax6* $^{+/-}$ mutants (Davis et al., 2003), which indicates inadequate tight junctions upon Pax6 loss. Several studies suggested interdependency in the formation of tight and adherens junction and the absence of adherens junction components lead to the failure in tight junction formation. So we speculate that the decrease in adherens junction components in CE cKO mutants could have an impact on the assembly of other cell junctions (Campbell et al., 2017; Capaldo and Macara, 2007; Ooshio et al., 2010; Sugrue and Zieske, 1997).

Krt12, a major IF with corneal specific expression (Chaloin-Dufau et al., 1993; Chaloin-Dufau et al., 1990), has been controlled by Pax6 together with reprogramming factors Klf4 and Oct4 (Liu et al., 1999; Sasamoto et al., 2016). Consistent with this, our data indicated the loss of Krt12 in CE cKO mutants. Corneal fragility is a characteristic of mutations in the human *KRT12* gene and in mice homozygous models (Nishida et al., 1997). Considering all together, loss of Krt12 might further worsen cell-cell adhesion in the CE cKO mutants. Additionally, the loss of Krt12 also implies an impaired differentiation program and this observation was further supported by the expansion of basal cell-specific expression of Krt14 to suprabasal cells in Pax6-depleted CE.

Conjunctivalisation and the presence of goblet cells were found in *Pax6* $^{+/-}$ mutants and these features are considered as the hallmarks of LSCD (Nishida et al., 1995; Puangsricharern and Tseng, 1995). We did not observe any expansion of Krt4 to CE in CE cKO mutants, implicating that depletion of Pax6 in the limbus is a prerequisite for the conjunctival outgrowth to the cornea. Whereas, at PN28, globet cells were found in the CE of CE cKO mutants. This could be explained by the globet cells arising from a complex niche located at the corneal-limbal border rather than being of conjunctival origin (Pajoohesh-Ganji et al., 2012).

The corneal development and homeostasis are maintained by a group of transcription factors such as Pax6, Ap2-α, Klf4, and EHF (Davis et al., 2003; Delp et al., 2015; Dwivedi et al., 2005; Swamynathan et al., 2007; Tiwari et al., 2017). But the hierarchical network of these regulators in CE is poorly understood. Further studies need to be done to identify downstream targets of Pax6 in CE. However, we are unable to continue our investigations due to the repopulation of Pax6^{+ve} cells by PN28 in the CE cKO mutant. Repopulation of Pax6^{+ve} cells can be attributed to the regulation of *Aldh3* promoter activity by Pax6 in co-operation with Oct1 and p300 (Davis et al., 2008).

Together, our data show that Pax6 is important for CE adhesion and corneal-specific differentiation.

Next, in an attempt to unravel the role of Pax6 in presumptive CE embryonically, we used *K14–Cre* (Andl et al., 2004). Even though, Cre activity starts at E14.5 (Andl et al., 2004), Pax6 was not deleted in OSE until PN2. Our data show that depletion of Pax6 in OSE during early postnatal stages (PN2-PN9), results in conjunctivalisation of CE, suggesting the importance of limbal Pax6 in preventing the expansion of conjunctival cells to CE. However, further analysis upon eye opening revealed keratinised cornea. We speculate that these are the outcomes of irritations and infections caused by ectopic eyelashes observed in OSE cKO mutants.

Wnt/β-catenin signalling plays an important role in the fate determination of OSE (Kreslova et al., 2007; Miller et al., 2006; Mizoguchi et al., 2015; Smith et al., 2005; Zhang et al., 2010). Active Wnt signalling is observed in the mesenchyme of the cornea, limbus and conjunctiva and conjunctival epithelium (Gage et al., 2008; Liu et al., 2003; Zhang et al., 2015). The barrier function of the limbal epithelium may require this regional specificity, and this could be possibly maintained by the active repression of this signalling pathway at different levels. This idea is favoured by the widespread expression of Wnt inhibitors Dkks and Sfrp1 in the cornea during embryonic and postnatal development (Ang et al., 2004; Liu et al., 2003; Mukhopadhyay et al., 2006). In addition to this, Pax6 is known to regulate the Wnt inhibitors like Dkk1, Sfrp1, and Sfpr2 in the central nervous system and lens (Duparc et al., 2006; Kim et al., 2001; Machon et al., 2010). Together, this suggests the possibility of deregulation of Wnt/ β-catenin in OSE upon Pax6 loss. Further experiments can help to reveal the possible connection between Wnt/ β-catenin and Pax6 in OSE. Nevertheless, mosaic deletion of Pax6 in PN2-PN6 in OSE and keratinisation of CE upon eyelid opening restrict us from conducting further research.

7.3 Distinct set of ocular phenotypes are associated with *Ovol2* promoter mutations in the mouse model

OVOL2 is a transcription factor involved in promoting MET by directly repressing mesenchymal genes such as TWIST, ZEB1 and ZEB2 (Aue et al., 2015; Kitazawa et al., 2016; Watanabe et al., 2019). OVOL2 maintains the epithelial nature of the CE by repressing mesenchymal genes (Kitazawa et al., 2016). In contrast to that, OVOL2 is absent in neural crest-derived CEn (Davidson et al., 2016). It has been demonstrated that mutations in the highly conserved promoter region of the *OVOL2* gene are the underlying cause of corneal dystrophy PPCD1 (Davidson et al., 2016). Further studies have shown that these mutations are resulting in the ectopic expression of (mRNA) *OVOL2* in CEn and the downregulation of the mesenchymal gene *ZEB1* (Chung et al., 2019). To further elucidate the molecular mechanisms associated with PPCD1, we generated an allelic series of promoter mutations including the human disease-associated variant c.-307T>C. Given the high level of promoter conservation within the mammals, we speculated that any mutations affecting this region could result in overexpression of Ovol2 in mice. However, to our surprise, out of seven mutations made, only two of them resulted in increased expression of (mRNA) *Ovol2* and some phenotypic traits. Considering the fact that PPCD1 is an autosomal dominant disorder, it is extremely likely that, CRISPR-Cas9 gene editing in the F0 generation selected against

the severe phenotypic modifications. This was further supported by the inability to generate a stable line for c.-370T>C linked to PPCD1 in the Czech family, despite numerous efforts.

Even though increased *Ovol2* mRNA levels are observed in CEn of mice harbouring c.-307T>C and c.-307_-320del mutations, these mutants didn't exhibit phenotypes associated with corneal endothelial dystrophy. We postulated that this could be due to the species-specific difference during the development of CEn.

Further analysis revealed that a minority of mice carrying c.-307T>C and c.-307_320del mutations exhibited a similar set of phenotypic traits such as iris hypoplasia, PHPV and dysplastic retina. It is interesting to note that an Ovol1 / Ovol2 binding site CCGTTA, is located next to c. -307T>C and in c.-307_-320del mutants, this binding site is deleted. A reasonable interpretation for this is that substitution of -307 T to C is altering the ability of Ovol1/ Ovol2 to bind to their consensus site and thus preventing Ovol2 autoregulation or repression by Ovol1 (Lee et al., 2014; Teng et al., 2007; Wells et al., 2009). Moreover, the lack of any phenotypic traits in c.-307_-311del mice mutants which accidentally restored the Ovol1/Ovol2 binding site lends credence to this notion.

The exact reason for the reduced penetrance of these phenotypic traits is uncertain. The reduced yield of heterozygotes and homozygotes was observed in these mutants, but that does not completely account for the reduced penetrance.

Ovol2 is expressed in inner cell mass and later in the derivatives of the epiblast, and as a result, embryonic lethality is observed in *Ovol2*$^{-/-}$ mice (Mackay et al., 2006). Furthermore, Ovol2 is also important for the skin, kidney, cornea, mammary epithelia, testis and ovary (Kitazawa et al., 2016; Li et al., 2002; Mackay et al., 2006; Unezaki et al., 2007; Watanabe et al., 2014). It has also been demonstrated that Ovol2 is required for the proper migration and survival of neural crest cells (Mackay et al., 2006). Considering the importance of Ovol2 during embryogenesis and postnatal development, we believe that the low yield of homozygotes or heterozygotes with phenotypic consequences was due to prenatal lethality.

Though it is uncertain whether Ovol2 governs migration and survival of neural crest cells directly or indirectly (Mackay et al., 2006), the ocular abnormalities noticed in c.307T>C mutants and c.-307_320del mutants are likely connected to abnormal migration of neural crest cells (Lin et al., 2020). Various structures in the eye including corneal stromal keratocytes, CEn, trabecular meshwork, primary vitreous and iris stoma are derived from neural crest cells (Bahn et al., 1984; Beauchamp and Knepper, 1984; Tripathi and Tripathi, 1989). Anterior segment dysgenesis, including aniridia, iris hypoplasia, Peters anomaly, congenital hereditary endothelial dystrophy, Axenfeld anomaly, and congenital iris ectropion, is caused by aberrant neural crest cell migration and differentiation during embryonic development (Churchill and Booth, 1996; Jat and Tripathy, 2023; Sridhar and Tripathy, 2023). Thus phenotypic consequences such as iridocorneal adhesion, lack of CEn and iris hypoplasia associated with c.-307T>C and c.-307_-320del mutations are indicative of aberrant neural crest cell migration or survival.

It has been demonstrated that PHPV can also arise due to abnormal migration or proliferation of neural crest cells during embryonic development (Hunt et al., 2005; Lin et al., 2020; Shastry, 2009). Consistent with this, we observed increased retrolental mass in c.-307T>C and c.-307_320del mutants from E14.5 and retained throughout the postnatal

stages. Collectively, these findings imply that the phenotypes observed in this study are linked to increased migration or proliferation of neural crest cells, which may be either a direct or indirect consequence of the changes in the Ovol2 expression set by the promoter mutations. However, we cannot exclude the possibility that increased migration of neural crest cells due to the delayed closure of optic fissure, since we observed coloboma in some of these mutants.

In summary, human PPCD1-associated c.-307T>C mutation in mice resulted in increased expression of (mRNA) *Ovol2* analogous to human patients. Even so, no corneal endothelial dystrophy was manifested in these mutants, suggesting that the development of CEn differs from humans to mice. The phenotypic consequences observed in a small percentage of c.-307T>C mice mutants suggest the possible role of Ovol2 in eye development. Additional research may clarify the precise function of the Ovol2 in the development of the eye and discover the downstream targets or pathways.

8. CONCLUSIONS

This PhD thesis can be summarized as follows:

1. We generated *Aldh3-Cre* transgenic mouse driver line which is beneficial for conditional gene inactivation in the postnatal cornea.
2. Pax6 is important for postnatal corneal development. Conditional depletion of Pax6 in early postnatal (PN1-PN9) OSE resulted in conjunctivalisation of limbal and CE, suggesting the role of limbal Pax6 in preventing the growth of conjunctiva to CE. Moreover, more restricted conditional depletion of Pax6 in postnatal CE coincident with eyelid opening (PN12 onwards) resulted in a thin cornea with differentiation and intercellular adhesion defects.
3. The genetic causation of human PPCD1 is the mutations affecting the highly conserved promoter region of the *OVOL2* gene resulting in increased *OVOL2* mRNA expression in CEn cells. We attempted to establish a mouse model, using the CRISPR-Cas9 approach by generating an allelic series with alterations in the *Ovol2* promoter region including pathogenic variant c.-307T>C as in human PPCD1 patients. Interestingly, despite the high degree of conservation among mammals, not all mutations in mice led to ocular abnormalities. Whereas mutation c.307T>C and c.-307_-320del (deletion of Ovol1/Ovol2 binding site next to c.307T>C) resulted in increased *Ovol2* mRNA levels analogous to human patients. Surprisingly, mouse endothelium is robust to these alterations, preventing the development of endothelial dystrophy. Notably, a small percentage of c.-307T>C and c.-307_-320del mutants showed iridocorneal adhesion, PHPV and dysplastic retina, suggesting the role of Ovol2 during embryonic eye development.
4. Snf2h is a chromatin remodeling factor expressed in RPC and post-mitotic retinal cells. Conditional depletion of Snf2h in RPC resulted in a thin retina with a lack of photoreceptors. Our further studies confirmed that Snf2h is not necessary for the specification of other retinal cell types. Contrarily, it is crucial for the proliferation of RPC. Loss of Snf2h in RPC caused discrepancies in the cell cycle and increased apoptosis, which eventually led to the death of photoreceptors and disrupted retinal lamination.

9. REFERENCES

Abedinia, M., Pain, T., Algar, E.M., Holmes, R.S., 1990. Bovine corneal aldehyde dehydrogenase: the major soluble corneal protein with a possible dual protective role for the eye. Experimental eye research 51, 419-426.

Aldave, A.J., Yellore, V.S., Yu, F., Bourla, N., Sonmez, B., Salem, A.K., Rayner, S.A., Sampat, K.M., Krafchak, C.M., Richards, J.E., 2007. Posterior polymorphous corneal dystrophy is associated with TCF8 gene mutations and abdominal hernia. American journal of medical genetics. Part A 143A, 2549-2556.

Andl, T., Ahn, K., Kairo, A., Chu, E.Y., Wine-Lee, L., Reddy, S.T., Croft, N.J., Cebra-Thomas, J.A., Metzger, D., Chambon, P., Lyons, K.M., Mishina, Y., Seykora, J.T., Crenshaw, E.B., 3rd, Millar, S.E., 2004. Epithelial Bmpr1a regulates differentiation and proliferation in postnatal hair follicles and is essential for tooth development. Development 131, 2257-2268.

Ang, S.J., Stump, R.J., Lovicu, F.J., McAvoy, J.W., 2004. Spatial and temporal expression of Wnt and Dickkopf genes during murine lens development. Gene expression patterns : GEP 4, 289-295.

Antosova, B., Smolikova, J., Klimova, L., Lachova, J., Bendova, M., Kozmikova, I., Machon, O., Kozmik, Z., 2016. The Gene Regulatory Network of Lens Induction Is Wired through Meis-Dependent Shadow Enhancers of Pax6. PLoS genetics 12, e1006441.

Ashery-Padan, R., Marquardt, T., Zhou, X., Gruss, P., 2000. Pax6 activity in the lens primordium is required for lens formation and for correct placement of a single retina in the eye. Genes & development 14, 2701-2711.

Aue, A., Hinze, C., Walentin, K., Ruffert, J., Yurtdas, Y., Werth, M., Chen, W., Rabien, A., Kilic, E., Schulzke, J.D., Schumann, M., Schmidt-Ott, K.M., 2015. A Grainyhead-Like 2/Ovo-Like 2 Pathway Regulates Renal Epithelial Barrier Function and Lumen Expansion. Journal of the American Society of Nephrology : JASN 26, 2704-2715

Beauchamp, G.R. and P.A. Knepper, Role of the neural crest in anterior segment development anddisease. J Pediatr Ophthalmol Strabismus, 1984. **21**(6): p. 209-14.

Bhinge, A., Poschmann, J., Namboori, S.C., Tian, X., Jia Hui Loh, S., Traczyk, A., Prabhakar, S., Stanton, L.W., 2014. MiR-135b is a direct PAX6 target and specifies human neuroectoderm by inhibiting TGF-beta/BMP signaling. The EMBO journal 33, 1271-1283.

Bonanno, J.A., 2012. Molecular mechanisms underlying the corneal endothelial pump. Experimental eye research 95, 2-7.

Bonnet, C., Roberts, J.S., Deng, S.X., 2021. Limbal stem cell diseases. Experimental eye research 205, 108437.

Bourgeois, J., Shields, M.B., Thresher, R., 1984. Open-angle glaucoma associated with posterior polymorphous dystrophy. A clinicopathologic study. Ophthalmology 91, 420-423.

Brown, A., McKie, M., van Heyningen, V., Prosser, J., 1998. The Human PAX6 Mutation Database. Nucleic acids research 26, 259-264.

Brault, V., Moore, R., Kutsch, S., Ishibashi, M., Rowitch, D.H., McMahon, A.P., Sommer, L., Boussadia, O., Kemler, R., 2001. Inactivation of the beta-catenin gene by Wnt1-Cre-

mediated deletion results in dramatic brain malformation and failure of craniofacial development. Development 128, 1253-1264.
Cadenas, U., 1955. Congenital aniridia. American journal of ophthalmology 40, 259-261.
Carriere, C., Plaza, S., Martin, P., Quatannens, B., Bailly, M., Stehelin, D., Saule, S., 1993. Characterization of quail Pax-6 (Pax-QNR) proteins expressed in the neuroretina. Molecular and cellular biology 13, 7257-7266.
Campbell, H.K., Maiers, J.L., DeMali, K.A., 2017. Interplay between tight junctions & adherens junctions. Experimental cell research 358, 39-44.
Capaldo, C.T., Macara, I.G., 2007. Depletion of E-cadherin disrupts establishment but not maintenance of cell junctions in Madin-Darby canine kidney epithelial cells. Molecular biology of the cell 18, 189-200.
Cepko, C., 2014. Intrinsically different retinal progenitor cells produce specific types of progeny. Nature reviews. Neuroscience 15, 615-627.
Chamcheu, J.C., Siddiqui, I.A., Syed, D.N., Adhami, V.M., Liovic, M., Mukhtar, H., 2011. Keratin gene mutations in disorders of human skin and its appendages. Archives of biochemistry and biophysics 508, 123-137.
Chaloin-Dufau, C., Pavitt, I., Delorme, P., Dhouailly, D., 1993. Identification of keratins 3 and 12 in corneal epithelium of vertebrates. Epithelial cell biology 2, 120-125.
Chaloin-Dufau, C., Sun, T.T., Dhouailly, D., 1990. Appearance of the keratin pair K3/K12 during embryonic and adult corneal epithelial differentiation in the chick and in the rabbit. Cell differentiation and development : the official journal of the International Society of Developmental Biologists 32, 97-108
Chen, J.J., Tseng, S.C., 1990. Corneal epithelial wound healing in partial limbal deficiency. Investigative ophthalmology & visual science 31, 1301-1314.
Chen, W., Hu, J., Zhang, Z., Chen, L., Xie, H., Dong, N., Chen, Y., Liu, Z., 2012. Localization and expression of zonula occludins-1 in the rabbit corneal epithelium following exposure to benzalkonium chloride. PloS one 7, e40893.
Chi, N., Epstein, J.A., 2002. Getting your Pax straight: Pax proteins in development and disease. Trends in genetics : TIG 18, 41-47.
Chiambaretta, F., Blanchon, L., Rabier, B., Kao, W.W., Liu, J.J., Dastugue, B., Rigal, D., Sapin, V., 2002. Regulation of corneal keratin-12 gene expression by the human Kruppel-like transcription factor 6. Investigative ophthalmology & visual science 43, 3422-3429.
Chow, R.L., Altmann, C.R., Lang, R.A., Hemmati-Brivanlou, A., 1999. Pax6 induces ectopic eyes in a vertebrate. Development 126, 4213-4222.
Chung, D.D., Frausto, R.F., Lin, B.R., Hanser, E.M., Cohen, Z., Aldave, A.J., 2017. Transcriptomic Profiling of Posterior Polymorphous Corneal Dystrophy. Investigative ophthalmology & visual science 58, 3202-3214.
Chung, D.D., Zhang, W., Jatavallabhula, K., Barrington, A., Jung, J., Aldave, A.J., 2019. Alterations in GRHL2-OVOL2-ZEB1 axis and aberrant activation of Wnt signaling lead to altered gene transcription in posterior polymorphous corneal dystrophy. Experimental eye research 188, 107696.
Churchill, A. and A. Booth, Genetics of aniridia and anterior segment dysgenesis. Br J Ophthalmol, 1996. 80(7): p. 669-73.

Cieply, B., Farris, J., Denvir, J., Ford, H.L., Frisch, S.M., 2013. Epithelial-mesenchymal transition and tumor suppression are controlled by a reciprocal feedback loop between ZEB1 and Grainyhead-like-2. Cancer research 73, 6299-6309.
Collinson, J.M., Morris, L., Reid, A.I., Ramaesh, T., Keighren, M.A., Flockhart, J.H., Hill, R.E., Tan, S.S., Ramaesh, K., Dhillon, B., West, J.D., 2002. Clonal analysis of patterns of growth, stem cell activity, and cell movement during the development and maintenance of the murine corneal epithelium. Developmental dynamics : an official publication of the American Association of Anatomists 224, 432-440.
Collinson, J.M., Quinn, J.C., Buchanan, M.A., Kaufman, M.H., Wedden, S.E., West, J.D., Hill, R.E., 2001. Primary defects in the lens underlie complex anterior segment abnormalities of the Pax6 heterozygous eye. Proceedings of the National Academy of Sciences of the United States of America 98, 9688-9693.
Cotsarelis, G., Cheng, S.Z., Dong, G., Sun, T.T., Lavker, R.M., 1989. Existence of slow-cycling limbal epithelial basal cells that can be preferentially stimulated to proliferate: implications on epithelial stem cells. Cell 57, 201-209.
Cvekl, A., Callaerts, P., 2017. PAX6: 25th anniversary and more to learn. Experimental eye research 156, 10-21.
Cvekl, A., Kashanchi, F., Brady, J.N., Piatigorsky, J., 1999. Pax-6 interactions with TATA-box-binding protein and retinoblastoma protein. Investigative ophthalmology & visual science 40, 1343-1350.
Cvekl, A., Piatigorsky, J., 1996. Lens development and crystallin gene expression: many roles for Pax-6. BioEssays : news and reviews in molecular, cellular and developmental biology 18, 621-630.
Cvekl, A., Tamm, E.R., 2004. Anterior eye development and ocular mesenchyme: new insights from mouse models and human diseases. BioEssays : news and reviews in molecular, cellular and developmental biology 26, 374-386.
Czerny, T., Busslinger, M., 1995. DNA-binding and transactivation properties of Pax-6: three amino acids in the paired domain are responsible for the different sequence recognition of Pax-6 and BSAP (Pax-5). Molecular and cellular biology 15, 2858-2871.
Czerny, T., Halder, G., Kloter, U., Souabni, A., Gehring, W.J., Busslinger, M., 1999. twin of eyeless, a second Pax-6 gene of Drosophila, acts upstream of eyeless in the control of eye development. Molecular cell 3, 297-307.
Czerny, T., Schaffner, G., Busslinger, M., 1993. DNA sequence recognition by Pax proteins: bipartite structure of the paired domain and its binding site. Genes & development 7, 2048-2061.
Darling, D.S., Stearman, R.P., Qi, Y., Qiu, M.S., Feller, J.P., 2003. Expression of Zfhep/deltaEF1 protein in palate, neural progenitors, and differentiated neurons. Gene expression patterns : GEP 3, 709-717.
Davidson, A.E., Liskova, P., Evans, C.J., Dudakova, L., Noskova, L., Pontikos, N., Hartmannova, H., Hodanova, K., Stranecky, V., Kozmik, Z., Levis, H.J., Idigo, N., Sasai, N., Maher, G.J., Bellingham, J., Veli, N., Ebenezer, N.D., Cheetham, M.E., Daniels, J.T., Thaung, C.M., Jirsova, K., Plagnol, V., Filipec, M., Kmoch, S., Tuft, S.J., Hardcastle, A.J., 2016. Autosomal-Dominant Corneal Endothelial Dystrophies CHED1 and PPCD1 Are

Allelic Disorders Caused by Non-coding Mutations in the Promoter of OVOL2. American journal of human genetics 98, 75-89.
Davis-Silberman, N., Ashery-Padan, R., 2008. Iris development in vertebrates; genetic and molecular considerations. Brain research 1192, 17-28.
Davis, J., Davis, D., Norman, B., Piatigorsky, J., 2008. Gene expression of the mouse corneal crystallin Aldh3a1: activation by Pax6, Oct1, and p300. Investigative ophthalmology & visual science 49, 1814-1826.
Davis, J., Duncan, M.K., Robison, W.G., Jr., Piatigorsky, J., 2003. Requirement for Pax6 in corneal morphogenesis: a role in adhesion. Journal of cell science 116, 2157-2167.
Davis, J., Piatigorsky, J., 2011. Overexpression of Pax6 in mouse cornea directly alters corneal epithelial cells: changes in immune function, vascularization, and differentiation. Investigative ophthalmology & visual science 52, 4158-4168.
DelMonte, D.W., Kim, T., 2011. Anatomy and physiology of the cornea. Journal of cataract and refractive surgery 37, 588-598.
Delp, E.E., Swamynathan, S., Kao, W.W., Swamynathan, S.K., 2015. Spatiotemporally Regulated Ablation of Klf4 in Adult Mouse Corneal Epithelial Cells Results in Altered Epithelial Cell Identity and Disrupted Homeostasis. Investigative ophthalmology & visual science 56, 3549-3558.
Douvaras, P., Mort, R.L., Edwards, D., Ramaesh, K., Dhillon, B., Morley, S.D., Hill, R.E., West, J.D., 2013. Increased corneal epithelial turnover contributes to abnormal homeostasis in the Pax6(+/-) mouse model of aniridia. PloS one 8, e71117.
Dua, H.S., Saini, J.S., Azuara-Blanco, A., Gupta, P., 2000. Limbal stem cell deficiency: concept, aetiology, clinical presentation, diagnosis and management. Indian journal of ophthalmology 48, 83-92.
Dublin, I., 1970. [Comparative embryologic studies of the early development of the cornea and the pupillary membrane in reptiles, birds and mammals]. Acta anatomica 76, 381-408.
Duncan, M.K., Cvekl, A., Li, X., Piatigorsky, J., 2000. Truncated forms of Pax-6 disrupt lens morphology in transgenic mice. Investigative ophthalmology & visual science 41, 464-473.
Duncan, M.K., Haynes, J.I., 2nd, Cvekl, A., Piatigorsky, J., 1998. Dual roles for Pax-6: a transcriptional repressor of lens fiber cell-specific beta-crystallin genes. Molecular and cellular biology 18, 5579-5586.
Duparc, R.H., Boutemmine, D., Champagne, M.P., Tetreault, N., Bernier, G., 2006. Pax6 is required for delta-catenin/neurojugin expression during retinal, cerebellar and cortical development in mice. Developmental biology 300, 647-655.
Dwivedi, D.J., Pontoriero, G.F., Ashery-Padan, R., Sullivan, S., Williams, T., West-Mays, J.A., 2005. Targeted deletion of AP-2alpha leads to disruption in corneal epithelial cell integrity and defects in the corneal stroma. Investigative ophthalmology & visual science 46, 3623-3630.
Dyer, M.A., Cepko, C.L., 2001. Regulating proliferation during retinal development. Nature reviews. Neuroscience 2, 333-342.
Epstein, J., Cai, J., Glaser, T., Jepeal, L., Maas, R., 1994a. Identification of a Pax paired domain recognition sequence and evidence for DNA-dependent conformational changes. The Journal of biological chemistry 269, 8355-8361.

Epstein, J.A., Glaser, T., Cai, J., Jepeal, L., Walton, D.S., Maas, R.L., 1994b. Two independent and interactive DNA-binding subdomains of the Pax6 paired domain are regulated by alternative splicing. Genes & development 8, 2022-2034.
Estey, T., Piatigorsky, J., Lassen, N., Vasiliou, V., 2007. ALDH3A1: a corneal crystallin with diverse functions. Experimental eye research 84, 3-12.
Evans, C.J., Liskova, P., Dudakova, L., Hrabcikova, P., Horinek, A., Jirsova, K., Filipec, M., Hardcastle, A.J., Davidson, A.E., Tuft, S.J., 2015. Identification of six novel mutations in ZEB1 and description of the associated phenotypes in patients with posterior polymorphous corneal dystrophy 3. Annals of human genetics 79, 1-9.
Fang, J., Zhang, T., Liu, Y., Li, Y., Zhou, S., Song, D., Zhao, Y., Feng, R., Zhang, X., Li, L., Wen, J., 2014. PAX6 downregulates miR-124 expression to promote cell migration during embryonic stem cell differentiation. Stem cells and development 23, 2297-2310.
Flugel-Koch, C., Ohlmann, A., Piatigorsky, J., Tamm, E.R., 2002. Disruption of anterior segment development by TGF-beta1 overexpression in the eyes of transgenic mice. Developmental dynamics : an official publication of the American Association of Anatomists 225, 111-125.
Fujimura, N., 2016. WNT/beta-Catenin Signaling in Vertebrate Eye Development. Frontiers in cell and developmental biology 4, 138.
Fujimura, N., Kuzelova, A., Ebert, A., Strnad, H., Lachova, J., Machon, O., Busslinger, M., Kozmik, Z., 2018. Polycomb repression complex 2 is required for the maintenance of retinal progenitor cells and balanced retinal differentiation. Developmental biology 433, 47-60.
Gage, P.J., Kuang, C., Zacharias, A.L., 2014. The homeodomain transcription factor PITX2 is required for specifying correct cell fates and establishing angiogenic privilege in the developing cornea. Developmental dynamics : an official publication of the American Association of Anatomists 243, 1391-1400.
Gage, P.J., Qian, M., Wu, D., Rosenberg, K.I., 2008. The canonical Wnt signaling antagonist DKK2 is an essential effector of PITX2 function during normal eye development. Developmental biology 317, 310-324.
Gatzioufas, Z., Charalambous, P., Thanos, S., 2008. Reduced expression of the gap junction protein Connexin 43 in keratoconus. Eye 22, 294-299.
Gehring, W.J., Ikeo, K., 1999. Pax 6: mastering eye morphogenesis and eye evolution. Trends in genetics : TIG 15, 371-377.
Gehring, W.J., 2004. Historical perspective on the development and evolution of eyes and photoreceptors. The International journal of developmental biology 48, 707-717.
Genis-Galvez, J.M., 1966. Role of the lens in the morphogenesis of the iris and cornea. Nature 210, 209-210.
Genis-Galvez, J.M., Santos-Gutierrez, L., Rios-Gonzalez, A., 1967. Causal factors in corneal development: an experimental analysis in the chick embryo. Experimental eye research 6, 48-56.
Glaser, T., Walton, D.S., Maas, R.L., 1992. Genomic structure, evolutionary conservation and aniridia mutations in the human PAX6 gene. Nature genetics 2, 232-239.
Global Burden of Disease Cancer, C., Fitzmaurice, C., Abate, D., Abbasi, N., Abbastabar, H., Abd-Allah, F., Abdel-Rahman, O., Abdelalim, A., Abdoli, A., Abdollahpour, I., Abdulle, A.S.M., Abebe, N.D., Abraha, H.N., Abu-Raddad, L.J., Abualhasan, A., Adedeji, I.A.,

Advani, S.M., Afarideh, M., Afshari, M., Aghaali, M., Agius, D., Agrawal, S., Ahmadi, A., Ahmadian, E., Ahmadpour, E., Ahmed, M.B., Akbari, M.E., Akinyemiju, T., Al-Aly, Z., AlAbdulKader, A.M., Alahdab, F., Alam, T., Alamene, G.M., Alemnew, B.T.T., Alene, K.A., Alinia, C., Alipour, V., Aljunid, S.M., Bakeshei, F.A., Almadi, M.A.H., Almasi-Hashiani, A., Alsharif, U., Alsowaidi, S., Alvis-Guzman, N., Amini, E., Amini, S., Amoako, Y.A., Anbari, Z., Anber, N.H., Andrei, C.L., Anjomshoa, M., Ansari, F., Ansariadi, A., Appiah, S.C.Y., Arab-Zozani, M., Arabloo, J., Arefi, Z., Aremu, O., Areri, H.A., Artaman, A., Asayesh, H., Asfaw, E.T., Ashagre, A.F., Assadi, R., Ataeinia, B., Atalay, H.T., Ataro, Z., Atique, S., Ausloos, M., Avila-Burgos, L., Avokpaho, E., Awasthi, A., Awoke, N., Ayala Quintanilla, B.P., Ayanore, M.A., Ayele, H.T., Babaee, E., Bacha, U., Badawi, A., Bagherzadeh, M., Bagli, E., Balakrishnan, S., Balouchi, A., Barnighausen, T.W., Battista, R.J., Behzadifar, M., Behzadifar, M., Bekele, B.B., Belay, Y.B., Belayneh, Y.M., Berfield, K.K.S., Berhane, A., Bernabe, E., Beuran, M., Bhakta, N., Bhattacharyya, K., Biadgo, B., Bijani, A., Bin Sayeed, M.S., Birungi, C., Bisignano, C., Bitew, H., Bjorge, T., Bleyer, A., Bogale, K.A., Bojia, H.A., Borzi, A.M., Bosetti, C., Bou-Orm, I.R., Brenner, H., Brewer, J.D., Briko, A.N., Briko, N.I., Bustamante-Teixeira, M.T., Butt, Z.A., Carreras, G., Carrero, J.J., Carvalho, F., Castro, C., Castro, F., Catala-Lopez, F., Cerin, E., Chaiah, Y., Chanie, W.F., Chattu, V.K., Chaturvedi, P., Chauhan, N.S., Chehrazi, M., Chiang, P.P., Chichiabellu, T.Y., Chido-Amajuoyi, O.G., Chimed-Ochir, O., Choi, J.J., Christopher, D.J., Chu, D.T., Constantin, M.M., Costa, V.M., Crocetti, E., Crowe, C.S., Curado, M.P., Dahlawi, S.M.A., Damiani, G., Darwish, A.H., Daryani, A., das Neves, J., Demeke, F.M., Demis, A.B., Demissie, B.W., Demoz, G.T., Denova-Gutierrez, E., Derakhshani, A., Deribe, K.S., Desai, R., Desalegn, B.B., Desta, M., Dey, S., Dharmaratne, S.D., Dhimal, M., Diaz, D., Dinberu, M.T.T., Djalalinia, S., Doku, D.T., Drake, T.M., Dubey, M., Dubljanin, E., Duken, E.E., Ebrahimi, H., Effiong, A., Eftekhari, A., El Sayed, I., Zaki, M.E.S., El-Jaafary, S.I., El-Khatib, Z., Elemineh, D.A., Elkout, H., Ellenbogen, R.G., Elsharkawy, A., Emamian, M.H., Endalew, D.A., Endries, A.Y., Eshrati, B., Fadhil, I., Fallah Omrani, V., Faramarzi, M., Farhangi, M.A., Farioli, A., Farzadfar, F., Fentahun, N., Fernandes, E., Feyissa, G.T., Filip, I., Fischer, F., Fisher, J.L., Force, L.M., Foroutan, M., Freitas, M., Fukumoto, T., Futran, N.D., Gallus, S., Gankpe, F.G., Gayesa, R.T., Gebrehiwot, T.T., Gebremeskel, G.G., Gedefaw, G.A., Gelaw, B.K., Geta, B., Getachew, S., Gezae, K.E., Ghafourifard, M., Ghajar, A., Ghashghaee, A., Gholamian, A., Gill, P.S., Ginindza, T.T.G., Girmay, A., Gizaw, M., Gomez, R.S., Gopalani, S.V., Gorini, G., Goulart, B.N.G., Grada, A., Ribeiro Guerra, M., Guimaraes, A.L.S., Gupta, P.C., Gupta, R., Hadkhale, K., Haj-Mirzaian, A., Haj-Mirzaian, A., Hamadeh, R.R., Hamidi, S., Hanfore, L.K., Haro, J.M., Hasankhani, M., Hasanzadeh, A., Hassen, H.Y., Hay, R.J., Hay, S.I., Henok, A., Henry, N.J., Herteliu, C., Hidru, H.D., Hoang, C.L., Hole, M.K., Hoogar, P., Horita, N., Hosgood, H.D., Hosseini, M., Hosseinzadeh, M., Hostiuc, M., Hostiuc, S., Househ, M., Hussen, M.M., Ileanu, B., Ilic, M.D., Innos, K., Irvani, S.S.N., Iseh, K.R., Islam, S.M.S., Islami, F., Jafari Balalami, N., Jafarinia, M., Jahangiry, L., Jahani, M.A., Jahanmehr, N., Jakovljevic, M., James, S.L., Javanbakht, M., Jayaraman, S., Jee, S.H., Jenabi, E., Jha, R.P., Jonas, J.B., Jonnagaddala, J., Joo, T., Jungari, S.B., Jurisson, M., Kabir, A., Kamangar, F., Karch, A., Karimi, N., Karimian, A., Kasaeian, A., Kasahun, G.G., Kassa, B., Kassa, T.D., Kassaw, M.W., Kaul, A., Keiyoro, P.N., Kelbore, A.G., Kerbo, A.A., Khader, Y.S., Khalilarjmandi,

M., Khan, E.A., Khan, G., Khang, Y.H., Khatab, K., Khater, A., Khayamzadeh, M., Khazaee-Pool, M., Khazaei, S., Khoja, A.T., Khosravi, M.H., Khubchandani, J., Kianipour, N., Kim, D., Kim, Y.J., Kisa, A., Kisa, S., Kissimova-Skarbek, K., Komaki, H., Koyanagi, A., Krohn, K.J., Bicer, B.K., Kugbey, N., Kumar, V., Kuupiel, D., La Vecchia, C., Lad, D.P., Lake, E.A., Lakew, A.M., Lal, D.K., Lami, F.H., Lan, Q., Lasrado, S., Lauriola, P., Lazarus, J.V., Leigh, J., Leshargie, C.T., Liao, Y., Limenih, M.A., Listl, S., Lopez, A.D., Lopukhov, P.D., Lunevicius, R., Madadin, M., Magdeldin, S., El Razek, H.M.A., Majeed, A., Maleki, A., Malekzadeh, R., Manafi, A., Manafi, N., Manamo, W.A., Mansourian, M., Mansournia, M.A., Mantovani, L.G., Maroufizadeh, S., Martini, S.M.S., Mashamba-Thompson, T.P., Massenburg, B.B., Maswabi, M.T., Mathur, M.R., McAlinden, C., McKee, M., Meheretu, H.A.A., Mehrotra, R., Mehta, V., Meier, T., Melaku, Y.A., Meles, G.G., Meles, H.G., Melese, A., Melku, M., Memiah, P.T.N., Mendoza, W., Menezes, R.G., Merat, S., Meretoja, T.J., Mestrovic, T., Miazgowski, B., Miazgowski, T., Mihretie, K.M.M., Miller, T.R., Mills, E.J., Mir, S.M., Mirzaei, H., Mirzaei, H.R., Mishra, R., Moazen, B., Mohammad, D.K., Mohammad, K.A., Mohammad, Y., Darwesh, A.M., Mohammadbeigi, A., Mohammadi, H., Mohammadi, M., Mohammadian, M., Mohammadian-Hafshejani, A., Mohammadoo-Khorasani, M., Mohammadpourhodki, R., Mohammed, A.S., Mohammed, J.A., Mohammed, S., Mohebi, F., Mokdad, A.H., Monasta, L., Moodley, Y., Moosazadeh, M., Moossavi, M., Moradi, G., Moradi-Joo, M., Moradi-Lakeh, M., Moradpour, F., Morawska, L., Morgado-da-Costa, J., Morisaki, N., Morrison, S.D., Mosapour, A., Mousavi, S.M., Muche, A.A., Muhammed, O.S.S., Musa, J., Nabhan, A.F., Naderi, M., Nagarajan, A.J., Nagel, G., Nahvijou, A., Naik, G., Najafi, F., Naldi, L., Nam, H.S., Nasiri, N., Nazari, J., Negoi, I., Neupane, S., Newcomb, P.A., Nggada, H.A., Ngunjiri, J.W., Nguyen, C.T., Nikniaz, L., Ningrum, D.N.A., Nirayo, Y.L., Nixon, M.R., Nnaji, C.A., Nojomi, M., Nosratnejad, S., Shiadeh, M.N., Obsa, M.S., Ofori-Asenso, R., Ogbo, F.A., Oh, I.H., Olagunju, A.T., Olagunju, T.O., Oluwasanu, M.M., Omonisi, A.E., Onwujekwe, O.E., Oommen, A.M., Oren, E., Ortega-Altamirano, D.D.V., Ota, E., Otstavnov, S.S., Owolabi, M.O., P, A.M., Padubidri, J.R., Pakhale, S., Pakpour, A.H., Pana, A., Park, E.K., Parsian, H., Pashaei, T., Patel, S., Patil, S.T., Pennini, A., Pereira, D.M., Piccinelli, C., Pillay, J.D., Pirestani, M., Pishgar, F., Postma, M.J., Pourjafar, H., Pourmalek, F., Pourshams, A., Prakash, S., Prasad, N., Qorbani, M., Rabiee, M., Rabiee, N., Radfar, A., Rafiei, A., Rahim, F., Rahimi, M., Rahman, M.A., Rajati, F., Rana, S.M., Raoofi, S., Rath, G.K., Rawaf, D.L., Rawaf, S., Reiner, R.C., Renzaho, A.M.N., Rezaei, N., Rezapour, A., Ribeiro, A.I., Ribeiro, D., Ronfani, L., Roro, E.M., Roshandel, G., Rostami, A., Saad, R.S., Sabbagh, P., Sabour, S., Saddik, B., Safiri, S., Sahebkar, A., Salahshoor, M.R., Salehi, F., Salem, H., Salem, M.R., Salimzadeh, H., Salomon, J.A., Samy, A.M., Sanabria, J., Santric Milicevic, M.M., Sartorius, B., Sarveazad, A., Sathian, B., Satpathy, M., Savic, M., Sawhney, M., Sayyah, M., Schneider, I.J.C., Schottker, B., Sekerija, M., Sepanlou, S.G., Sepehrimanesh, M., Seyedmousavi, S., Shaahmadi, F., Shabaninejad, H., Shahbaz, M., Shaikh, M.A., Shamshirian, A., Shamsizadeh, M., Sharafi, H., Sharafi, Z., Sharif, M., Sharifi, A., Sharifi, H., Sharma, R., Sheikh, A., Shirkoohi, R., Shukla, S.R., Si, S., Siabani, S., Silva, D.A.S., Silveira, D.G.A., Singh, A., Singh, J.A., Sisay, S., Sitas, F., Sobngwi, E., Soofi, M., Soriano, J.B., Stathopoulou, V., Sufiyan, M.B., Tabares-Seisdedos, R., Tabuchi, T., Takahashi, K., Tamtaji, O.R., Tarawneh, M.R., Tassew, S.G., Taymoori, P., Tehrani-Banihashemi, A.,

Temsah, M.H., Temsah, O., Tesfay, B.E., Tesfay, F.H., Teshale, M.Y., Tessema, G.A., Thapa, S., Tlaye, K.G., Topor-Madry, R., Tovani-Palone, M.R., Traini, E., Tran, B.X., Tran, K.B., Tsadik, A.G., Ullah, I., Uthman, O.A., Vacante, M., Vaezi, M., Varona Perez, P., Veisani, Y., Vidale, S., Violante, F.S., Vlassov, V., Vollset, S.E., Vos, T., Vosoughi, K., Vu, G.T., Vujcic, I.S., Wabinga, H., Wachamo, T.M., Wagnew, F.S., Waheed, Y., Weldegebreal, F., Weldesamuel, G.T., Wijeratne, T., Wondafrash, D.Z., Wonde, T.E., Wondmieneh, A.B., Workie, H.M., Yadav, R., Yadegar, A., Yadollahpour, A., Yaseri, M., Yazdi-Feyzabadi, V., Yeshaneh, A., Yimam, M.A., Yimer, E.M., Yisma, E., Yonemoto, N., Younis, M.Z., Yousefi, B., Yousefifard, M., Yu, C., Zabeh, E., Zadnik, V., Moghadam, T.Z., Zaidi, Z., Zamani, M., Zandian, H., Zangeneh, A., Zaki, L., Zendehdel, K., Zenebe, Z.M., Zewale, T.A., Ziapour, A., Zodpey, S., Murray, C.J.L., 2019. Global, Regional, and National Cancer Incidence, Mortality, Years of Life Lost, Years Lived With Disability, and Disability-Adjusted Life-Years for 29 Cancer Groups, 1990 to 2017: A Systematic Analysis for the Global Burden of Disease Study. JAMA oncology 5, 1749-1768.

Graw, J., 2010. Eye development. Current topics in developmental biology 90, 343-386.

Grayson, M., 1974. The nature of hereditary deep polymorphous dystrophy of the cornea: its association with iris and anterior chamber dygenesis. Transactions of the American Ophthalmological Society 72, 516-559.

Gu, H., Marth, J.D., Orban, P.C., Mossmann, H., Rajewsky, K., 1994. Deletion of a DNA polymerase beta gene segment in T cells using cell type-specific gene targeting. Science 265, 103-106.

Gu, H., Zou, Y.R., Rajewsky, K., 1993. Independent control of immunoglobulin switch recombination at individual switch regions evidenced through Cre-loxP-mediated gene targeting. Cell 73, 1155-1164.

Gumbiner, B.M., 2005. Regulation of cadherin-mediated adhesion in morphogenesis. Nature reviews. Molecular cell biology 6, 622-634.

Halder, G., Callaerts, P., Gehring, W.J., 1995. Induction of ectopic eyes by targeted expression of the eyeless gene in Drosophila. Science 267, 1788-1792.

Hanson, I., Van Heyningen, V., 1995. Pax6: more than meets the eye. Trends in genetics : TIG 11, 268-272.

Hanson, I.M., Seawright, A., Hardman, K., Hodgson, S., Zaletayev, D., Fekete, G., van Heyningen, V., 1993. PAX6 mutations in aniridia. Human molecular genetics 2, 915-920.

Harada, N., Tamai, Y., Ishikawa, T., Sauer, B., Takaku, K., Oshima, M., Taketo, M.M., 1999. Intestinal polyposis in mice with a dominant stable mutation of the beta-catenin gene. The EMBO journal 18, 5931-5942.

Hardwick, L.J., Ali, F.R., Azzarelli, R., Philpott, A., 2015. Cell cycle regulation of proliferation versus differentiation in the central nervous system. Cell and tissue research 359, 187-200.

Hartsock, A., Nelson, W.J., 2008. Adherens and tight junctions: structure, function and connections to the actin cytoskeleton. Biochimica et biophysica acta 1778, 660-669.

Hassan, H., Thaung, C., Ebenezer, N.D., Larkin, G., Hardcastle, A.J., Tuft, S.J., 2013. Severe Meesmann's epithelial corneal dystrophy phenotype due to a missense mutation in the helix-initiation motif of keratin 12. Eye 27, 367-373.

Hay, E.D., 1980. Development of the vertebrate cornea. International review of cytology 63, 263-322.
Hill, R.E., Favor, J., Hogan, B.L., Ton, C.C., Saunders, G.F., Hanson, I.M., Prosser, J., Jordan, T., Hastie, N.D., van Heyningen, V., 1991. Mouse small eye results from mutations in a paired-like homeobox-containing gene. Nature 354, 522-525.
Hogan, B.L., Horsburgh, G., Cohen, J., Hetherington, C.M., Fisher, G., Lyon, M.F., 1986. Small eyes (Sey): a homozygous lethal mutation on chromosome 2 which affects the differentiation of both lens and nasal placodes in the mouse. Journal of embryology and experimental morphology 97, 95-110.
Hong, T., Watanabe, K., Ta, C.H., Villarreal-Ponce, A., Nie, Q., Dai, X., 2015. An Ovol2-Zeb1 Mutual Inhibitory Circuit Governs Bidirectional and Multi-step Transition between Epithelial and Mesenchymal States. PLoS computational biology 11, e1004569.
Huang, J., Rajagopal, R., Liu, Y., Dattilo, L.K., Shaham, O., Ashery-Padan, R., Beebe, D.C., 2011. The mechanism of lens placode formation: a case of matrix-mediated morphogenesis. Developmental biology 355, 32-42.
Hunt, A., et al., Outcomes in persistent hyperplastic primary vitreous. Br J Ophthalmol, 2005.89(7): p. 859-63.
Jat, N.S. and K. Tripathy, Peters Anomaly, in StatPearls. 2023: Treasure Island (FL).
Jester, J.V., 2008. Corneal crystallins and the development of cellular transparency. Seminars in cell & developmental biology 19, 82-93.
Joo, J.H., Kim, Y.H., Dunn, N.W., Sugrue, S.P., 2010. Disruption of mouse corneal epithelial differentiation by conditional inactivation of pnn. Investigative ophthalmology & visual science 51, 1927-1934.
Jordan, T., Hanson, I., Zaletayev, D., Hodgson, S., Prosser, J., Seawright, A., Hastie, N., van Heyningen, V., 1992. The human PAX6 gene is mutated in two patients with aniridia. Nature genetics 1, 328-332.
Jun, S., Desplan, C., 1996. Cooperative interactions between paired domain and homeodomain. Development 122, 2639-2650.
Kammandel, B., Chowdhury, K., Stoykova, A., Aparicio, S., Brenner, S., Gruss, P., 1999. Distinct cis-essential modules direct the time-space pattern of the Pax6 gene activity. Developmental biology 205, 79-97.
Kanakubo, S., Nomura, T., Yamamura, K., Miyazaki, J., Tamai, M., Osumi, N., 2006. Abnormal migration and distribution of neural crest cells in Pax6 heterozygous mutant eye, a model for human eye diseases. Genes to cells : devoted to molecular & cellular mechanisms 11, 919-933.
Kao, W.W., 2020. Keratin expression by corneal and limbal stem cells during development. Experimental eye research 200, 108206.
Kao, W.W., Liu, C.Y., Converse, R.L., Shiraishi, A., Kao, C.W., Ishizaki, M., Doetschman, T., Duffy, J., 1996. Keratin 12-deficient mice have fragile corneal epithelia. Investigative ophthalmology & visual science 37, 2572-2584.
Kays, W.T., Piatigorsky, J., 1997. Aldehyde dehydrogenase class 3 expression: identification of a cornea-preferred gene promoter in transgenic mice. Proceedings of the National Academy of Sciences of the United States of America 94, 13594-13599.

Kenchegowda, D., Swamynathan, S., Gupta, D., Wan, H., Whitsett, J., Swamynathan, S.K., 2011. Conditional disruption of mouse Klf5 results in defective eyelids with malformed meibomian glands, abnormal cornea and loss of conjunctival goblet cells. Developmental biology 356, 5-18.
Kenyon, K.R., Tseng, S.C., 1989. Limbal autograft transplantation for ocular surface disorders. Ophthalmology 96, 709-722; discussion 722-703.
Kidson, S.H., Kume, T., Deng, K., Winfrey, V., Hogan, B.L., 1999. The forkhead/winged-helix gene, Mf1, is necessary for the normal development of the cornea and formation of the anterior chamber in the mouse eye. Developmental biology 211, 306-322.
Kim, A.S., Anderson, S.A., Rubenstein, J.L., Lowenstein, D.H., Pleasure, S.J., 2001. Pax-6 regulates expression of SFRP-2 and Wnt-7b in the developing CNS. The Journal of neuroscience : the official journal of the Society for Neuroscience 21, RC132.
Kreslova, J., Machon, O., Ruzickova, J., Lachova, J., Wawrousek, E.F., Kemler, R., Krauss, S., Piatigorsky, J., Kozmik, Z., 2007. Abnormal lens morphogenesis and ectopic lens formation in the absence of beta-catenin function. Genesis 45, 157-168.
Kim, J., Lauderdale, J.D., 2006. Analysis of Pax6 expression using a BAC transgene reveals the presence of a paired-less isoform of Pax6 in the eye and olfactory bulb. Developmental biology 292, 486-505.
Kitazawa, K., Hikichi, T., Nakamura, T., Mitsunaga, K., Tanaka, A., Nakamura, M., Yamakawa, T., Furukawa, S., Takasaka, M., Goshima, N., Watanabe, A., Okita, K., Kawasaki, S., Ueno, M., Kinoshita, S., Masui, S., 2016. OVOL2 Maintains the Transcriptional Program of Human Corneal Epithelium by Suppressing Epithelial-to-Mesenchymal Transition. Cell reports 15, 1359-1368.
Kleinjan, D.A., Seawright, A., Childs, A.J., van Heyningen, V., 2004. Conserved elements in Pax6 intron 7 involved in (auto)regulation and alternative transcription. Developmental biology 265, 462-477.
Kleinjan, D.A., Seawright, A., Schedl, A., Quinlan, R.A., Danes, S., van Heyningen, V., 2001. Aniridia-associated translocations, DNase hypersensitivity, sequence comparison and transgenic analysis redefine the functional domain of PAX6. Human molecular genetics 10, 2049-2059.
Klyce, S.D., 2020. 12. Endothelial pump and barrier function. Experimental eye research 198, 108068.
Koizumi, N., Okumura, N., Kinoshita, S., 2012. Development of new therapeutic modalities for corneal endothelial disease focused on the proliferation of corneal endothelial cells using animal models. Experimental eye research 95, 60-67.
Kokado, M., Miyajima, M., Okada, Y., Ichikawa, K., Yamanaka, O., Liu, C.Y., Kao, W.W., Shou, W., Saika, S., 2018. Lack of plakoglobin impairs integrity and wound healing in corneal epithelium in mice. Laboratory investigation; a journal of technical methods and pathology 98, 1375-1383.
Kokotas, H., Petersen, M.B., 2010. Clinical and molecular aspects of aniridia. Clinical genetics 77, 409-420.
Koppaka, V., Chen, Y., Mehta, G., Orlicky, D.J., Thompson, D.C., Jester, J.V., Vasiliou, V., 2016. ALDH3A1 Plays a Functional Role in Maintenance of Corneal Epithelial Homeostasis. PloS one 11, e0146433.

Koroma, B.M., Yang, J.M., Sundin, O.H., 1997. The Pax-6 homeobox gene is expressed throughout the corneal and conjunctival epithelia. Investigative ophthalmology & visual science 38, 108-120.
Kowalczyk, A.P., Green, K.J., 2013. Structure, function, and regulation of desmosomes. Progress in molecular biology and translational science 116, 95-118.
Kozmik, Z., 2005. Pax genes in eye development and evolution. Current opinion in genetics & development 15, 430-438.
Krachmer, J.H., 1985. Posterior polymorphous corneal dystrophy: a disease characterized by epithelial-like endothelial cells which influence management and prognosis. Transactions of the American Ophthalmological Society 83, 413-475.
Krafchak, C.M., Pawar, H., Moroi, S.E., Sugar, A., Lichter, P.R., Mackey, D.A., Mian, S., Nairus, T., Elner, V., Schteingart, M.T., Downs, C.A., Kijek, T.G., Johnson, J.M., Trager, E.H., Rozsa, F.W., Mandal, M.N., Epstein, M.P., Vollrath, D., Ayyagari, R., Boehnke, M., Richards, J.E., 2005. Mutations in TCF8 cause posterior polymorphous corneal dystrophy and ectopic expression of COL4A3 by corneal endothelial cells. American journal of human genetics 77, 694-708.
Kucerova, R., Dora, N., Mort, R.L., Wallace, K., Leiper, L.J., Lowes, C., Neves, C., Walczysko, P., Bruce, F., Fowler, P.A., Rajnicek, A.M., McCaig, C.D., Zhao, M., West, J.D., Collinson, J.M., 2012. Interaction between hedgehog signalling and PAX6 dosage mediates maintenance and regeneration of the corneal epithelium. Molecular vision 18, 139-150.
Kucerova, R., Ou, J., Lawson, D., Leiper, L.J., Collinson, J.M., 2006. Cell surface glycoconjugate abnormalities and corneal epithelial wound healing in the pax6+/- mouse model of aniridia-related keratopathy. Investigative ophthalmology & visual science 47, 5276-5282.
Lassen, N., Bateman, J.B., Estey, T., Kuszak, J.R., Nees, D.W., Piatigorsky, J., Duester, G., Day, B.J., Huang, J., Hines, L.M., Vasiliou, V., 2007. Multiple and additive functions of ALDH3A1 and ALDH1A1: cataract phenotype and ocular oxidative damage in Aldh3a1(-/-)/Aldh1a1(-/-) knock-out mice. The Journal of biological chemistry 282, 25668-25676.
Lavker, R.M., Dong, G., Cheng, S.Z., Kudoh, K., Cotsarelis, G., Sun, T.T., 1991. Relative proliferative rates of limbal and corneal epithelia. Implications of corneal epithelial migration, circadian rhythm, and suprabasally located DNA-synthesizing keratinocytes. Investigative ophthalmology & visual science 32, 1864-1875.
Le, Q., Chauhan, T., Yung, M., Tseng, C.H., Deng, S.X., 2020. Outcomes of Limbal Stem Cell Transplant: A Meta-analysis. JAMA ophthalmology 138, 660-670.
Lee, B., et al., Transcriptional mechanisms link epithelial plasticity to adhesion and differentiation of epidermal progenitor cells. Dev Cell, 2014. 29(1): p. 47-58.
Lee, H., Khan, R., O'Keefe, M., 2008. Aniridia: current pathology and management. Acta ophthalmologica 86, 708-715.
Li, B., et al., Ovol2, a mammalian homolog of Drosophila ovo: gene structure, chromosomal mapping, and aberrant expression in blind-sterile mice. Genomics, 2002. 80(3): p. 319-25.
Lima Cunha, D., Arno, G., Corton, M., Moosajee, M., 2019. The Spectrum of PAX6 Mutations and Genotype-Phenotype Correlations in the Eye. Genes 10.
Lin, S., et al., Neogenin-loss in neural crest cells results in persistent hyperplastic primary

vitreous formation. J Mol Cell Biol, 2020. 12(1): p. 17-31.
Lin, Z.N., Chen, J., Cui, H.P., 2016. Characteristics of corneal dystrophies: a review from clinical, histological and genetic perspectives. International journal of ophthalmology 9, 904-913.
Liskova, P., Dudakova, L., Evans, C.J., Rojas Lopez, K.E., Pontikos, N., Athanasiou, D., Jama, H., Sach, J., Skalicka, P., Stranecky, V., Kmoch, S., Thaung, C., Filipec, M., Cheetham, M.E., Davidson, A.E., Tuft, S.J., Hardcastle, A.J., 2018. Ectopic GRHL2 Expression Due to Non-coding Mutations Promotes Cell State Transition and Causes Posterior Polymorphous Corneal Dystrophy 4. American journal of human genetics 102, 447-459.
Liskova, P., Evans, C.J., Davidson, A.E., Zaliova, M., Dudakova, L., Trkova, M., Stranecky, V., Carnt, N., Plagnol, V., Vincent, A.L., Tuft, S.J., Hardcastle, A.J., 2016. Heterozygous deletions at the ZEB1 locus verify haploinsufficiency as the mechanism of disease for posterior polymorphous corneal dystrophy type 3. European journal of human genetics : EJHG 24, 985-991.
Liu, J.J., Kao, W.W., Wilson, S.E., 1999. Corneal epithelium-specific mouse keratin K12 promoter. Experimental eye research 68, 295-301.
Liu, Y., El-Naggar, S., Darling, D.S., Higashi, Y., Dean, D.C., 2008. Zeb1 links epithelial-mesenchymal transition and cellular senescence. Development 135, 579-588.
Liu, H., Mohamed, O., Dufort, D., Wallace, V.A., 2003. Characterization of Wnt signaling components and activation of the Wnt canonical pathway in the murine retina. Developmental dynamics : an official publication of the American Association of Anatomists 227, 323-334.
Livesey, F.J., Cepko, C.L., 2001. Vertebrate neural cell-fate determination: lessons from the retina. Nature reviews. Neuroscience 2, 109-118.
Lloyd, C., Yu, Q.C., Cheng, J., Turksen, K., Degenstein, L., Hutton, E., Fuchs, E., 1995. The basal keratin network of stratified squamous epithelia: defining K15 function in the absence of K14. The Journal of cell biology 129, 1329-1344.
Logan, C.Y., Nusse, R., 2004. The Wnt signaling pathway in development and disease. Annual review of cell and developmental biology 20, 781-810.
Loughner, C.L., Tiwari, A., Kenchegowda, D., Swamynathan, S., Swamynathan, S.K., 2017. Spatiotemporally Controlled Ablation of Klf5 Results in Dysregulated Epithelial Homeostasis in Adult Mouse Corneas. Investigative ophthalmology & visual science 58, 4683-4693.
Lu, H., Lu, Q., Zheng, Y., Li, Q., 2012. Notch signaling promotes the corneal epithelium wound healing. Molecular vision 18, 403-411.
Lu, H., Zimek, A., Chen, J., Hesse, M., Bussow, H., Weber, K., Magin, T.M., 2006. Keratin 5 knockout mice reveal plasticity of keratin expression in the corneal epithelium. European journal of cell biology 85, 803-811.
Machon, O., Kreslova, J., Ruzickova, J., Vacik, T., Klimova, L., Fujimura, N., Lachova, J., Kozmik, Z., 2010. Lens morphogenesis is dependent on Pax6-mediated inhibition of the canonical Wnt/beta-catenin signaling in the lens surface ectoderm. Genesis 48, 86-95.

Mackay, D.R., et al., The mouse Ovol2 gene is required for cranial neural tube development. Dev Biol, 2006. 291(1): p. 38-52.
Magana-Acosta, M., Valadez-Graham, V., 2020. Chromatin Remodelers in the 3D Nuclear Compartment. Frontiers in genetics 11, 600615.
Mantelli, F., Mauris, J., Argueso, P., 2013. The ocular surface epithelial barrier and other mechanisms of mucosal protection: from allergy to infectious diseases. Current opinion in allergy and clinical immunology 13, 563-568.
Marquardt, T., Ashery-Padan, R., Andrejewski, N., Scardigli, R., Guillemot, F., Gruss, P., 2001. Pax6 is required for the multipotent state of retinal progenitor cells. Cell 105, 43-55.
Masterton, S., Ahearne, M., 2018. Mechanobiology of the corneal epithelium. Experimental eye research 177, 122-129.
Matsuo, T., Osumi-Yamashita, N., Noji, S., Ohuchi, H., Koyama, E., Myokai, F., Matsuo, N., Taniguchi, S., Doi, H., Iseki, S., et al., 1993. A mutation in the Pax-6 gene in rat small eye is associated with impaired migration of midbrain crest cells. Nature genetics 3, 299-304.
Maurice, D.M., 1962. The cornea and sclera, Vegetative physiology and biochemistry. Elsevier, pp. 289-368.
Menzel-Severing, J., 2011. Emerging techniques to treat limbal epithelial stem cell deficiency. Discovery medicine 11, 57-64.
Merbs, S.L., Khan, M.A., Hackler, L., Jr., Oliver, V.F., Wan, J., Qian, J., Zack, D.J., 2012. Cell-specific DNA methylation patterns of retina-specific genes. PloS one 7, e32602.
Mikkola, I., Bruun, J.A., Bjorkoy, G., Holm, T., Johansen, T., 1999. Phosphorylation of the transactivation domain of Pax6 by extracellular signal-regulated kinase and p38 mitogen-activated protein kinase. The Journal of biological chemistry 274, 15115-15126.
Mikkola, I., Bruun, J.A., Holm, T., Johansen, T., 2001. Superactivation of Pax6-mediated transactivation from paired domain-binding sites by dna-independent recruitment of different homeodomain proteins. The Journal of biological chemistry 276, 4109-4118.
Miller, L.A., Smith, A.N., Taketo, M.M., Lang, R.A., 2006. Optic cup and facial patterning defects in ocular ectoderm beta-catenin gain-of-function mice. BMC developmental biology 6, 14.
Mizoguchi, S., Suzuki, K., Zhang, J., Yamanaka, O., Liu, C.Y., Okada, Y., Miyajima, M., Kokado, M., Kao, W.W., Yamada, G., Saika, S., 2015. Disruption of eyelid and cornea morphogenesis by epithelial beta-catenin gain-of-function. Molecular vision 21, 793-803.
Mohan, R., Lee, B., Panjwani, N., 1995. Molecular cloning of the E-cadherin cDNAs from rabbit corneal epithelium. Current eye research 14, 1136-1145.
Moll, R., Divo, M., Langbein, L., 2008. The human keratins: biology and pathology. Histochemistry and cell biology 129, 705-733.
Mooney, S.M., Talebian, V., Jolly, M.K., Jia, D., Gromala, M., Levine, H., McConkey, B.J., 2017. The GRHL2/ZEB Feedback Loop-A Key Axis in the Regulation of EMT in Breast Cancer. Journal of cellular biochemistry 118, 2559-2570.
Mort, R.L., Bentley, A.J., Martin, F.L., Collinson, J.M., Douvaras, P., Hill, R.E., Morley, S.D., Fullwood, N.J., West, J.D., 2011. Effects of aberrant Pax6 gene dosage on mouse corneal pathophysiology and corneal epithelial homeostasis. PloS one 6, e28895.

Mukhopadhyay, M., Gorivodsky, M., Shtrom, S., Grinberg, A., Niehrs, C., Morasso, M.I., Westphal, H., 2006. Dkk2 plays an essential role in the corneal fate of the ocular surface epithelium. Development 133, 2149-2154.
Nagasaki, T., Zhao, J., 2003. Centripetal movement of corneal epithelial cells in the normal adult mouse. Investigative ophthalmology & visual science 44, 558-566.
Nielsen, M.S., Axelsen, L.N., Sorgen, P.L., Verma, V., Delmar, M., Holstein-Rathlou, N.H., 2012. Gap junctions. Comprehensive Physiology 2, 1981-2035.
Nieto, M.A., 2001. The early steps of neural crest development. Mechanisms of development 105, 27-35.
Nishida, K., Honma, Y., Dota, A., Kawasaki, S., Adachi, W., Nakamura, T., Quantock, A.J., Hosotani, H., Yamamoto, S., Okada, M., Shimomura, Y., Kinoshita, S., 1997. Isolation and chromosomal localization of a cornea-specific human keratin 12 gene and detection of four mutations in Meesmann corneal epithelial dystrophy. American journal of human genetics 61, 1268-1275.
Nishida, K., Kinoshita, S., Ohashi, Y., Kuwayama, Y., Yamamoto, S., 1995. Ocular surface abnormalities in aniridia. American journal of ophthalmology 120, 368-375.
Nishimura, T., Takeichi, M., 2009. Remodeling of the adherens junctions during morphogenesis. Current topics in developmental biology 89, 33-54.
Norman, B., Davis, J., Piatigorsky, J., 2004. Postnatal gene expression in the normal mouse cornea by SAGE. Investigative ophthalmology & visual science 45, 429-440.
Numayama-Tsuruta, K., Arai, Y., Takahashi, M., Sasaki-Hoshino, M., Funatsu, N., Nakamura, S., Osumi, N., 2010. Downstream genes of Pax6 revealed by comprehensive transcriptome profiling in the developing rat hindbrain. BMC developmental biology 10, 6.
Nusslein-Volhard, C., Wieschaus, E., 1980. Mutations affecting segment number and polarity in Drosophila. Nature 287, 795-801.
Ooshio, T., Kobayashi, R., Ikeda, W., Miyata, M., Fukumoto, Y., Matsuzawa, N., Ogita, H., Takai, Y., 2010. Involvement of the interaction of afadin with ZO-1 in the formation of tight junctions in Madin-Darby canine kidney cells. The Journal of biological chemistry 285, 5003-5012.
Ouyang, J., Shen, Y.C., Yeh, L.K., Li, W., Coyle, B.M., Liu, C.Y., Fini, M.E., 2006. Pax6 overexpression suppresses cell proliferation and retards the cell cycle in corneal epithelial cells. Investigative ophthalmology & visual science 47, 2397-2407.
Park, S., Leonard, B.C., Raghunathan, V.K., Kim, S., Li, J.Y., Mannis, M.J., Murphy, C.J., Thomasy, S.M., 2021. Animal models of corneal endothelial dysfunction to facilitate development of novel therapies. Annals of translational medicine 9, 1271.
Pajoohesh-Ganji, A., Pal-Ghosh, S., Tadvalkar, G., Stepp, M.A., 2012. Corneal goblet cells and their niche: implications for corneal stem cell deficiency. Stem cells 30, 2032-2043.
Pei, Y.F., Rhodin, J.A., 1970. The prenatal development of the mouse eye. The Anatomical record 168, 105-125.
Pellegrini, G., Traverso, C.E., Franzi, A.T., Zingirian, M., Cancedda, R., De Luca, M., 1997. Long-term restoration of damaged corneal surfaces with autologous cultivated corneal epithelium. Lancet 349, 990-993.
Perez-Moreno, M., Fuchs, E., 2006. Catenins: keeping cells from getting their signals crossed. Developmental cell 11, 601-612.

Peters, B., Kirfel, J., Bussow, H., Vidal, M., Magin, T.M., 2001. Complete cytolysis and neonatal lethality in keratin 5 knockout mice reveal its fundamental role in skin integrity and in epidermolysis bullosa simplex. Molecular biology of the cell 12, 1775-1789.
Pichaud, F., Desplan, C., 2002. Pax genes and eye organogenesis. Current opinion in genetics & development 12, 430-434.
Plaza, S., Dozier, C., Langlois, M.C., Saule, S., 1995a. Identification and characterization of a neuroretina-specific enhancer element in the quail Pax-6 (Pax-QNR) gene. Molecular and cellular biology 15, 892-903.
Plaza, S., Dozier, C., Turque, N., Saule, S., 1995b. Quail Pax-6 (Pax-QNR) mRNAs are expressed from two promoters used differentially during retina development and neuronal differentiation. Molecular and cellular biology 15, 3344-3353.
Pokutta, S., Weis, W.I., 2007. Structure and mechanism of cadherins and catenins in cell-cell contacts. Annual review of cell and developmental biology 23, 237-261.
Popova, E.Y., Barnstable, C.J., Zhang, S.S., 2014. Cell type-specific epigenetic signatures accompany late stages of mouse retina development. Advances in experimental medicine and biology 801, 3-8.
Popova, E.Y., Grigoryev, S.A., Fan, Y., Skoultchi, A.I., Zhang, S.S., Barnstable, C.J., 2013. Developmentally regulated linker histone H1c promotes heterochromatin condensation and mediates structural integrity of rod photoreceptors in mouse retina. The Journal of biological chemistry 288, 17895-17907.
Price, M.O., Mehta, J.S., Jurkunas, U.V., Price, F.W., Jr., 2021. Corneal endothelial dysfunction: Evolving understanding and treatment options. Progress in retinal and eye research 82, 100904.
Puangsricharern, V., Tseng, S.C., 1995. Cytologic evidence of corneal diseases with limbal stem cell deficiency. Ophthalmology 102, 1476-1485.
Quiring, R., Walldorf, U., Kloter, U., Gehring, W.J., 1994. Homology of the eyeless gene of Drosophila to the Small eye gene in mice and Aniridia in humans. Science 265, 785-789.
Ramaesh, T., Collinson, J.M., Ramaesh, K., Kaufman, M.H., West, J.D., Dhillon, B., 2003. Corneal abnormalities in Pax6+/- small eye mice mimic human aniridia-related keratopathy. Investigative ophthalmology & visual science 44, 1871-1878.
Ramaesh, T., Ramaesh, K., Martin Collinson, J., Chanas, S.A., Dhillon, B., West, J.D., 2005. Developmental and cellular factors underlying corneal epithelial dysgenesis in the Pax6+/- mouse model of aniridia. Experimental eye research 81, 224-235.
Reneker, L.W., Silversides, D.W., Xu, L., Overbeek, P.A., 2000. Formation of corneal endothelium is essential for anterior segment development - a transgenic mouse model of anterior segment dysgenesis. Development 127, 533-542.
Roca, H., Hernandez, J., Weidner, S., McEachin, R.C., Fuller, D., Sud, S., Schumann, T., Wilkinson, J.E., Zaslavsky, A., Li, H., Maher, C.A., Daignault-Newton, S., Healy, P.N., Pienta, K.J., 2013. Transcription factors OVOL1 and OVOL2 induce the mesenchymal to epithelial transition in human cancer. PloS one 8, e76773.
Sasamoto, Y., Hayashi, R., Park, S.J., Saito-Adachi, M., Suzuki, Y., Kawasaki, S., Quantock, A.J., Nakai, K., Tsujikawa, M., Nishida, K., 2016. PAX6 Isoforms, along with Reprogramming Factors, Differentially Regulate the Induction of Cornea-specific Genes. Scientific reports 6, 20807.

Sansom, S.N., Griffiths, D.S., Faedo, A., Kleinjan, D.J., Ruan, Y., Smith, J., van Heyningen, V., Rubenstein, J.L., Livesey, F.J., 2009. The level of the transcription factor Pax6 is essential for controlling the balance between neural stem cell self-renewal and neurogenesis. PLoS genetics 5, e1000511.
Sax, C.M., Kays, W.T., Salamon, C., Chervenak, M.M., Xu, Y.S., Piatigorsky, J., 2000. Transketolase gene expression in the cornea is influenced by environmental factors and developmentally controlled events. Cornea 19, 833-841.
Schweitzer, J.M., 1981. An evaluation of 50 years of reconstructive dentistry. Part I: Jaw relations and occlusion. The Journal of prosthetic dentistry 45, 383-388.
Senoo, T., Joyce, N.C., 2000. Cell cycle kinetics in corneal endothelium from old and young donors. Investigative ophthalmology & visual science 41, 660-667.
Shaham, O., Gueta, K., Mor, E., Oren-Giladi, P., Grinberg, D., Xie, Q., Cvekl, A., Shomron, N., Davis, N., Keydar-Prizant, M., Raviv, S., Pasmanik-Chor, M., Bell, R.E., Levy, C., Avellino, R., Banfi, S., Conte, I., Ashery-Padan, R., 2013. Pax6 regulates gene expression in the vertebrate lens through miR-204. PLoS genetics 9, e1003357.
Shaham, O., Menuchin, Y., Farhy, C., Ashery-Padan, R., 2012. Pax6: a multi-level regulator of ocular development. Progress in retinal and eye research 31, 351-376.
Shastry, B.S., Persistent hyperplastic primary vitreous: congenital malformation of the eye.ClinExp Ophthalmol, 2009. **37**(9): p. 884-90.
Shiraishi, A., Converse, R.L., Liu, C.Y., Zhou, F., Kao, C.W., Kao, W.W., 1998. Identification of the cornea-specific keratin 12 promoter by in vivo particle-mediated gene transfer. Investigative ophthalmology & visual science 39, 2554-2561.
Simpson, T.I., Price, D.J., 2002. Pax6; a pleiotropic player in development. BioEssays : news and reviews in molecular, cellular and developmental biology 24, 1041-1051.
Singh, S., Tang, H.K., Lee, J.Y., Saunders, G.F., 1998. Truncation mutations in the transactivation region of PAX6 result in dominant-negative mutants. The Journal of biological chemistry 273, 21531-21541.
Sivak, J.M., West-Mays, J.A., Yee, A., Williams, T., Fini, M.E., 2004. Transcription Factors Pax6 and AP-2alpha Interact To Coordinate Corneal Epithelial Repair by Controlling Expression of Matrix Metalloproteinase Gelatinase B. Molecular and cellular biology 24, 245-257.
Soriano, P., 1999. Generalized lacZ expression with the ROSA26 Cre reporter strain. Nature genetics 21, 70-71.
Sridhar, M.S., 2018. Anatomy of cornea and ocular surface. Indian journal of ophthalmology 66, 190-194.
Sridhar, U. and K. Tripathy, Iris Ectropion Syndrome, in StatPearls. 2023: Treasure Island (FL).
Sturtevant, A.H., 1951. A map of the fourth chromosome of Drosophila melanogaster, based on crossing over in triploid females. Proceedings of the National Academy of Sciences of the United States of America 37, 405-407.
Sugrue, S.P., Zieske, J.D., 1997. ZO1 in corneal epithelium: association to the zonula occludens and adherens junctions. Experimental eye research 64, 11-20.
Sun, J., Rockowitz, S., Xie, Q., Ashery-Padan, R., Zheng, D., Cvekl, A., 2015. Identification of in vivo DNA-binding mechanisms of Pax6 and reconstruction of Pax6-dependent gene

regulatory networks during forebrain and lens development. Nucleic acids research 43, 6827-6846.
Swamynathan, S., Kenchegowda, D., Piatigorsky, J., Swamynathan, S., 2011. Regulation of corneal epithelial barrier function by Kruppel-like transcription factor 4. Investigative ophthalmology & visual science 52, 1762-1769.
Swamynathan, S.K., 2013. Ocular surface development and gene expression. Journal of ophthalmology 2013, 103947.
Swamynathan, S.K., Davis, J., Piatigorsky, J., 2008. Identification of candidate Klf4 target genes reveals the molecular basis of the diverse regulatory roles of Klf4 in the mouse cornea. Investigative ophthalmology & visual science 49, 3360-3370.
Swamynathan, S.K., Katz, J.P., Kaestner, K.H., Ashery-Padan, R., Crawford, M.A., Piatigorsky, J., 2007. Conditional deletion of the mouse Klf4 gene results in corneal epithelial fragility, stromal edema, and loss of conjunctival goblet cells. Molecular and cellular biology 27, 182-194.
Takeichi, M., 1988b. Cadherins: key molecules for selective cell-cell adhesion. IARC scientific publications, 76-79.
Takeichi, M., 1988a. The cadherins: cell-cell adhesion molecules controlling animal morphogenesis. Development 102, 639-655.
Tang, H.K., Singh, S., Saunders, G.F., 1998. Dissection of the transactivation function of the transcription factor encoded by the eye developmental gene PAX6. The Journal of biological chemistry 273, 7210-7221.
Tanifuji-Terai, N., Terai, K., Hayashi, Y., Chikama, T., Kao, W.W., 2006. Expression of keratin 12 and maturation of corneal epithelium during development and postnatal growth. Investigative ophthalmology & visual science 47, 545-551.
Teng, A., et al., Strain-dependent perinatal lethality of Ovol1-deficient mice and identification of Ovol2 as a downstream target of Ovol1 in skin epidermis. Biochim Biophys Acta, 2007. 1772(1): p. 89-95.
Thoft, R.A., Friend, J., 1983. The X, Y, Z hypothesis of corneal epithelial maintenance. Investigative ophthalmology & visual science 24, 1442-1443.
Tiwari, A., Loughner, C.L., Swamynathan, S., Swamynathan, S.K., 2017. KLF4 Plays an Essential Role in Corneal Epithelial Homeostasis by Promoting Epithelial Cell Fate and Suppressing Epithelial-Mesenchymal Transition. Investigative ophthalmology & visual science 58, 2785-2795.
Tiwari, A., Swamynathan, S., Alexander, N., Gnalian, J., Tian, S., Kinchington, P.R., Swamynathan, S.K., 2019. KLF4 Regulates Corneal Epithelial Cell Cycle Progression by Suppressing Canonical TGF-beta Signaling and Upregulating CDK Inhibitors P16 and P27. Investigative ophthalmology & visual science 60, 731-740.
Tripathi, B.J. and R.C. Tripathi, Neural crest origin of human trabecular meshwork and its implications for the pathogenesis of glaucoma. Am J Ophthalmol, 1989. **107**(6): p. 583-90.
Tseng, S.C., 1989. Concept and application of limbal stem cells. Eye 3 (Pt 2), 141-157.
Tuft, S.J., Coster, D.J., 1990. The corneal endothelium. Eye 4 (Pt 3), 389-424.
van Raamsdonk, C.D., Tilghman, S.M., 2000. Dosage requirement and allelic expression of PAX6 during lens placode formation. Development 127, 5439-5448.

Unezaki, S., et al., Ovol2/Movo, a homologue of Drosophila ovo, is required for angiogenesis, heart formation and placental development in mice. Genes Cells, 2007. 12(6): p. 773-85.
Vandewalle, C., Van Roy, F., Berx, G., 2009. The role of the ZEB family of transcription factors in development and disease. Cellular and molecular life sciences : CMLS 66, 773-787.
Walcher, T., Xie, Q., Sun, J., Irmler, M., Beckers, J., Ozturk, T., Niessing, D., Stoykova, A., Cvekl, A., Ninkovic, J., Gotz, M., 2013. Functional dissection of the paired domain of Pax6 reveals molecular mechanisms of coordinating neurogenesis and proliferation. Development 140, 1123-1136.
Walker, H., Akula, M., West-Mays, J.A., 2020. Corneal development: Role of the periocular mesenchyme and bi-directional signaling. Experimental eye research 201, 108231.
Walther, C., Gruss, P., 1991. Pax-6, a murine paired box gene, is expressed in the developing CNS. Development 113, 1435-1449.
Wang, Z., Liu, C.H., Huang, S., Chen, J., 2019. Wnt Signaling in vascular eye diseases. Progress in retinal and eye research 70, 110-133.
Watanabe, K., et al., Mammary morphogenesis and regeneration require the inhibition of EMT at terminal end buds by Ovol2 transcriptional repressor. Dev Cell, 2014. 29(1): p. 59-74.
Watanabe, K., Liu, Y., Noguchi, S., Murray, M., Chang, J.C., Kishima, M., Nishimura, H., Hashimoto, K., Minoda, A., Suzuki, H., 2019. OVOL2 induces mesenchymal-to-epithelial transition in fibroblasts and enhances cell-state reprogramming towards epithelial lineages. Scientific reports 9, 6490.
Weiss, J.S., Moller, H.U., Aldave, A.J., Seitz, B., Bredrup, C., Kivela, T., Munier, F.L., Rapuano, C.J., Nischal, K.K., Kim, E.K., Sutphin, J., Busin, M., Labbe, A., Kenyon, K.R., Kinoshita, S., Lisch, W., 2015. IC3D classification of corneal dystrophies--edition 2. Cornea 34, 117-159.
Wells, J., et al., Ovol2 suppresses cell cycling and terminal differentiation of keratinocytes by directly repressing c-Myc and Notch1. J Biol Chem, 2009. 284(42): p. 29125-35.
Weng, D.Y., Zhang, Y., Hayashi, Y., Kuan, C.Y., Liu, C.Y., Babcock, G., Weng, W.L., Schwemberger, S., Kao, W.W., 2008. Promiscuous recombination of LoxP alleles during gametogenesis in cornea Cre driver mice. Molecular vision 14, 562-571.
Werner, S., Frey, S., Riethdorf, S., Schulze, C., Alawi, M., Kling, L., Vafaizadeh, V., Sauter, G., Terracciano, L., Schumacher, U., Pantel, K., Assmann, V., 2013. Dual roles of the transcription factor grainyhead-like 2 (GRHL2) in breast cancer. The Journal of biological chemistry 288, 22993-23008.
West-Mays, J.A., Sivak, J.M., Papagiotas, S.S., Kim, J., Nottoli, T., Williams, T., Fini, M.E., 2003. Positive influence of AP-2alpha transcription factor on cadherin gene expression and differentiation of the ocular surface. Differentiation; research in biological diversity 71, 206-216.
West-Mays, J.A., Zhang, J., Nottoli, T., Hagopian-Donaldson, S., Libby, D., Strissel, K.J., Williams, T., 1999. AP-2alpha transcription factor is required for early morphogenesis of the lens vesicle. Developmental biology 206, 46-62.

Williams, S.C., Altmann, C.R., Chow, R.L., Hemmati-Brivanlou, A., Lang, R.A., 1998. A highly conserved lens transcriptional control element from the Pax-6 gene. Mechanisms of development 73, 225-229.
Wilson, D., Sheng, G., Lecuit, T., Dostatni, N., Desplan, C., 1993. Cooperative dimerization of paired class homeo domains on DNA. Genes & development 7, 2120-2134.
Wilson, D.S., Guenther, B., Desplan, C., Kuriyan, J., 1995. High resolution crystal structure of a paired (Pax) class cooperative homeodomain dimer on DNA. Cell 82, 709-719.
Wolf, L., Harrison, W., Huang, J., Xie, Q., Xiao, N., Sun, J., Kong, L., Lachke, S.A., Kuracha, M.R., Govindarajan, V., Brindle, P.K., Ashery-Padan, R., Beebe, D.C., Overbeek, P.A., Cvekl, A., 2013. Histone posttranslational modifications and cell fate determination: lens induction requires the lysine acetyltransferases CBP and p300. Nucleic acids research 41, 10199-10214.
Wolf, L.V., Yang, Y., Wang, J., Xie, Q., Braunger, B., Tamm, E.R., Zavadil, J., Cvekl, A., 2009. Identification of pax6-dependent gene regulatory networks in the mouse lens. PloS one 4, e4159.
Xiang, P., Jia, Y., Wang, K., Li, M.Y., Qin, Y.S., He, R.W., Gao, P., Liu, Y., Liu, X., Ma, L.Q., 2018. Water extract of indoor dust induces tight junction disruption in normal human corneal epithelial cells. Environmental pollution 243, 301-307.
Xie, Q., Cvekl, A., 2011. The orchestration of mammalian tissue morphogenesis through a series of coherent feed-forward loops. The Journal of biological chemistry 286, 43259-43271.
Xu, H.E., Rould, M.A., Xu, W., Epstein, J.A., Maas, R.L., Pabo, C.O., 1999a. Crystal structure of the human Pax6 paired domain-DNA complex reveals specific roles for the linker region and carboxy-terminal subdomain in DNA binding. Genes & development 13, 1263-1275.
Xu, L., Overbeek, P.A., Reneker, L.W., 2002. Systematic analysis of E-, N- and P-cadherin expression in mouse eye development. Experimental eye research 74, 753-760.
Xu, P.X., Zhang, X., Heaney, S., Yoon, A., Michelson, A.M., Maas, R.L., 1999b. Regulation of Pax6 expression is conserved between mice and flies. Development 126, 383-395.
Xu, Z.P., Saunders, G.F., 1997. Transcriptional regulation of the human PAX6 gene promoter. The Journal of biological chemistry 272, 3430-3436.
Yi, X., Wang, Y., Yu, F.S., 2000. Corneal epithelial tight junctions and their response to lipopolysaccharide challenge. Investigative ophthalmology & visual science 41, 4093-4100.
Yoon, J.J., Ismail, S., Sherwin, T., 2014. Limbal stem cells: Central concepts of corneal epithelial homeostasis. World journal of stem cells 6, 391-403.
Yu, Q.C., Geng, A., Preusch, C.B., Chen, Y., Peng, G., Xu, Y., Jia, Y., Miao, Y., Xue, H., Gao, D., Bao, L., Pan, W., Chen, J., Garcia, K.C., Cheung, T.H., Zeng, Y.A., 2022. Activation of Wnt/beta-catenin signaling by Zeb1 in endothelial progenitors induces vascular quiescence entry. Cell reports 41, 111694.
Zhang, J., Taylor, R.J., La Torre, A., Wilken, M.S., Cox, K.E., Reh, T.A., Vetter, M.L., 2015a. Ezh2 maintains retinal progenitor proliferation, transcriptional integrity, and the timing of late differentiation. Developmental biology 403, 128-138.

Zhang, L., Wang, Y.C., Okada, Y., Zhang, S., Anderson, M., Liu, C.Y., Zhang, Y., 2019. Aberrant expression of a stabilized beta-catenin mutant in keratocytes inhibits mouse corneal epithelial stratification. Scientific reports 9, 1919.

Zhang, Y., Call, M.K., Yeh, L.K., Liu, H., Kochel, T., Wang, I.J., Chu, P.H., Taketo, M.M., Jester, J.V., Kao, W.W., Liu, C.Y., 2010. Aberrant expression of a beta-catenin gain-of-function mutant induces hyperplastic transformation in the mouse cornea. Journal of cell science 123, 1285-1294.

Zhang, Y., Yeh, L.K., Zhang, S., Call, M., Yuan, Y., Yasunaga, M., Kao, W.W., Liu, C.Y., 2015b. Wnt/beta-catenin signaling modulates corneal epithelium stratification via inhibition of Bmp4 during mouse development. Development 142, 3383-3393.

Zieske, J.D., 2004. Corneal development associated with eyelid opening. The International journal of developmental biology 48, 903-911.

Zieske, J.D., 2000. Expression of cyclin-dependent kinase inhibitors during corneal wound repair. Progress in retinal and eye research 19, 257-270.